

Oil & Natural Gas Technology

DOE Award No.: DE-FC26-06NT42962

Full Scale Reservoir Simulation Studies (Topical Report)

Characterization and Quantification of the Methane Hydrate Resource Potential Associated with the Barrow Gas Fields

Submitted by:
Petrotechnical Resources of Alaska, LLC
3601 C. Street, Suite 822
Anchorage, AK 99503

Prepared for:
United States Department of Energy
National Energy Technology Laboratory

June, 2008



Office of Fossil Energy

Topical Report:

**Full Scale Reservoir Simulation Studies for the
East Pool of the Barrow Gas Field and the Walakpa Gas Field**

June 2008

**CHARACTERIZATION AND QUANTIFICATION
OF THE METHANE HYDRATE RESOURCE POTENTIAL ASSOCIATED WITH THE
BARROW GAS FIELDS**

DOE Project Number: DE-FC26-06NT42962

Awarded to

North Slope Borough, Alaska

Project Director/Manager: Kent Grinage

Principal Investigator: Thomas P. Walsh

Prepared by

Praveen Singh
University of Alaska – Fairbanks
College of Engineering & Mines
PO Box 755880
Fairbanks AK 99775-5880

and

Manmath Panda and Peter J. Stokes
Petrotechnical Resources of Alaska, LLC
3601 C. Street, Suite 822
Anchorage, AK 99503

Prepared for:

U.S. Department of Energy
National Energy Technology Laboratory
626 Cochrane Mills Road
P.O. Box 10940
Pittsburgh, PA 15236-0940

DISCLAIMER

This report was prepared as an account of work sponsored by an agency of the United States Government. Neither the United States Government nor any agency thereof, nor any of their employees, makes any warranty, express or implied, or assumes any legal liability or responsibility for the accuracy, completeness, or usefulness of any information, apparatus, product, or process disclosed, or represents that its use would not infringe privately owned rights. Reference herein to any specific commercial product, process, or service by trade name, trademark, manufacturer, or otherwise does not necessarily constitute or imply its endorsement, recommendation, or favoring by the United States Government or any agency thereof. The views and opinions of authors expressed herein do not necessarily state or reflect those of the United States Government or any agency thereof.

TABLE OF CONTENTS

Section	Page
TABLE OF CONTENTS	iii
LIST OF TABLES	v
LIST OF FIGURES	vi
EXECUTIVE SUMMARY	1
INTRODUCTION	2
MODELING OBJECTIVE	2
EAST BARROW METHODOLOGY	3
I. EAST BARROW CMG-STARS RESERVOIR SIMULATOR	3
II. EAST BARROW MODEL INITIALIZATION	8
III. EAST BARROW HISTORY MATCHING	51
IV. EAST BARROW SENSITIVITY STUDY	57
V. EAST BARROW FORECASTING STUDY	63
EAST BARROW RESULTS AND DISCUSSIONS	68
I. EAST BARROW HISTORY MATCHING	68
II. EAST BARROW DATA ANALYSIS	80
III. SELECTING LOCATIONS FOR INFILL AND HYDRATE TEST WELLS FOR EAST BARROW	93
IV. EAST BARROW SENSITIVITY STUDY	95
V. EAST BARROW FORECASTING STUDY	115
EAST BARROW CONCLUSIONS	119
WALAKPA METHODOLOGY	121
WALAKPA MODEL INITIALIZATION	121

TABLE OF CONTENTS, CONT.

Section	Page
WALAKPA RESULTS AND DISCUSSIONS	134
I. WALAKPA HISTORY MATCHING - SMALL MODEL	134
II. WALAKPA DATA ANALYSIS	138
III. WALAKPA FORECASTING STUDY	139
WALAKPA CONCLUSIONS	143
REFERENCES	145

LIST OF TABLES

Table	Page
Table E-1: Initial condition of East Barrow reservoir	27
Table E-2: Thermal properties initialized for East Barrow reservoir	28
Table E-3: Fluid and component properties initialized for East Barrow reservoir	29
Table E-4: End point and hydrate-water relative permeability data for East Barrow	31
Table E-5: End point and gas-hydrate relative permeability data for East Barrow	33
Table E-6: Location (co-ordinates) and dimension of East Barrow Wells	36
Table E-7: History matching scenarios for East Barrow	53
Table E-8a: Initial Condition for Scenario A (Only Gas Model) for East Barrow	54
Table E-8b: Initial Condition for Scenario B (Gas + Aquifer Model) for East Barrow	54
Table E-8c: Initial Condition for Scenario C (HYD + Gas + Aquifer Model) for East Barrow	55
Table E-8d: Initial Condition for Scenario D (Only HYD Model) for East Barrow	55
Table E-8e: Initial Condition for Scenario E (HYD + Gas Model) for East Barrow	56
Table E-8f: Initial Condition for Scenario F (HYD + Aquifer Model) for East Barrow	56
Table E-9a: Initial estimates of free gas, hydrate and water for East Barrow	68
Table E-9b: Initial Gas In Place (Free Gas + Hydrate Associated Gas) for East Barrow	69
Table E-10: Cumulative gas production (September 2007) for East Barrow	70
Table E-11: Cumulative water production (September 2007) for East Barrow	71
Table E-12: RMS Error (Reservoir Pressure Data vs. Model Output) for East Barrow	73
Table E-13: Hydrate Contribution in recharging gas reservoir for East Barrow	92
Table E-14: Optimum locations for drilling future infill wells for East Barrow	94
Table E-15: Cumulative gas production and recovery (Forecast Study) for East Barrow	118
Table W-1: Walakpa reservoir model – Initial reservoir condition	131
Table W-2: Production history data – Walakpa gas field	132
Table W-3: Location (co-ordinates) and dimension of Walakpa Wells	133
Table W-4: Initial estimates of free gas, hydrate and water for Walakpa	134
Table W-5: Initial Gas In Place (Free Gas + Hydrate Associated Gas) for Walakpa	134
Table W-6: Cumulative gas production (to September 2007) for Walakpa	135
Table W-7: RMS Error-Scenario A (Res Press Data vs. Model Output) for Walakpa	136
Table W-8: RMS Error-Scenario B (Res Press Data vs. Model Output) for Walakpa	137
Table W-9: Hydrate Contribution in recharging gas reservoir for Walakpa	139
Table W-10: Initialization of Forecasting Study for Walakpa	139
Table W-11: Summary of forecast run from Forecasting Study for Walakpa	140
Table W-12: Initial in-place gas and hydrate volumes Walakpa reservoir models	142
Table W-13: Comparison of simulation results between the Small and Large models for Walakpa	142

LIST OF FIGURES

Figure	Page
Figure 1: Map of Barrow Gas Fields in North Slope Borough of Alaska	1
Figure 2: 3D reservoir grid (Grid Top)– East Barrow Reservoir Model	9
Figure 3: East Barrow IJ Plane view reservoir grid (K layer 1)	9
Figure 4: East Barrow IJ Plane view reservoir grid (K layer 12)	10
Figure 5: East Barrow IJ Plane view reservoir grid (K layer 25)	10
Figure 6: East Barrow Porosity (3D view)	11
Figure 7: East Barrow Layer 16th, shaley layer (Porosity) - IJ plane view	12
Figure 8: East Barrow Permeability-I (3D view)	13
Figure 9: East Barrow Permeability-J (3D view)	13
Figure 10: East Barrow Permeability-K (3D view)	14
Figure 11: East Barrow Layer 16th, shaley layer (Permeability I,J and K) - IJ plane view	14
Figure 12: Formula editor (CMG-STARs) - Initializing temperature distribution	15
Figure 13: East Barrow Temperature, Deg F (3D view)	16
Figure 14: East Barrow Temperature, Deg F (3D view)	17
Figure 15: Initial Condition CMG-STARs (No Vertical Equilibrium Calculation)	17
Figure 16: Pressure-Temperature equilibrium relationship for water-hydrate-free gas system	18
Figure 17: Formula editor (CMG-STARs) - Initializing hydrate saturation	19
Figure 18: East Barrow Hydrate Saturation, Sh (3D view)	20
Figure 19: East Barrow Hydrate Saturation (IJ Plane view, K Layer-1)	20
Figure 20: East Barrow Hydrate -Free Gas Zone Contact at 2050' (IK Plane view)	21
Figure 21: Formula editor (CMG-STARs) - Initializing gas saturation	22
Figure 22: East Barrow Gas Saturation, Sg (3D view)	23
Figure 23: East Barrow Gas Saturation (IJ Plane view, K Layer-1)	23
Figure 24: East Barrow Hydrate-Gas Contact at 2050' and GWC at 2080' (IK Plane view)	24
Figure 25: Formula editor (CMG-STARs) - Initializing water saturation	25
Figure 26: East Barrow Water Saturation (3D view)	26
Figure 27: East Barrow Water Saturation (IJ Plane view, K Layer-1)	26
Figure 28: East Barrow Gas-Water Contact at 2080' (IK Plane view)	27
Figure 29: Hydrate - Water relative permeability curve (CMG keyword *SWT)	32
Figure 30: Water capillary pressure (CMG keyword *SWT)	32
Figure 31: Gas - Hydrate relative permeability curve (CMG keyword *SLT)	34
Figure 32: Gas capillary pressure (CMG keyword *SLT)	34
Figure 33: East Barrow Well locations (IJ Plane View)	36
Figure 34: East Barrow Wellbore diagram of Well #EB-14	37
Figure 35: East Barrow Wellbore diagram of Well #EB-15	38
Figure 36: East Barrow Wellbore diagram of Well #EB-18	39
Figure 37: East Barrow Wellbore diagram of Well #EB-19	40
Figure 38: East Barrow Wellbore diagram of Well #EB-21	41
Figure 39: Choose the file containing well production data (Step 1)	43
Figure 40: Choose the file option (Step 2)	44
Figure 41: Choose delimiters (Step 3)	45
Figure 42: Choose column details (Step 4)	46
Figure 43: Check well names and primary constraint (Step 5)	47
Figure 44: Gas production rate for Well #EB-14 (Production data vs. Model Output)	48
Figure 45: Gas production rate for Well #EB-15 (Production data vs. Model Output)	49
Figure 46: Gas production rate for Well #EB-18 (Production data vs. Model Output)	49
Figure 47: Gas production rate for Well #EB-19 (Production data vs. Model Output)	50
Figure 48: Gas production rate for Well #EB-21 (Production data vs. Model Output)	50

LIST OF FIGURES, CONT.

Figure	Page
Figure 49: East Barrow Block 19,19,1 representing average reservoir pressure	52
Figure 50: Aquifer Options (CMG-STARs)	58
Figure 51: Initializing bottom aquifer (infinite size)	59
Figure 52: Initializing bottom aquifer (finite size)	60
Figure 53: Initializing region aquifer (infinite size)	61
Figure 54: Initializing region aquifer (finite size)	62
Figure 55: Wellbore diagram of EB#14 (completed in horizontal section)	64
Figure 56: Wellbore diagram of EB#19 (completed in horizontal section)	65
Figure 57: Wellbore diagram of Vertical Test Well (New Infill Well) for East Barrow	66
Figure 58: Wellbore diagram of Horizontal Test Well (New Infill Well) for East Barrow	67
Figure 59: East Barrow Cumulative gas production profile (History Matching)	70
Figure 60: East Barrow Cumulative water production profile (History Matching)	71
Figure 61: East Barrow Average Reservoir Pressure Match (History Matching)	73
Figure 62: Gas production rate matching - Well EB#14	74
Figure 63: Gas production rate matching - Well EB#15	75
Figure 64: Gas production rate matching - Well EB#18	75
Figure 65: Gas production rate matching - Well EB#19	76
Figure 66: Gas production rate matching - Well EB#21	76
Figure 67: Water production rate matching - Well EB#14	77
Figure 68: Water production rate matching - Well EB#15	78
Figure 69: Water production rate matching - Well EB#18	78
Figure 70: Water production rate matching - Well EB#19	79
Figure 71: Water production rate matching - Well EB#21	79
Figure 72: Hydrate Saturation Profile (Location 19, 19 (k=1 to 25)) for East Barrow	80
Figure 73: Gas Saturation Profile (Location 19, 19 (k=1 to 25)) for East Barrow	81
Figure 74: Water Saturation Profile (Location 19, 19 (k=1 to 25)) for East Barrow	82
Figure 75: Location 29,8, 1 (Representing Hydrate-Free Gas-Aquifer Zone) for East Barrow	83
Figure 76: Hydrate Saturation Profile (Location 29, 8 (k=1 to 8)) for East Barrow	83
Figure 77: Gas Saturation Profile (Location 29, 8 (k=1 to 22)) for East Barrow	84
Figure 78: Water Saturation Profile (Location 29, 8 (k=1 to 22)) for East Barrow	85
Figure 79: Reservoir pressure (Sep 2007, 3D View) for East Barrow	86
Figure 80: Reservoir temperature (Sep 2007, 3D View) for East Barrow	86
Figure 81: Hydrate saturation (Sep 2007, 3D View) for East Barrow	87
Figure 82: Gas saturation (Sep 2007, 3D View) for East Barrow	87
Figure 83: Water Saturation (Sep 2007, 3D View) for East Barrow	88
Figure 84: Initial Hydrate-Free Gas Contact (2050', December 1981) for East Barrow	89
Figure 85: Current Hydrate-Free Gas Contact (2045', Sep 2007) for East Barrow	89
Figure 86: Initial Free Gas-Water Contact (2080', Dec 1981) for East Barrow	90
Figure 87: Current Free Gas-Water Contact (2070', Sep 2007) for East Barrow	90
Figure 88: Hydrate per Unit Area-Total (Dec 1981) for East Barrow	91
Figure 89: Hydrate per Unit Area-Total (Sep 2007) for East Barrow	91
Figure 90: Free Gas per Unit Area-Total (Dec 1981) for East Barrow	92
Figure 91: Free Gas per Unit Area-Total (Sep 2007) for East Barrow	93
Figure 92: Selected location for infill wells (Free Gas per Unit Area-Total) for East Barrow	94
Figure 93: Cumulative Gas Production (Sensitivity - Free Gas Zone Size) for East Barrow	96
Figure 94: Cumulative Water Production (Sensitivity - Free Gas Zone Size) for East Barrow	96
Figure 95: Average Reservoir Pressure (Sensitivity - Free Gas Zone Size) for East Barrow	97
Figure 96: Cumulative Gas Production (Sensitivity - Hydrate Saturation) for East Barrow	98

LIST OF FIGURES, CONT.

Figure	Page
Figure 97: Cumulative Water Production (Sensitivity - Hydrate Saturation) for East Barrow	99
Figure 98: Average Reservoir Pressure (Sensitivity - Hydrate Saturation) for East Barrow	99
Figure 99: Cumulative Gas Production (Sensitivity - Hydrate Zone Size) for East Barrow	101
Figure 100: Cumulative Water Production (Sensitivity - Hydrate Zone Size) for East Barrow	101
Figure 101: Average Reservoir Pressure (Sensitivity - Hydrate Zone Size) for East Barrow	102
Figure 102: Cumulative Gas Production (Sensitivity - Aquifer Shape and Size for East Barrow	103
Figure 103: Cumulative Water Production (Sensitivity - Aquifer Shape and Size for East Barrow	104
Figure 104: Average Reservoir Pressure (Sensitivity - Aquifer Shape and Size for East Barrow	104
Figure 105: Cumulative Water Production (Sensitivity - Bottom Aquifer) for East Barrow	105
Figure 106: Average Reservoir Pressure (Sensitivity - Bottom Aquifer) for East Barrow	106
Figure 107: Cumulative Water Production (Sensitivity - Edge Aquifer) for East Barrow	107
Figure 108: Average Reservoir Pressure (Sensitivity - Edge Aquifer) for East Barrow	107
Figure 109: Cumulative Water Production (Sensitivity - Infinite Aquifer) for East Barrow	108
Figure 110: Average Reservoir Pressure (Sensitivity - Infinite Aquifer) for East Barrow	109
Figure 111: Cumulative Water Production (Sensitivity - Finite Aquifer) for East Barrow	110
Figure 112: Average Reservoir Pressure (Sensitivity - Finite Aquifer) for East Barrow	110
Figure 113: Cumulative Water Production (Sensitivity - GWC 2080') for East Barrow	112
Figure 114: Average Reservoir Pressure (Sensitivity - GWC 2080') for East Barrow	112
Figure 115: Cumulative Water Production (Sensitivity - GWC 2070') for East Barrow	113
Figure 116: Average Reservoir Pressure (Sensitivity - GWC 2070') for East Barrow	113
Figure 117: Cumulative Water Production (Sensitivity - GWC 2045') for East Barrow	114
Figure 118: Average Reservoir Pressure (Sensitivity - GWC 2045') for East Barrow	114
Figure 119: Average Reservoir Pressure (Forecasting Study) for East Barrow	115
Figure 120: Cumulative Water Production (Forecasting Study) for East Barrow	116
Figure 121: Cumulative gas production (Forecast Study) for East Barrow	117
Figure 122: East Barrow % Recovery (Forecast Study)	117
Figure 123: 3D reservoir grid (Grid Top) – Walakpa Reservoir Model – SMALL MODEL	122
Figure 124: Porosity (3D view) – Walakpa Reservoir Model – SMALL MODEL	123
Figure 125: Walakpa Permeability-I (3D view) – SMALL MODEL	124
Figure 126: Walakpa Temperature, Deg F (3D view) – SMALL MODEL	125
Figure 127: Walakpa Pressure, psi (3D view) – SMALL MODEL	126
Figure 128: Pressure-temperature equilibrium relationship for water-hydrate-free gas system	126
Figure 129: Walakpa Hydrate Saturation, S_h (3D view) – SMALL MODEL	127
Figure 130: Walakpa Hydrate-Free Gas Zone Contact at 2000' (JK Plane view) – SMALL MODEL	128
Figure 131: Walakpa Gas Saturation, S_g (3D view) – SMALL MODEL	129
Figure 132: Walakpa Hydrate-Gas Contact at 2000' and GWC at 2750' (JK Plane view)	129
Figure 133: Walakpa Water Saturation, S_w (3D view) – SMALL MODEL	130
Figure 134: Gas-Water Contact at 2750' (JK Plane view) for Walakpa – SMALL MODEL	131
Figure 135: Well locations (IJ Plane View) for Walakpa	133
Figure 136: Cumulative gas production profile (History Matching) for Walakpa	135
Figure 137: Reservoir Pressure Match (Scenario-A) for Walakpa – SMALL MODEL	136
Figure 138: Reservoir Pressure Match (Scenario-B) for Walakpa – SMALL MODEL	137
Figure 139: Pressure co-ordinates selected to represent reservoir pressure for Walakpa	138
Figure 140: Cumulative gas production from Forecasting Study for Walakpa	140
Figure 141: Cumulative gas production rate from Forecasting Study for Walakpa	141
Figure 142: Reservoir Pressure from Forecasting Study for Walakpa	141
Figure 143: Walakpa LARGE MODEL Hydrate dissociation over forecast	142

EXECUTIVE SUMMARY

This Topical Report details the full scale reservoir simulation that was performed for the East Pool of the Barrow Gas Field and the Walakpa Gas Field (Figure 1) to evaluate and quantify methane hydrate resource potential that appears to exist adjacent and up-dip of the free gas producing reservoirs. Geologic models were uploaded to CGM-STARS reservoir simulation application and history matched to actual production offtake, field pressure and temperature. The models were then used to predict future hydrate dissociation to recharge the free gas reservoirs.

Model forecasts predict that 100% of the 26 BSCF of in-place methane hydrates will be dissociated and produced from the East Barrow Pool over its production life of 1981-2037 with one additional well added to the existing well set, and 20% of the 284 BSCF of in-place methane hydrates will be dissociated and produced from the Walakpa Field reservoir over a production life of 1992-2037 using the current production rates from existing wells.

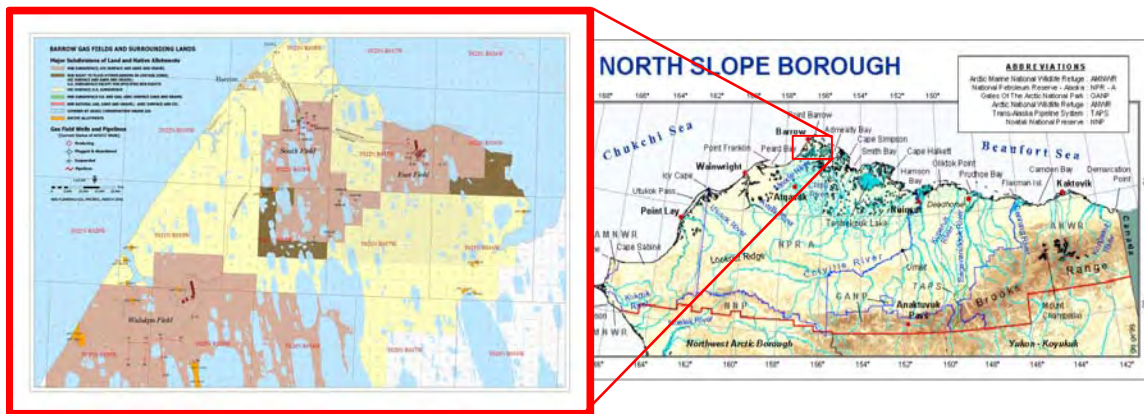


Figure 1: Map of Barrow Gas Fields in North Slope Borough of Alaska

INTRODUCTION

This topical report describes the results of the reservoir simulation studies for East Barrow and Walakpa reservoirs.

Several hydrate production mechanisms and phenomenon have been discussed in the literature^{2,3,4} to date. Hydrate production modeling has been described based on 3D mechanistic models, simulating different reservoir conditions and production patterns. Sensitivity of several parameters has also been discussed in published literature^{2,3,4}; however, limited information on full field simulation has been reported for hydrate bearing reservoirs.

Gas production from a hydrate capped free gas reservoir has been reported to be the best candidate for producing gas from insitu hydrates^{2,3,4,5}. The material balance study for East Barrow gas reservoir¹⁷ suggests existence of a thick hydrate cap over a free gas pool. Hence this reservoir becomes an ideal candidate for dissociating hydrate by depressurization and producing the liberated methane gas via conventional production methodology.

A number of reservoir simulators are available that are capable of performing simulations for hydrate-free gas-aquifer systems. A detailed reservoir code comparison study was recently completed by the USDOE in order to compare the effectiveness of these simulators⁵. The reservoir simulators showed close agreement in model output. The recently concluded code comparison study (refer NETL methane hydrate program at www.netl.doe.gov) and previous simulation efforts with CMG-STARS^{8,14} was the basis of selecting STARS reservoir simulator for developing hydrate production models for East Barrow and Walakpa gas reservoirs.

The history matched and tested reservoir models were used as a predictive tool to formulate future plans of reservoir development and hydrate production testing. The simulation model is capable of quantifying the contribution of dissociating hydrates in recharging the gas reservoir. The model was also evaluated to select optimum locations for drilling infill wells. Several forecasting runs were simulated to compare the impact of drilling a new well vs. producing from existing infrastructure, and also the performance of a new horizontal well vs. a vertical well.

MODELING OBJECTIVE

Based on hydrate stability modeling work⁶ and material balance modeling¹⁷, a full field simulation model for the East Barrow and Walakpa gas reservoirs have been developed in CMG-STARS. The model results are validated by performing both field level and well level history match. The best case model was used to decide location for infill drilling. This model is capable of evaluating and testing sensitivity of all reservoir parameters. The objective of this study was to develop a full field reservoir model capable of evaluating and quantifying methane hydrate resource potential associated with the East Barrow and Walakpa Gas Fields. A top down approach has been employed to build the reservoir model and match the production history using an advanced reservoir simulator.

A primary focus of this study was to build a robust reservoir model, for a free gas and hydrate bearing system, capable of predicting future reservoir performance. We have thus developed full scale field models for East Barrow and Walakpa reservoirs that have been used to study performance and to influence future development strategies. The models can be easily adapted or customized to represent similar hydrate bearing reservoirs.

The East Barrow modeling was completed first, followed by the Walakpa modeling, and many of the details of the two models are the same. This report will present the East Barrow modeling work in detail, with the Walakpa modeling presented as a modification of input to the same procedure in somewhat less detail.

EAST BARROW METHODOLOGY

I. CMG-STARS RESERVOIR SIMULATOR

STARS (*Steam, Thermal and Advanced Process Reservoir Simulator*) developed by Computer Modeling Group (CMG) was used to model gas production from hydrate reservoirs. STARS can model the flow of three-phase, multi-component fluids using cartesian, cylindrical or mixed coordinates. The input parameters to the model can be in the forms of field data or they can be generated by correlations built into the model. It also incorporates a unique discretized wellbore option, which allows improved modeling of horizontal wells. STARS is designed to simulate a variety of complex oilfield production and enhancement processes; however, it is primarily used for conventional black oil studies. To simulate gas production by hydrate dissociation in STARS, adjustments are made to accommodate the properties of hydrate. In this study, hydrate is considered as the oil phase with very high viscosity and low relative permeability. Discussed below are the salient features/options available with CMG-STARS.

A. Reservoir Grid

CMG-STARS offers two ways to initialize reservoir grid. The first method is by specifying the dimensions and number of blocks in a grid using the graphic user interface, and the second method is by directly importing the grid dimensions from an external data file. These external data source must be CMG-STARS compatible.

Based on reservoir geology and well log data, a detailed reservoir model, depicting East Barrow gas reservoir was built using RMS¹⁹. The data file generated using RMS software was directly imported into CMG by using *INCLUDE keyword. The geological description and the geostatistical modeling procedure are described in separate reports¹⁹.

B. Reservoir Properties

The graphic user interface in CMG-STARS allows layer-wise (K-direction) initialization of all reservoir properties. This method is an approximate way to represent the reservoir and may not provide true representation of reservoir conditions. A detailed geostatistical modeling approach¹⁹ was followed in this study to obtain reservoir properties like porosity and permeability (in all three directions). The properties are directly imported in CMG-STARS using *INCLUDE keyword.

Reservoir properties like pressure, temperature, permeability (I, J and K direction), water, hydrate and gas saturations are specified by using key information like initial reservoir pressure data, geothermal gradient, Hydrate Free Gas Contact (HGC) and Gas Water Contact (GWC). A formula is written using CMG's Add/Edit formula feature. The new formula is loaded for specific/all layers (k-direction) using "specify property" and "region/sector" options. The formula can then be easily loaded for respective property.

C. Thermal Properties

Thermal rock properties, like volumetric heat capacity and thermal conductivity can be specified under this section. Provision for initializing overburden temperature has also been provided under this section. Apart from dissociation by depressurization (due to free gas production), hydrate dissociation is also controlled by heat supply from matrix and overburden/underburden rocks. Hence, option of choosing overburden temperature is critical with respect to hydrate dissociation. For this case, a constant overburden temperature was chosen. A single rock type has been considered for the reservoir model. The thermal properties can also be directly initialized in CMG data file using the following keywords.

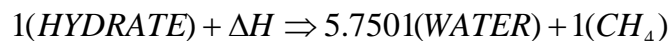
- *ROCKCP - volumetric heat capacity (rock),
- *THCONR - Thermal Heat Conductivity (rock),
- *THCONO - Thermal Heat Conductivity (oil),
- *THCONW – Thermal Heat Conductivity (water)
- *THCONG – Thermal Heat Conductivity (gas)
- *THCONMIX – Thermal Conductivity Phase Mixing
- *HLOSST – Overburden Temperature
- *HLOSSPROP – Directional Heat Loss Property
- *ROCKTYPE.- Reservoir Rock Type

D. Fluid/Component Properties

For a hydrate-gas-water system, properties of three components are initialized. Water is modeled as aqueous phase, methane as gaseous phase. The hydrate is modeled as an oil phase in STARS, using a very high viscosity such as 1000 centipoise, assuming hydrate to be the immobile phase. Component properties like $P_{critical}$, $T_{critical}$, MW, density, viscosity, ethalpies etc are provided under respective sections. Dissolution of methane gas in water has been neglected, hence each phase is independent and holds a mole fraction of 1 within its phase (i.e. no dissolved gas in oil or water).

When hydrate dissociates, it splits into methane and water initially, and as the production continues, the reservoir conditions change, due to the fact that one hydrate molecule gives off approximately 1 molecule of methane and 5.75 molecules of water. This hydrate dissociation mechanism is represented by a first order chemical reaction where hydrate reactant undergoes physical change into water and free gas in the presence of additional heat of dissociation acting as a catalyst.

The chemical reaction is represented by



Where,
HYDRATE – hydrate phase
 ΔH – heat of dissociation
WATER – aqueous phase
 CH_4 – methane gas phase

The reaction rate constant ' k_d ' is defined by Arrhenius equation. The value of each component of Arrhenius equation can be easily provided through user interface or using keywords *FREQFAC, *RENTH, *EACT.

Arrhenius Equation :

$$k_d = k_d^o \exp\left(-\frac{E_a}{RT}\right)$$

Where,

k_d = reaction rate constant

k_d^o = Frequency Factor, (CMG Keyword *FRQFAC)

E_a = Activation Energy, (CMG Keyword, *EACT)

R = Universal Gas Constant, (CMG inbuilt property)

T = Reservoir Temperature

The rate of hydrate decomposition is given by Kim Bishnoi Model⁷.

Rate of hydrate decomposition

$$\frac{dC_H}{dt} = k_d A_d (p_e(t) - p_g(t))$$

Where,

$\frac{dC_H}{dt}$ = Rate of Hydrate decomposition

k_d = reaction rate constant

A_d = Surface Area per unit Volume

p_e = equilibrium pressure (based on reservoir temperature)

p_g = average reservoir pressure (current)

As observed above, the rate of reaction is governed by the extent of deviation observed from equilibrium⁸. This deviation from equilibrium is governed by the value K, also called the equilibrium parameter. The model K parameter is initialized using the three phase pressure-temperature equilibrium correlation proposed by Kamath et. al.⁹. The correlation is a good approximation of hydrate thermodynamic relationship and was derived from empirical data obtained from laboratory experiments. Following CMG keywords are used to define K parameter - rxk1, rxk2, rxk3, rxk4 and rxk5⁸

Three phase equilibrium parameter

$$K = p_e/p_g$$

Three phase equilibrium relationship, Kamath et.al⁹

$$p_e = \exp\left(\lambda - \frac{\beta}{T_{se}}\right)$$

Where,

p_e = Equilibrium pressure, kPa

λ = 38.98, dimensionless

β = 8533.80, Kelvin

T_{se} = Equilibrium temperature

Hence, K value is given by the expression

$$K = \left(\frac{1}{P_g}\right) \exp\left(\lambda - \frac{\beta}{T_{se}}\right)$$

In CMG-STARS, the above expression is re-arranged and K value is represented by

$$K = \left(\frac{rxk1}{P_g} + rxk2 * P + rxk3\right) \exp\left(\frac{rxk4}{T - rxk5}\right)$$

Where,

rxk1, rxk2, rxk3, rxk4 and rxk5 are coefficients defining equilibrium parameter K.

E. Relative Permeabilities and Capillary Pressure Functions

Relative permeability calculations for hydrates have not been published to date. The values used in the model are calculated using equations presented by Hong and Darvish (2003)¹⁰. Hong and Darvish modified the correlations suggested by Van Genuchten (1980)¹¹ and Parker et al (1987)¹². These models are modified in order to incorporate the presence of a hydrate phase. The new models are given as:

Relative Permeability of water:
$$k_{rw} = k_{rwo} \bar{S}_w^{-0.5} [1 - (1 - \bar{S}_w^{-1/m})^m]^2$$

Relative Permeability of gas:
$$k_{rg} = k_{rgo} \bar{S}_g^{-0.5} (1 - \bar{S}_{wH}^{-1/m})^{2m}$$

Capillary pressure between gaseous and aqueous phases:
$$p_c = p_{co} [(\bar{S}_w)^{-1/m} - 1]^{1-m}$$

Where,

Normalized Water Saturation
$$\bar{S}_w = \frac{S_w - S_{wr}}{1 - S_{wr} - S_{gr}}$$

Normalized Hydrate Saturation
$$\bar{S}_{wH} = \frac{S_w + S_H - S_{wr}}{1 - S_{wr} - S_{gr}}$$

$$\bar{S}_g = \frac{1 - S_w - S_H - S_{gr}}{1 - S_{wr} - S_{gr}}$$

Normalized Gas Saturation

Also,

S_w = Water Saturation

S_{wr} = Irreducible Water Saturation

S_{gr} = Residual Gas Saturation

k_{rwo} = Water relative permeability at residual gas saturation (single phase flow)

k_{rgo} = Gas relative permeability at irreducible water saturation (single phase flow)

$m = 0.45$ (rock type - sandstone)

The three phase (hydrate-gas-water) relative permeability has been calculated in CMG-STARS using Stone's second model (normalized). The rock type has been considered water wet (default). In CMG-STARS, relative permeability data is represented by two relative permeability curves (water-oil (hydrate) table and liquid (hydrate)-gas table). For the East Barrow model a single rock type has been considered. CMG-STARS also allows customizing relative permeability data by providing an option of end point rescaling. Based on reservoir end point data, the three phase relative permeability can be easily re-scaled to desired limits.

F. Production Well Modeling

CMG-STARS offers a powertool to initialize well utility as producer or injector. The wells can be easily constructed horizontal or vertical based on requirement. The wells can be completed and produced/shut in at any time or time period during the production life of the reservoir, depending on the actual field conditions. Well completions can also be altered at any point of time during the production based on well history.

The wells are produced with the help of constraints. These constraints range from operating at MIN flowing bottom hole pressure, to MAX gas production rate. One can also monitor other important parameters like Gas Oil Ratio in order to shut in the well whenever the set limit is reached. Any number of constraints can be given to each well. The first constraint given to any well is called the primary constraint. Well production closely follows the primary constraint and tries to maintain other constraints, if given. These constraints can be altered at any time based on production data. The well constraints can also be imported from production data files. For the East Barrow reservoir, monthly production data has been loaded (imported) for each well.

II. EAST BARROW MODEL INTIALIZATION

East Barrow Reservoir Model - Base Case

Several models were intialized and results were matched with reservoir production history. The history match criteria and results are discussed in subsequent chapters. Based on history match studies a best case (base case) model has been selected. In this section the model intialization (in CMG-STARS) for the best case has been explained in detail.

The best case scenario consists of hydrate cap lying over free gas and underlain with model aquifer. This section will discuss the reservoir properties and wellbore model intialized for the base case. All parameters have been initialized in field units.

A. Reservoir Grid

Based on reservoir geology and well log data, a detailed reservoir model, depicting the East Barrow reservoir was built using RMS¹⁹. The data file generated using RMS software was directly imported into CMG-STARS by using *INCLUDE keyword. The geological description and the geostatistical modeling procedure are described in separate reports¹⁹.

The model has been generated using a Cartesian co-ordinate system by choosing a grid having 54 blocks in the 'I' direction, 37 blocks in 'J' direction and 25 blocks in 'K' direction making a total of 49,950 grid blocks. Based on geologic information, several grid blocks have been rendered inactive by using *NULL keyword. These grid blocks are not part of the active reservoir volume. The dimension of each grid block is 600' by 600' (IJ plane). The grid block thickness in K direction is variable and ranges anywhere between 1.09 ft and 3.22 ft. The grid blocks are thinner in the updip section (west direction) and thicker in downdip locations (east direction). The topmost section of the reservoir is at a depth of 1900 ft below sea level, whereas the deepest section is at a depth of 2330 ft below sea level. However, the pay zone depth ranges between 1901 ft to 2328 ft below sea level.

The 3D reservoir grid is shown in Figure 2 below. Figures 3, 4 and 5 show the IJ plane view of reservoir grid at plane 1 (k=1), plane 12 (K=12) and plane 25 (K=25), respectively.

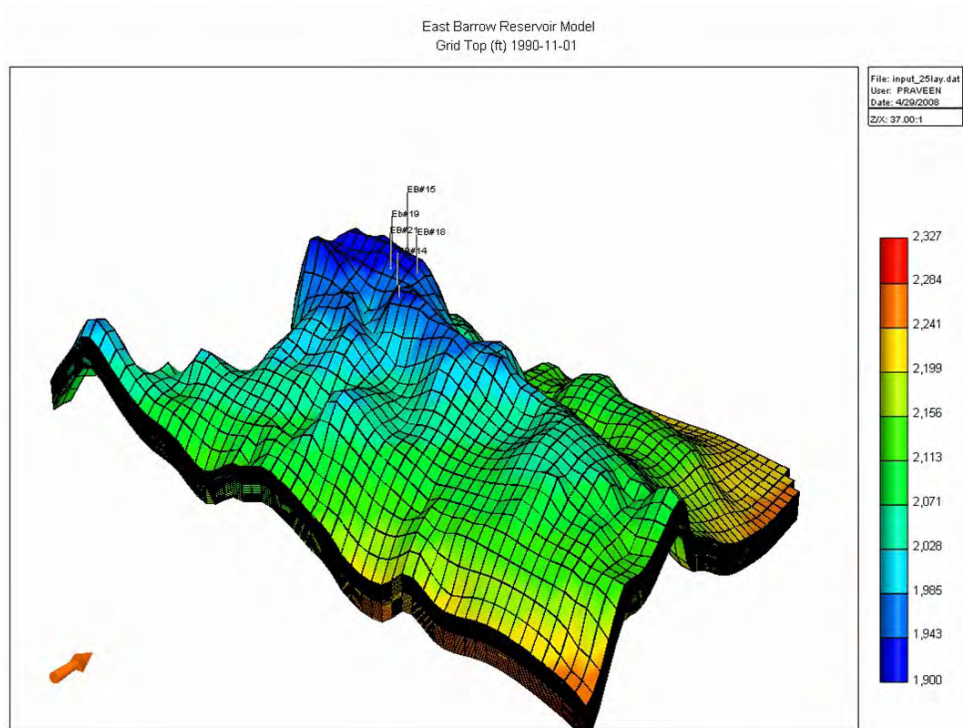


Figure 2: 3D reservoir grid (Grid Top)– East Barrow Reservoir Model

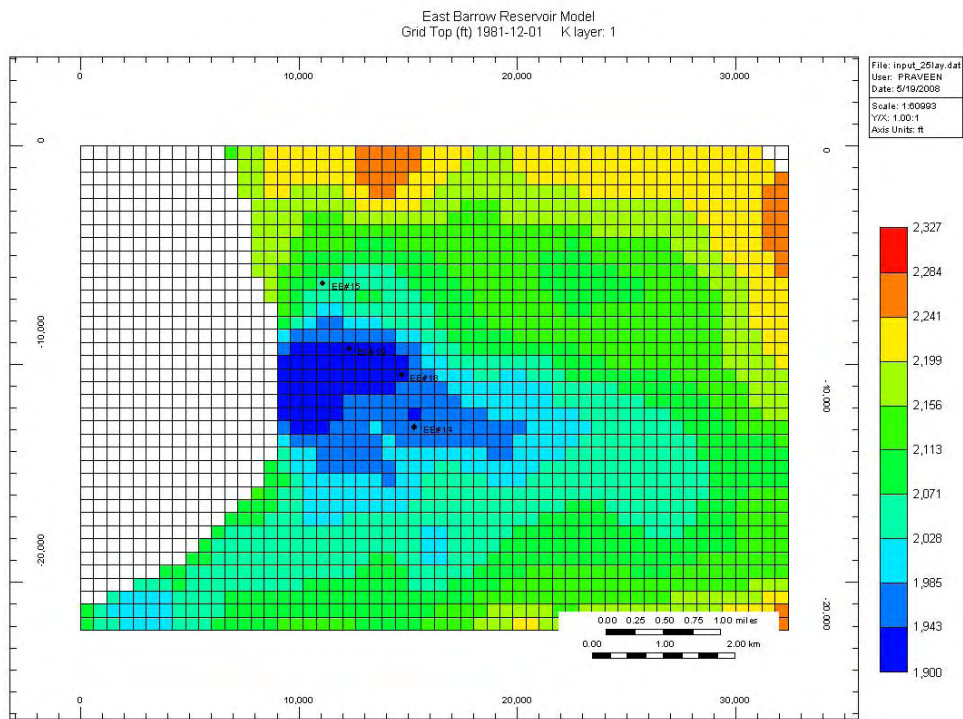


Figure 3: East Barrow IJ Plane view reservoir grid (K layer 1)

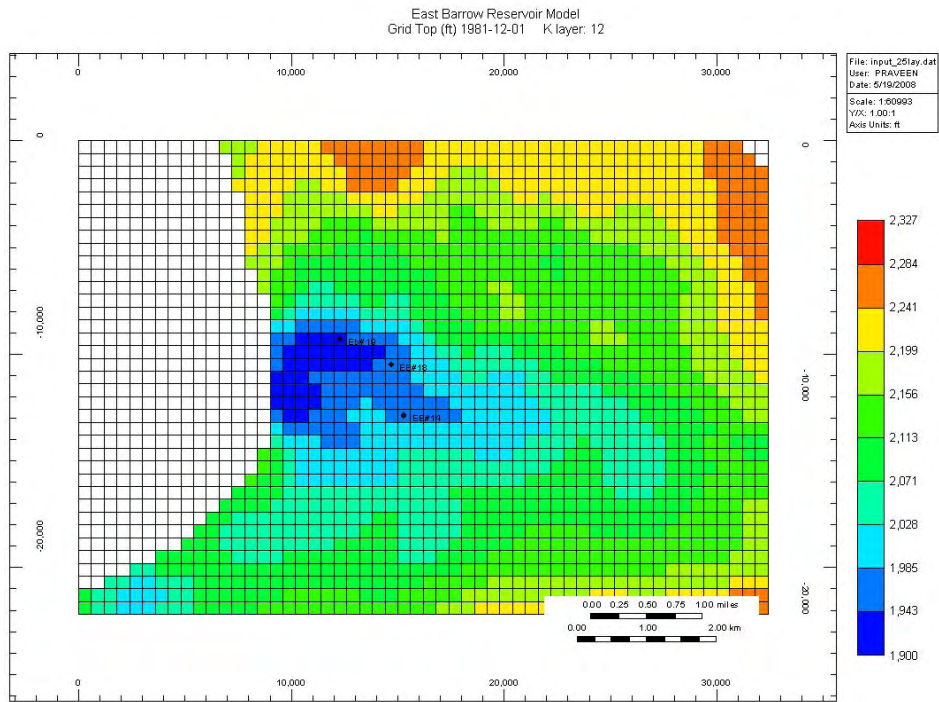


Figure 4: East Barrow IJ Plane view reservoir grid (K layer 12)

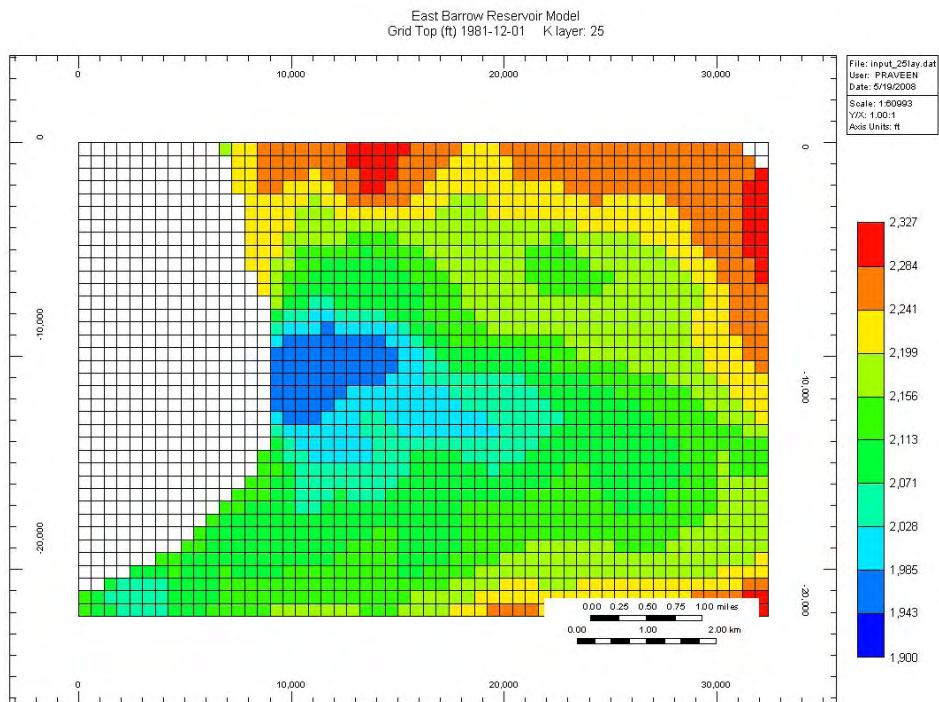


Figure 5: East Barrow IJ Plane view reservoir grid (K layer 25)

B. Reservoir Properties

1. Porosity

For details regarding porosity distribution and estimation procedure, the reader is referred to the reports on reservoir geology and geo-statistical modeling¹⁹. The porosity distribution data file is loaded into the CMG-STARs data file using *INCLUDE keyword. The porosity of the reservoir ranges from 5% (min) to 24% (max). The geologic study on the reservoir has identified the existence of a semi permeable barrier (a shaley layer) between Upper and Lower Barrow sands. To represent this condition, layer 16 (K=16) has been assigned lower porosity value of 5%. Figure 6 shows a 3D view of porosity distribution within the reservoir. Figure 7 shows the IJ plane view of layer 16 (shaley layer).

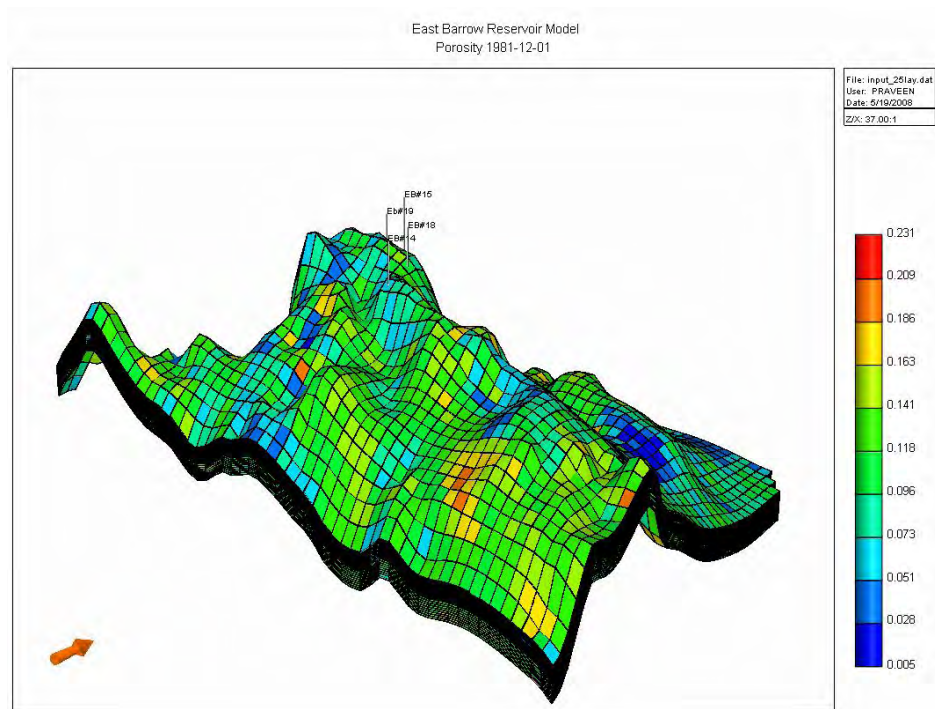


Figure 6: East Barrow Porosity (3D view)

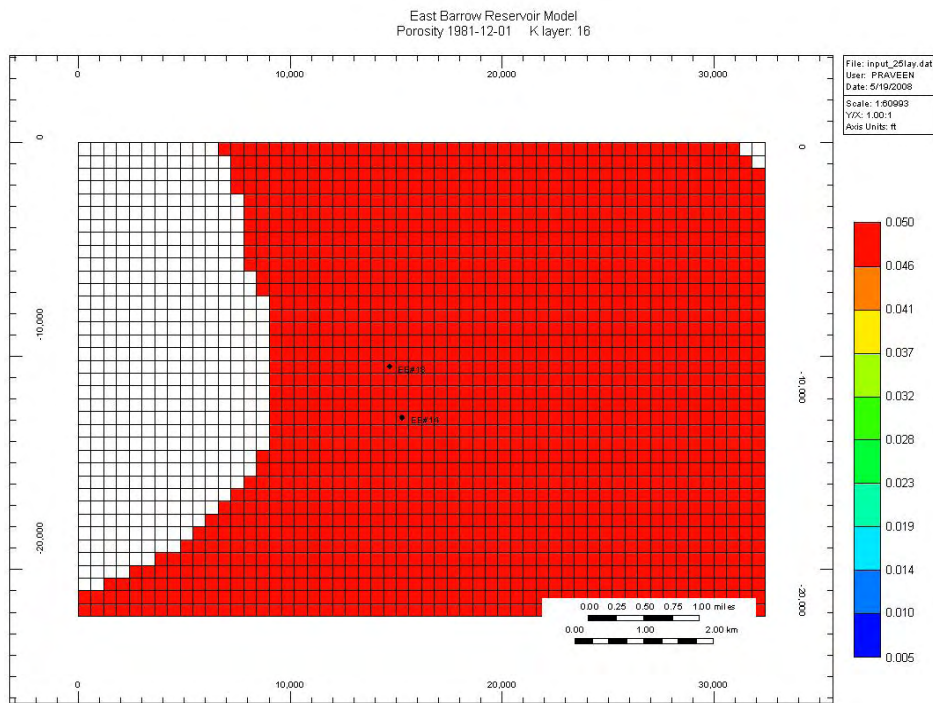


Figure 7: East Barrow Layer 16th, shaley layer (Porosity) – IJ plane view

2. Permeability

Reservoir permeability is calculated on the basis of well log data. Details about reservoir characterization and geostatistical modeling approach are discussed in a separate report¹⁹. *INCLUDE keyword is used to load these permeability data directly into the reservoir model. The reservoir permeability (I-J-K directions) is predominately low, mostly in the range of 1-50 mD. Layer 16 (K=16) has been identified as a permeability barrier (shaley layer), hence the entire layer has been assigned a constant permeability of 5 mD. Figures 8, 9, and 10 show 3D views of permeability distribution within the reservoir in I, J and K directions and Figure 10 shows IJ Plane view of permeability in I direction (valid for J and K direction as well) for layer 16 (shaley layer).

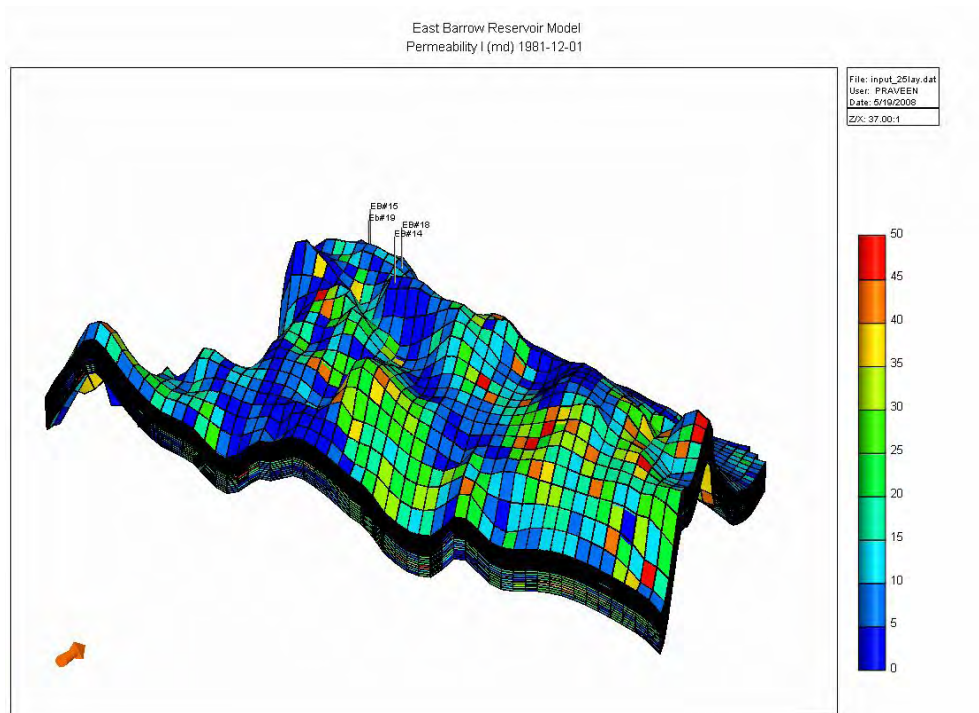


Figure 8: East Barrow Permeability - I (3D view)

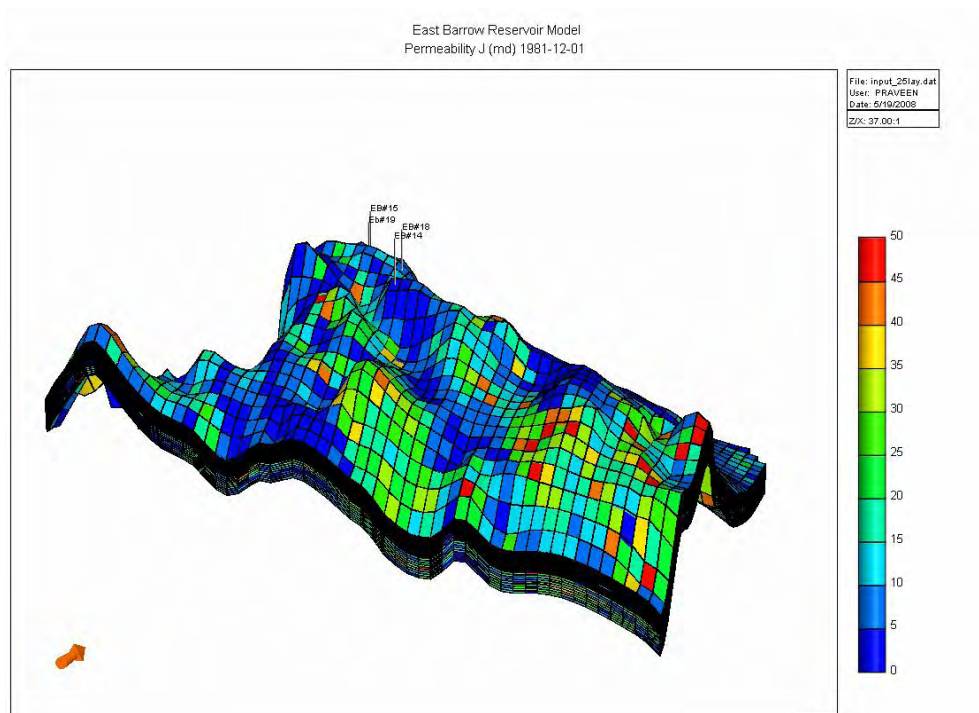


Figure 9: East Barrow Permeability - J (3D view)

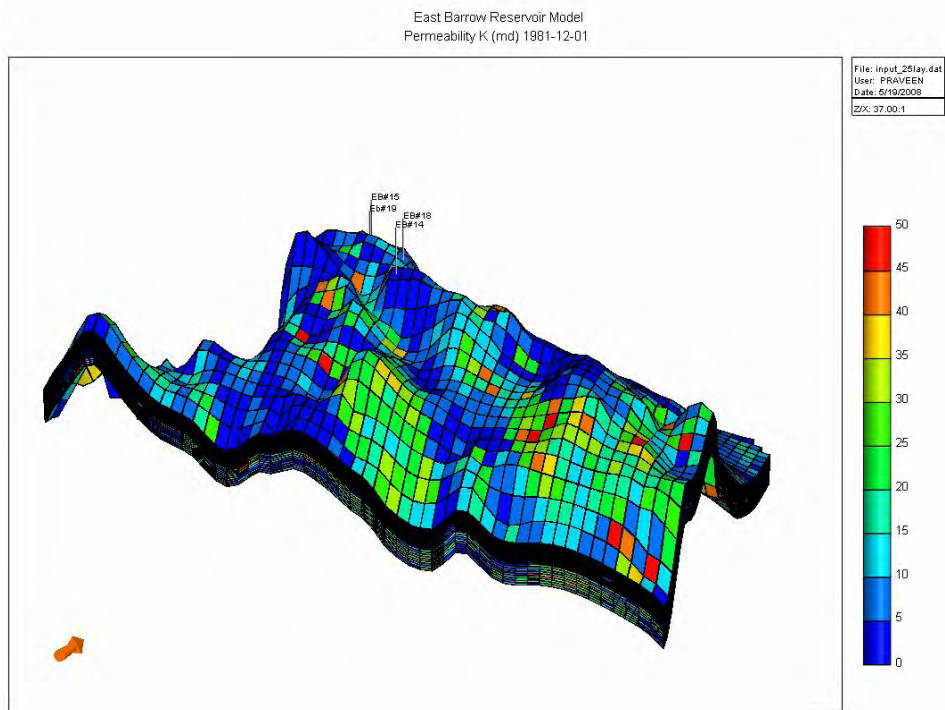


Figure 10: East Barrow Permeability - K (3D view)

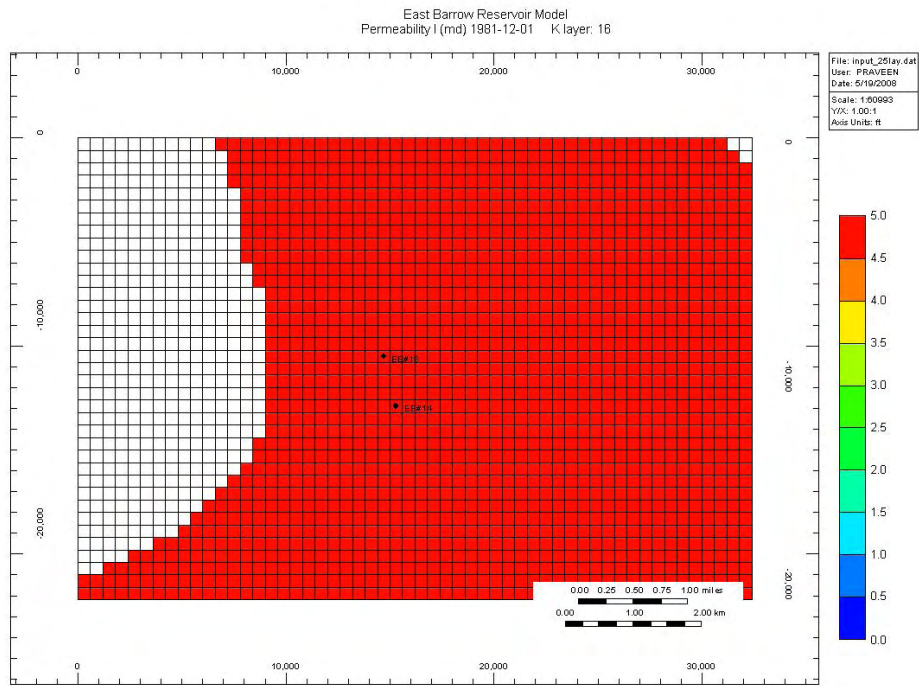


Figure 11: East Barrow Layer 16th, shaley layer (Permeability I,J and K) - IJ plane view

3. Initial Temperature

Geothermal gradient data obtained for East Barrow reservoir is 1.6⁰F/100ft. The reservoir top temperature is 41⁰F and bottommost region has a temperature of 47.7⁰F. The temperature distribution within the reservoir is initialized on the basis of reservoir depth. A formula is written in formula editor and then it is loaded for the entire grid. The formula calculates the reservoir temperature at respective depths and initializes each grid block. The formula editor and temperature distribution are shown below as Figure 12 and Figure 13, respectively. Note that '1900' in formula editor is the depth to the top of the reservoir and 41 is the corresponding temperature whereas X0 (variable) is the depth of the reservoir for a particular grid block.

Formula: Grid block Temperature = X0 (Grid Top) * 0.016 + 41

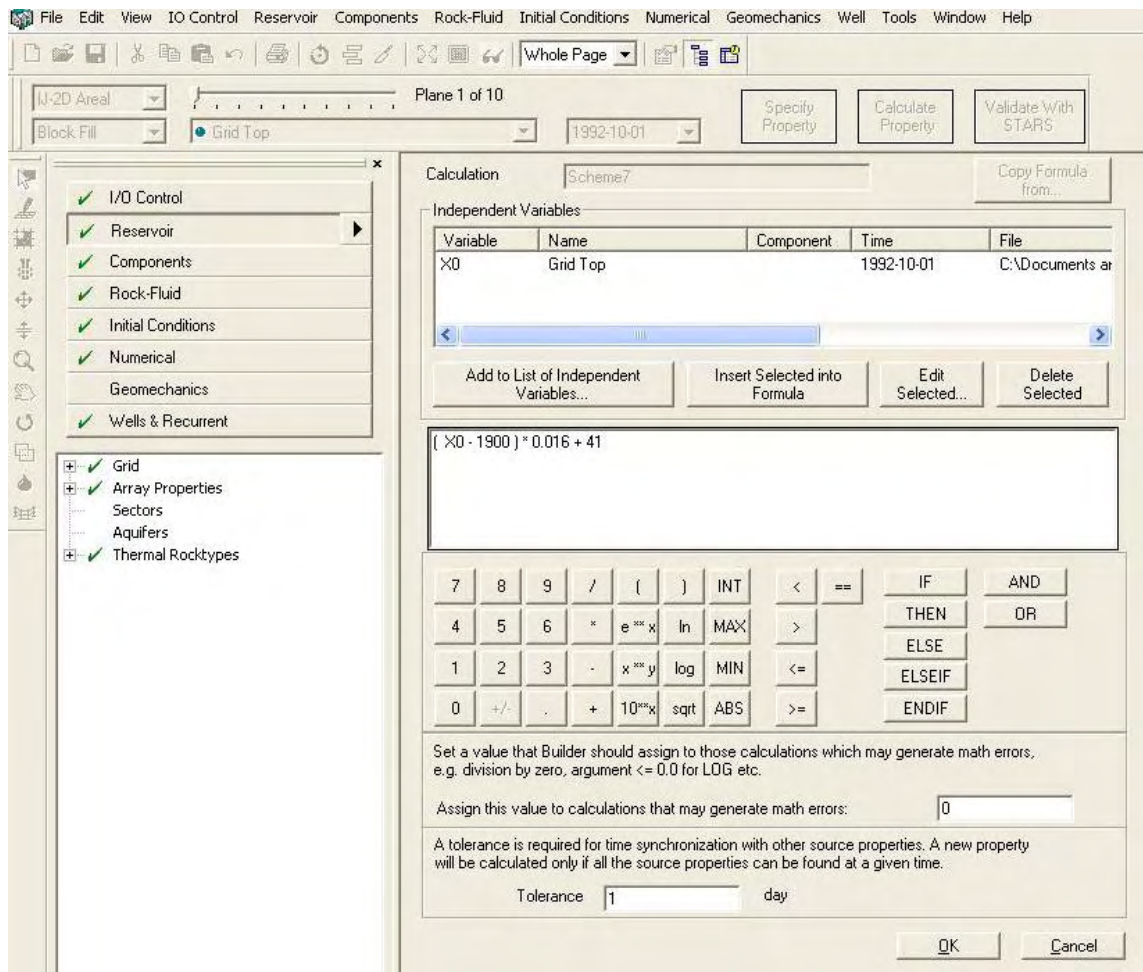


Figure 12: Formula editor (CMG-STARS) – Initializing temperature distribution

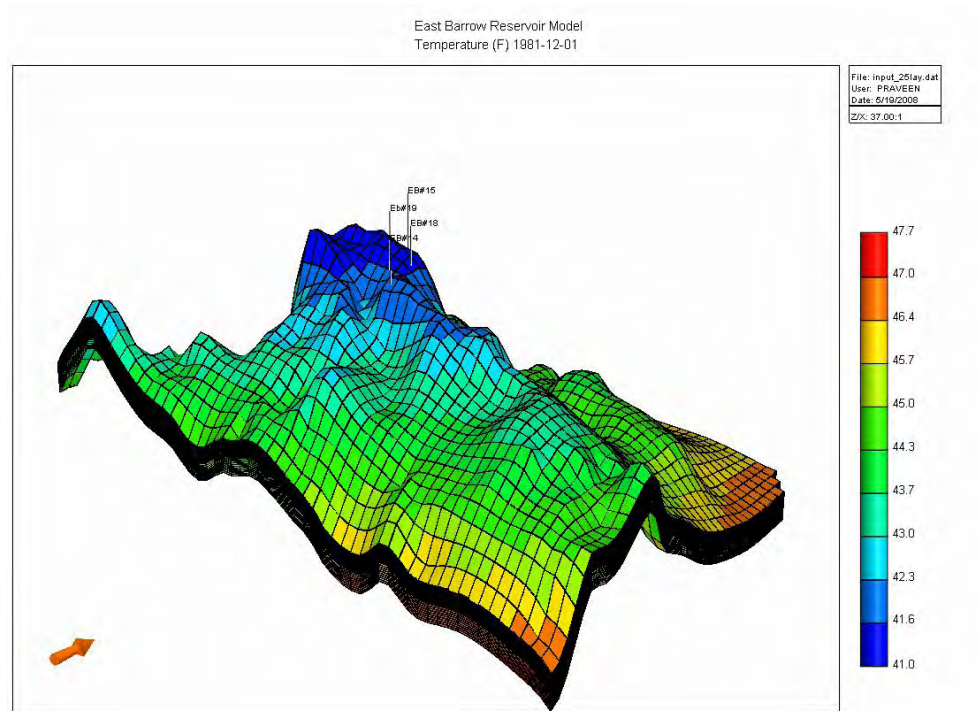


Figure 13: East Barrow Temperature, Deg F (3D view)

4. Initial Reservoir Pressure

Well testing and pressure gradient data reported in previous studies¹³ conducted for East Barrow gas pool, indicates that the initial reservoir pressure is 975 psi. Since the model is comprised of a hydrate cap and free gas zone underlain with model aquifer, the effect of gravity on reservoir pressure in the free gas zone has been neglected. The entire reservoir has been initialized with an average reservoir pressure of 975 psi. The effect of gravity can be neglected in CMG-STARS by switching “vertical equilibrium calculations” to OFF mode. Figure 14 shows the initial pressure of the reservoir and Figure 15 shows the initial condition as specified in CMG-STARS.

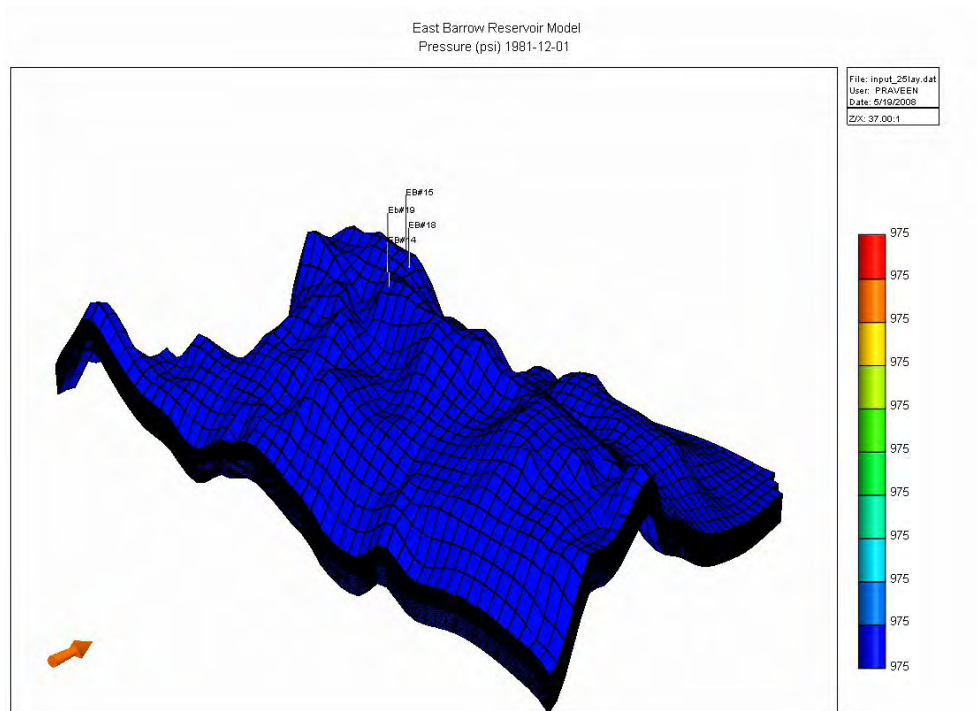


Figure 14: East Barrow Temperature, Deg F (3D view)

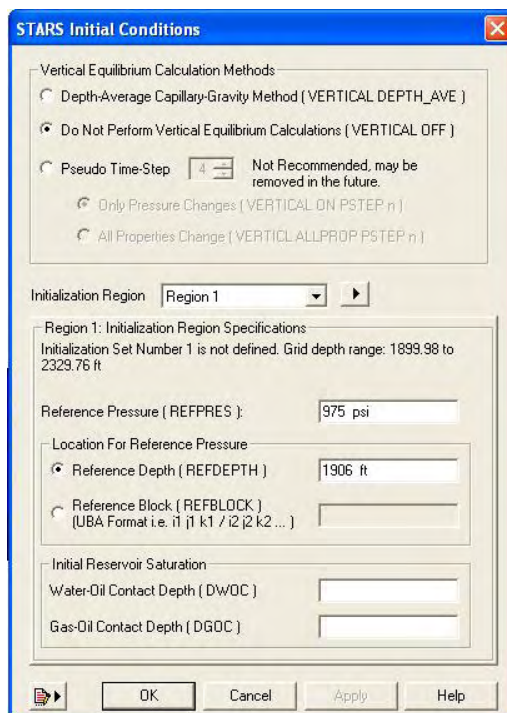


Figure 15: Initial Condition CMG-STARs (No Vertical Equilibrium Calculation)

5. Hydrate Saturation

The history matching study (discussed later) shows that the East Barrow reservoir is overlain with a thick hydrate cap. Well log studies have also supported this argument (refer technical reports on geological description and geostatistical modeling¹⁹). The hydrate-free gas contact for East Barrow gas reservoir is estimated to be 2050', based on hydrate stability modeling.

The pressure-temperature condition (refer to Figure 16) for East Barrow gas field lies very close to the three phase pressure-temperature equilibrium curve (Lw-H-V, basis 100% methane) of Moridis (2003)¹⁸. This suggests that the three phases i.e. hydrates, free gas and bounded water exist in thermodynamic equilibrium within the hydrate zone. The hydrate saturation in the hydrate zone was initialized as 31%. This was based on sensitivity and history matching studies (discussed later). A hydrate saturation of 0% is initialized in the free gas and aquifer zones.

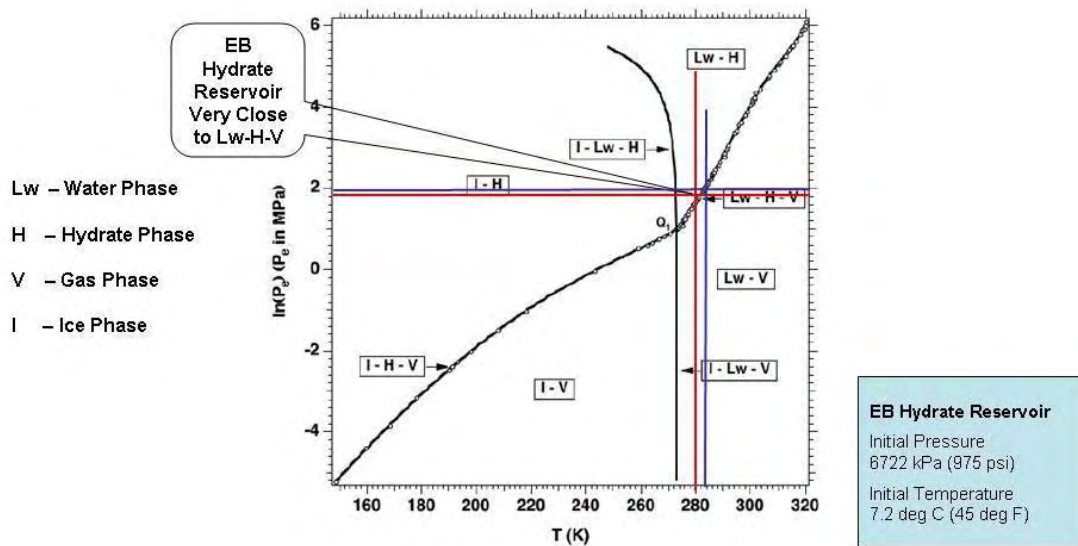


Figure 16 – Pressure-temperature equilibrium relationship in the phase diagram of the water-CH₄-hydrate system (Moridis, 2003), Lw: Liquid water; H: Hydrate; V: Vapor (gas phase); I: Ice; Q₁: Quadruple point = I + Lw + H + V

To initialize hydrate saturation, a formula is written using the formula editor. The formula is developed using grid bottom depth, hydrate (defined as oil in CMG-STARS) saturation parameter and hydrate-free gas contact data. The formula defines hydrate saturation of 31% to all grid blocks whose depth is shallower than or equal to 2050', but deeper than 1900'. For all other grid blocks the formula assigns a hydrate saturation of 0%. Figure 17 shows a formula editor (CMG-STARS) initializing hydrate saturation. Figure 18 shows a 3D view of hydrate distribution. Figure 19 is a 2D (IJ Plane) view of the top layer showing hydrate distribution. Figure 20 is a magnified 2D (IK plane) image showing hydrate saturation in the hydrate zone up to the Hydrate-Free Gas Contact (at 2050').

Formula:

IF ((X0 > 1900) AND (X0 <= 2050)) THEN ((X1 * 0.31)) ELSE ((X1 * 0))

Where,

X0 = Grid Bottom Depth (ft)

X1 = Oil (Hydrate) Saturation

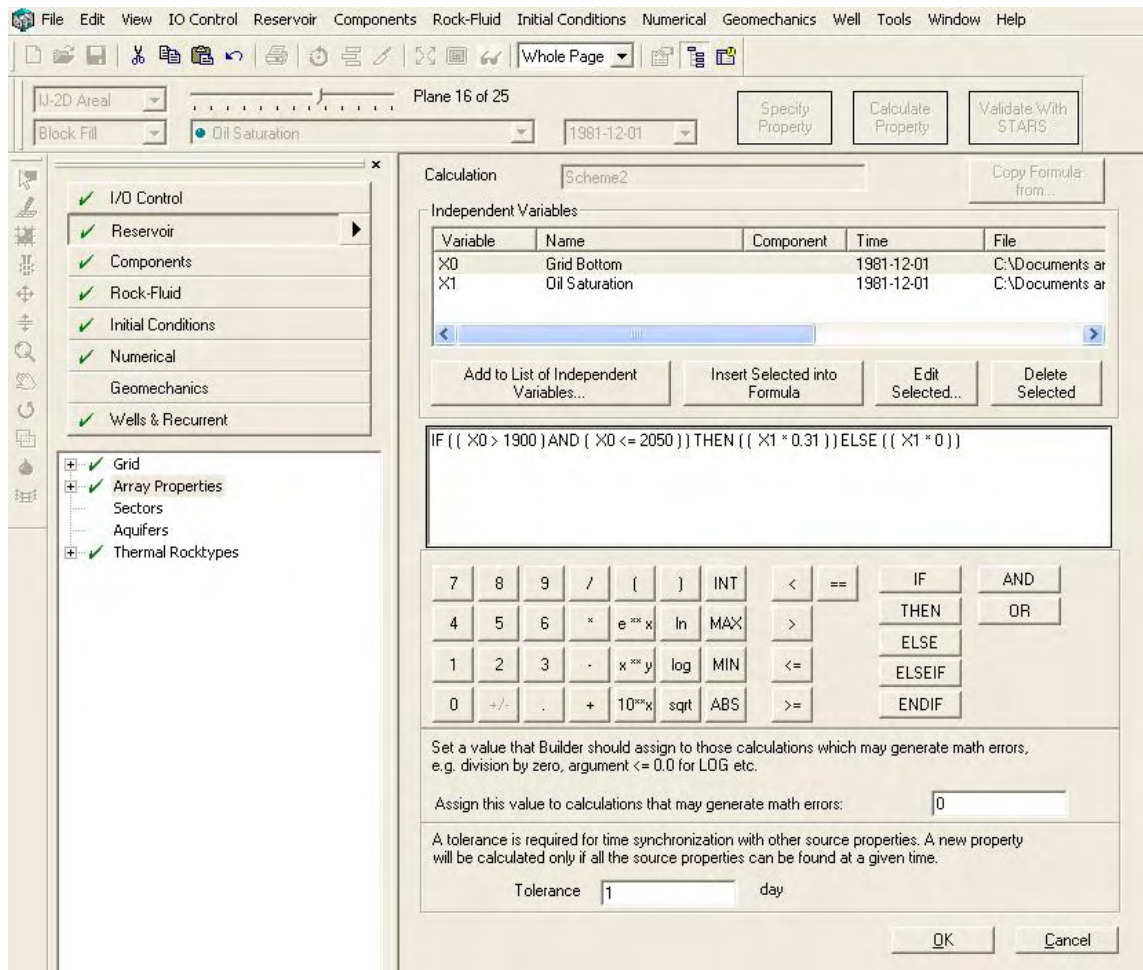


Figure 17: Formula editor (CMG-STARs) – Initializing hydrate saturation

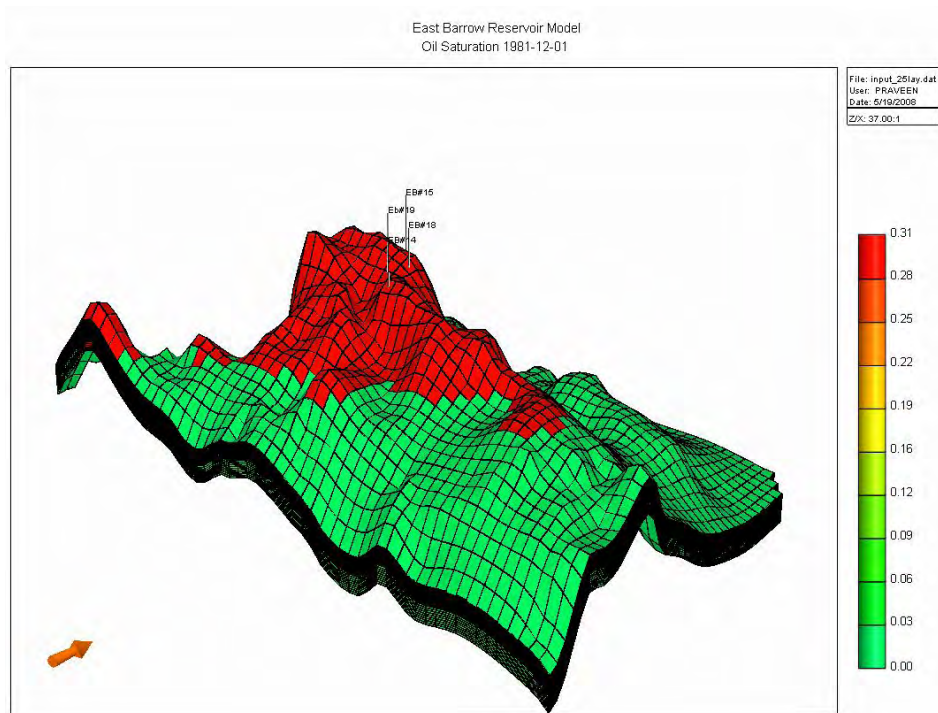


Figure 18: East Barrow Hydrate Saturation, S_h (3D view)

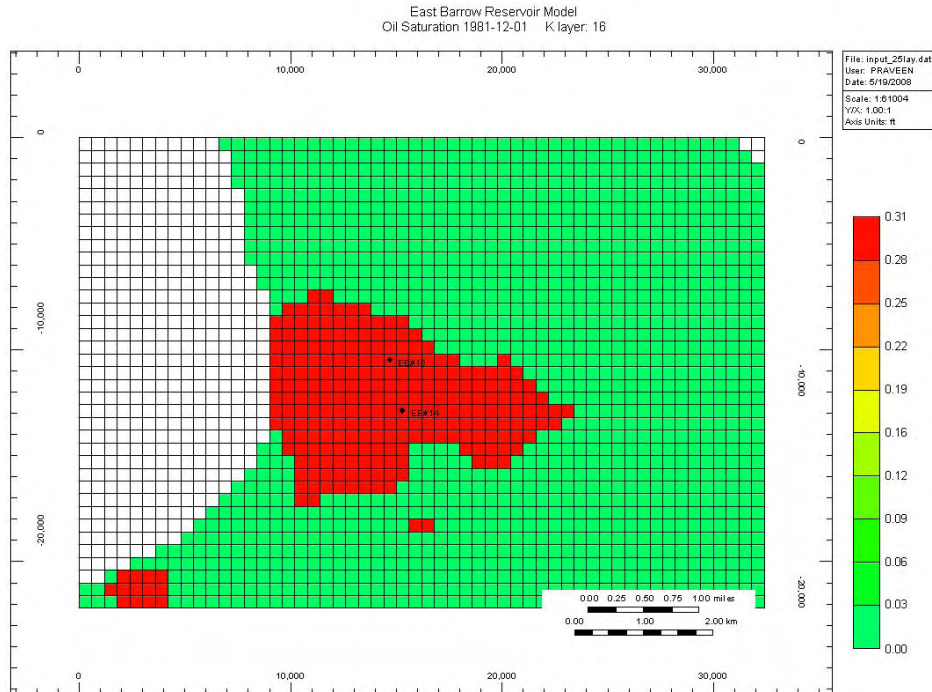


Figure 19: East Barrow Hydrate Saturation (IJ Plane view, K Layer-1)

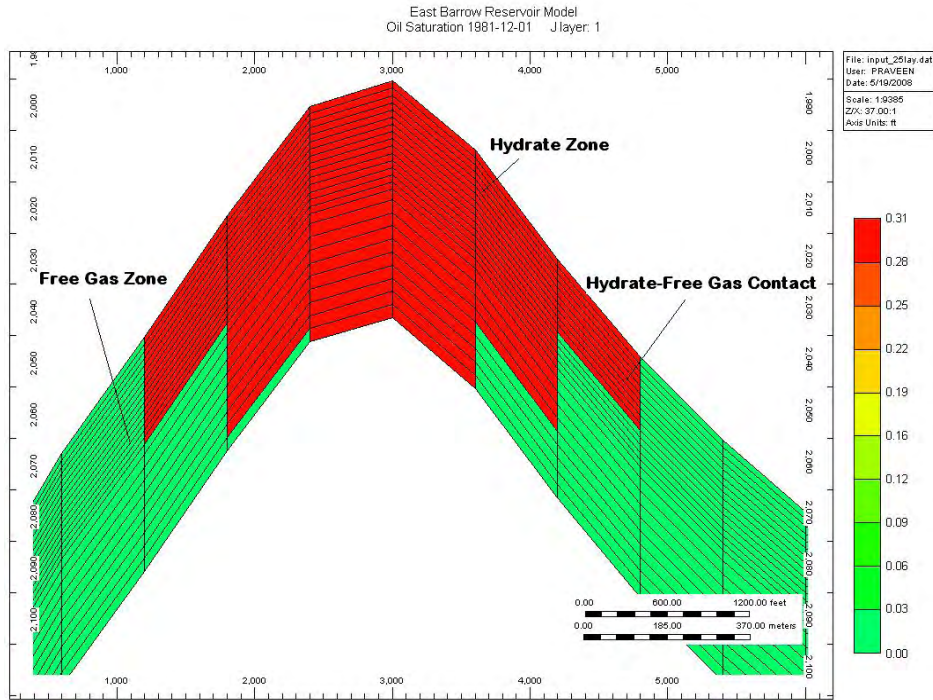


Figure 20: East Barrow Hydrate-Free Gas Zone Contact at 2050' (IK Plane view)

5. Gas Saturation

Below the hydrate cap lays the free gas zone. However, since the thermodynamic condition of hydrates are such that the hydrate phase exists in equilibrium with free gas and bounded water, the gas phase saturation needs to be defined both for the hydrate and free gas zones. Well logs have shown that the irreducible (bounded) water saturation for the hydrate and free gas zone is 55% and the gas water contact was at 2080'. Hence, the free gas saturation initialized in the hydrate zone is 14% and within the free gas zone is 45%.

To initialize free gas saturation, a formula is written using the formula editor. The formula is developed using grid bottom, gas saturation, hydrate-free gas contact and gas-water contact data. The formula defines a gas saturation of 14% to all grid blocks whose depth is shallower or equal to 2050' but deeper than 1900'. For a depth range of 2050' and 2080' the gas saturation is initialized as 45%. For all other grid blocks (those lying outside the range) the formula assigns a gas saturation of 0%. Figure 21 shows a formula editor (CMG-STARS) initializing gas saturation. Figure 22 shows a 3D view of gas distribution. Figure 23 is a 2D (IJ Plane) view showing gas distribution. Figure 24 is a 2D (IK plane) image showing hydrate-free gas and free gas-water contacts at 2050' and 2080', respectively.

Formula:

IF ((X0 > 1900) AND (X0 <= 2050)) THEN ((X1 * 0.14)) ELSEIF ((X0 > 2050) AND (X0 <= 2080)) THEN ((X1 * 0.45)) ELSE ((X1 * 0))

Where,

X0 = Grid Bottom Depth (ft)

X1 = Gas Saturation

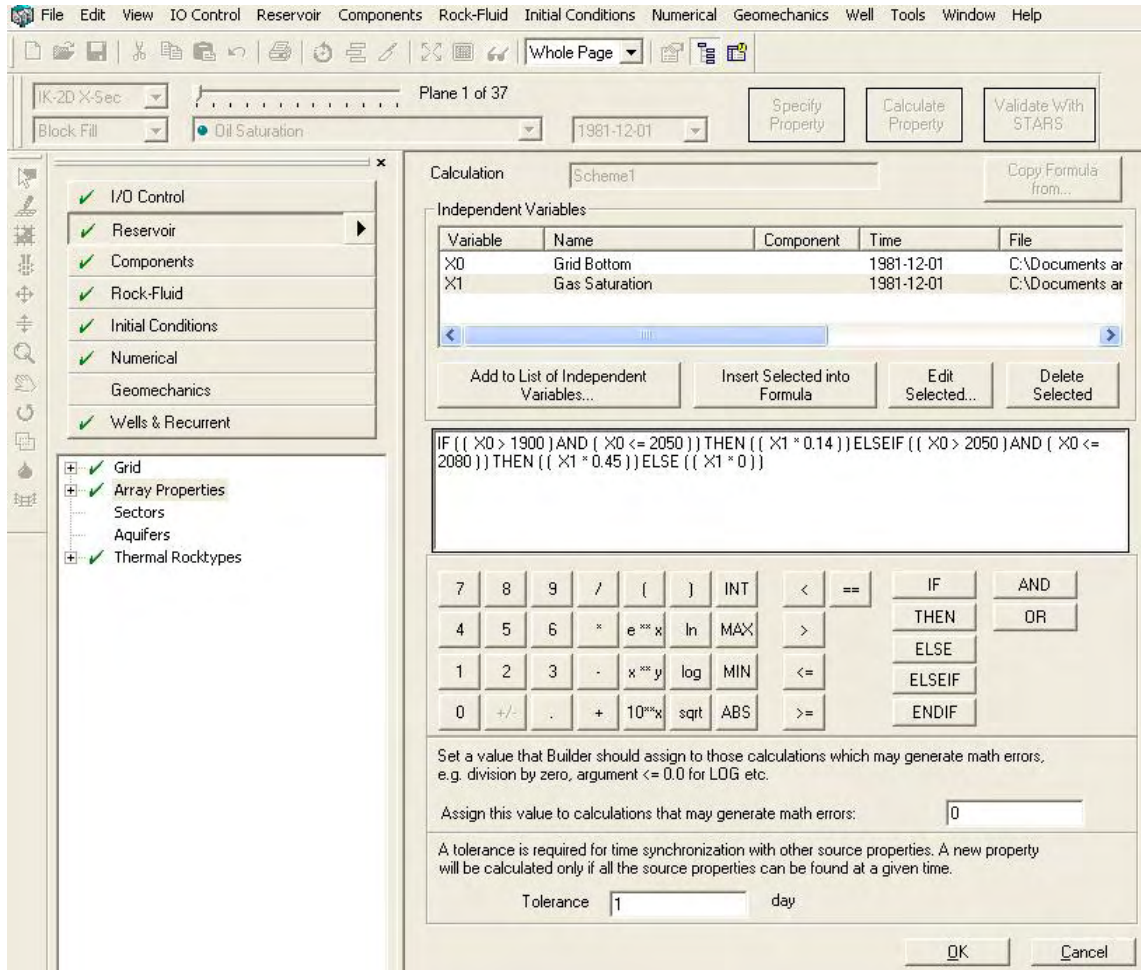


Figure 21: Formula editor (CMG-STARS) – Initializing gas saturation

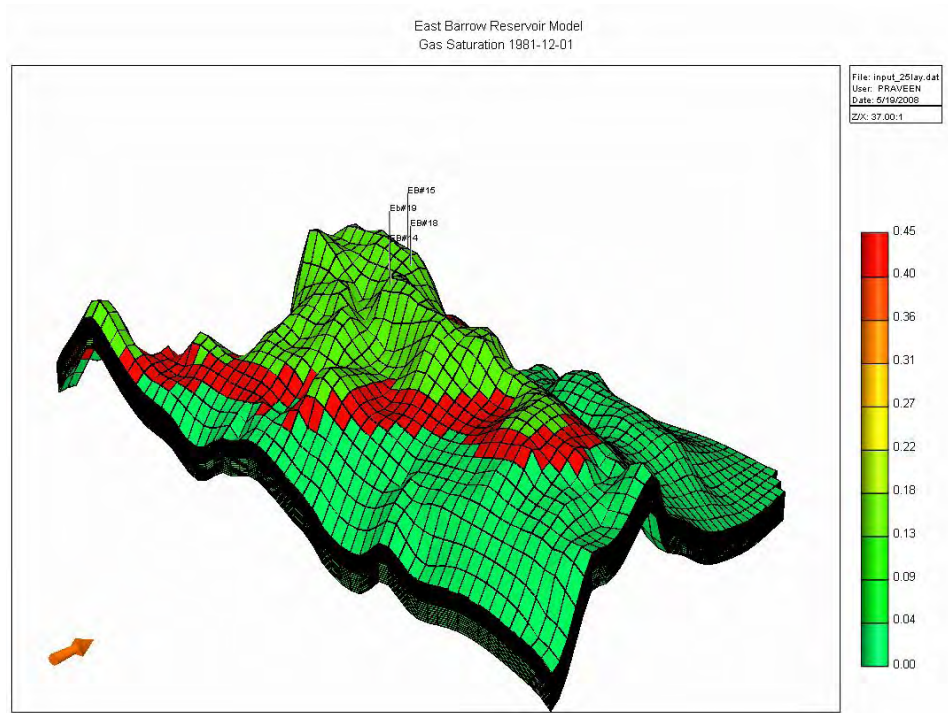


Figure 22: East Barrow Gas Saturation, S_g (3D view)

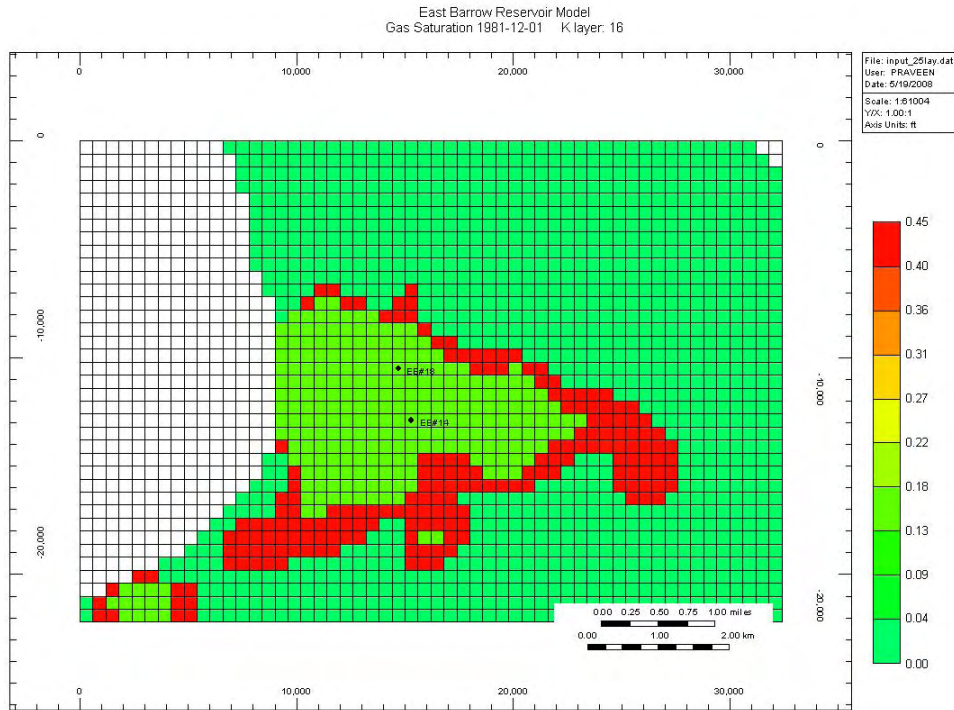


Figure 23: East Barrow Gas Saturation (IJ Plane view, K Layer-1)

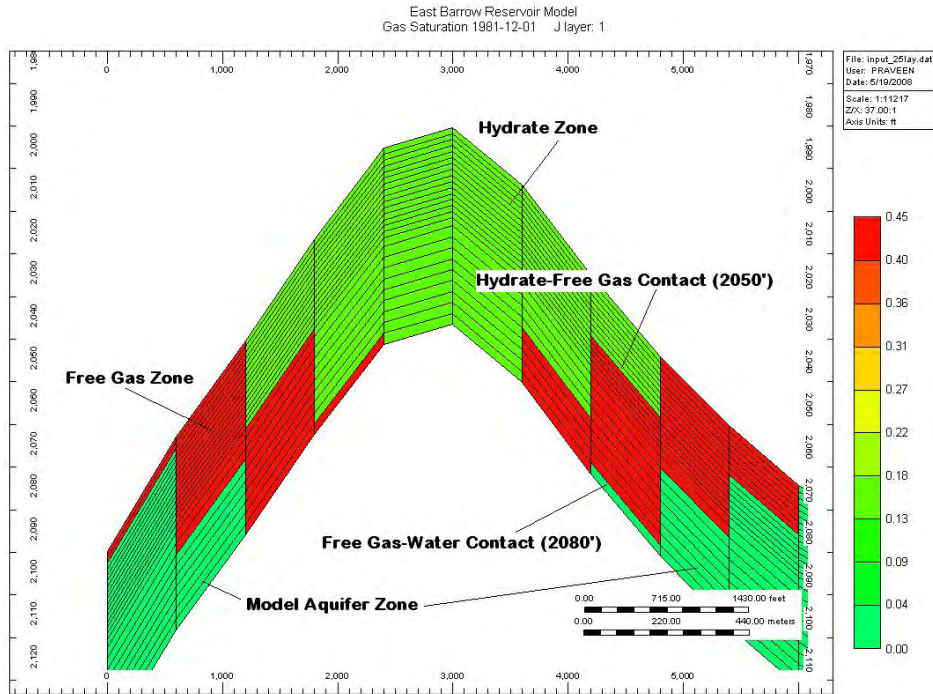


Figure 24: East Barrow Hydrate-Gas Contact at 2050' and GWC at 2080' (IK Plane view)

6. Water Saturation

As stated earlier, well log data suggest that the irreducible/connate water saturation in the hydrate and free gas zones is very high i.e. 55%. This is supported by core analysis as well, although both well log and core analysis are considered to represent high-side estimates of water saturation, due to potential invasion effects. Well log data and recently concluded material balance study results have shown the existence of an aquifer below the free gas zone. CMG-STARS offers several aquifer models (also called numerical aquifers) that can be easily attached to the hydrate free gas system, but in order to improve reservoir accuracy, the aquifer has been constructed as part of the reservoir model (also called a model aquifer). To initialize water saturation in the aquifer zone, we keep water saturation as 100% in the aquifer zone.

A new formula is written using formula editor in order to initialize model water saturation. The formula is developed using grid bottom, water saturation parameters and gas-water contact data. The formula defines a water saturation of 55% to all grid blocks whose grid depth is shallower or equal to 2080' but deeper than 1900'. For all other grid blocks (those lying outside the range) the formula assigns a water saturation of 100%. Figure 25 shows a formula editor (CMG-STARS) initializing water saturation. Figure 26 shows a 3D view of water distribution. Figure 27 is a 2D (IJ Plane) view showing water distribution. Figure 28 is a 2D (IK plane) image showing free gas-water contact 2080'.

Formula

IF ((X0 > 1900) AND (X0 <= 2080)) THEN ((X1 * 0.55)) ELSE ((X1 * 1))

Where,

X0 = Grid Bottom Depth (ft)

X1 = Water Saturation

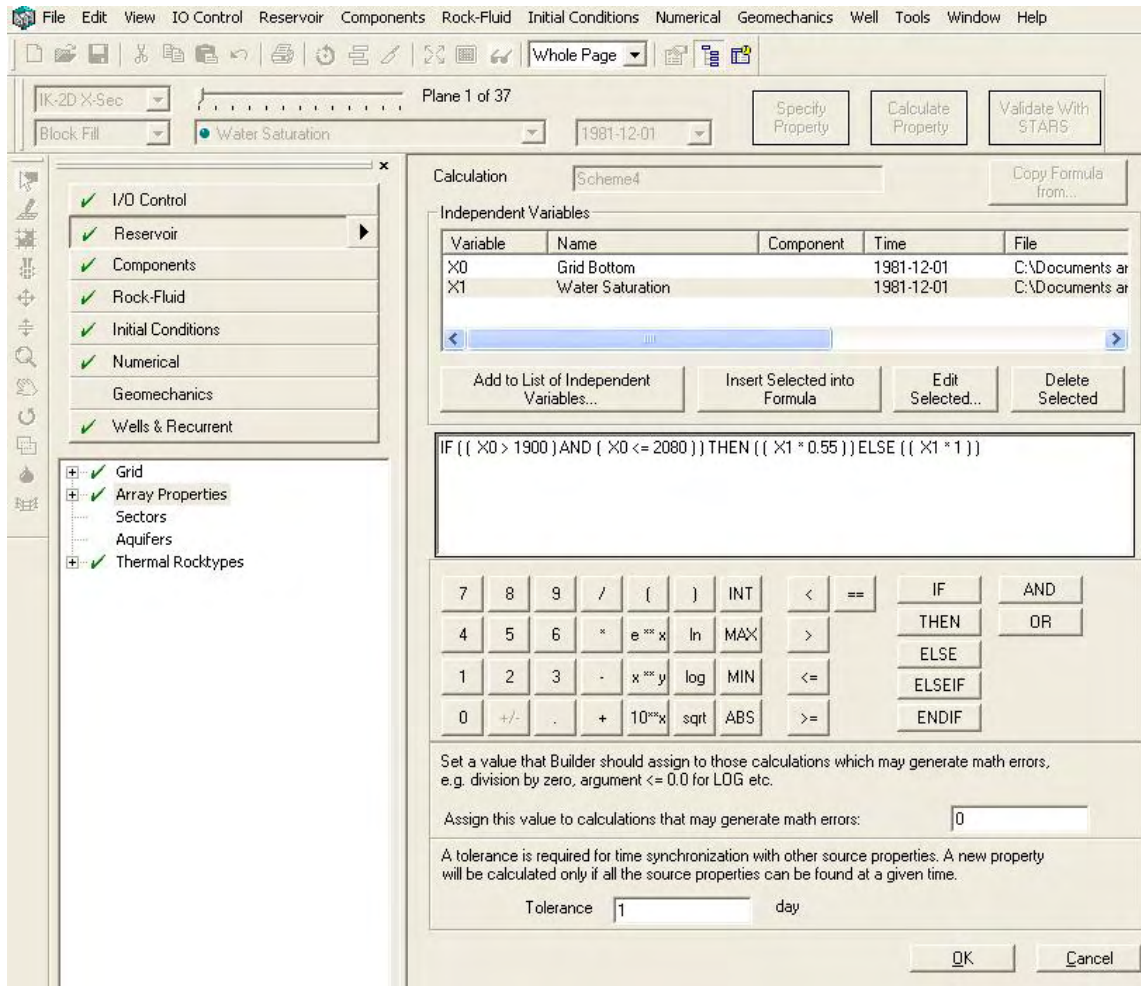


Figure 25: Formula editor (CMG-STARs) – Initializing water saturation

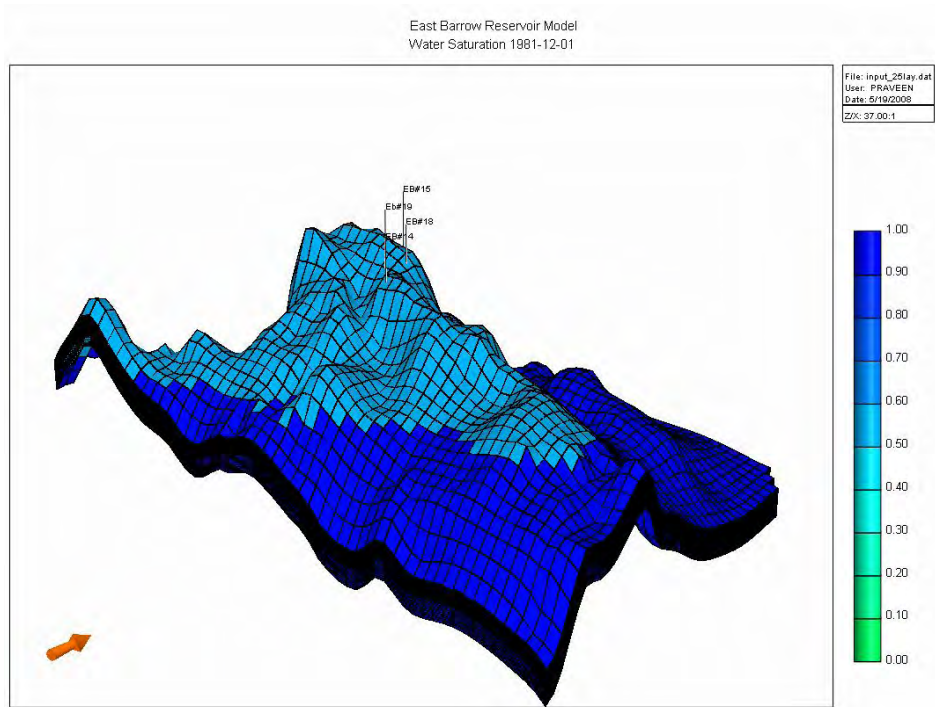


Figure 26: East Barrow Water Saturation, S_w (3D view)

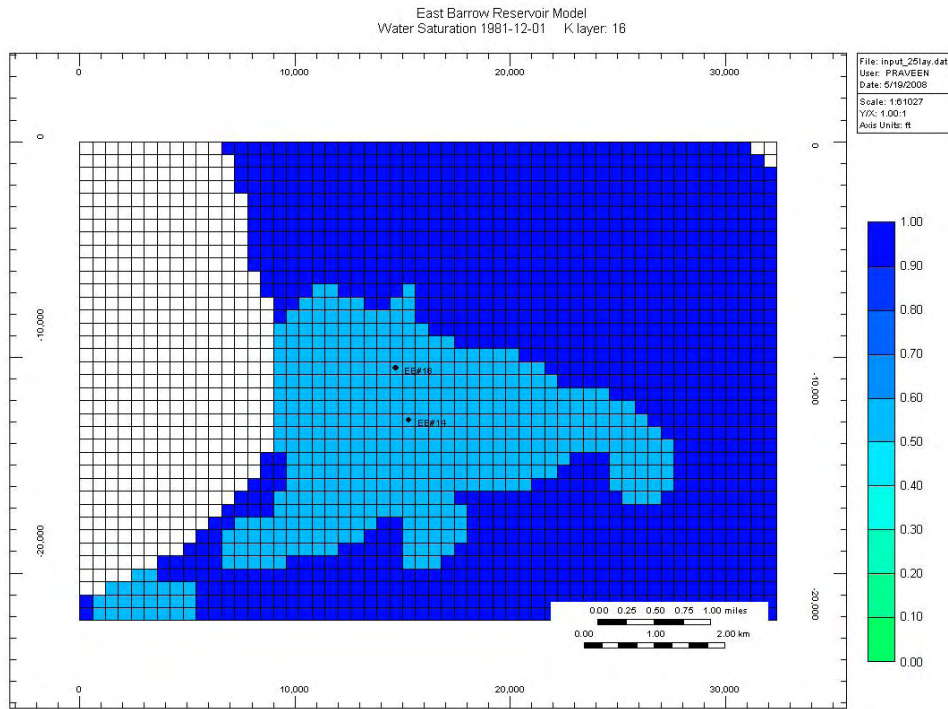


Figure 27: East Barrow Water Saturation (IJ Plane view, K Layer-1)

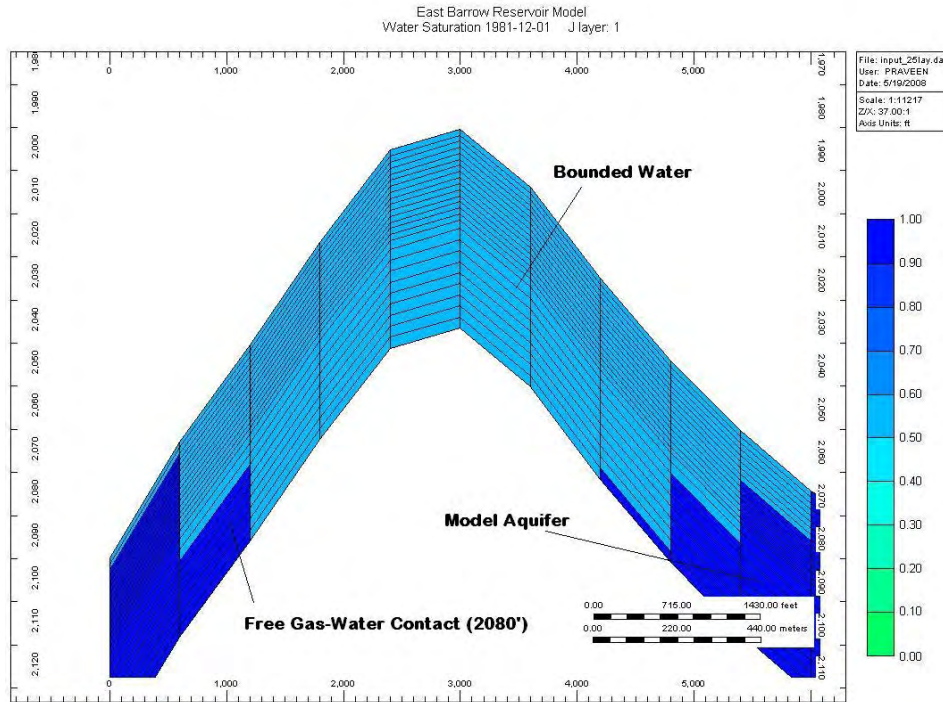


Figure 28: East Barrow Gas-Water Contact at 2080' (IK Plane view)

The initial condition of East Barrow Reservoir has been summarized in Table E-1 presented below.

Zone	Pressure	Temperature	Saturation	Remarks
Hydrate	975 psi	Temperature Gradient 1.6 ⁰ F/100ft Top Temp 41 ⁰ F	S _h = 31% S _g = 14% S _w = 55%	(Lw-H-V) close to Equilibrium
Free Gas*			S _g = 45% S _w = 55%	*Hydrate-Free Gas Contact- 2050'
Aquifer**			S _w = 100%	**Free Gas-Water Contact-2080'

Table E-1: Initial Condition of East Barrow reservoir

C. Thermal Properties

Table E-2 summarizes the thermal properties (rock & fluids) initialized for East Barrow Gas reservoir. These properties have been modified from Stephen Howe's (2004)¹⁴ work on Alaska North Slope gas hydrate reservoir.

Description	CMG-STARS Keyword	Value (Field Units)	
Reservoir Rock Type	*ROCKTYPE	1	
Volumetric Heat Capacity (Rock)	*ROCKCP	34 BTU/(ft ³ - ⁰ F)	
Thermal Heat Conductivity (rock)	*THCONR	24.01043 BTU/(ft-day- ⁰ F)	
Thermal Heat Conductivity (oil/hydrate)	*THCONO	265.30236 BTU/(ft-day- ⁰ F)	
Thermal Heat Conductivity (water)	*THCONW	8.586616 BTU/(ft-day- ⁰ F)	
Thermal Heat Conductivity (gas)	*THCONG	1.1876815 BTU/(ft-day- ⁰ F)	
Thermal Conductivity Phase Mixing	*THCONMIX	SIMPLE	
Overburden / Underburden Temperature	*HLOSST	48 ⁰ F	
Directional Heat Loss Property	*HLOSSPROP	Volumetric Heat Capacity	Thermal Conductivity
		BTU/(ft ³ - ⁰ F)	BTU/(ft-day- ⁰ F)
		+I 34.99531654	+I 24.010425
		-I 34.99531654	-I 24.010425
		+J 34.99531654	+J 24.010425
		-J 34.99531654	-J 24.010425
		+K 34.99531654	+K 24.010425
-K 34.99531654	-K 24.010425		

Table E-2: Thermal Properties initialized for East Barrow reservoir

D. Fluid/Component Properties

Table E-3 summarizes the fluid/component properties initialized for East Barrow Gas reservoir, these properties have been modified from Stephen Howe's (2004)¹⁴ work on Alaska North Slope gas hydrate reservoir.

Description	CMG-STARS Keyword	Water/Hydrate/Methane
		Value (Field Units)
Component Name/Definition	*COMPNAME	'WATER' / 'HYDRATE' / 'CH4'
Molecular Weight	*CMM	18 / 119.54408 / 16.043 (lb/lbmole)
Critical Pressure	*PRCIT	0 / 1450.377 / 667.174 (psi)
Critical Temperature	*TCRIT	32 / 1832 / -116.59 (°F)
Molar Density (Liquid)	*MOLDEN	3.46818 / 0.480455 / NA (lbmole/ft ³)
Liquid Phase Viscosity (Using temperature dependent correlation)	*AVISC	0 / 1000 / NA (cp)
	*BVISC	32 / 32 / NA (°F)
Gas Phase Viscosity (Using correlation)	*AVG	NA / NA / 0.00211 (cp/°F)
	*BVG	NA / NA / 0 (dimensionless)
Liquid Compressibility	*CP	0 / 0 / NA (1/psi)
Coefficient of thermal expansion		
First Coefficient	*CT1	0 / 0 / NA (1/°F)
Second Coefficient	*CT2	0 / 0 / NA (1/°F-°F)

Table E-3: Fluid and component properties initialized for East Barrow reservoir

Table E-3 Fluid and component properties initialized for East Barrow reservoir, continued

Description	CMG-STARS Keyword	Water/Hydrate/Methane Value (Field Units)
Heat Capacity in the liquid phase	*CPL1 *CPL2 *CPL3 *CPL4	0 / 45.6678 / 0 (BTU/lbmole- ⁰ F) 0 / 0 / 0 (BTU/lbmole- ⁰ F ⁰ F) 0 / 0 / 0 (BTU/lbmole- ⁰ F ⁰ F ⁰ F) 0 / 0 / 0 (BTU/lbmole- ⁰ F ⁰ F ⁰ F ⁰ F)
Heat Capacity in the gas phase (Using Correlation)	*CPG1 *CPG2 *CPG3 *CPG4	0 / 0 / 4.59807 (BTU/lbmole- ⁰ F) 0 / 0 / 0.00691333 (BTU/lbmole- ⁰ F ⁰ F) 0 / 0 / 1.588e-6 (BTU/lbmole- ⁰ F ⁰ F ⁰ F) 0 / 0 / -1.50209e-9 (BTU/lbmole- ⁰ F ⁰ F ⁰ F ⁰ F)
NOTE: (0 – CMG default values shall be taken		
Reactant Stoichiometry	*STOREAC	0 / 1 / 0
Product Stoichiometry	*STOPROD	5.7501 / 0 / 1
Component Reaction Order	*RORDER	0 / 1 / 0
Reaction Frequency Factor	*FREQFAC	1.35878e30
Activation Energy	*EACT	-22295.1255 BTU/lbmole
K values (For reactant only) (using correlation)	*rxk1 *rxk2 *rxk3 *rxk4 *rxk5	NA / 6.3507334e15 / NA (psi) NA / 0 / NA (1/psi) NA / 0 / NA (dimensionless) NA / -14967.7002 / NA (⁰ K) NA / -459.67 / NA (⁰ F)

E. Relative Permeabilities and Capillary Pressure Functions

Stone’s second model is used to represent three phase relative permeability data. The three phase relative permeability data given in Stephen Howe’s¹⁴ work has a very low irreducible water saturation value of 20%. Since the connate water saturation in East Barrow is very high (55%), endpoint rescaling has been performed on the given data to match the reservoir conditions. Figures 29 and 30 show the hydrate-water two phase relative permeability curve and water capillary pressure relationship, respectively.

Figures 31 and 32 show the gas-hydrate two phase relative permeability curve and gas capillary pressure relationship, respectively.

Table E-4 summarizes the end point saturations and relative permeability data for hydrate-water (*SWT) relative permeability curve.

End Point Saturations	
Critical Water Saturation (S_{wcrit})	0.55
Irreducible Oil (hydrate) Saturation (S_{oirw})	0.00
Connate Water Saturation (S_{wcon})	0.55
Residual Oil (hydrate) Saturation (S_{orw})	0.40
End Point Relative Permeability	
Water Relative Permeability (single phase flow) k_{rw} end point (max. k_{rw})	0.70
Hydrate Relative Permeability (single phase flow) k_{row} end point (max. k_{row})	0.0001

Table E-4: End point and hydrate-water relative permeability data for East Barrow.

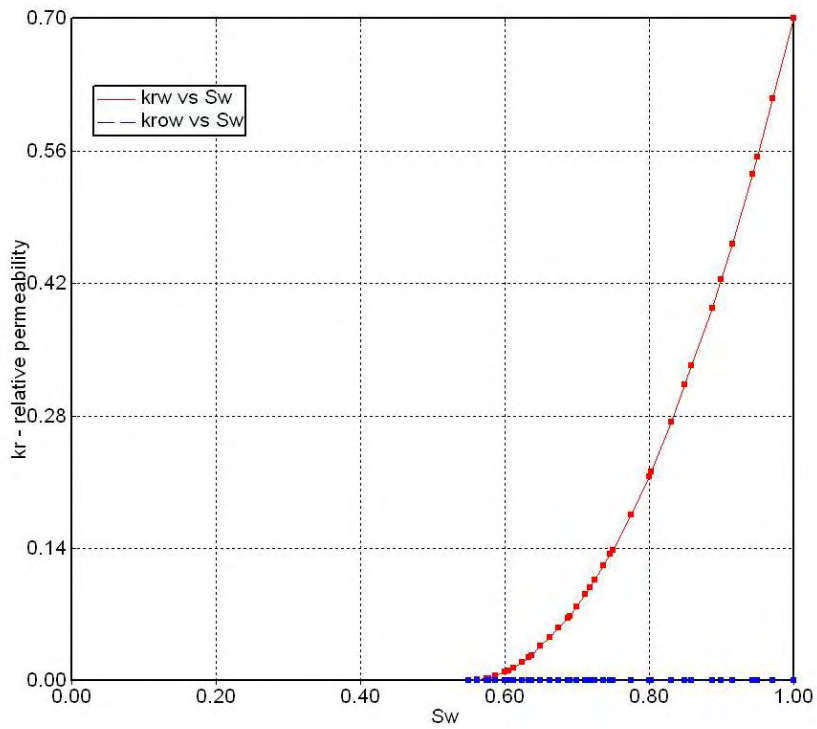


Figure 29: Hydrate-Water relative permeability curve (CMG keyword *SWT)

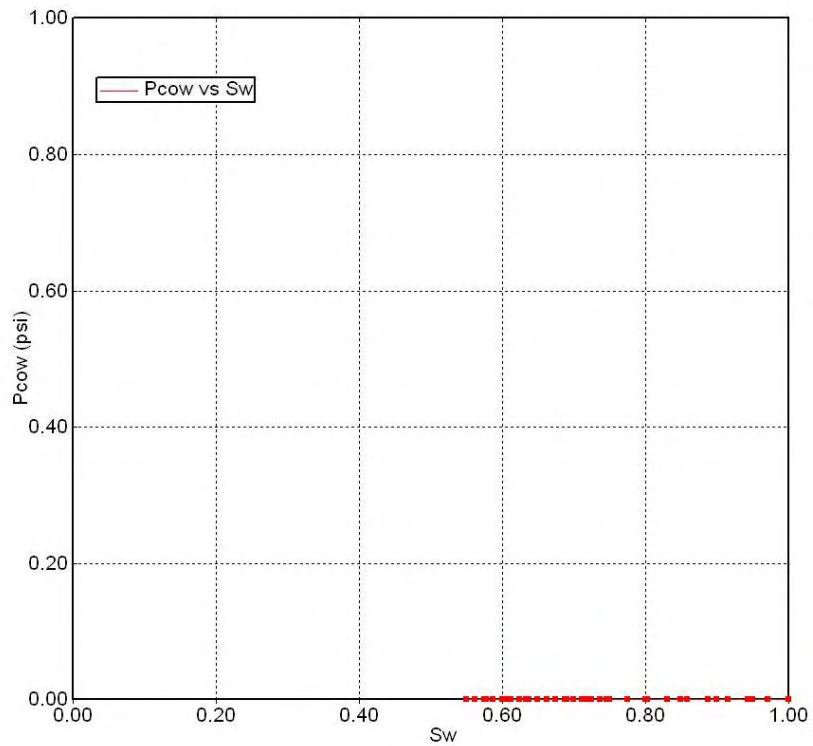


Figure 30: Water capillary pressure (CMG keyword *SWT)

Table E-5 summarizes the end point saturations and relative permeability data for gas-hydrate (*SLT) relative permeability curve.

End Point Saturations	
Critical Gas Saturation (S_{gcrit})	0.05
Connate Liquid Saturation (S_{lcon})	0.55
Connate Gas Saturation (S_{gcon})	0.05
Residual Oil (hydrate) Saturation (S_{orl})	0.70
End Point Relative Permeability	
Gas Relative Permeability (single phase flow) k_{rg} end point (max. k_{rg})	0.90
Hydrate Relative Permeability (single phase flow) k_{rog} end point (max. k_{rog})	9e-005

Table E-5: End point and gas-hydrate relative permeability data for East Barrow

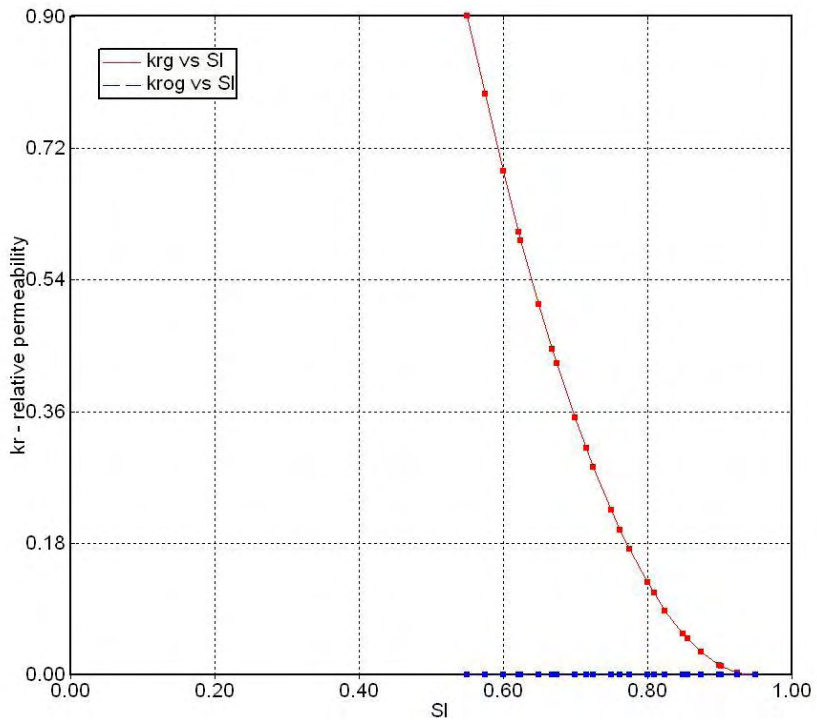


Figure 31: Gas-hydrate relative permeability curve (CMG keyword *SLT)

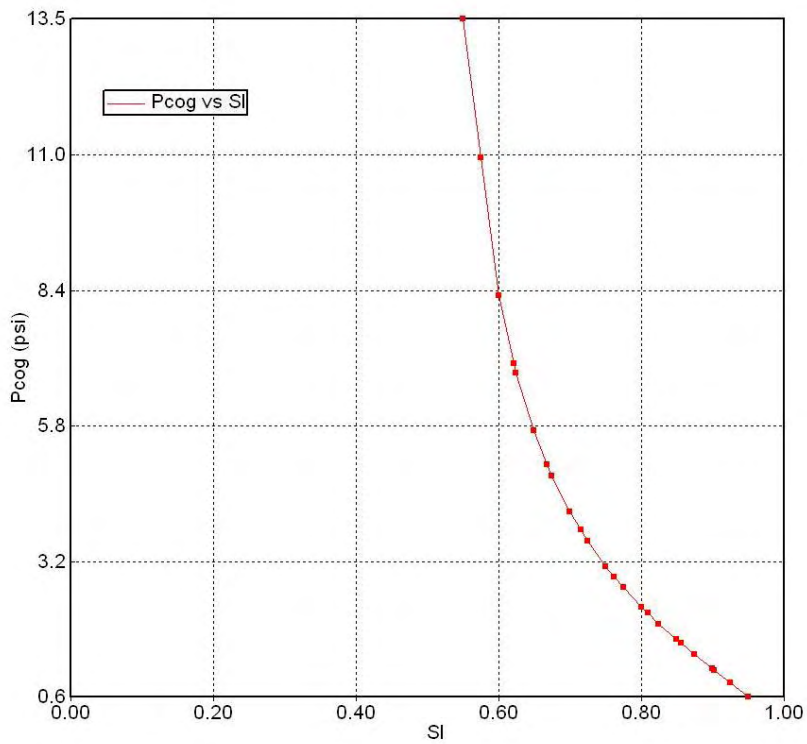


Figure 32: Gas capillary pressure (CMG keyword *SLT)

F. Production Well Modeling

The East Barrow gas pool was first opened to production in the month of December 1981. A total of five wells have produced over 8 BCF of methane gas to September 2007. Several wells that produced initially were later abandoned due to maintenance issues. Currently, two wells are the most active wells in the region and they contribute substantially to the overall gas produced.

1. Production History Data

Production history data for the East Barrow gas reservoir was acquired from a previous PRA engineering report¹⁵. The production history data is available from December 1981 to September 2007. The production history data includes monthly gas and water production rate for each well, and cumulative gas and water production rate for the entire reservoir. Flowing bottom hole pressure data is not available, but based on previous studies/reports^{13,15,16}, average pressure data for the reservoir has been collected. The pressure data is limited, but is sufficient to perform history match analysis.

The five wells of the East Barrow gas pool are EB#14, EB#15, EB#18, EB#19, EB#21. Gas production started in four wells in December 1981. These wells are EB#14, EB#15, EB#18 and EB#19. Production started from EB#21 in November 1990. By the end of September 2007, EB#14 was the only producing well.

2. Well location and positioning of perforations

The well files and other engineering reports¹⁵ indicate the location, type and dimensions of all five wells in the region. All wells were drilled vertically in up dip locations of the reservoir and completed within the reservoir section. Table-4 below lists the location of each well based on the model coordinate system. The location of each well is shown in Figure 33.

Wells are perforated using CMG-STARs interactive “PERF” module. Initially all wells were perforated based on individual well files. Several runs were performed in order to validate gas/water production rate and obtain optimum number and positioning of the perforations. All efforts have been made to avoid over-perforation of the well. The specifications and methodology followed to validate well production rates will be discussed later in this report.

Figures 34 to 38 are wellbore diagrams of each well, showing well orientation and positioning of the perforations. These images show the perforations for each well obtained after numerous trial and validation runs.

Well Name	Co-ordinate (Reservoir Top) I, J, K	Well Direction	Well Radius	Well Completion Date
EB#14	26 16 1	K-Direction (Vertical Well)	0.4583 ft	Dec 01, 1981
EB#15	19 27 1	K-Direction (Vertical Well)	0.5833 ft	Dec 01, 1981
EB#18	25 20 1	K-Direction (Vertical Well)	0.5833 ft	Dec 01, 1981
EB#19	21 22 1	K-Direction (Vertical Well)	0.5833 ft	Dec 01, 1981
EB#21	23 19 1	K-Direction (Vertical Well)	0.5833 ft	Nov 01, 1990

Table E-6: Location (co-ordinates) and dimension of East Barrow Wells

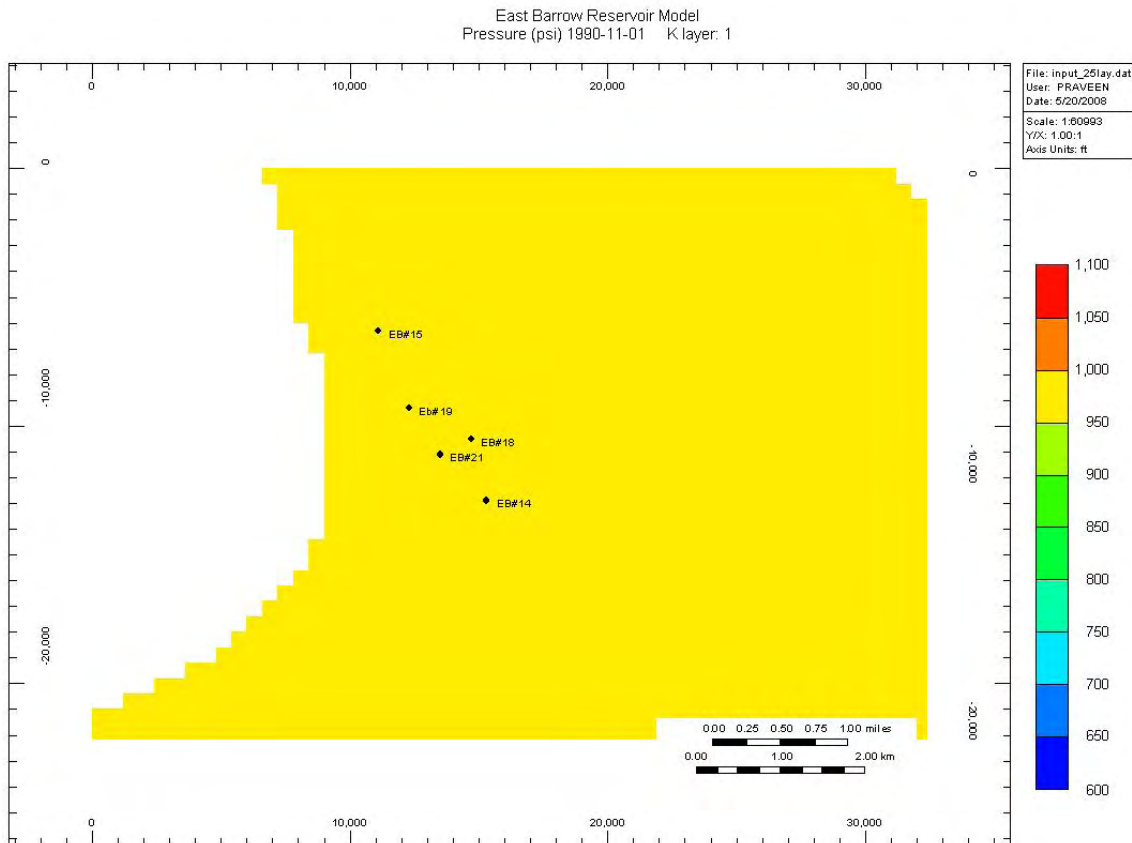


Figure 33: East Barrow Well locations (IJ Plane View)

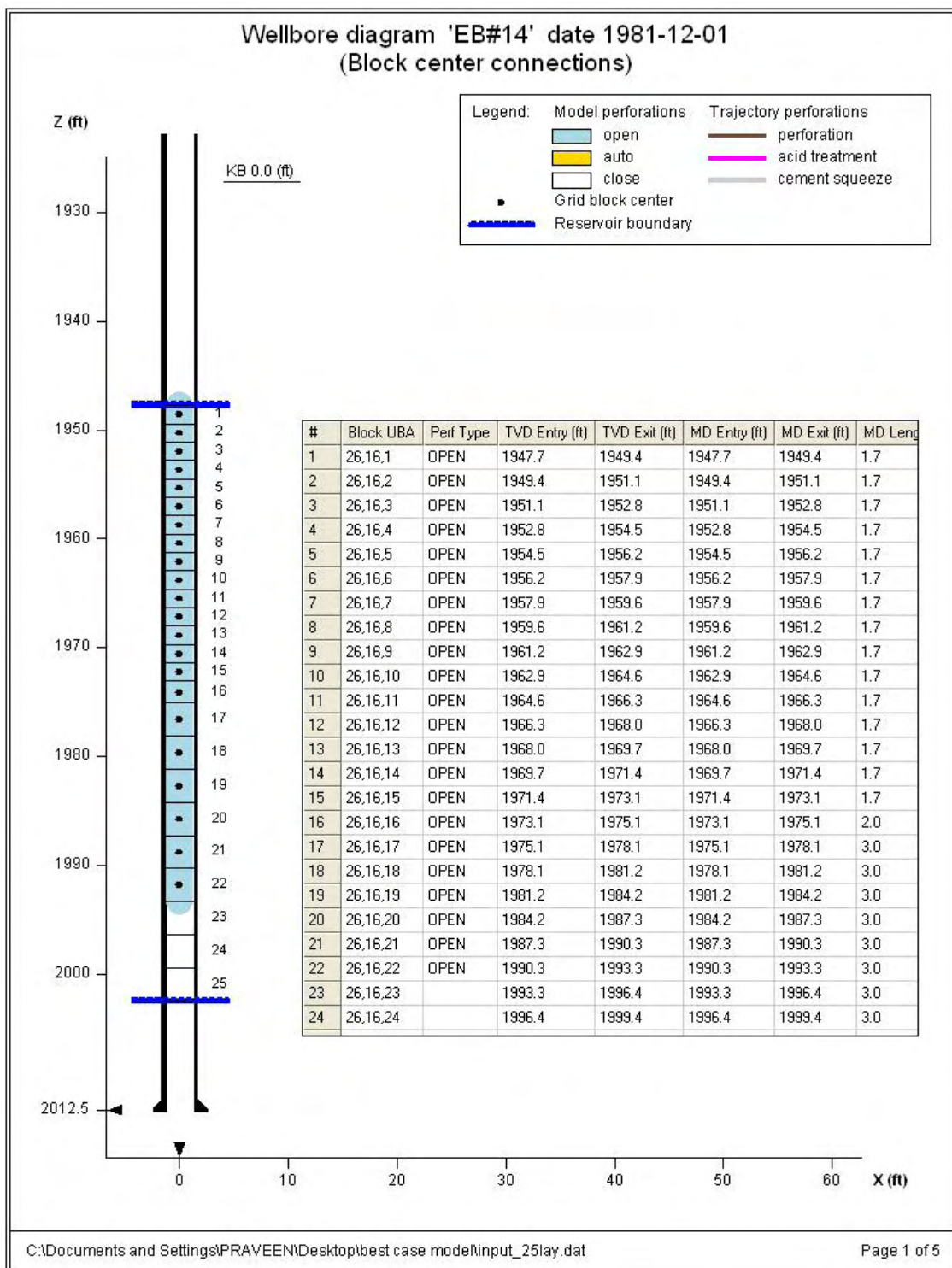


Figure 34: Wellbore diagram of Well EB#14

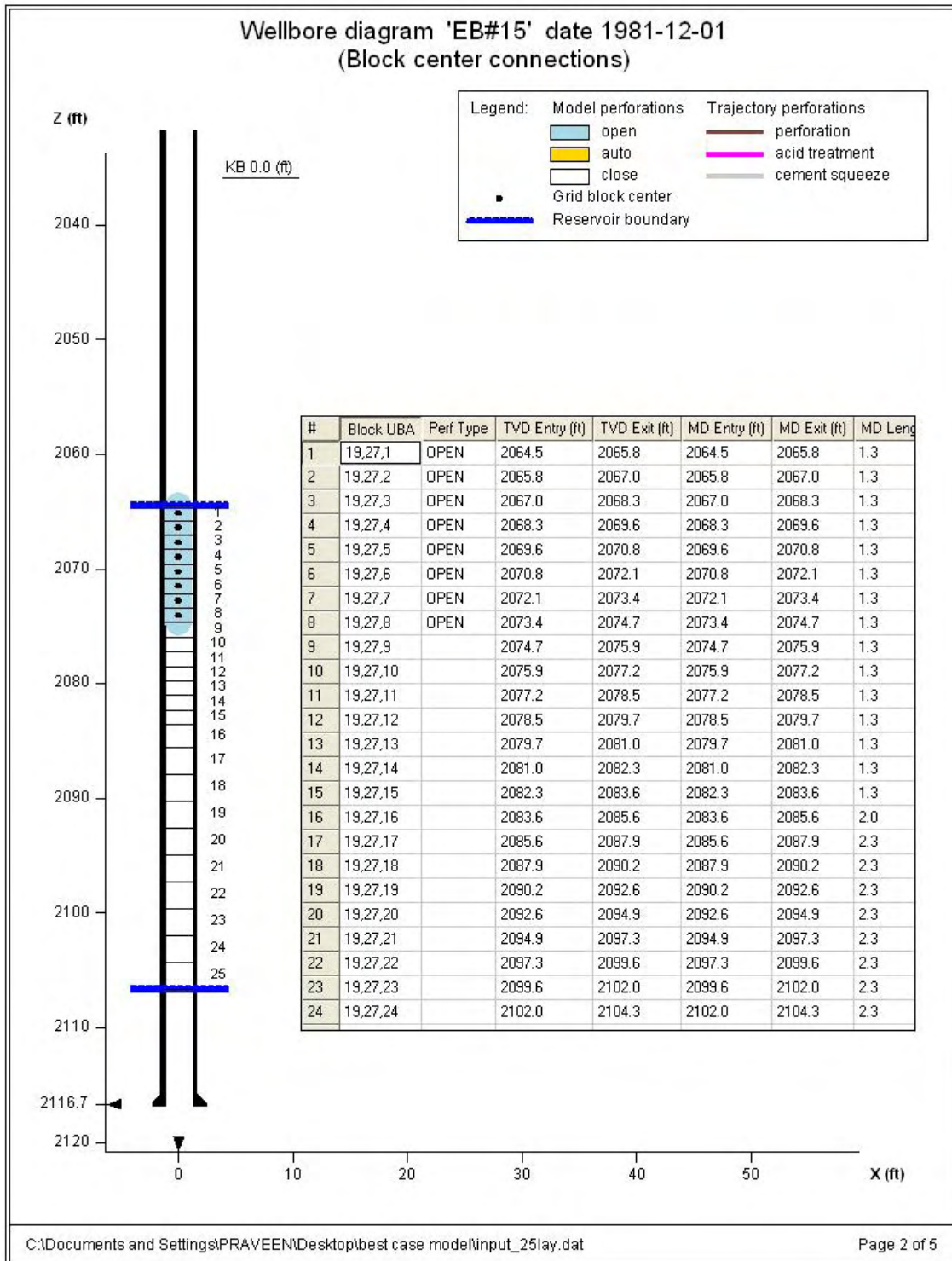


Figure 35: Wellbore diagram of Well EB#15

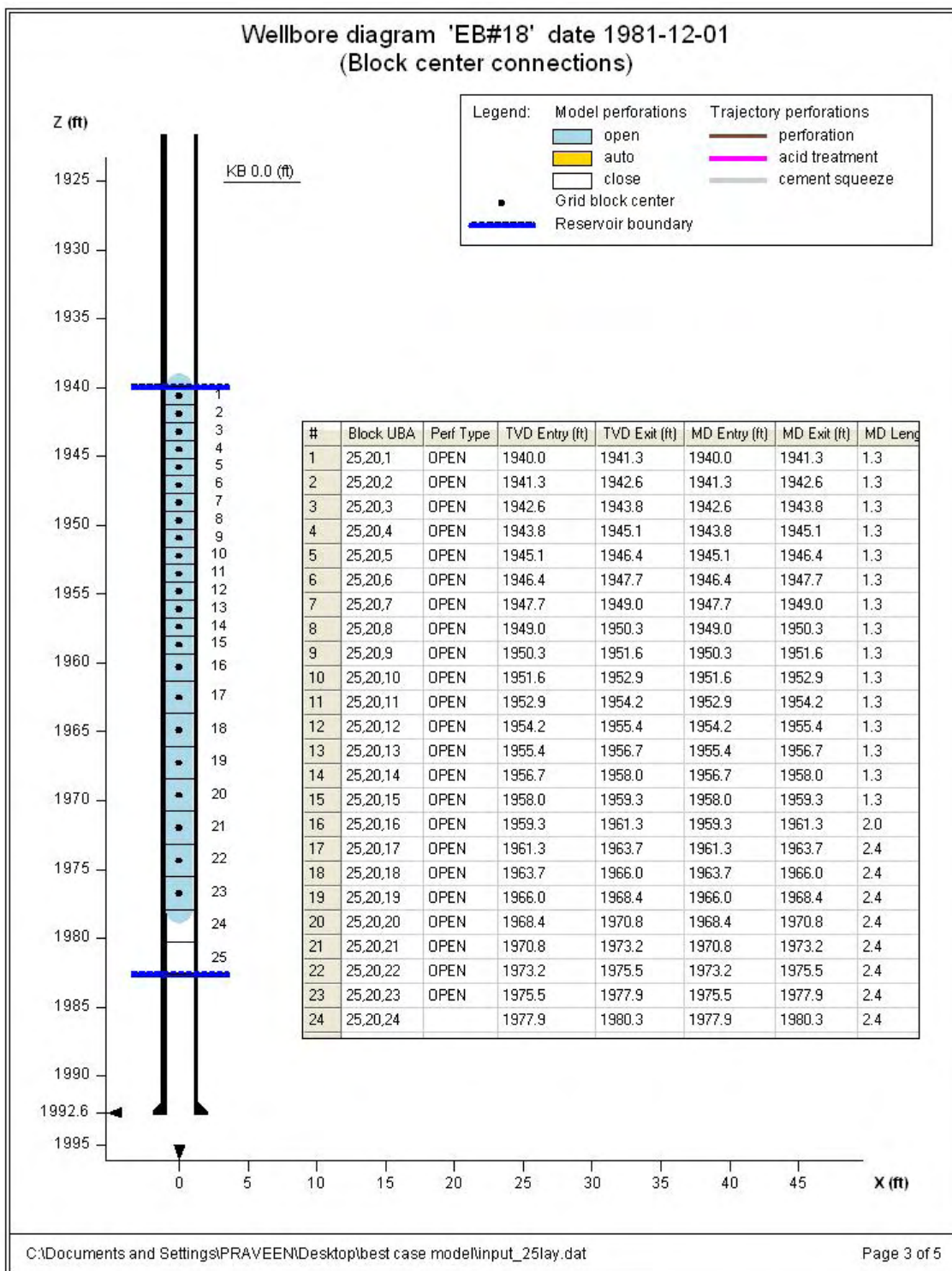


Figure 36: Wellbore diagram of Well EB#18

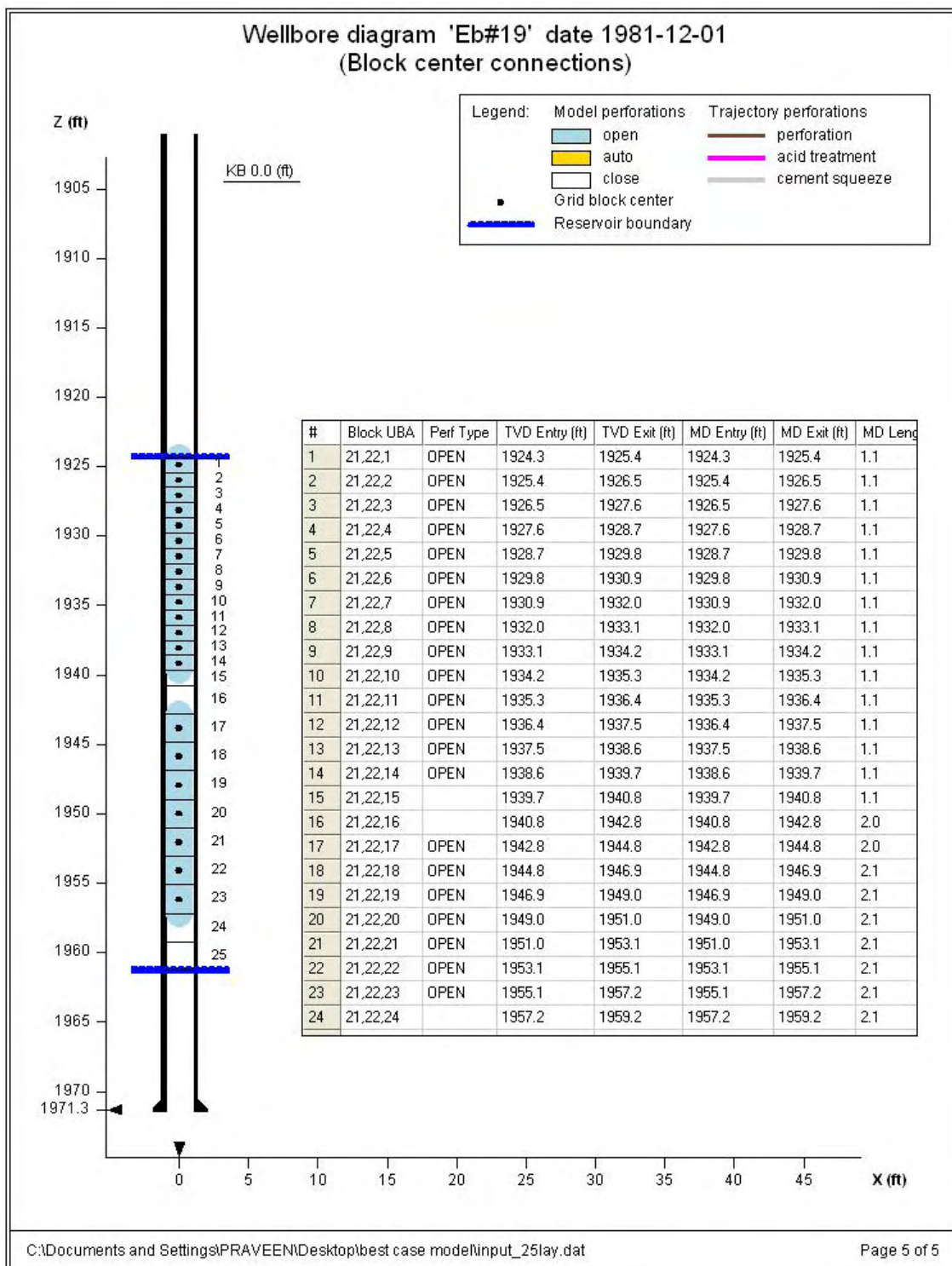


Figure 37: Wellbore diagram of Well EB#19

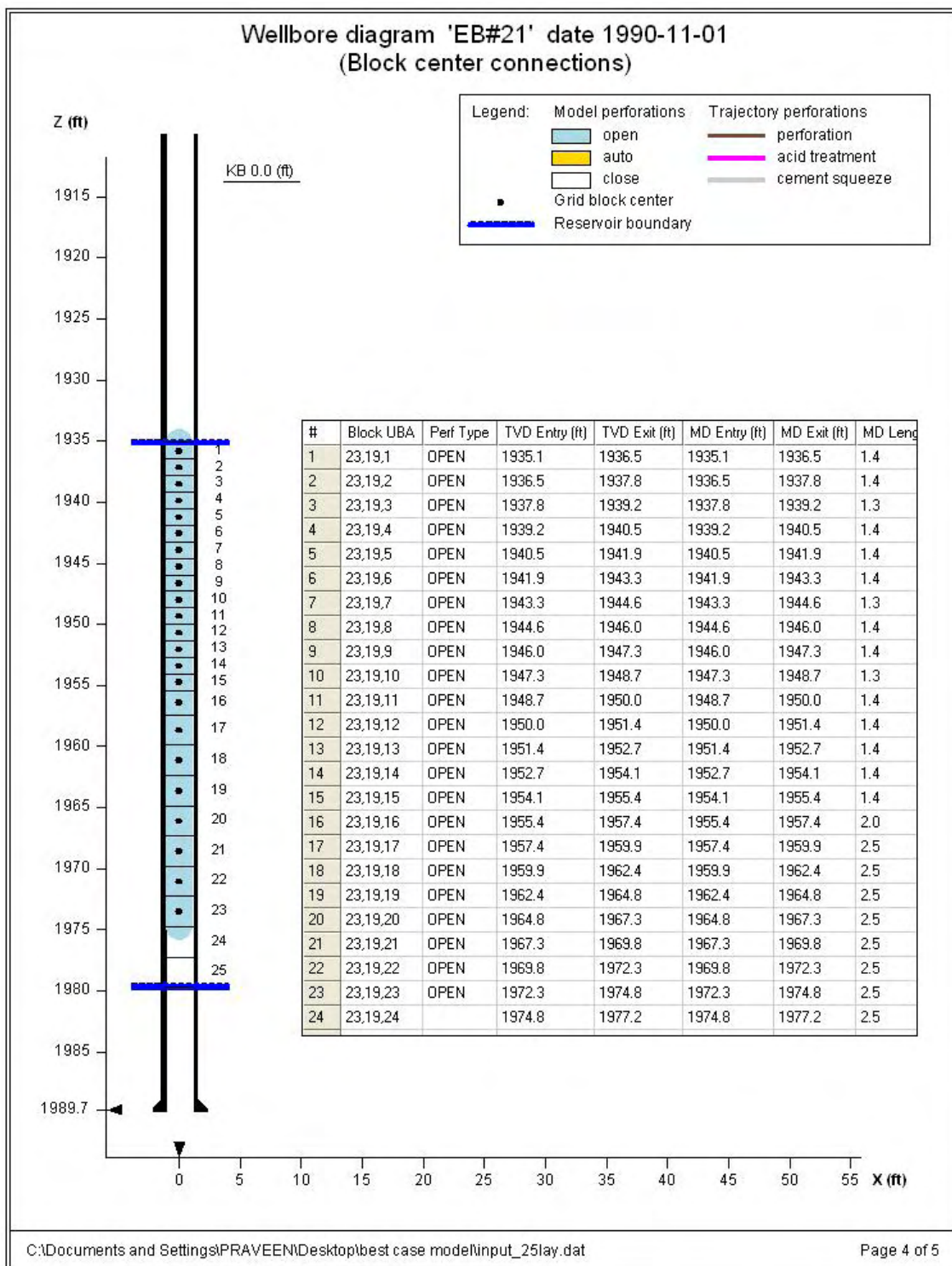


Figure 38: Wellbore diagram of Well EB#21

3. Production rate specifications and data importing procedures

Due to the lack of bottom hole flowing pressure data, the only production constraint (primary constraint) that can be used to model well production is the monthly gas production. The well production data for each well is re-written in a special format and initialized in CMG-STARS using “Import Production Data” option. CMG-STARS keyword *ALTER can also be used directly to change monthly production rate.

The primary operating constraint is the FIRST constraint entered for the well using the *OPERATE keyword. *ALTER allows modification of only the primary operating constraint for the specified wells.

The following steps are followed in order to initialize and alter well production rates.

Step 1: Choose the file containing well production data.

Construct gas production data file for each well. A specific format is followed. An example case is given below.

```
WELL: EB#14
11717000    12/1/1981
14530000    1/1/1982
...
```

Upon loading this data file in CMG, a monthly gas production rate of 11,717,000 SCF for the month of December 1981 will be initialized and later ALTER the same with a new gas production rate of 14,530,000 SCF for the month of January 1982, and so on.

Import Production/Injection Data

Step 1: Choose the file containing well production data

For the Generalized File Reading of production, injection, or pressure data:

1. The data should be organized into columns, with one type of data in each column.
2. The data can be read in free or fixed format mode.
3. A well name must be one of the columns of data, or the well name is identified by unique text (eg. Well: 03-17, in which case the unique text is Well:).

Please verify that years are 4 digits, since a 2 digit year is not accepted.

Select type of production/injection data file:

General

Name of the file containing the well production/injection data:

C:\Documents and Settings\PPRAVEEN\Desktop\WELL_14.txt Browse...

Data field type

Fixed Width - Data is present in columns of fixed width.

Delimited - Characters such as commas, spaces or tabs separate data fields. Columns can vary in width.

How are commas used in the file?

Commas separate data

Commas for thousands (eg: 5,000 = five thousand)

Commas as decimals (eg:5,2 = five + 2/10)

Help View Original File Cancel < Back Next > Finish

Figure 39: Choose the file containing well production data (Step 1)

Step 2: Choose the file option

Well name and data are identified by CMG-STARS upon highlighting the same under each section.

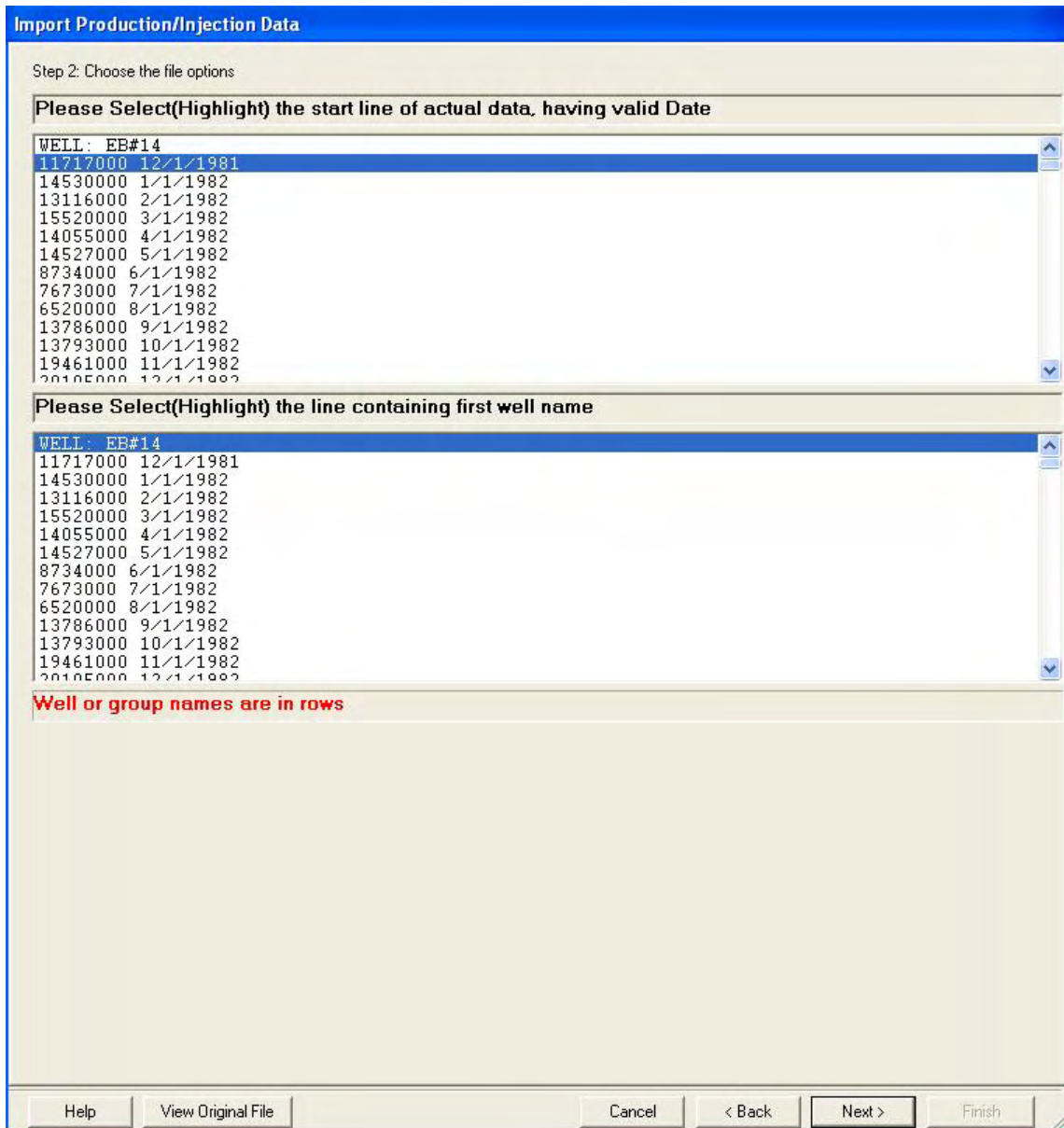


Figure 40: Choose the file option (Step 2)

Step 3: Choose delimiters

Choose appropriate delimiters. For this case, all delimiters were chosen to avoid any data mixing or data loss.

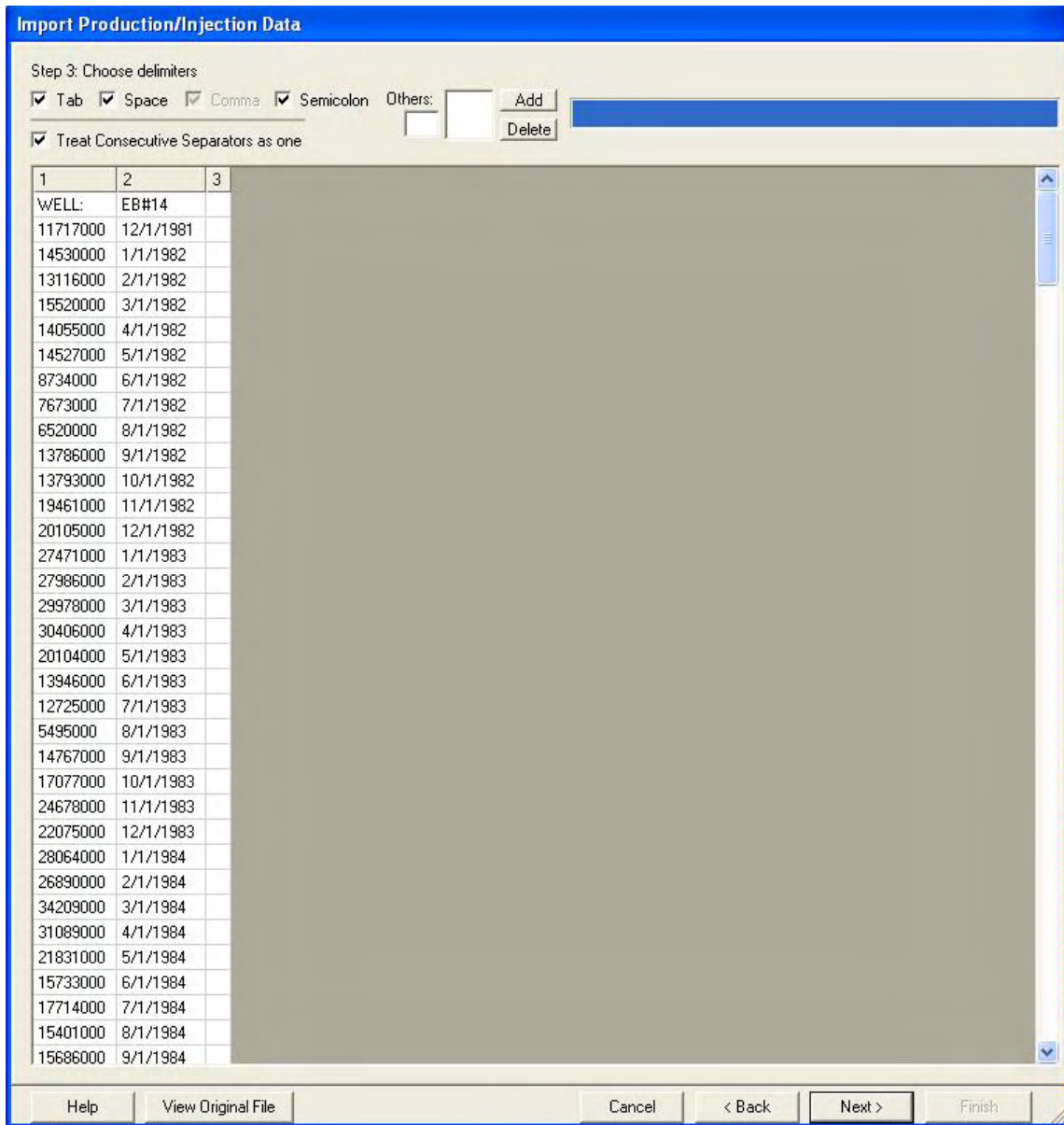


Figure 41: Choose delimiters (Step 3)

Step 4: Choose column details

The first column is identified as follows:

- a. Identifier – Gas Produced
- b. Related Info – Volume for period
- c. Units – SCF
- d. Expected period – Monthly
- e. Missing dates – take zero value

The second column is identified as follows.

- a. Identifier – Date/Time
- b. Related Info – MM/DD/YYYY

Import Production/Injection Data

Step 4: Choose column details

Note: For date formats that span multiple columns (eg. 26 02 1998), please do selection for each column.

	1	2	3
Identifier	Gas Produced	Date/ Time	Ignore Column
Related info	Volume for p...	M D Y (eg. 0...	
Units	SCF		
Expected period	Monthly		
Missing dates	zero(take ze...		
1	WELL:	EB#14	
2	11717000	12/1/1981	
3	14530000	1/1/1982	
4	13116000	2/1/1982	
5	15520000	3/1/1982	
6	14055000	4/1/1982	
7	14527000	5/1/1982	
8	8734000	6/1/1982	
9	7673000	7/1/1982	
10	6520000	8/1/1982	
11	13786000	9/1/1982	
12	13793000	10/1/1982	
13	19461000	11/1/1982	
14	20105000	12/1/1982	
15	27471000	1/1/1983	
16	27986000	2/1/1983	
17	29978000	3/1/1983	
18	30406000	4/1/1983	
19	20104000	5/1/1983	
20	13946000	6/1/1983	
21	12725000	7/1/1983	
22	5495000	8/1/1983	
23	14767000	9/1/1983	
24	17077000	10/1/1983	
25	24678000	11/1/1983	
26	22075000	12/1/1983	
27	28064000	1/1/1984	
28	26890000	2/1/1984	
29	34209000	3/1/1984	

Ignore a column for a well if all data are zero or blanks

Help View Original File Cancel < Back Next > Finish

Figure 42: Choose column details (Step 4)

Step 5: Check well names and primary constraint

CMG-STARs provides an opportunity to check and modify all initialized parameters.

Step 5: Check well/group names and primary constraints

Injector name suffix: Water injectors: iw, Gas injectors: ig, Solvent injectors: is

Buttons: Add All, Add Only Producers, Add Only Injectors, Add None, Add Only Matched

For changing primary constraints, please right click on the selected cell(s).

This table lists the existing well/group names that do not match the names in the production file. Select a well/group name by single click and then drag and drop it to the New Name column to the left if you want to use it.

	Import Name	Group	Matched	New Name	Add	Primary Constraint	Fraction
1	● EB#14	<input type="checkbox"/>	<input checked="" type="checkbox"/>		<input checked="" type="checkbox"/>	Gas Produced	1.0

	Unmatched Names
1	● EB#15
2	● EB#18
3	● EB#21
4	● Eb#19

Group adjacent periods with rates within 0 % of each (will result in less ALTER keywords)

Import Data Options

- Import data after this date: 1981-12-01
- For each well/group, apply data after last date of old data (new data append to the end of old data)
- For each well/group, apply data after first date of new data (new data overwrite the old data)

Buttons: Help, View Original File, Cancel, < Back, Next >, Finish

Figure 43: Check well names and primary constraint (Step 5)

Step 6: Finish

Pressing the 'Finish' button will automatically initialize a new well (example EB#14) and load the gas production data.

4. Well production rate validation

Following all the steps previously mentioned, the gas production data for all five East Barrow wells are loaded in CMG-STARS. The initialized well production models are tested and validated with actual production history data. This step is a necessary quality check, required before running the full field model.

To validate the well production model, a simple model is developed in CMG. The East Barrow reservoir is considered as a free gas reservoir with no associated hydrate cap or aquifer. A free gas saturation of 45% and bounded water of 55% is considered. All parameters initialized for the base case model (as discussed previously) are applied to this case. The model is simulated from 1981 to 2007, producing gas from all five wells based on production history. Well location and perforations are kept the same as initialized previously.

The monthly gas production output for each well is plotted with actual production history data. Any change or deviation in gas production rates are corrected and simulated again. Upon achieving a close agreement with production history data, the CMG-STARS well model is considered accurate and ready to be used for performing history match and sensitivity analysis. Figure 44 to 48 presents validated monthly gas production rate.

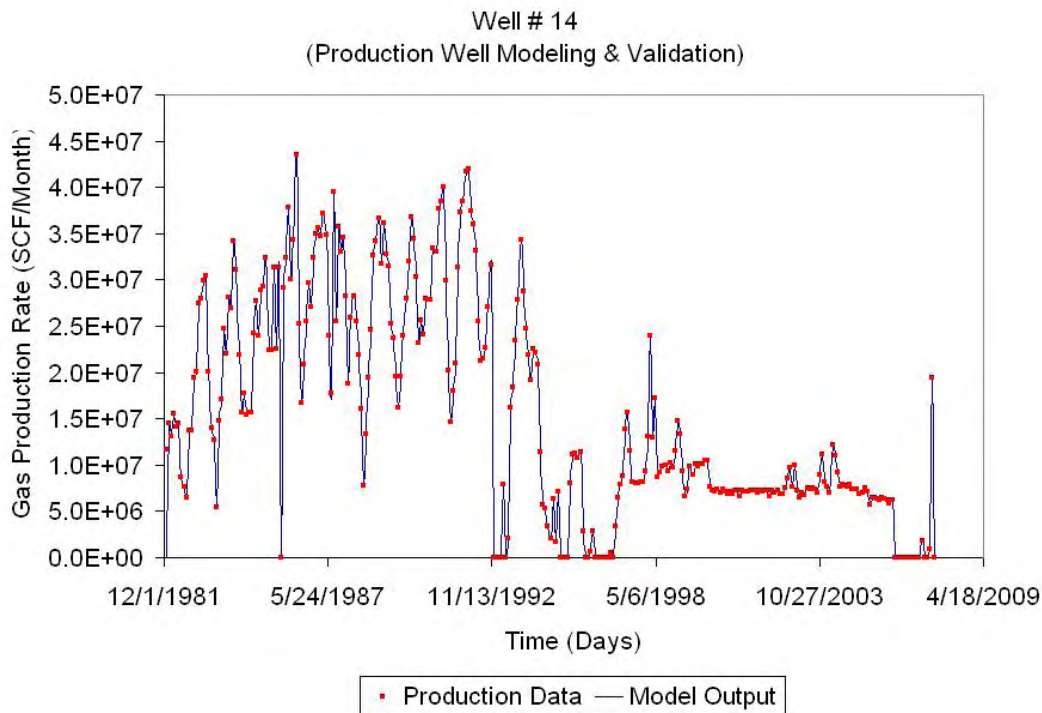


Figure 44: Gas production rate for EB#14 (Production data vs Model Output)

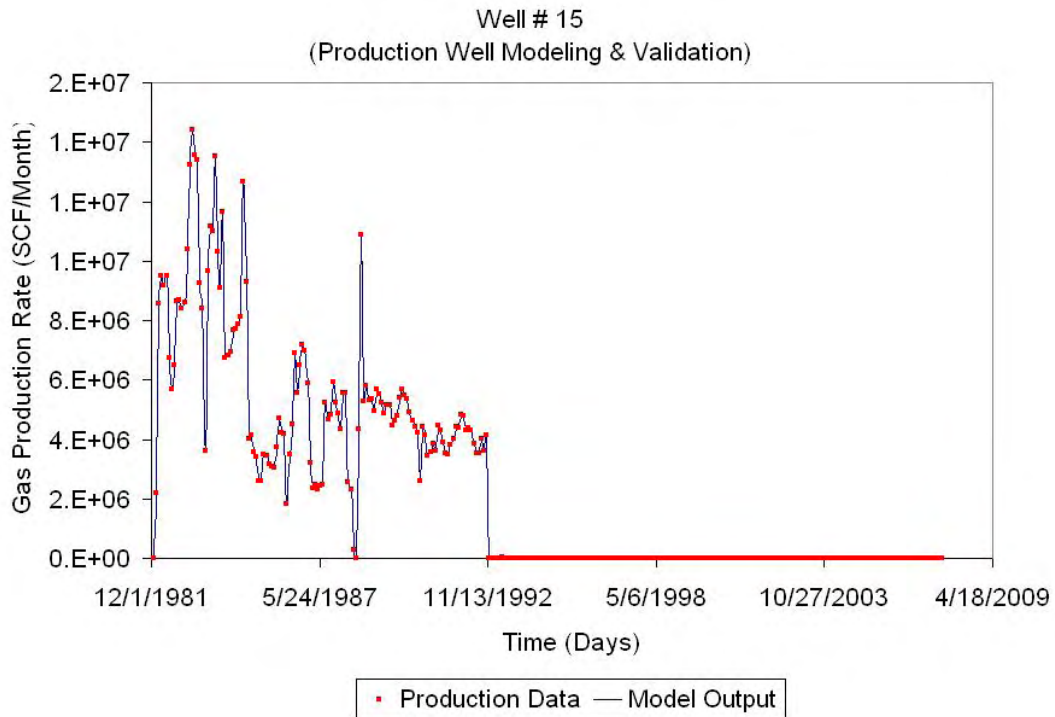


Figure 45: Gas production rate for EB#15 (Production data vs Model Output)

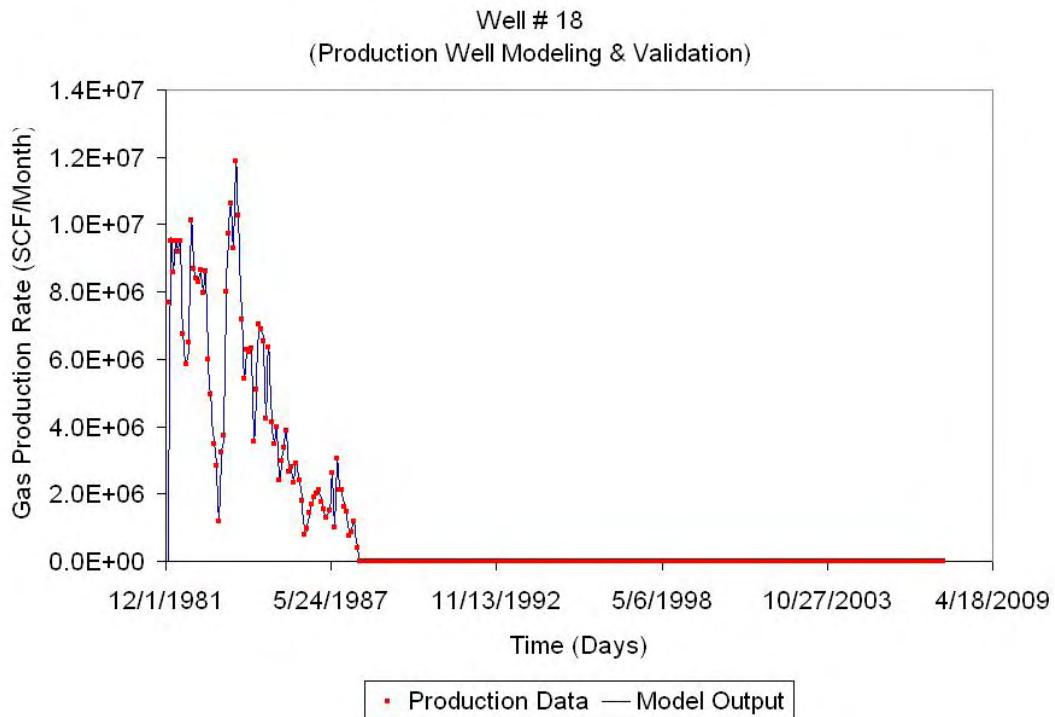


Figure 46: Gas production rate for EB#18 (Production data vs Model Output)

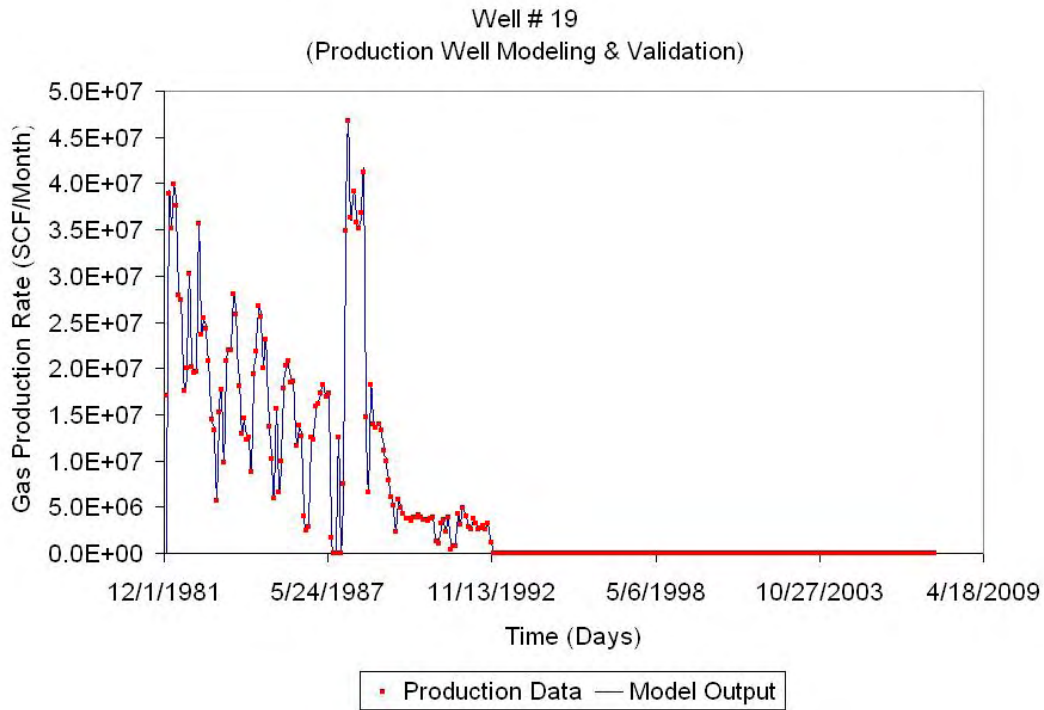


Figure 47: Gas production rate for EB#19 (Production data vs Model Output)

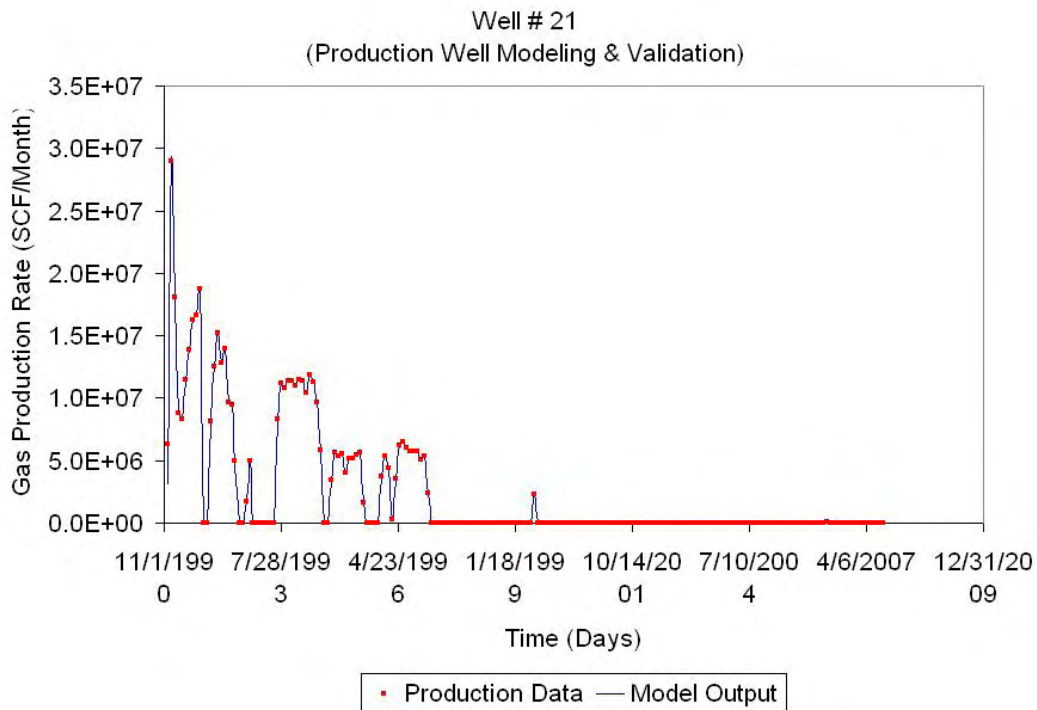


Figure 48: Gas production rate for EB#21 (Production data vs Model Output)

III. EAST BARROW HISTORY MATCHING

The objective of history matching analysis is to build a reservoir model that closely matches the performance of the East Barrow gas field. The quality and accuracy of predicting future reservoir behavior lies in developing the best suited model. Hence, the criteria followed in performing history matching plays a crucial role. Availability and quality of production history data, geologic data and well log data will be the governing parameters.

The East Barrow gas reservoir is data limited. Hence, an attempt has been made to develop a reservoir model that can best describe the historical performance of the reservoir and which is capable of predicting future behaviors with greater accuracy.

A topdown approach has been followed while performing the history matching study. Reservoir level match is performed followed by individual well level match. The history match criteria chosen for this study is as follows:

Field level match criteria

1. Cumulative gas production

The cumulative gas production obtained from model output is compared with production history data. While evaluating different scenarios, this can become a crucial parameter to be compared.

2. Cumulative water production

There is no control on water production in any well. Negligible water production has been observed to date. Hence, the cumulative water production comparison can provide vital information about the mobile water distribution near wellbore region.

3. Average reservoir pressure:

Pressure is a block property. CMG-STARS performs material balance calculations on each grid block. Based on these calculations the pressure for each block is estimated. However, due to pressure variation within the reservoir, there is no provision to directly obtain average reservoir pressure. Blockwise pressure data can be used to generate average reservoir pressure. The task is cumbersome and time consuming. To approximate similar results, several grid blocks were chosen and their pressure profiles were compared with each other and also with production history data.

The pressure profile in downdip location (far away from producing well) remained unaffected most of the time due to the presence of an aquifer. Also, the production history data were collected from active wells. These wells represent average drainage pressure of near well location. Based on these observations, a grid block in updip location (block number 19, 19, 1) was chosen to represent average reservoir pressure. Figure 48 shows the location of this grid block.

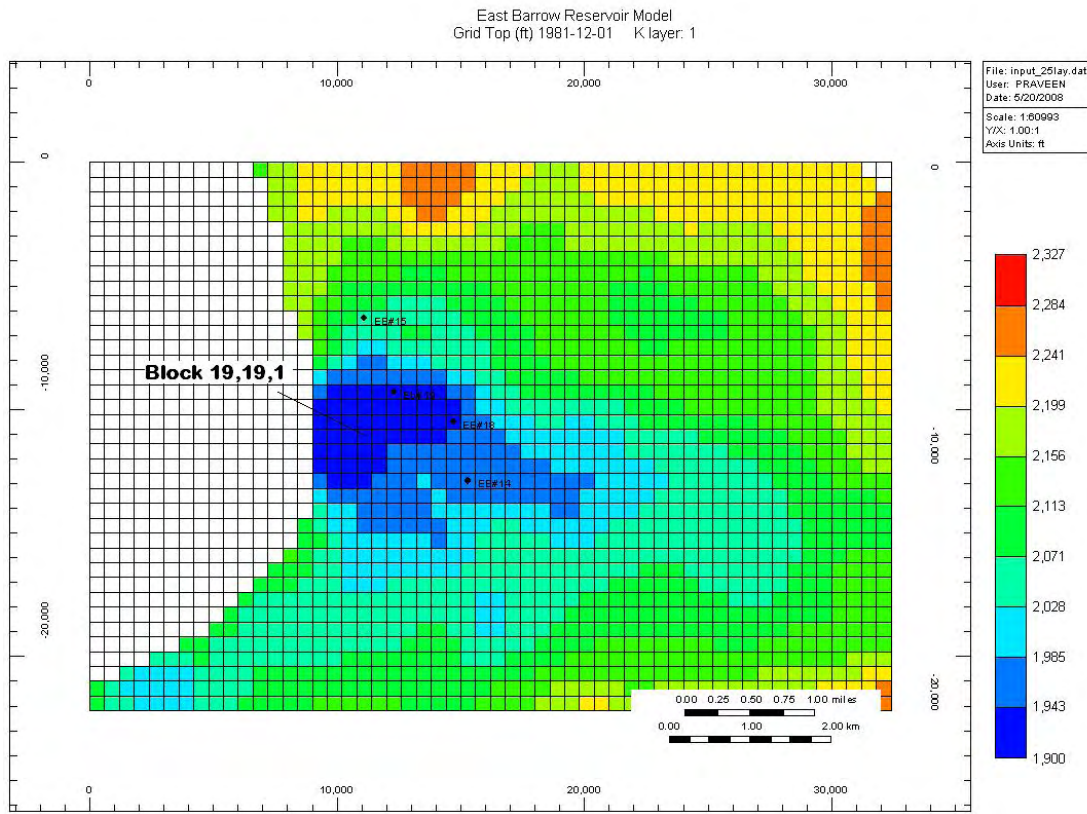


Figure 49: East Barrow Block 19,19,1 representing average reservoir pressure

Well level match criteria

1. Gas production rate

Field level match is followed by initiating well level match. The model results are obtained for individual wells and compared with production data.

2. Water production rate

Water production rate match can also be performed to compare the water production data on well to well basis. As negligible quantities of water have been produced to date, well level match may not be a good parameter to rely on. However, comparing water production rate for each well will surely strengthen the basis on which the matching exercise has been performed.

Approach

Based on the previous material balance study and preliminary history matching efforts¹ it was concluded that the East Barrow gas reservoir is associated with thick hydrate layer and associated with weak aquifer support. The material balance study followed a simple step by step approach in analyzing the reservoir drive mechanism. A similar approach has been adopted in evaluating the reservoir response for the entire gas pool.

Scenario	Reservoir Model	Description
A.	Free Gas Reservoir <i>(Only Gas model)</i>	A simple free gas reservoir model with no hydrate cap and aquifer support
B.	Free Gas Reservoir with associated aquifer <i>(Gas + Aquifer model)</i>	Free gas reservoir model associated with aquifer support (model aquifer)
C.	Free Gas Reservoir with associated hydrate cap and aquifer supports <i>(HYD + Gas + Aquifer model)</i>	Free gas reservoir model associated with thick hydrate cap on the top and model aquifer support at the bottom.
D.	Hydrate Reservoir <i>(Only HYD model)</i>	A reservoir model saturated with methane hydrates, bounded water and free gas (respecting thermodynamic equilibrium)
E.	Hydrate cap associated with free gas <i>(HYD + Gas model)</i>	Free gas reservoir model associated with thick hydrate zone
F.	Hydrate associated with model aquifer <i>(HYD + Aquifer model)</i>	A hydrate rich reservoir model associated model aquifer support. (No free gas)

Table E-7: History matching scenarios for East Barrow

The history matching scenarios are developed and initialized in CMG-STARS. The model output is evaluated by comparing the field level and well level data. The model initialization procedure is the same as discussed previously. The scenarios studied are tabulated below in Table-7. The parameters initialized for different scenarios are listed in Table-8a to 8f, all other parameters remain the same as discussed for the base case model.

Zone	Pressure	Temperature	Saturation	Remarks
Hydrate	975 psi	Temperature Gradient 1.6 ⁰ F/100ft Top Temp 41 ⁰ F	No Hydrate Zone	
Free Gas			S _g = 45% S _w = 55%	Covers entire reservoir
Aquifer			No Aquifer Zone	

Table E-8a: Initial Condition for Scenario A (*Only Gas Model*) for East Barrow

Zone	Pressure	Temperature	Saturation	Remarks
Hydrate	975 psi	Temperature Gradient 1.6 ⁰ F/100ft Top Temp 41 ⁰ F	No Hydrate Zone	
Free Gas			S _g = 45% S _w = 55%	Free Gas-Water Contact-2080'
Aquifer			S _w = 100%	

Table E-8b: Initial Condition for Scenario B (*Gas + Aquifer Model*) for East Barrow

Zone	Pressure	Temperature	Saturation	Remarks
Hydrate	975 psi	Temperature Gradient 1.6 ⁰ F/100ft Top Temp 41 ⁰ F	S _h = 31% S _g = 14% S _w = 55%	(Lw-H-V) close to Equilibrium
Free Gas			S _g = 45% S _w = 55%	Hydrate-Free Gas Contact- 2050'
Aquifer			S _w = 100%	Free Gas-Water Contact-2080'

Table E-8c: Initial Condition for Scenario C (*HYD + Gas + Aquifer Model*) for East Barrow

Zone	Pressure	Temperature	Saturation	Remarks
Hydrate	975 psi	Temperature Gradient 1.6 ⁰ F/100ft Top Temp 41 ⁰ F	S _h = 31% S _g = 14% S _w = 55%	(Lw-H-V) close to Equilibrium Hydrate covers entire reservoir
Free Gas			No Free Gas Zone	
Aquifer			No Aquifer Zone	

Table E-8d: Initial Condition for Scenario D (*Only HYD Model*) for East Barrow

Zone	Pressure	Temperature	Saturation	Remarks
Hydrate	975 psi	Temperature Gradient 1.6 ⁰ F/100ft Top Temp 41 ⁰ F	S _h = 31% S _g = 14% S _w = 55%	(Lw-H-V) close to Equilibrium
Free Gas			S _g = 45% S _w = 55%	Hydrate-Free Gas Contact- 2050'
Aquifer			No Aquifer Zone	

Table E-8e: Initial Condition for Scenario E (*HYD + Gas Model*) for East Barrow

Zone	Pressure	Temperature	Saturation	Remarks
Hydrate	975 psi	Temperature Gradient 1.6 ⁰ F/100ft Top Temp 41 ⁰ F	S _h = 31% S _g = 14% S _w = 55%	(Lw-H-V) close to Equilibrium
Free Gas			No Free Gas Zone	
Aquifer			S _w = 100%	Hydrate-Water Contact-2080'

Table E-8f: Initial Condition for Scenario F (*HYD + Aquifer Model*) for East Barrow

IV. SENSITIVITY STUDY

The best case (history matched) scenario is subjected to sensitivity analysis. The CMG-STARS model developed here provides an easy means to study sensitivity of all parameters. The primary goal of performing a sensitivity study is to quantify the effect of changing parameters on overall reservoir performance. Also, these sensitivity studies provide additional support to the argument of choosing the best case model (history matched case) for future forecasting work. For this study the sensitivity parameters have been categorized into four major groups. These categories have been identified based on their importance in quantifying methane hydrate resource potential of the East Barrow gas field. These are:

1. Free Gas Zone Size
2. Hydrate Saturation
3. Hydrate Zone Size
4. Aquifer Strength and Size

1. Free Gas Zone Size

The effect of changing free gas zone size on reservoir performance has been studied as one of the sensitivity elements. The free gas zone size is altered by changing the free gas-water contact. CMG-STARS formula editor was used to edit gas-water contact for different case studies. The size of the hydrate zone was kept the same. Changing hydrate cap thickness has been studied separately. The effect of changing the free gas zone size is observed by plotting average reservoir pressure, cumulative gas and water production.

Five different free gas zone sizes have been studied. These are:

- a. Free Gas Water Contact – 2060'
- b. Free Gas Water Contact – 2070'
- c. Free Gas Water Contact – 2080' (best case model)
- d. Free Gas Water Contact – 2090'
- e. No Free Gas Water Contact (HYD + Free Gas model)

2. Hydrate Saturation

Hydrate thermodynamic studies for the East Barrow gas reservoir (Figure 15) show that the hydrate exists in equilibrium with free gas and bounded water in the hydrate zone. A hydrate saturation of 31% was used to match pressure history (best case model). The effect of hydrate saturation on reservoir performance has been studied as a part of the sensitivity analysis. This analysis helped in choosing a hydrate saturation of 31% for the best case model.

Five different cases were studied by changing hydrate saturation. These are:

- a. Hydrate Saturation = 0% (Gas + Aquifer Model)
- b. Hydrate Saturation = 5%
- c. Hydrate Saturation = 15%
- d. Hydrate Saturation = 31% (Best case model)
- e. Hydrate Saturation = 40%

3. Hydrate Zone Size

Hydrate zone size is changed by altering the depth of the hydrate-free gas contact. Changing hydrate zone size changes the cumulative water production and average reservoir pressure.

Hydrate stability modeling estimated the depth to the base of the hydrate stability zone to be at 2050' tvdss. The best case model was developed by using a contact at the depth of 2050'. This sensitivity study supports that basis.

Six different cases were studied by changing hydrate zone size. These are:

- a. No Hydrate Zone (Gas + Aquifer model)
- b. Hydrate – Free Gas Contact – 2030'
- c. Hydrate – Free Gas Contact – 2040'
- d. Hydrate – Free Gas Contact – 2050' (Best case model)
- e. Hydrate – Free Gas Contact – 2060'
- f. Hydrate – Water Contact – 2080' (HYD + Aquifer model)

4. Aquifer Strength and Size

The material balance study indicates that the reservoir is not volumetric. The reservoir is under the effect of strong external support. This support is either from dissociating hydrates or a strong aquifer. Detailed analysis showed a combined effect of these two sources. This became the basis of developing the best case model during the history matching study. However, it is important to investigate the effect of aquifer support on the free gas reservoir. The aquifer model developed for best case was created as part of the reservoir grid system. This is called the model aquifer. The aquifer sensitivity is studied by attaching the numerical aquifer available in CMG-STARS. The size and strength of such numerical aquifers have been changed, performance recorded and compared with production data. It should be noted that the aquifer study has been performed on free gas- model aquifer system, no hydrate cap has been considered in this case.

The numerical aquifer is initialized in CMG-STARS by using graphic user interface “aquifers”. The interface provide three options - BOTTOM aquifer model, BOUNDARY model and REGION model. The numerical aquifer is initalized using *AQUIFER keyword followed by desired aquifer model.

*AQUIFER - Specifies the aquifer location, via one of three methods:

*BOTTOM to connect aquifer to the bottom of the reservoir.

*BOUNDARY to connect aquifer to all boundary blocks in the sides of the reservoir.

*REGION to connect aquifer to an arbitrary list of fundamental grid blocks via I-J-K address ranges i1(:i2) j1(:j2) k1(:k2).

Figure 50 presents the option available with CMG-STARS.

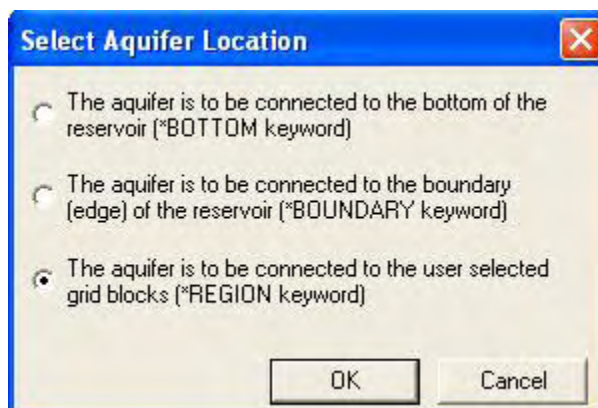
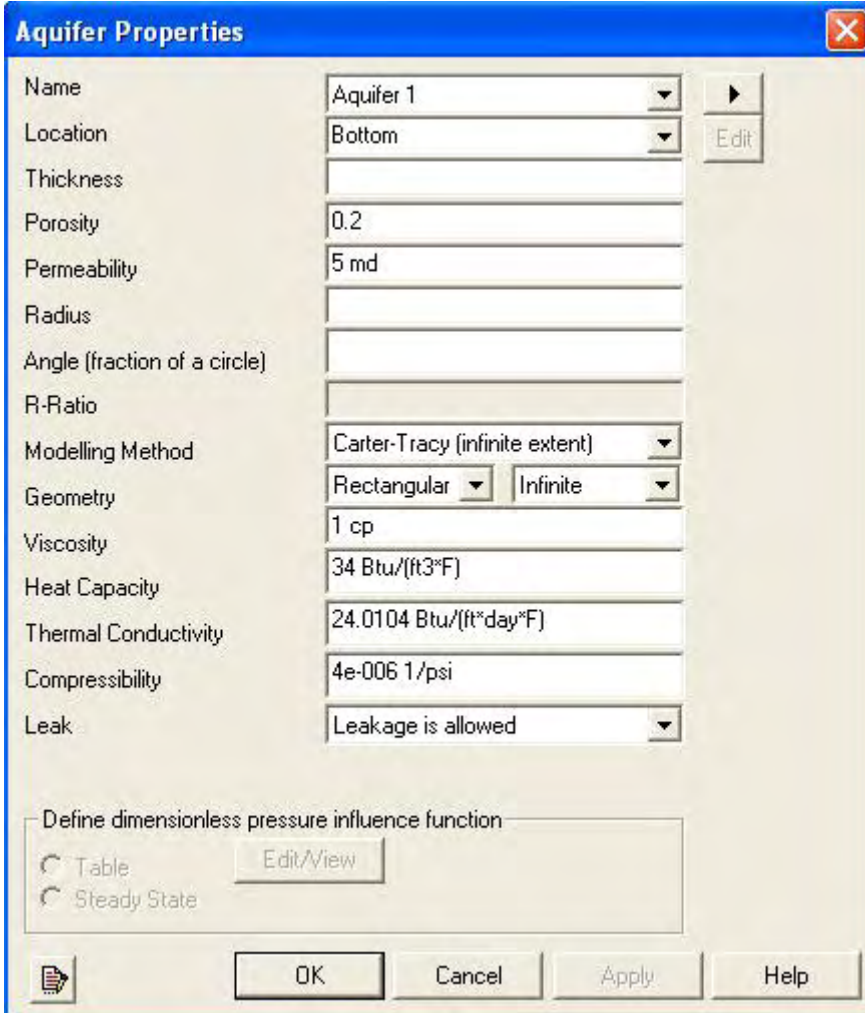


Figure 50: Aquifer Options (CMG-STARS)

Initializing Bottom Aquifer

Figure 51 shows the parameters initialized in order to include bottom numerical aquifer to the gas-model aquifer system. The aquifer is infinitely strong in this case. This can be easily made finite by making the numerical aquifer size finite. Figure 52 shows an example of finite bottom aquifer.



The screenshot shows a software dialog box titled "Aquifer Properties" with a close button (X) in the top right corner. The dialog contains the following fields and controls:

- Name: Aquifer 1 (dropdown menu)
- Location: Bottom (dropdown menu) with an "Edit" button to its right.
- Thickness: (empty text field)
- Porosity: 0.2 (text field)
- Permeability: 5 md (text field)
- Radius: (empty text field)
- Angle (fraction of a circle): (empty text field)
- R-Ratio: (empty text field)
- Modelling Method: Carter-Tracy (infinite extent) (dropdown menu)
- Geometry: Rectangular (dropdown menu) and Infinite (dropdown menu)
- Viscosity: 1 cp (text field)
- Heat Capacity: 34 Btu/(ft³*F) (text field)
- Thermal Conductivity: 24.0104 Btu/(ft*day*F) (text field)
- Compressibility: 4e-006 1/psi (text field)
- Leak: Leakage is allowed (dropdown menu)

At the bottom of the dialog, there is a section titled "Define dimensionless pressure influence function" with two radio buttons: "Table" and "Steady State". An "Edit/View" button is located to the right of these radio buttons. At the very bottom of the dialog are four buttons: "OK", "Cancel", "Apply", and "Help".

Figure 51: Initializing bottom aquifer (infinite size)

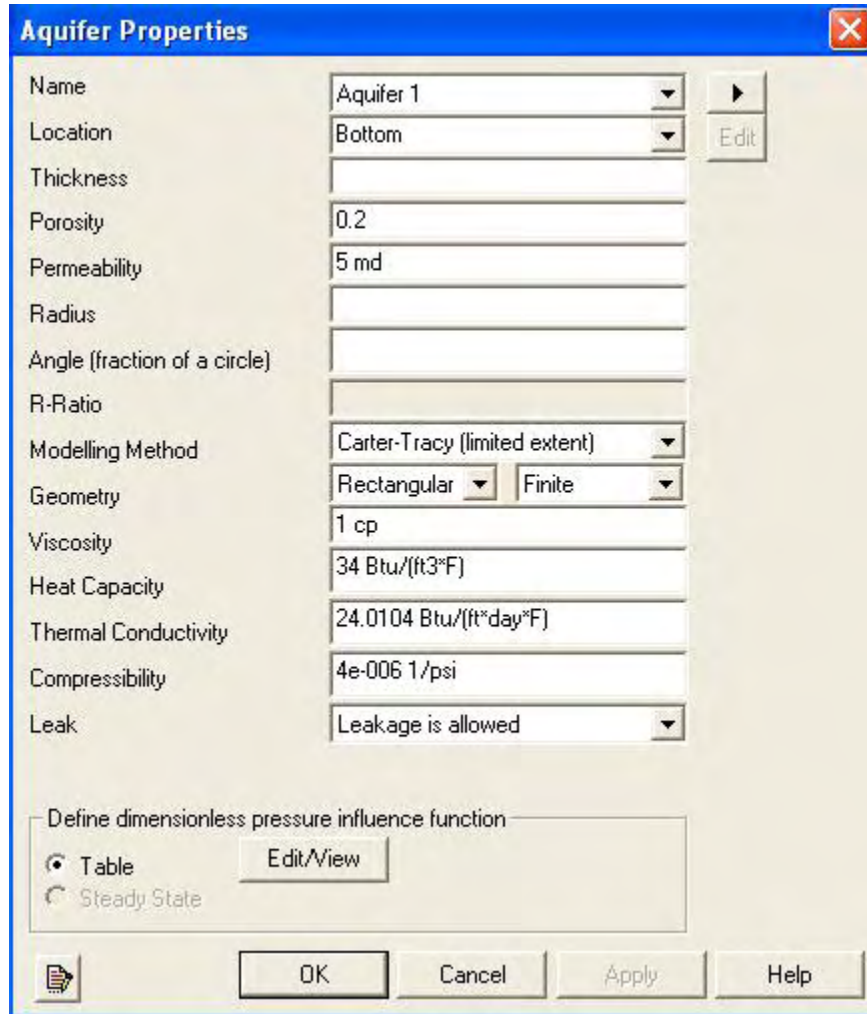


Figure 52: Initializing bottom aquifer (finite size)

Initializing Edge Aquifer

*REGION keyword is used to attach numerical aquifer to specific regions only. The numerical aquifer is attached to the north, east and south direction of the reservoir. The strength of the reservoir can be kept finite or infinite.

Figure 53 shows parameters initialized to attach infinite edge water aquifer to the reservoir model. Figure 54 shows data utilized to initialize finite edge water aquifer.

Property	Value
Name	Aquifer 1
Location	Regions
Thickness	
Porosity	0.2
Permeability	5 md
Radius	
Angle (fraction of a circle)	
R-Ratio	
Modelling Method	Carter-Tracy (infinite extent)
Geometry	Rectangular Infinite
Viscosity	1 cp
Heat Capacity	34 Btu/(ft ³ *F)
Thermal Conductivity	24.0104 Btu/(ft*day*F)
Compressibility	4e-006 1/psi
Leak	Leakage is allowed

Define dimensionless pressure influence function

Table Steady State

Buttons: OK, Cancel, Apply, Help

Figure 53: Initializing region aquifer (infinite size)

Aquifer Properties ✕

Name	Aquifer 1	▶
Location	Regions	Edit
Thickness		
Porosity	0.2	
Permeability	5 md	
Radius		
Angle (fraction of a circle)		
R-Ratio		
Modelling Method	Carter-Tracy (limited extent)	
Geometry	Rectangular	Infinite
Viscosity	1 cp	
Heat Capacity	34 Btu/(ft ³ *F)	
Thermal Conductivity	24.0104 Btu/(ft*day*F)	
Compressibility	4e-006 1/psi	
Leak	Leakage is allowed	

Define dimensionless pressure influence function

Table Edit/View
 Steady State

📄 OK Cancel Apply Help

Figure 54: Initializing region aquifer (finite size)

Following are the scenarios studied as part of numerical aquifer sensitivity study.

1. All Aquifer Sensitivity
2. Bottom Aquifer Sensitivity
3. Edge Aquifer Sensitivity
4. Infinite Aquifer Sensitivity
5. Finite Aquifer Sensitivity
6. Aquifer Sensitivity at Gas-Water contact 2080'
7. Aquifer Sensitivity at Gas-Water contact 2070'
8. Aquifer Sensitivity at Gas-Watre contact 2045'

V. EAST BARROW FORECASTING STUDY

The best case model provides a useful tool to locate sweet spot (high gas and hydrate concentration zones) in the reservoir. Based on such reservoir mapping studies, location for future infill wells can be selected. Horizontal and vertical infill wells can be drilled and simulated to predict the reservoir performance for the next 30 years. Several such models have been simulated to compare the technical feasibility of adding a horizontal or vertical test well, or completing existing wells laterally. However, it should be noted that this forecast study does not include economic modeling and hence, would require a separate study.

CMG-STARS keyword *RESTART offers an easy way to start a new simulation run from the last simulation date. For the East Barrow gas reservoir, the last simulation date is September 2007. The model loads simulation run data from the best case model and model run extends from September 2007 to September 2037.

Eight different forecasting runs are simulated in this study. These runs are as follows:

1. Producing EB#14 (only)
2. Producing EB#19 (only)
3. Producing EB#14 and EB#19 together
4. Completing and producing EB#14 in horizontal plane (~1000' long)
5. Completing and producing EB#19 in horizontal plane (~1000' long)
6. Completing and producing EB#14 and EB#19 in horizontal plane (~1000' long)
7. Producing EB#14 and EB#19 with Vertical Infill Well (New Test Well)
8. Producing EB#14 and EB#19 with Horizontal Infill Well (New Test Well, ~1000')

The wellbore diagrams of EB#14 and EB#19, completed in horizontal plane (both vertical and horizontal section open to flow), vertical and horizontal infill wells are shown in Figure 55-58. The wellbore diagram of EB#14 and EB#19 when produced without any completion remained unchanged (refer to Figures 34 and 37). The selection of location for drilling infill wells have been discussed under East Barrow Results and Discussion section.

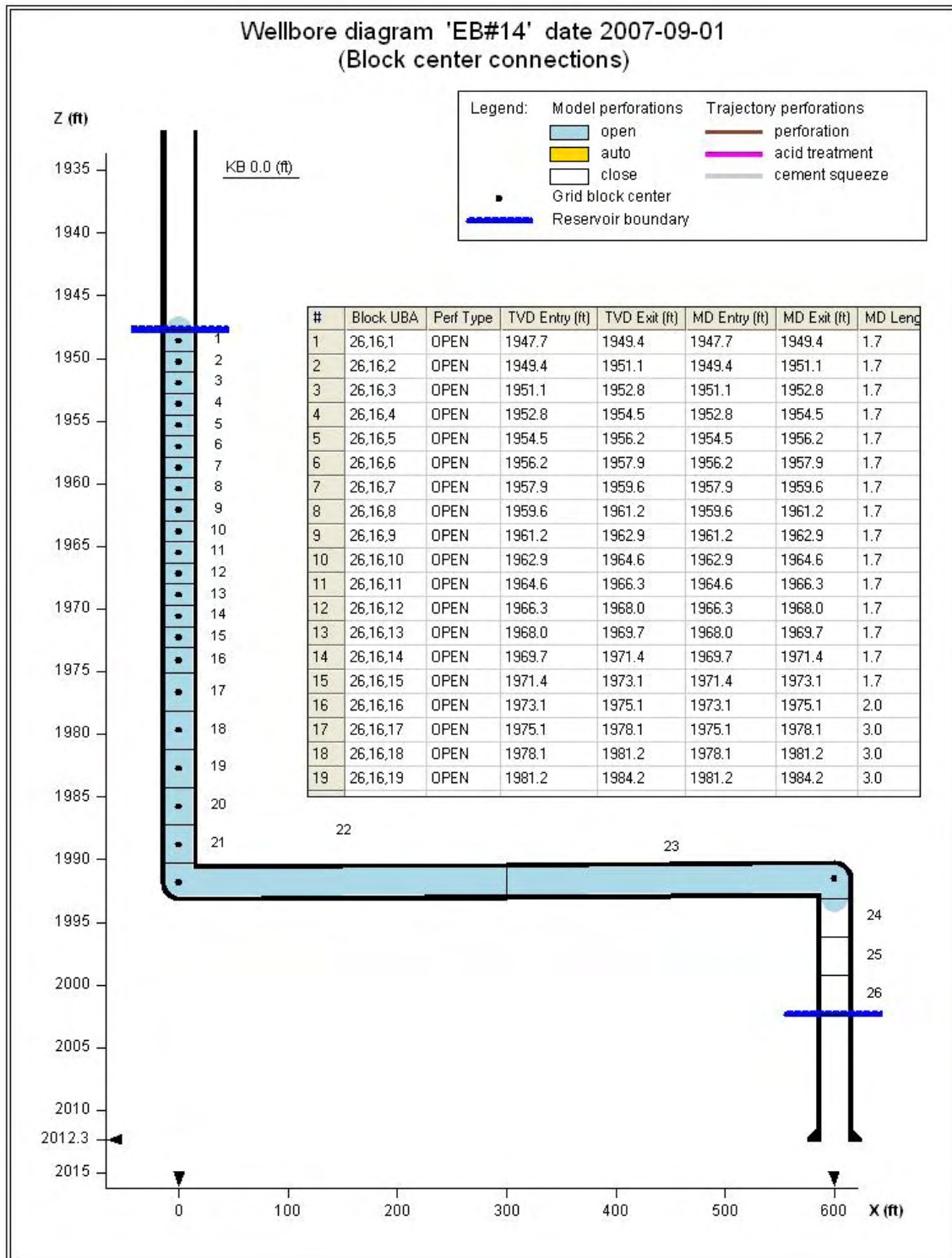


Figure 55: Wellbore diagram of EB#14 (completed in horizontal section)

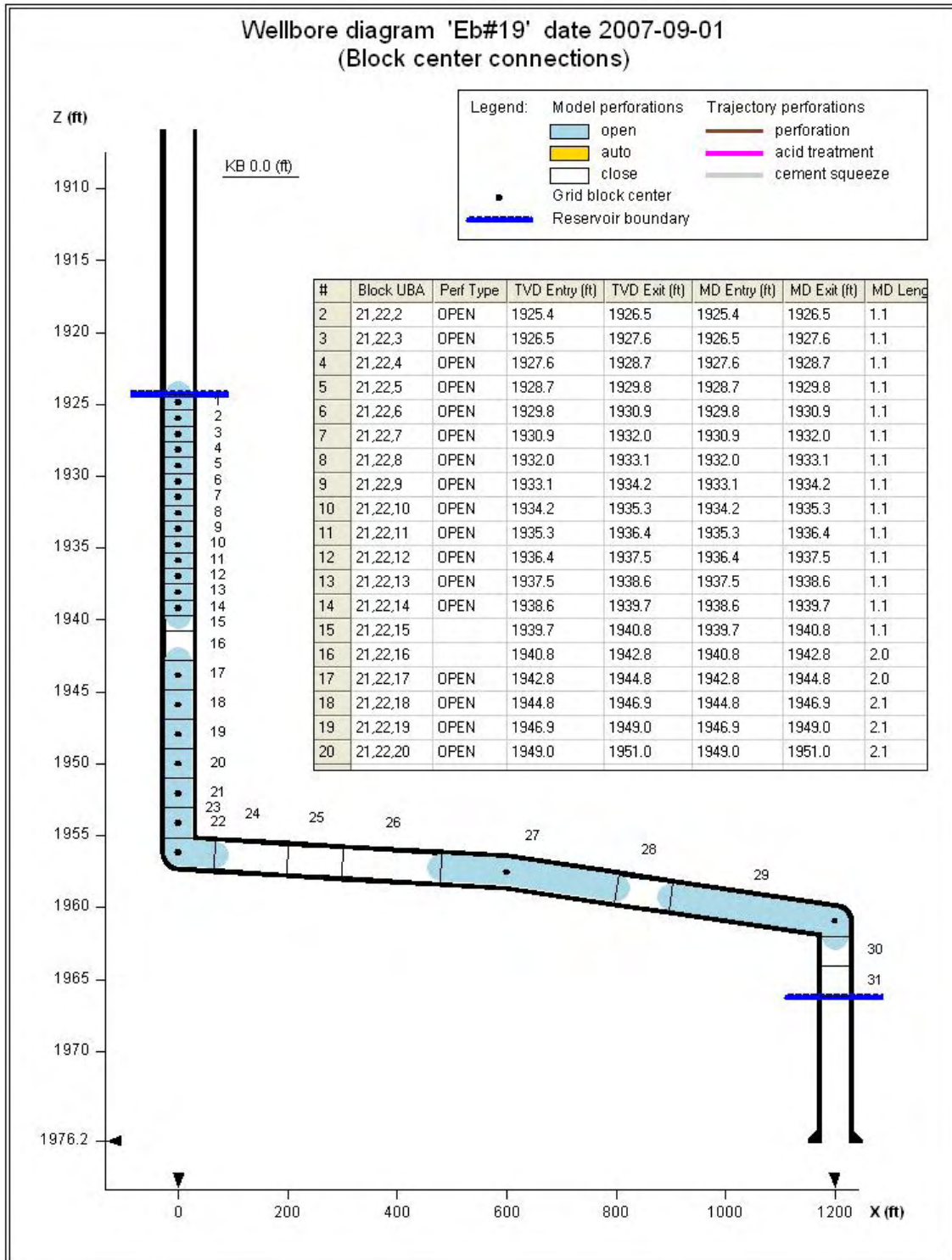


Figure 56: Wellbore diagram of EB#19 (completed in horizontal section)

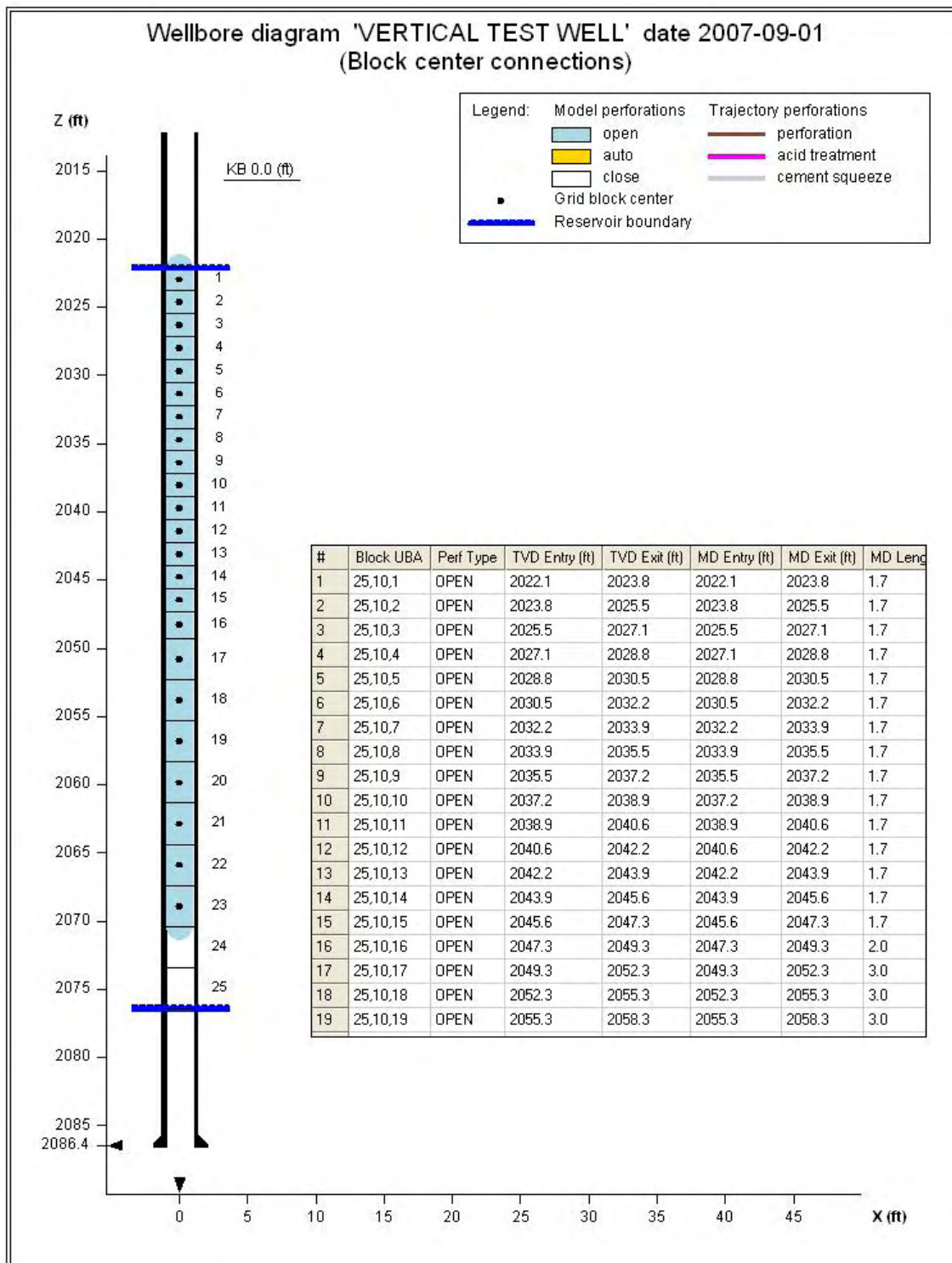


Figure 57: Wellbore diagram of Vertical Test Well (New Infill Well for East Barrow)

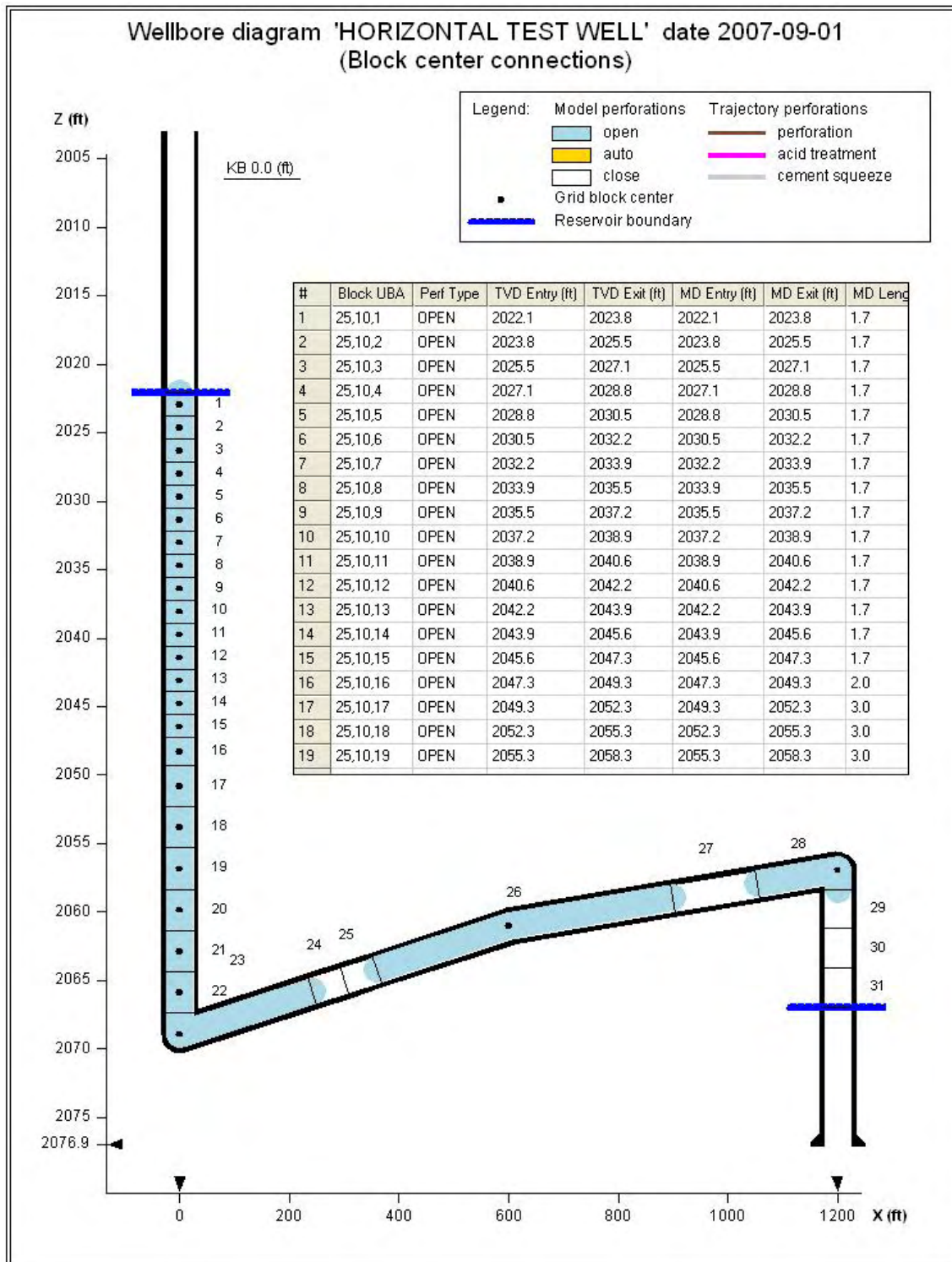


Figure 58: Wellbore diagram of Horizontal Test Well (New Infill Well for East Barrow)

EAST BARROW RESULTS AND DISCUSSIONS

I. EAST BARROW HISTORY MATCHING

As discussed previously, six different scenarios are developed and the performance is studied and matched with reservoir history data. The history matching is performed both at the reservoir level and well level. The reservoir level match has been initiated for all scenarios. Upon achieving a close match, individual well level match has been performed for best case scenario. The initial estimates of free gas, hydrates and associated (bounded) water have been estimated for each scenario. Table E-9a presents the estimates for each case.

Scenario	Reservoir Model	Hydrate	Free Gas		Water
		reservoir ft ³	reservoir ft ³	SCF	reservoir ft ³
A.	<i>Only Gas model</i>	0.00	1.23 E+9	94.21 E+9	1.51 E+9
B.	<i>Gas + Aquifer model</i>	0.00	3.57 E+8	27.32 E+9	2.38 E+9
C.	<i>HYD + Gas + Aquifer model (Best Case)</i>	1.50 E+8	2.07 E+8	15.84 E+9	2.38 E+9
D.	<i>Only HYD model</i>	8.48 E+8	3.83 E+8	29.31 E+9	1.51E+9
E.	<i>HYD + Gas model</i>	1.5 E+8	1.08 E+9	82.62 E+9	1.51E+9
F.	<i>HYD + Aquifer model</i>	2.46 E+8	1.11 E+8	8.49 E+9	2.38 E+9

Table E-9a: Initial estimates of free gas, hydrate and water for East Barrow

Table E-9b shows initial free gas estimates (at STD condition). These estimates include gas associated with hydrates. The basis for calculating hydrate associated gas is: one reservoir volume of hydrate (res ft3) is equal to 174 SCF of free gas.

Scenario	Reservoir Model	Hydrate Associated Free Gas, ft3	Free Gas	Total Initial Gas In Place (Free + Hydrate Associated)
		SCF	SCF	SCF
A.	<i>Only Gas model</i>	0.00	94.21 E+9	94.21 E+9
B.	<i>Gas + Aquifer model</i>	0.00	27.32 E+9	27.32 E+9
C.	<i>HYD + Gas + Aquifer model (Best Case)</i>	26.13 E+9	15.84 E+9	41.96 E+9
D.	<i>Only HYD model</i>	147.62 E+9	29.31 E+9	176.93 E+9
E.	<i>HYD + Gas model</i>	26.1 E+9	82.62 E+9	108.72 E+9
F.	<i>HYD + Aquifer model</i>	42.8 E+9	8.49 E+9	51.30 E+9

Table E-9b: Initial Gas In Place (Free Gas + Hydrate Associated Gas) for East Barrow

Field Level Match

1. Cumulative gas production

Figure 59 is a plot showing cumulative gas production obtained for several scenarios. The production history data has also been plotted on the same graph. The cumulative gas production profile for all cases matches perfectly with the production data. However, Scenario-F (HYD+Aquifer model) has produced slightly less than actual production data. This can be attributed to the unavailability of free gas for production. Table E-10 shows cumulative gas production for each case.

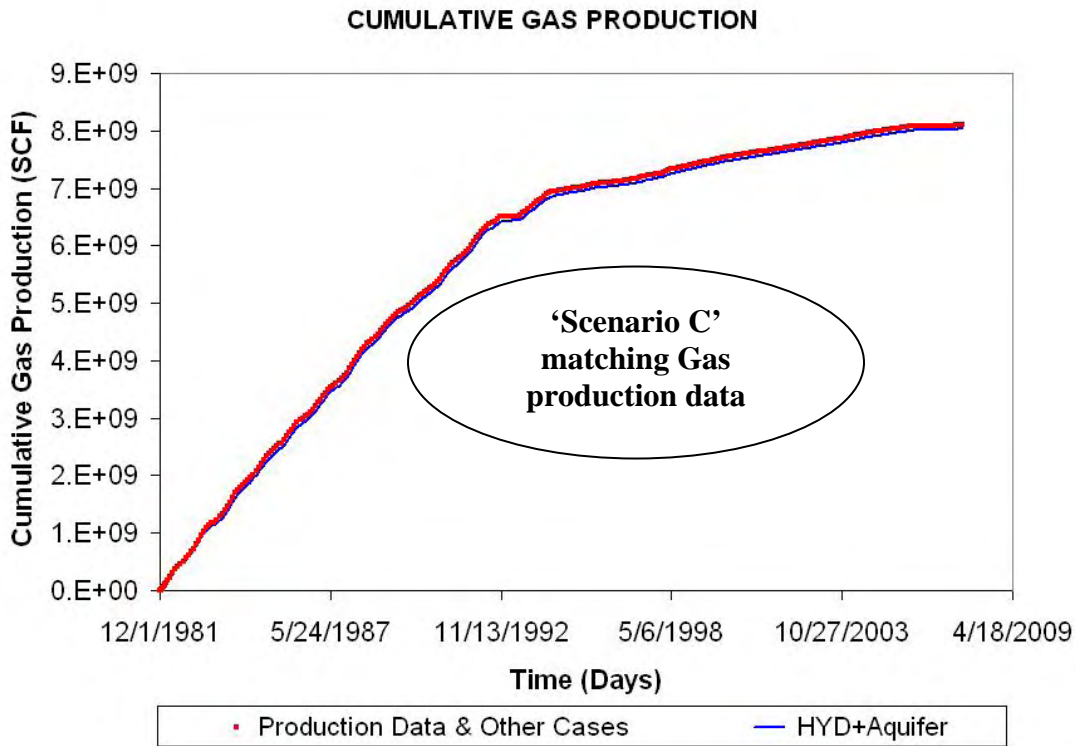


Figure 59: East Barrow Cumulative gas production profile (History Matching)

SCENARIO	SIMULATION RESULT Cumulative Gas Production (September 2007)
Production History Data	8.11 E+9 SCF
Scenario A to E	8.11 E+9 SCF
Scenario F	8.04 E+9 SCF

Table E-10: Cumulative gas production (September 2007) for East Barrow

2. Cumulative Water Production

The cumulative water production plot is shown in Figure 60. Water production is reported in barrels. As seen from the plot, the cumulative water production for different scenarios ranges from 20 barrels of water in case of Scenario-A to 9000 barrels of water in case of Scenario-B. Table E-11 presents the cumulative water production at the end of the simulation run.

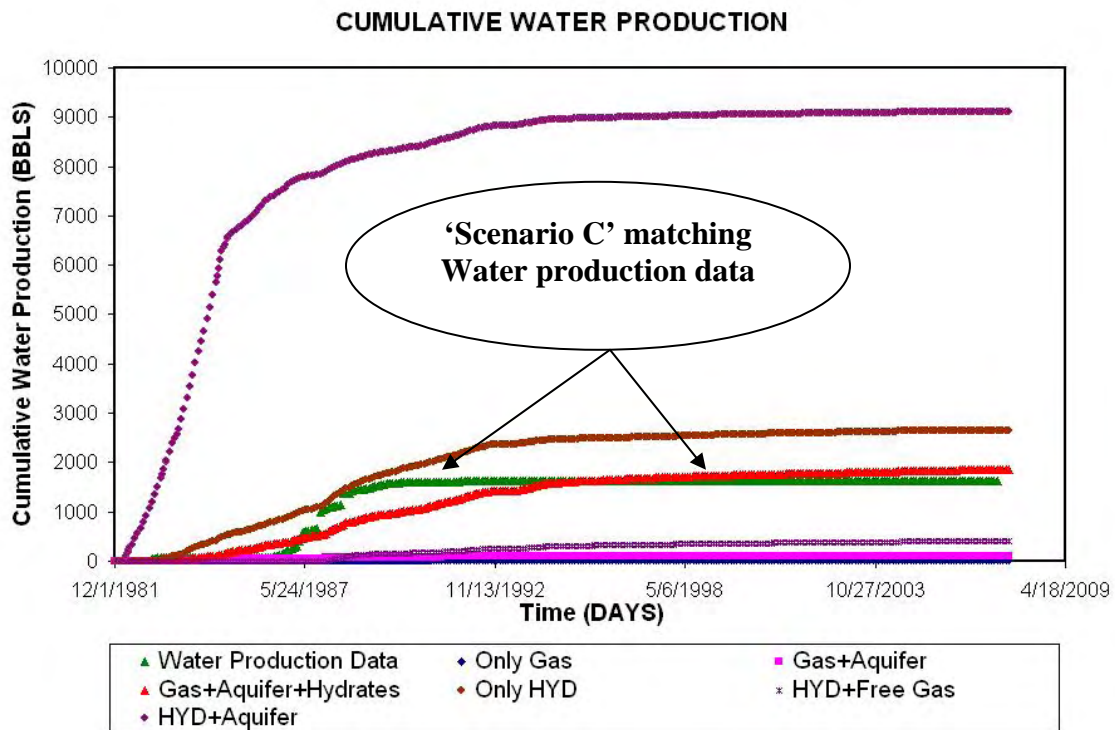


Figure 60: Cumulative water production profile (History Matching) for East Barrow

SCENARIO	SIMULATION RESULT Cumulative Gas Production (Septemeber 2007)
Production History Data	1631 BBLS
Scenario A (Gas Only)	19 BBLS
Scenario B (Gas + Aquifer)	106 BBLS
Scenario C (HYD + Gas + Aquifer)	1850 BBLS
Scenario D (HYD Only)	2660 BBLS
Scenario E (HYD + Free Gas)	406 BBLS
Scenario F (HYD + Aquifer)	9110 BBLS

Table E-11: Cumulative water production (September 2007) for East Barrow

The plot and table results clearly suggest that the Scenario C (Hydrate + Free Gas + Aquifer) closely matches the water production profile and the cumulative water production at the end of the simulation.

Another important observation made between Scenario C and the production data is the initial and final slope of cumulative water production profile. Initially, water production is lower than at later times; however, the gas production profile is completely opposite (refer to Figure 60). This phenomenon is a typical signature of hydrate dissociation. With free gas-water contact far away from the producing well (completed in hydrate zone), the only source of water is dissociating hydrates. High gas production reduces reservoir pressure initially, causing hydrate dissociation. Dissociation is a slow process, and produced water during hydrate dissociation initially gets trapped within the pore spaces and remains immobile. With continuous hydrate dissociation, a critical water saturation is achieved and then water becomes mobile. Being heavier than gas, mobile water falls by gravity segregation and is produced along with gas. This explains the late stage water production being higher in the case of the East Barrow gas reservoir and Scenario C.

Water production in the case of other scenarios corresponds to the availability of free water. With no free water available in Scenario A, the water production is near zero. However, with similar conditions in Scenario D, the water production is as high as 2660 BBLS. This is primarily due to the hydrate dissociation effect, hence producing lots of free and mobile water that gets produced along with gas. The water production exceeds limits in the case of a hydrate-aquifer system (Scenario F). The combined effect of available water, scarcity of free gas and dissociating hydrates causes large volumes of produced water in this case.

3. Average reservoir pressure

Pressure at grid block 19, 19 1 has been chosen to represent average reservoir pressure. Figure 61 shows average reservoir pressure response for all scenarios. Actual reservoir pressure response has also been plotted on the same graph. Table E-12 presents the root mean square error between available reservoir pressure history data and model output. Table E-12 quantifies the reservoir pressure match and helps in analyzing the results.

The plot in Figure 61 shows a close match between pressure data and model response for Scenario C and Scenario F. The error check for the two scenarios shows a better match in case of Scenario F. In other words, this means that a reservoir model with hydrates and aquifer presents a better match than hydrate+free gas+aquifer type model. But, Scenario C was able to successfully match production data during field level match (refer cumulative gas production match and cumulative water production match discussed above). On the other hand, Scenario F was unsuccessful in matching gas production and water production data. Also, the absence of hydrate-free gas contact in case of Scenario F violates observations from well log data.

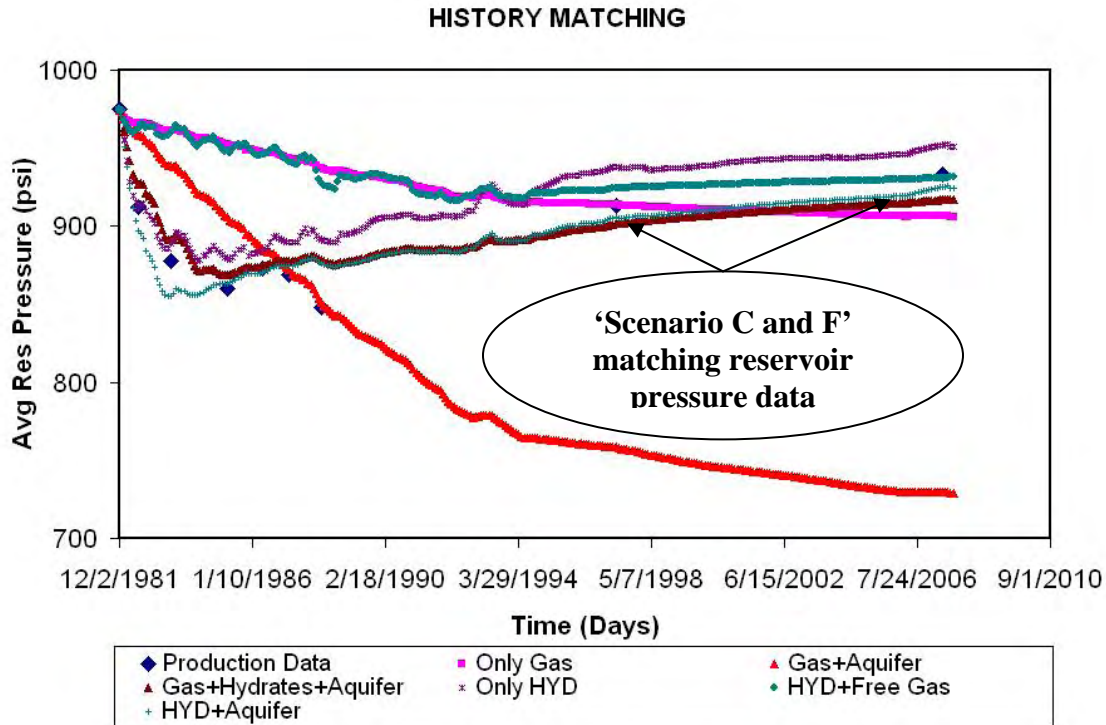


Figure 61: Average Reservoir Pressure Match (History Matching) for East Barrow

To summarize, Scenario C i.e. a reservoir model with hydrate free gas contact at 2050’ and free gas-water contact at 2080’ closely matching the field level response. Based on this conclusion, the best case model has been chosen for further fine tuning to match individual well response.

SCENARIO	SIMULATION RESULT Root Mean Square Error
Production History Data	N/A
Scenario A (Gas Only)	7.10
Scenario B (Gas + Aquifer)	9.30
Scenario C (HYD + Gas + Aquifer)	1.56
Scenario D (HYD Only)	2.28
Scenario E (HYD + Free Gas)	6.69
Scenario F (HYD + Aquifer)	1.50

Table E-12: Root Mean Square Error (Reservoir Pressure Data vs Model Output) for East Barrow

Well Level Match

1. Gas Production Rate

The best case model has been chosen to match individual well level match. The first attempt was made to obtain a match between the gas production data. Figures 62-66 clearly show a perfect match between individual well production and monthly production history data of each well.

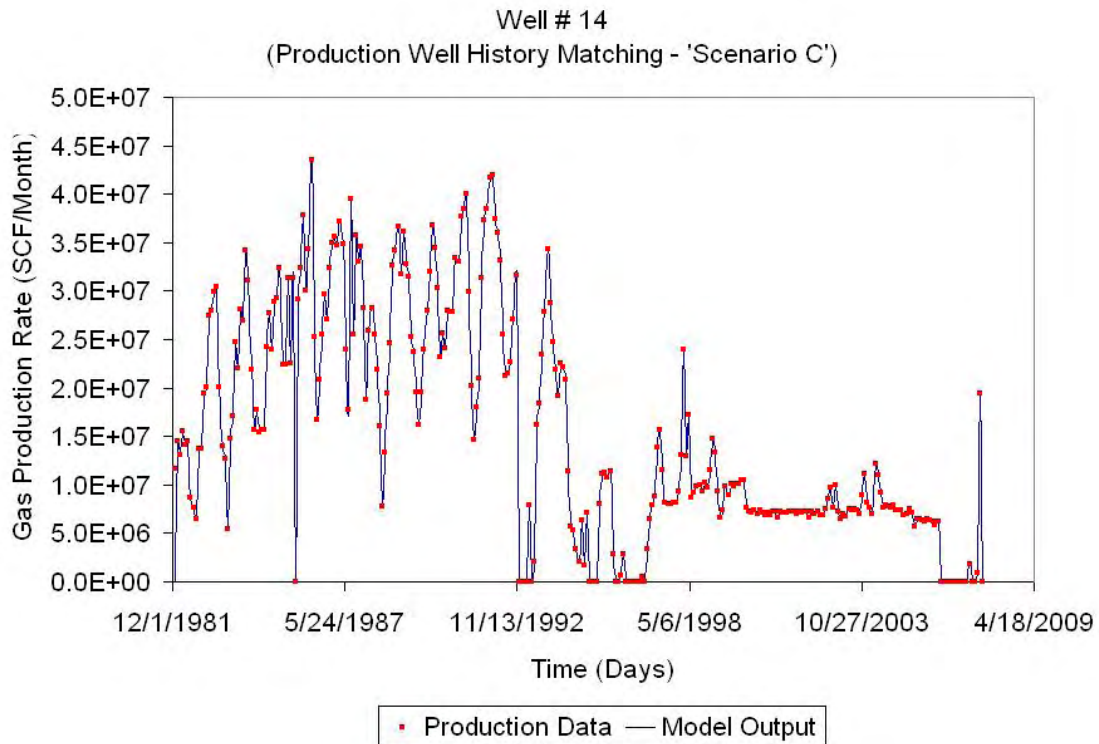


Figure 62: Gas production rate matching - Well EB#14

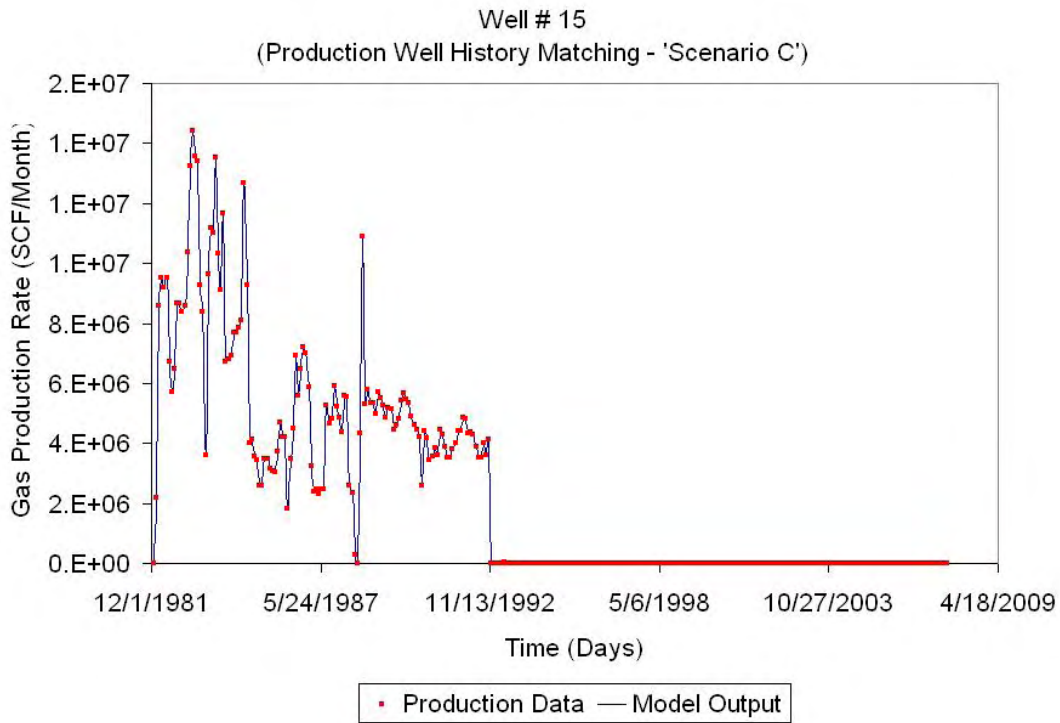


Figure 63: Gas production rate matching - Well EB#15

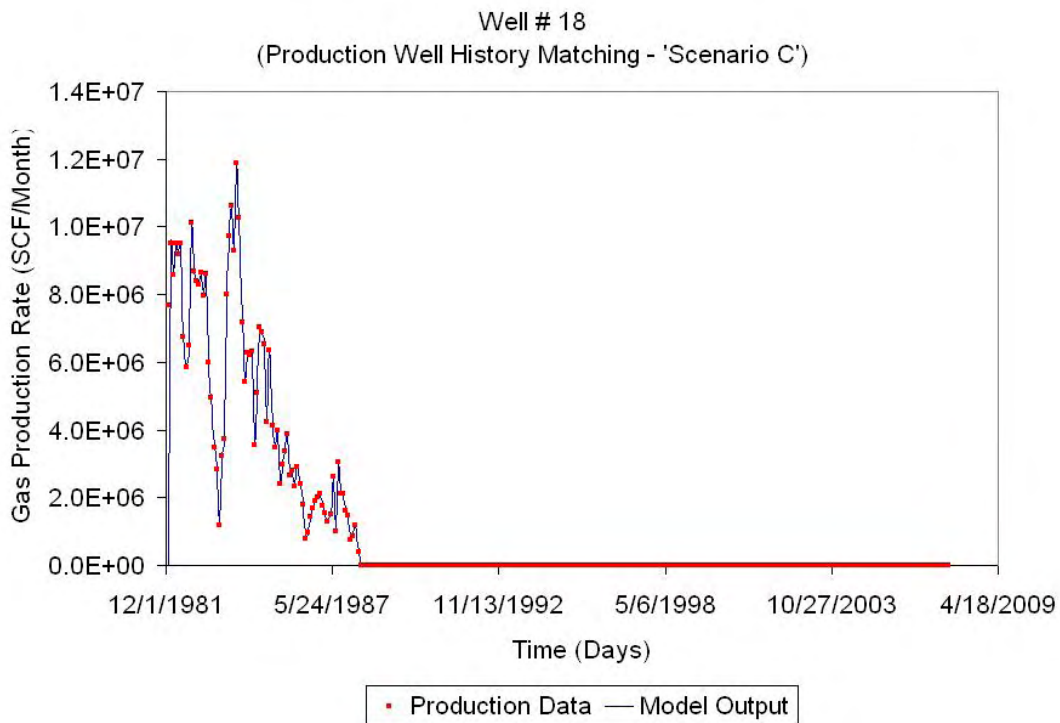


Figure 64: Gas production rate matching - Well EB#18

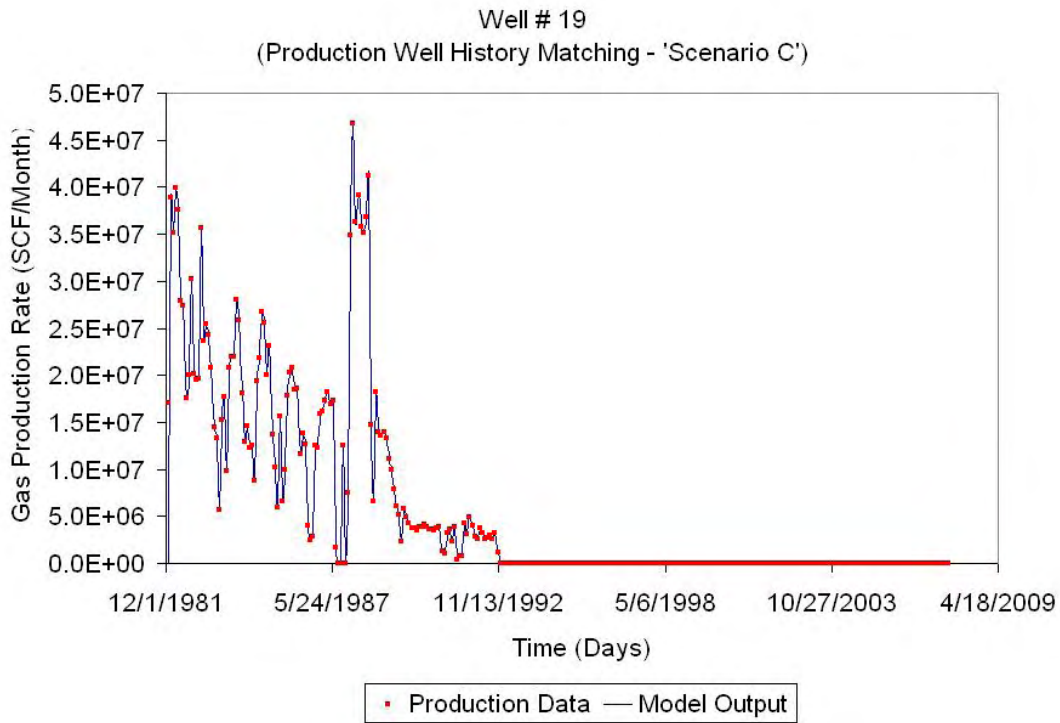


Figure 65: Gas production rate matching - Well EB#19

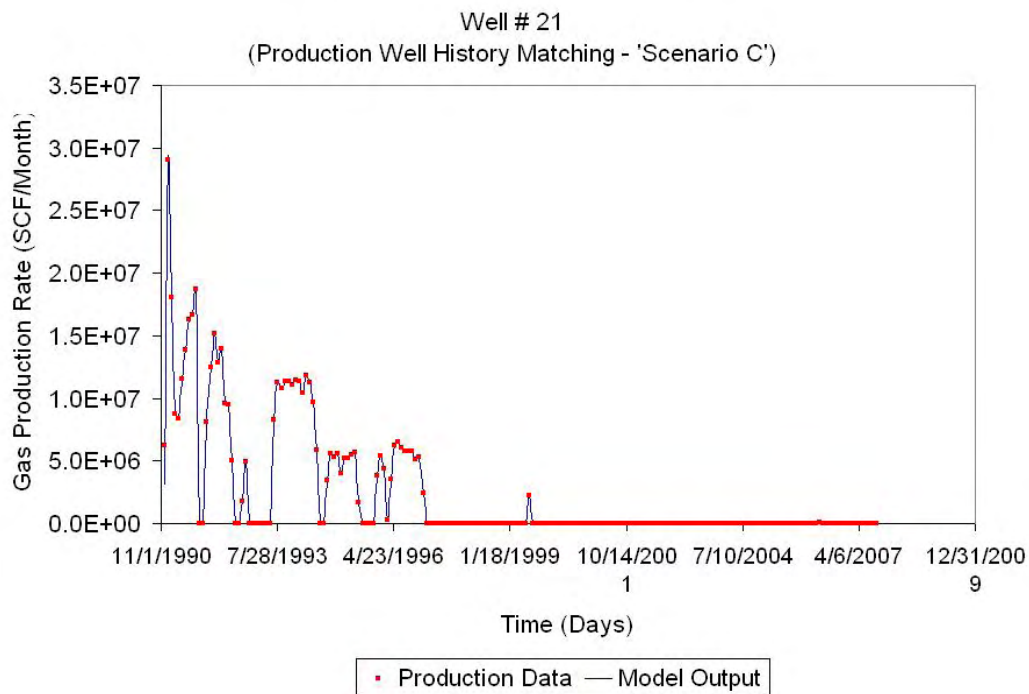


Figure 66: Gas production rate matching - Well EB#21

2. Water Production Rate

The second parameter matched at the individual well level is the water production rate. The cumulative water production data for the East Barrow gas pool is around 1630 BBLS, the quantity is negligible and well level matching may not be a good estimate. However, well level match has been performed for comparison purposes. Figures 67-71 compare the water production rate for wells EB#14, EB#15, EB#18, EB#19, EB#21, respectively.

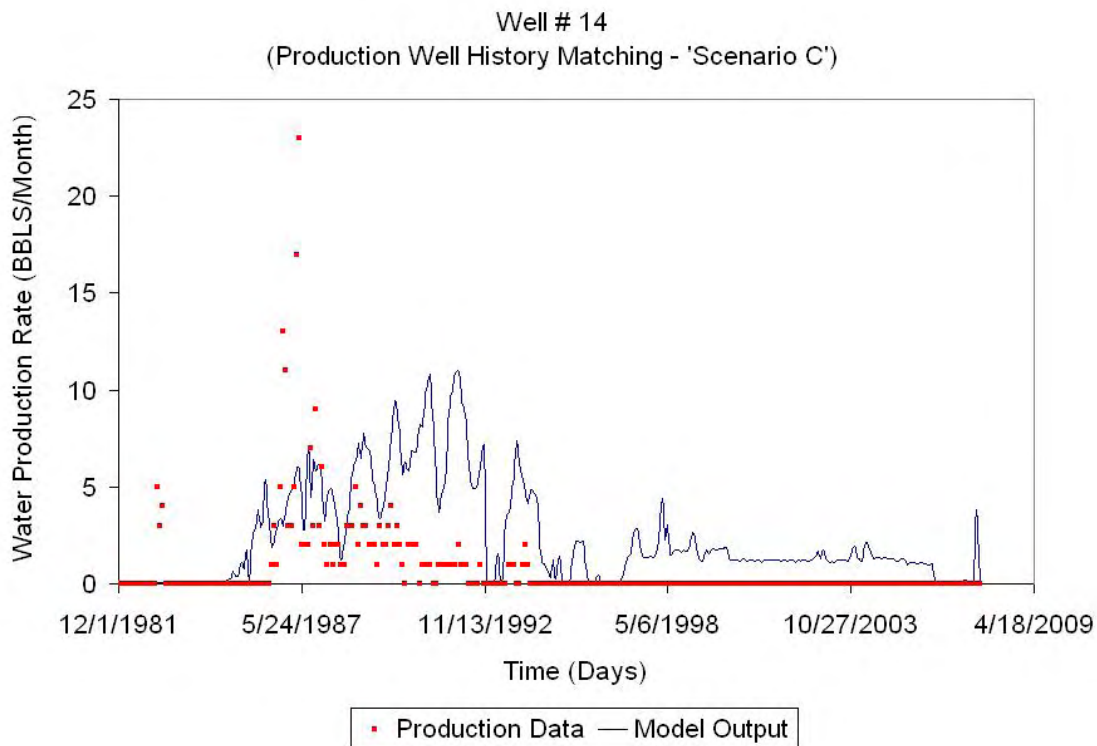


Figure 67: Water production rate matching - Well EB#14

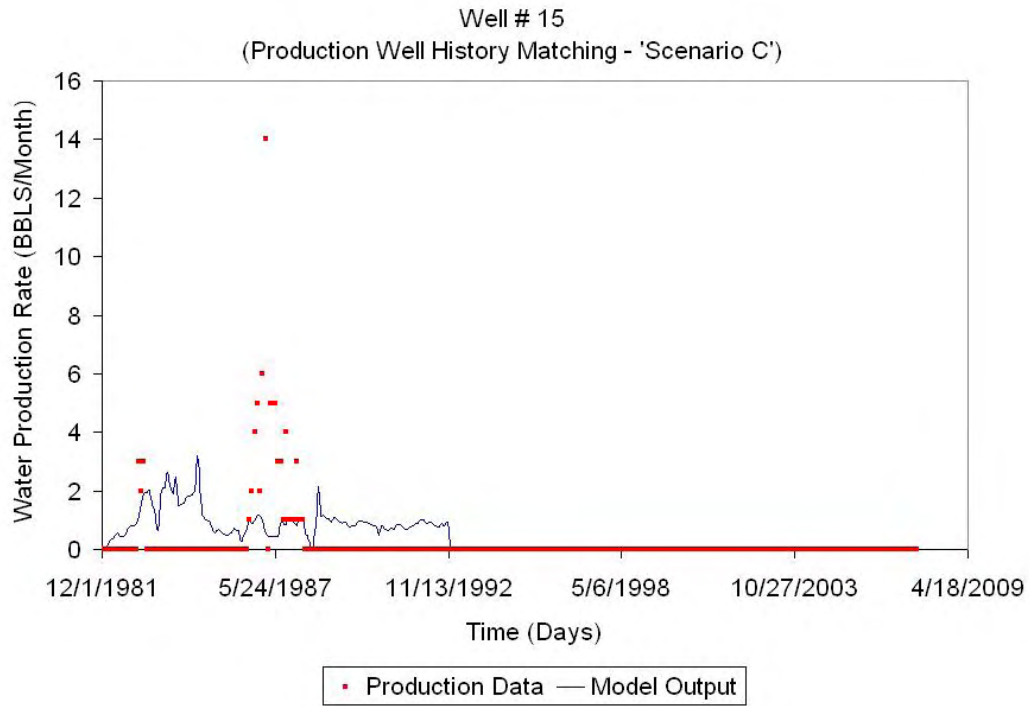


Figure 68: Water production rate matching - Well EB#15

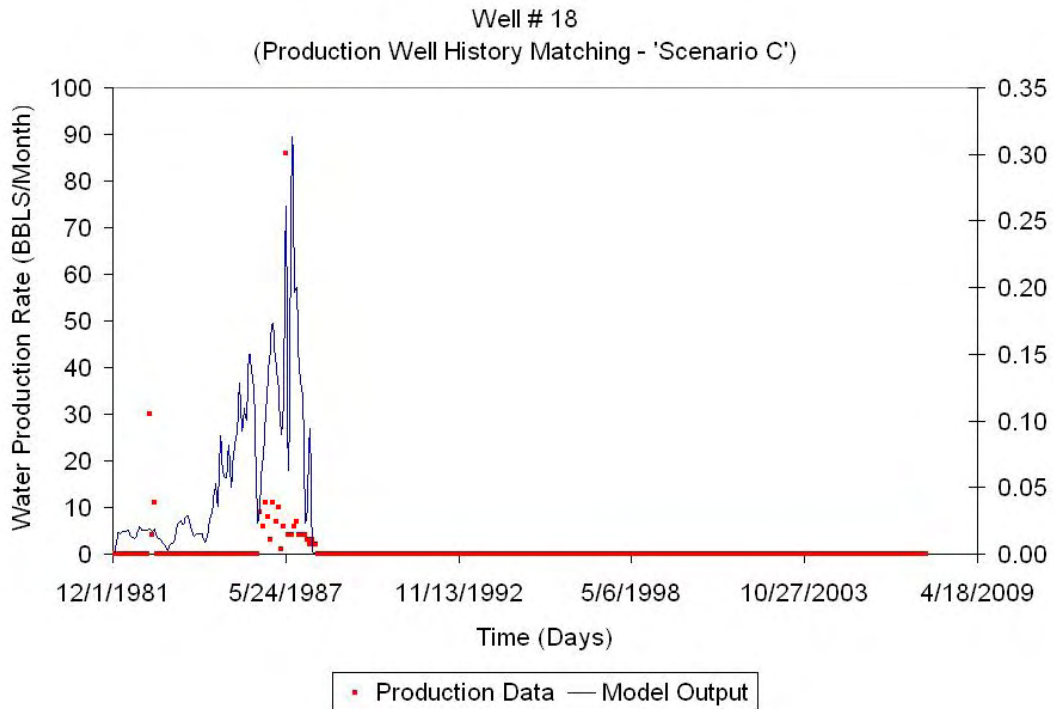


Figure 69: Water production rate matching - Well EB#18

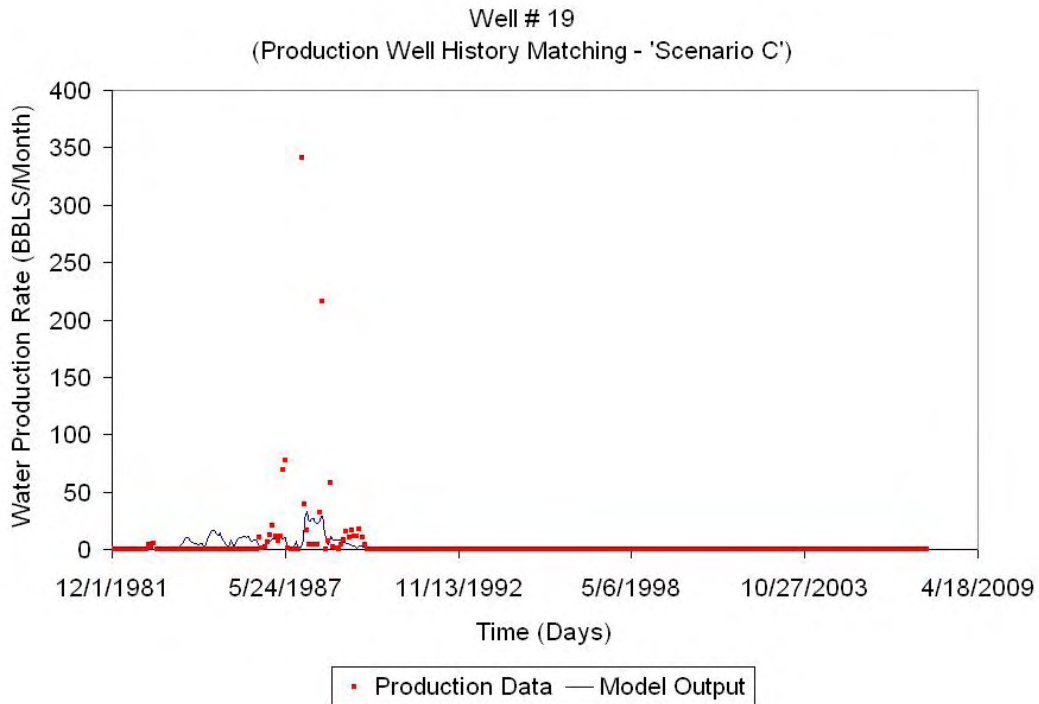


Figure 70: Water production rate matching - Well EB#19

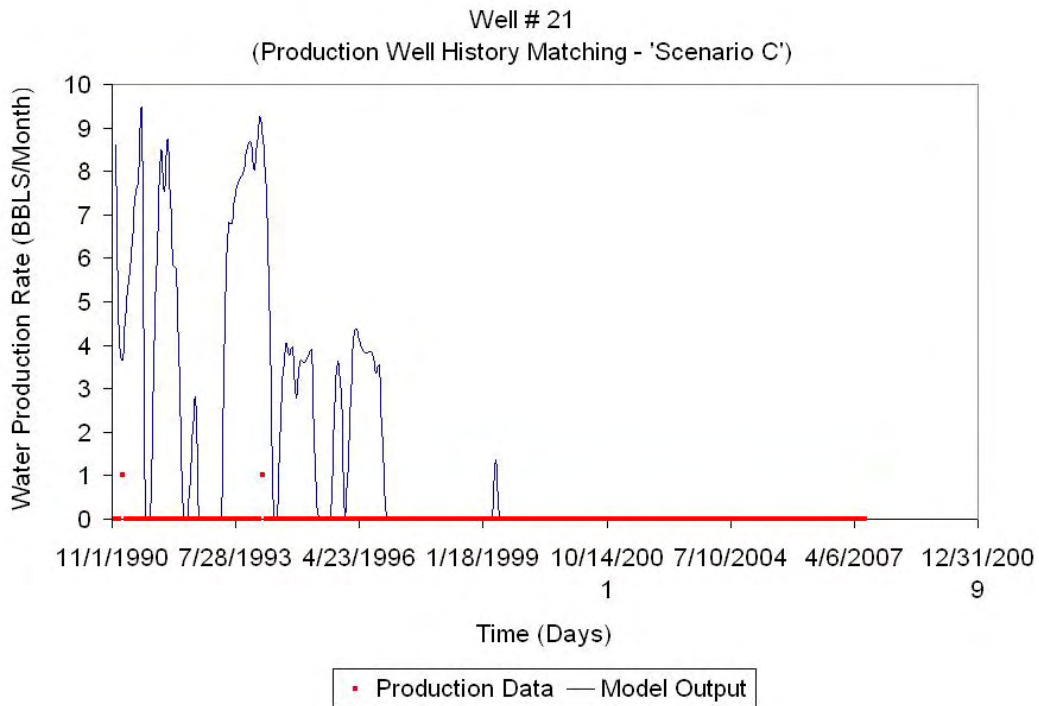


Figure 71: Water production rate matching - Well EB#21

II. EAST BARROW DATA ANALYSIS

A. Three phase saturation profile within hydrate zone (all layers in hydrate zone)

The initial conditions for the best case model have already been discussed under Model Initialization. The simulated output can be used to study the current reservoir condition after 26 years of gas production. The aim is to investigate the active zones/regions of hydrate dissociation, zones of higher water saturation and increasing gas saturation. To understand the profile of three phases, grid blocks 19, 19 (K =1 to 25) (refer Figure 32) have been chosen. All the grid blocks in K direction lay within the hydrate zone and hence, provide an excellent opportunity to study reservoir dynamics within the hydrate zone. Figures 72, 73 and 74 show hydrate, gas and water phase variation within the hydrate zone during the production life of the reservoir.

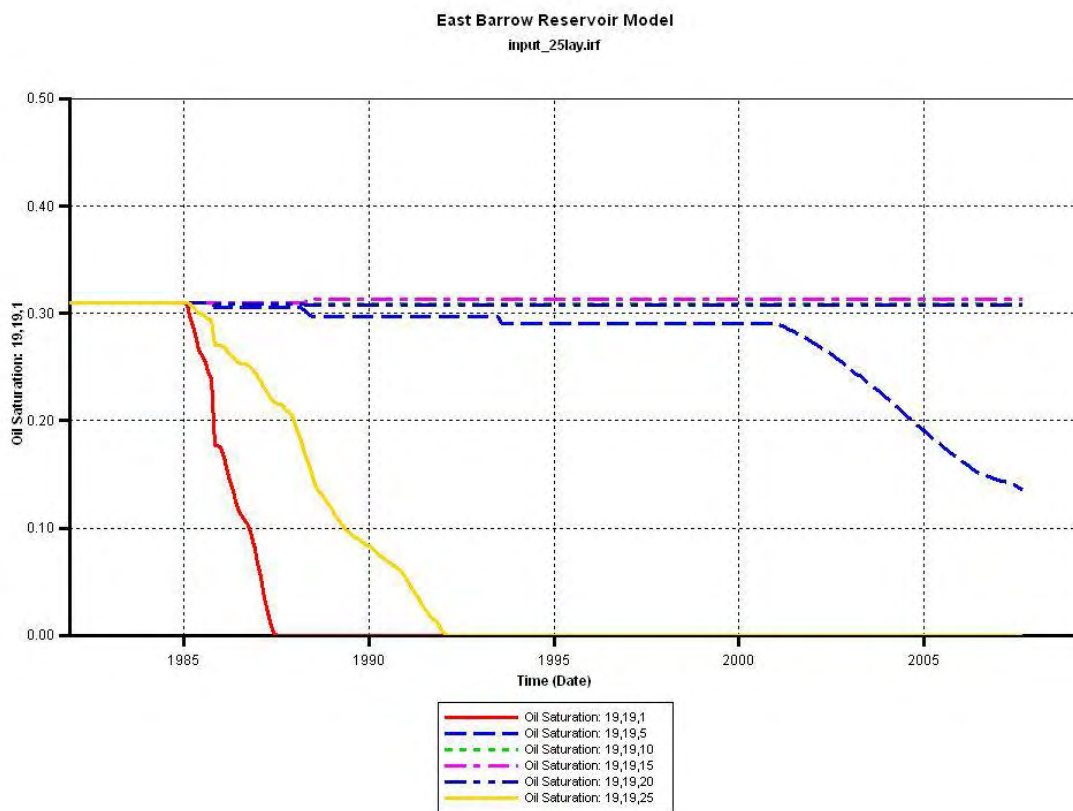


Figure 72: Hydrate Saturation Profile (Location 19,19 (k=1 to 25)) for East Barrow

The plot shows rapid reduction in hydrate saturation at and near the top and bottom of the reservoir. This suggests that for locations where all grid blocks (k = 1 to 25) of the model are in the hydrate zone, hydrate dissociation is governed by heat transfer from overburden and underburden rocks.

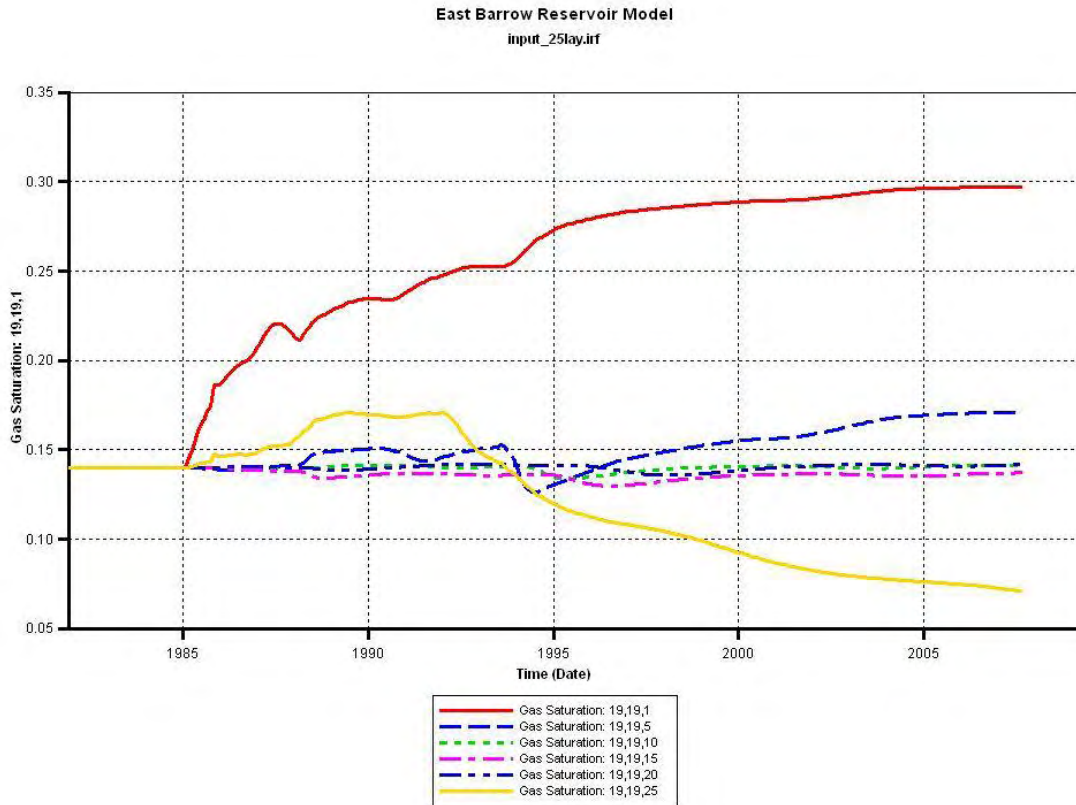


Figure 73: Gas Saturation Profile (Location 19,19 (k=1 to 25)) for East Barrow

Figure 73 displays the gas saturation profile within the hydrate zone for grid blocks 19 19 (k=1 to 25). The decrease in hydrate saturation at and near the top of the reservoir is partially occupied by produced gas and partially by water. However, at the bottom of the reservoir (at and near K =25), the hydrate dissociation initially increases the gas saturation but later due to gravity segregation the mobile water falls to the bottom of the reservoir and thereby decreases the gas saturation and correspondingly increases the water saturation. Figure 74 follows a similar trend. Water saturation at the top of the reservoir rises due to hydrate dissociation followed by saturation decrease due to falling water. Similarly water saturation increases by many fold at the bottom of the reservoir due to gravity segregation.

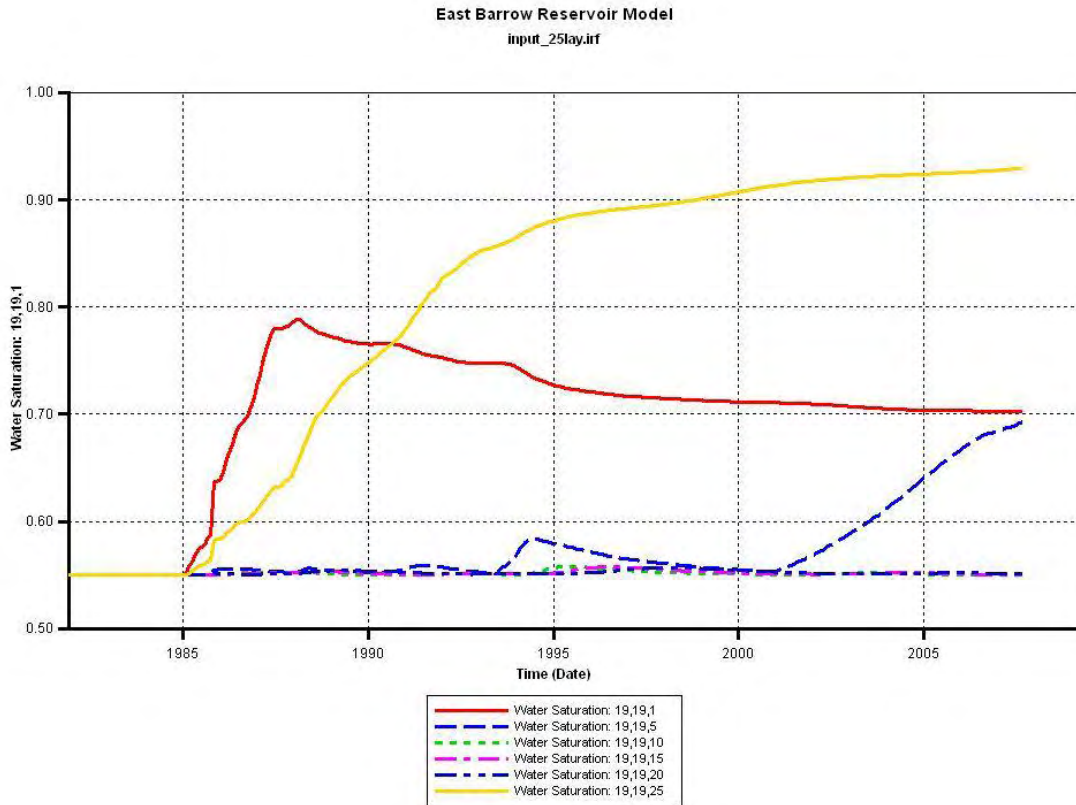


Figure 74: Water Saturation Profile (Location 19,19 (k=1 to 25)) for East Barrow

B. Three phase saturation profile within Hydrate-Free Gas-Aquifer zone

Grid blocks 29, 8, (K=1 to 25) (refer to Figure 75) have been chosen to understand the reservoir dynamics during gas production. The grid blocks in k-directions include all the three zones (hydrate-free gas-aquifer). The hydrate-free gas contact was found at K=8, whereas the free gas-water contact was found at K=22. Three plots are generated to study the impact of free gas production on hydrate dissociation and the effect of gravity on water saturation.

Figure 76 shows the variation in hydrate saturation within the hydrate zone. It can be seen that the effect of gas production and overburden temperature increases the rate of hydrate dissociation at and near the top of the reservoir. However, near the hydrate-free gas interface, the rate of hydrate dissociation is mainly governed by depressurization.

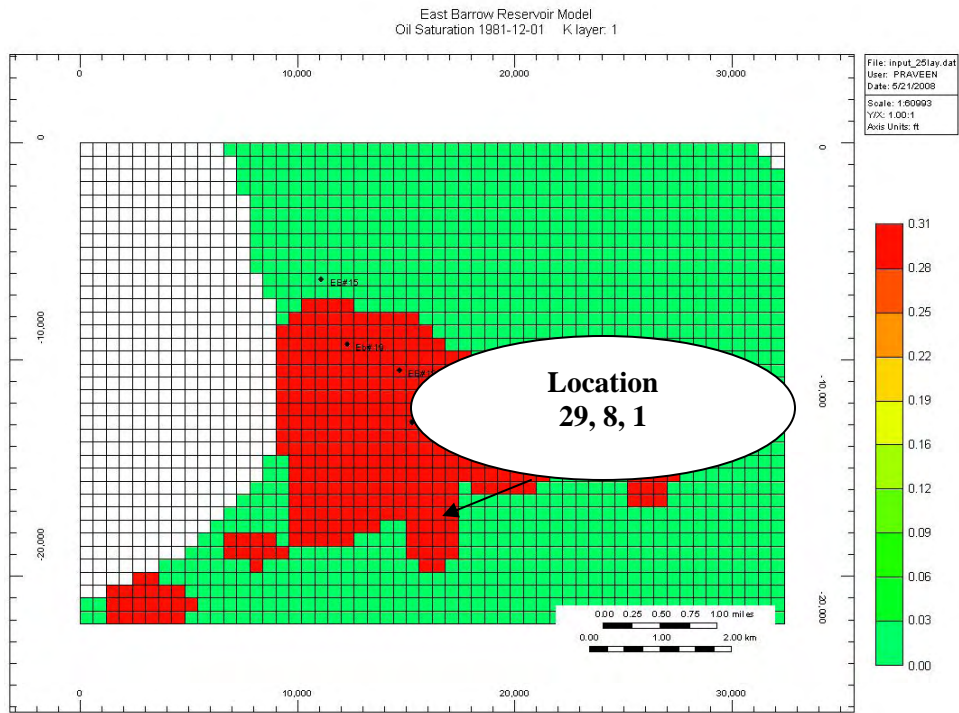


Figure 75: Location 29,8,1 (Representing Hydrate-Free Gas-Aquifer Zone) for East Barrow

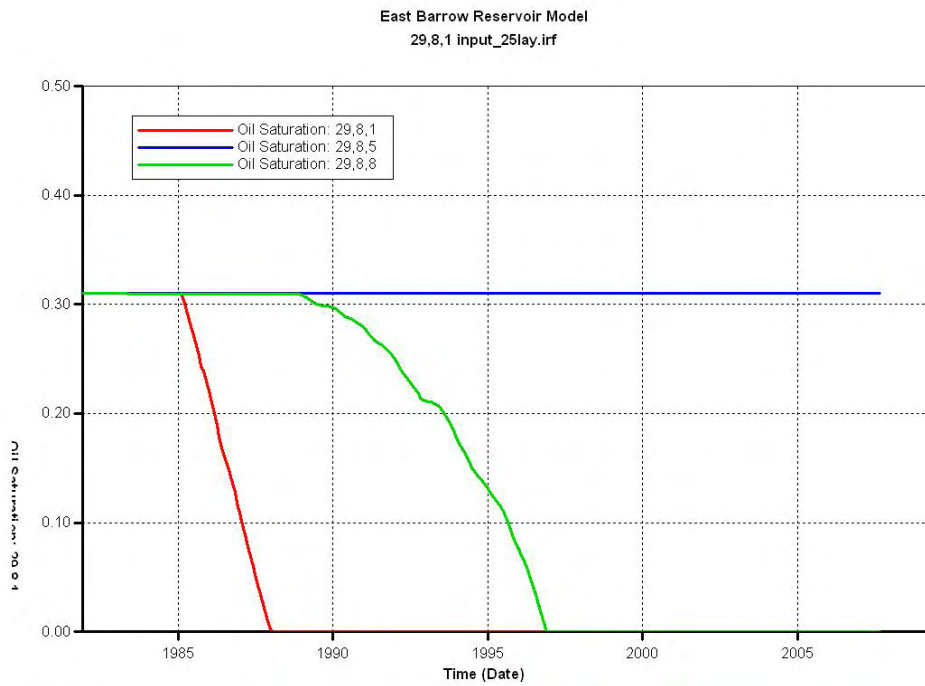


Figure 76: Hydrate Saturation Profile (Location 29,8 (k=1 to 8)) for East Barrow

East Barrow Reservoir Model
29,8,1 input_25lay.irf

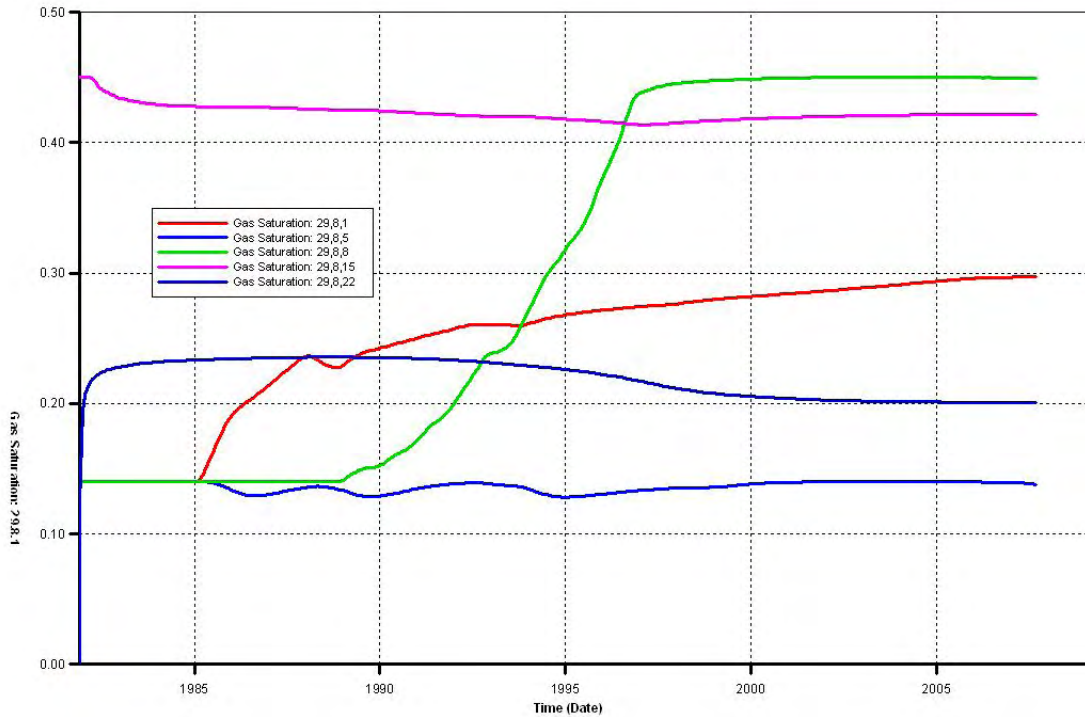


Figure 77: Gas Saturation Profile (Location 29,8 (k=1 to 22)) for East Barrow

The gas saturation profile is presented in Figure 77. The gas saturation at the top of the reservoir has increased due to hydrate dissociation. However, the gas saturation increase is limited to 30% as the rest of the reservoir pores are occupied by free water. The gas saturation at K=5 remains unchanged as hydrate saturation remains undissociated so far. Near the hydrate-free gas interface (k=8), the gas saturation increases slowly with hydrate dissociation and reaches a maxima of 45% upon complete dissociation, it shows that the free water has reached the bottom of the reservoir. As expected, the gas saturation in free gas zone (k=15) remains unchanged. Near free gas-aquifer interface (k=22), the gas saturation has dropped from initial saturation of 45% to 20%. The primary reason for this reduction is the water influx from the aquifer zone. The mobile water falling from the hydrate zone may also be collecting near this zone causing reduction in gas saturation. It should be noted that the effect of gas dissolution in water was not considered while initializing the model.

East Barrow Reservoir Model
29,8,1 input_25lay.irf

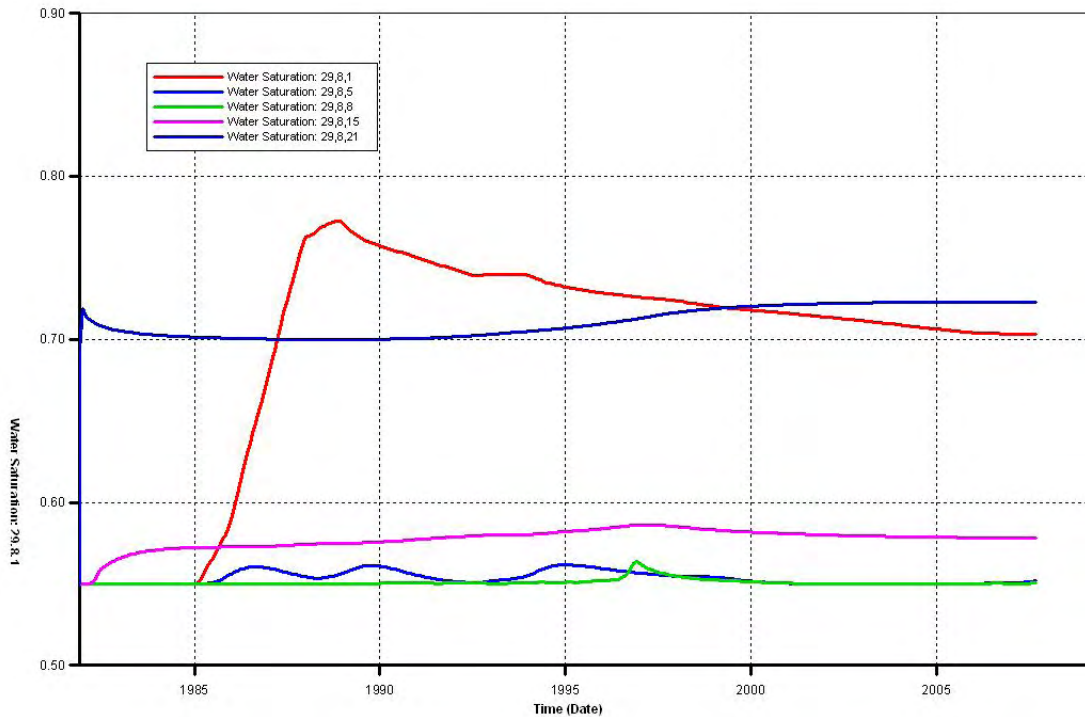


Figure 78: Water Saturation Profile (Location 29,8 (k=1 to 22)) for East Barrow

As discussed previously, the hydrate dissociation causes an increase in water saturation at the top of the reservoir (k=1), but with falling water and rising gas, the water saturation starts to decrease. With no hydrate dissociation near the hydrate-free gas (k=5) zone there is no change in water saturation. Again, the water saturation remains the same in the gas zone. Near the free gas-water contact the water saturation increases from 55% to 70%. This is attributed to water influx from the aquifer zone (during gas production) and hydrate dissociated free water occupying pore spaces at the bottom of the reservoir.

C. Reservoir Properties

Figures 79, 80, 81, 82 and 83 are 3D views of the East Barrow reservoir model showing current distribution of properties like pressure, temperature, hydrate phase, gas phase and water phase saturations, respectively.

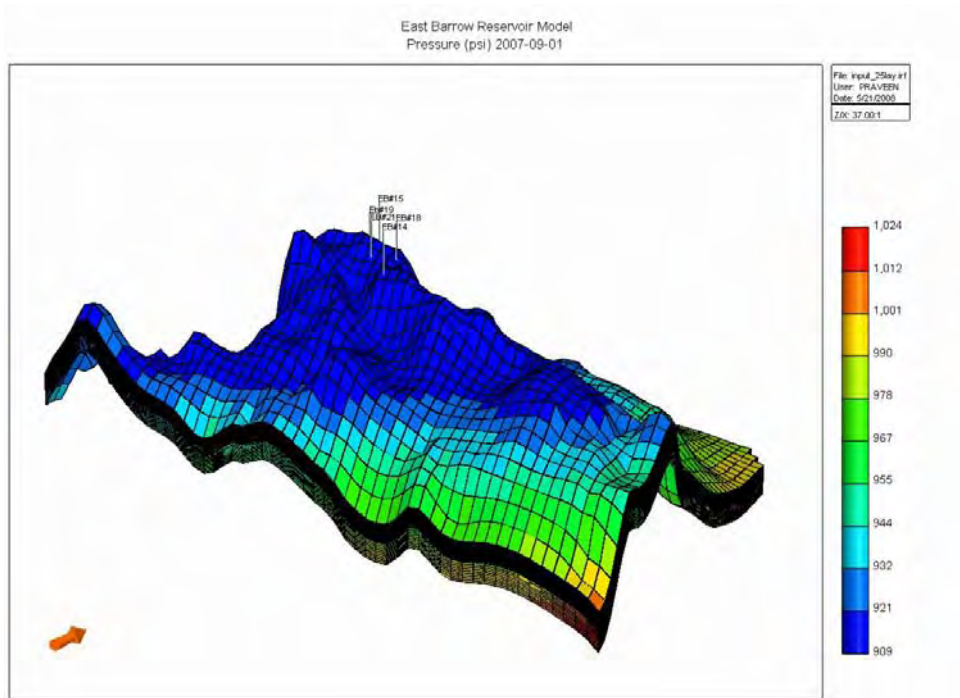


Figure 79: Reservoir pressure (Sep 2007, 3D View) for East Barrow

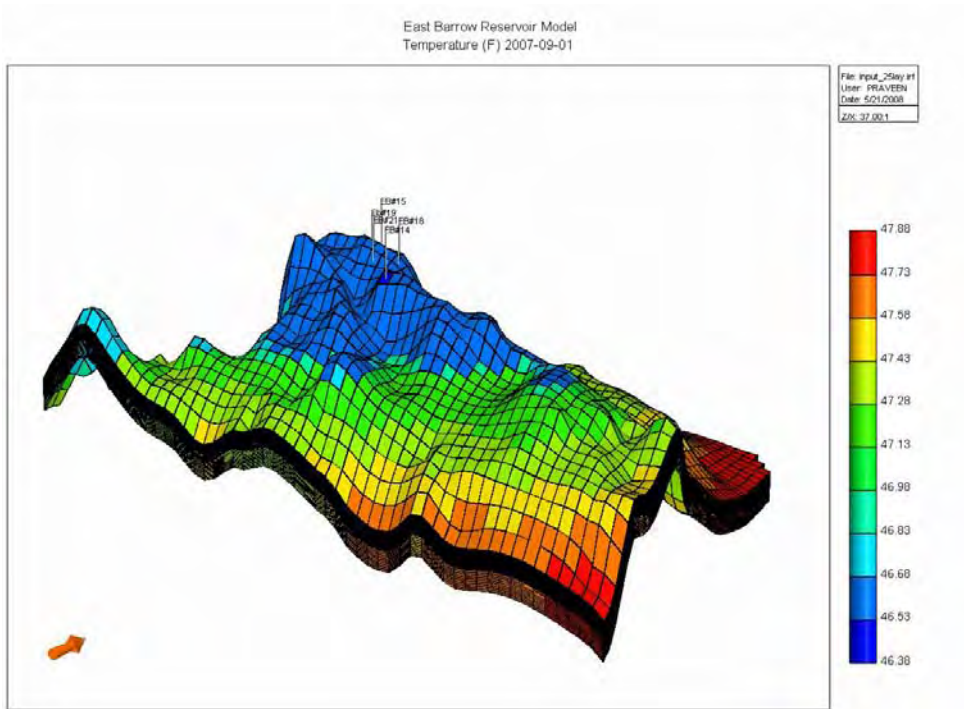


Figure 80: Reservoir temperature (Sep 2007, 3D View) for East Barrow

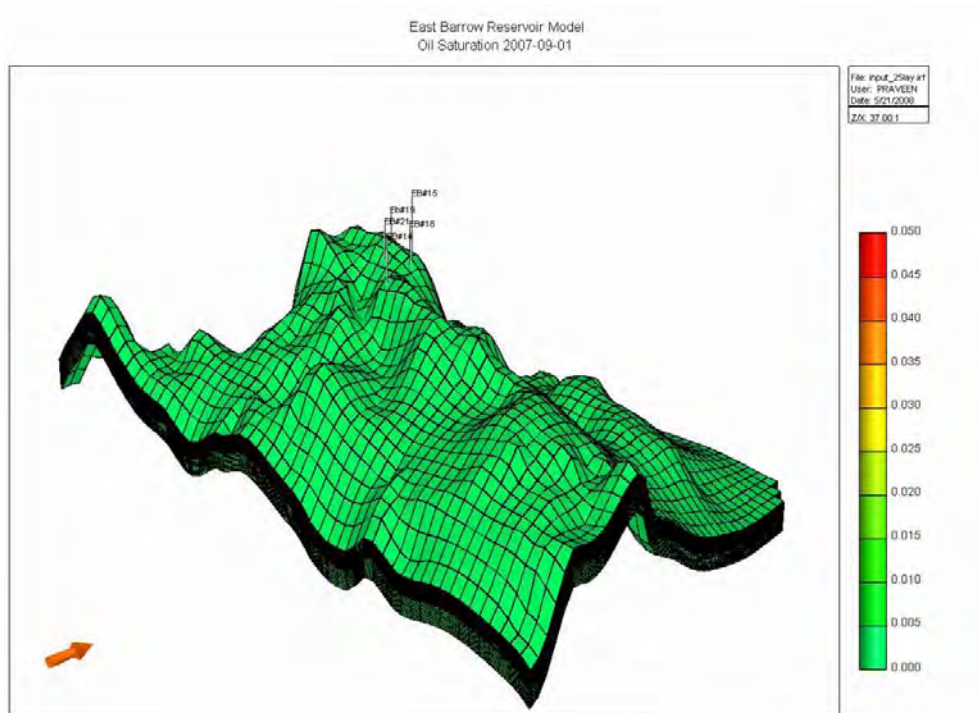


Figure 81: Hydrate saturation (Sep 2007, 3D View) for East Barrow

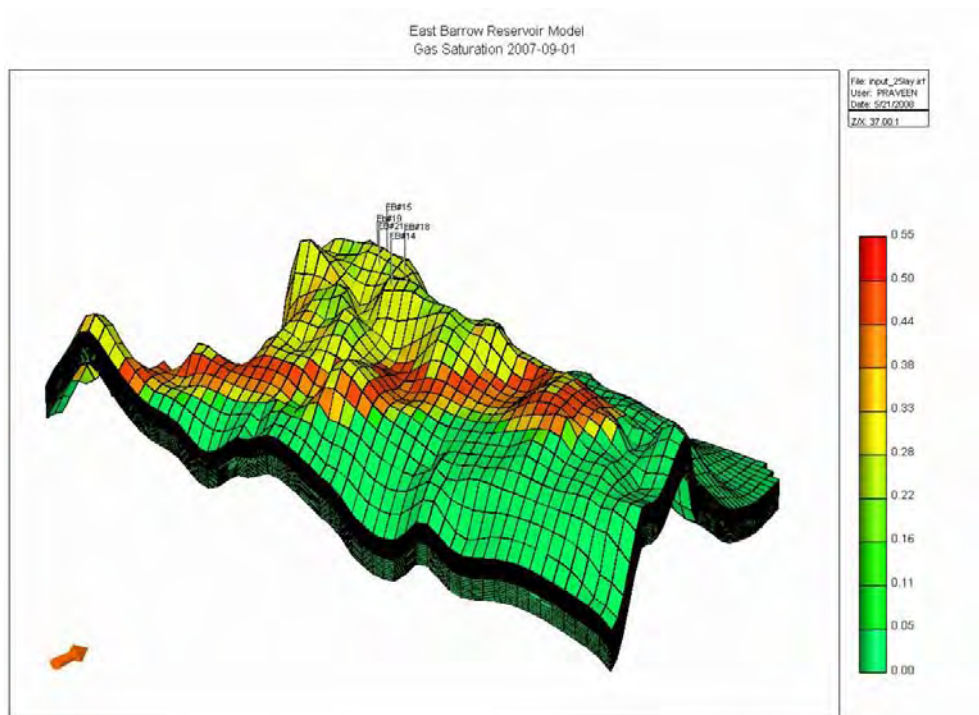


Figure 82: Gas saturation (Sep 2007, 3D View) for East Barrow

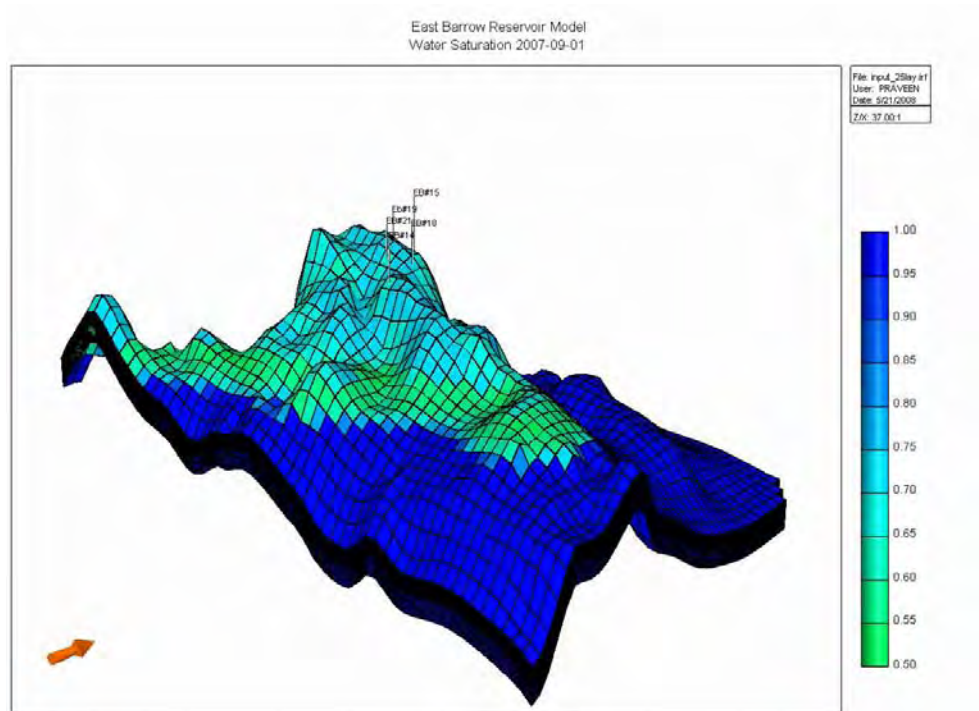


Figure 83: Water Saturation (Sep 2007, 3D View) for East Barrow

D. Hydrate-Free Gas Contact and Free Gas-Water Contact

Figures 84 and 85 show the changes in hydrate-free gas contact. As discussed previously, the hydrate-free gas contact was initialized as 2050'. With hydrate dissociation the contact shifts upward to ~2045'. Figures 86 and 87 show the change in free gas-water contact in the reservoir. The contact shifts upward from an initial depth of 2080' (Dec 1981) to 2070' (Sep 2007).

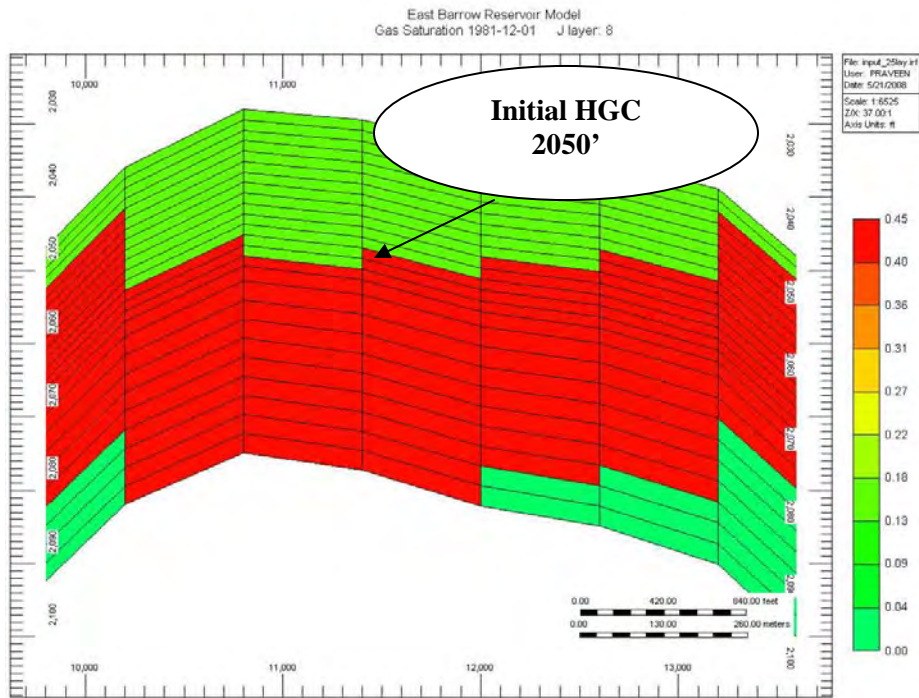


Figure 84: Initial Hydrate-Free Gas Contact (2050', December 1981) for East Barrow

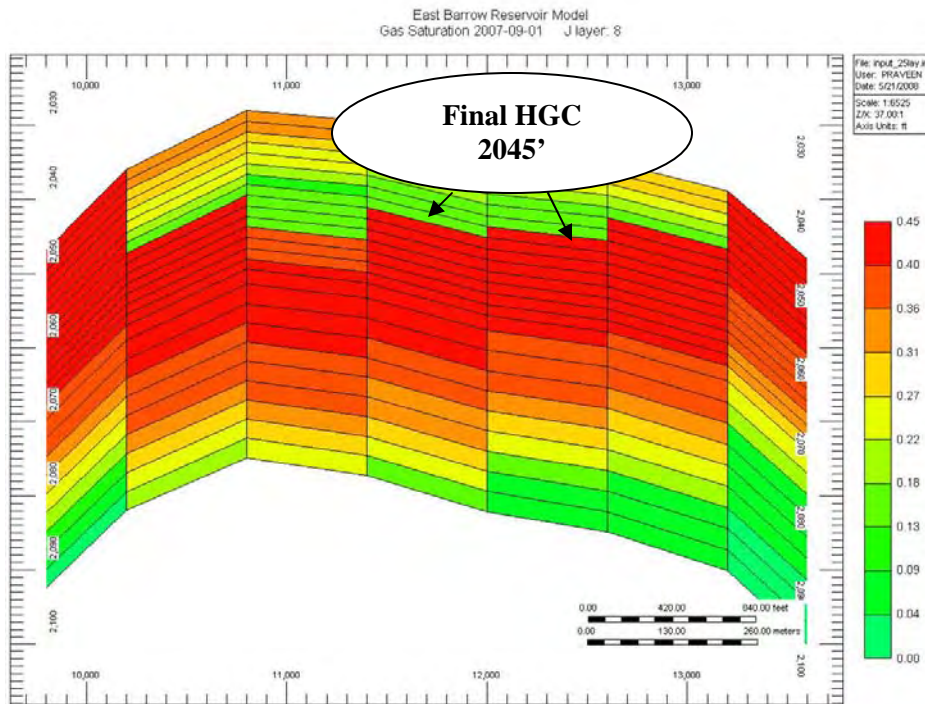


Figure 85: Current Hydrate-Free Gas Contact (2045', Sep 2007) for East Barrow

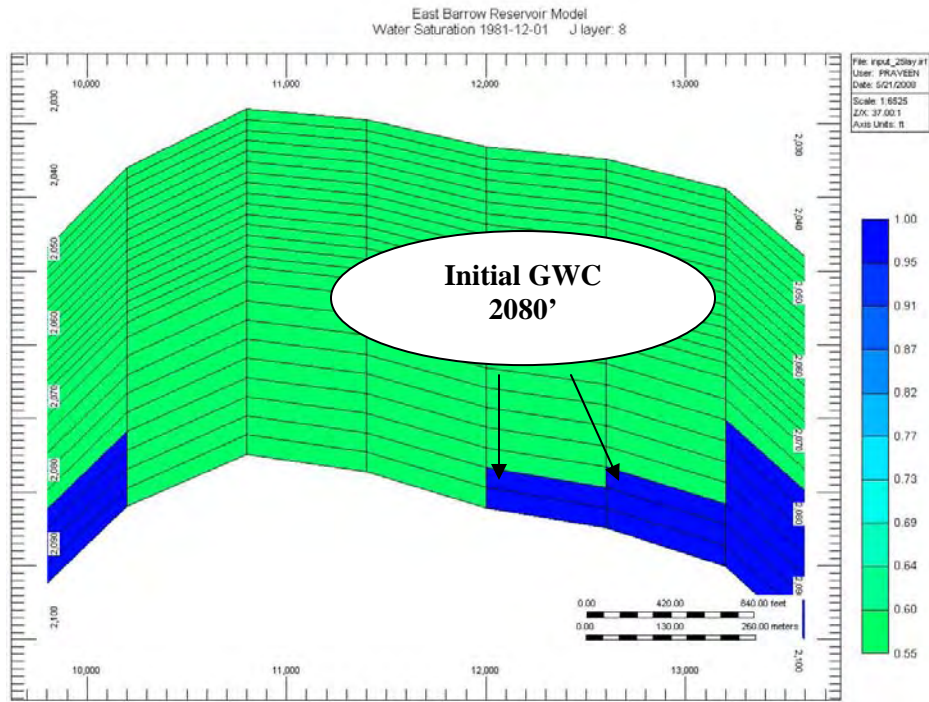


Figure 86: Initial Free Gas-Water Contact (2080', Dec 1981) for East Barrow

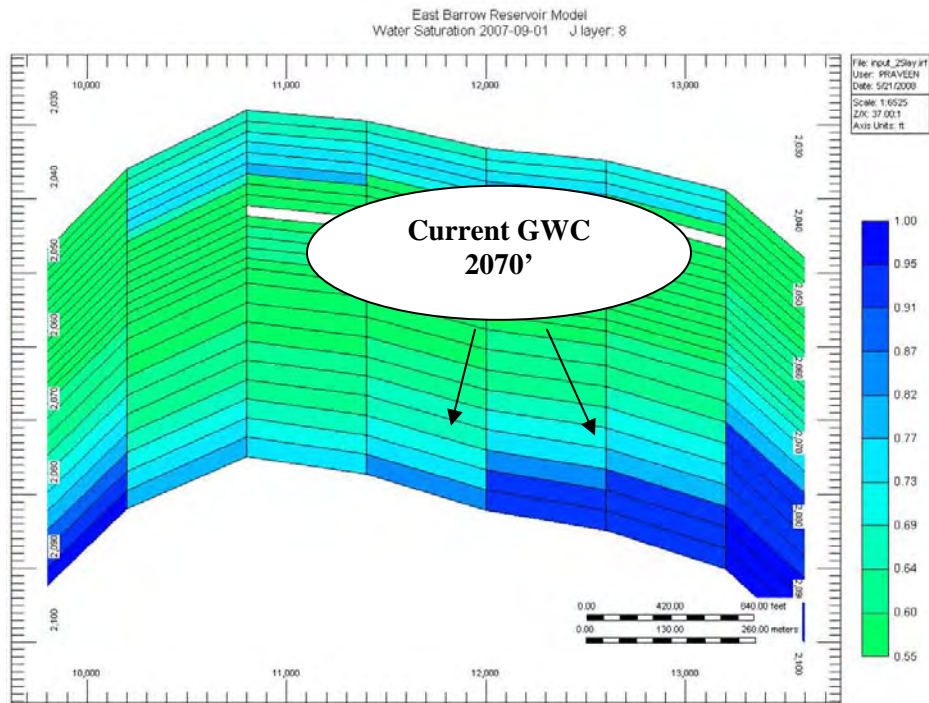


Figure 87: Current Free Gas-Water Contact (2070', Sep 2007) for East Barrow

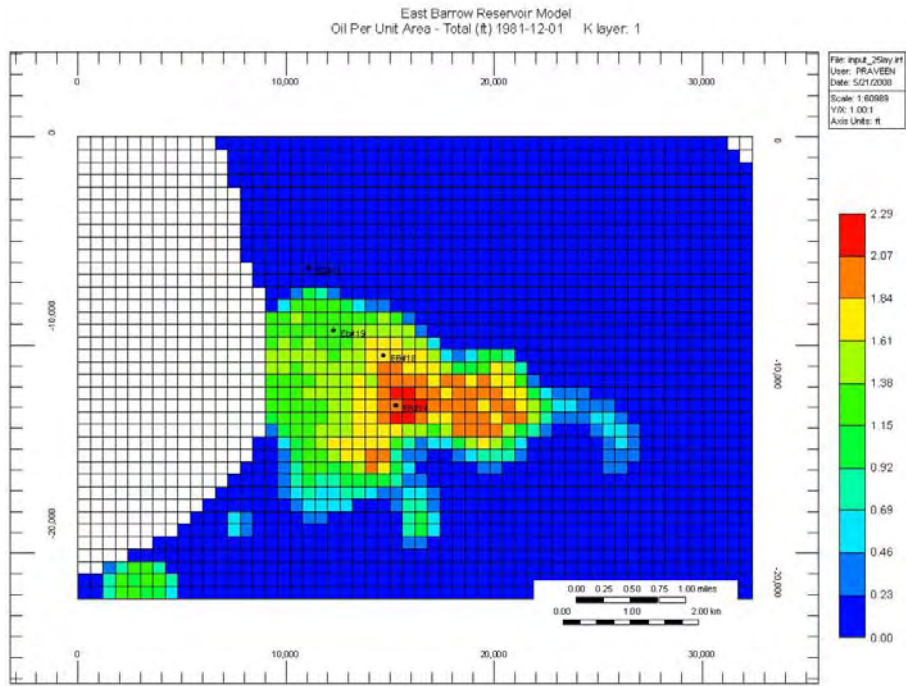


Figure 88: Hydrate per Unit Area-Total (Dec 1981) for East Barrow

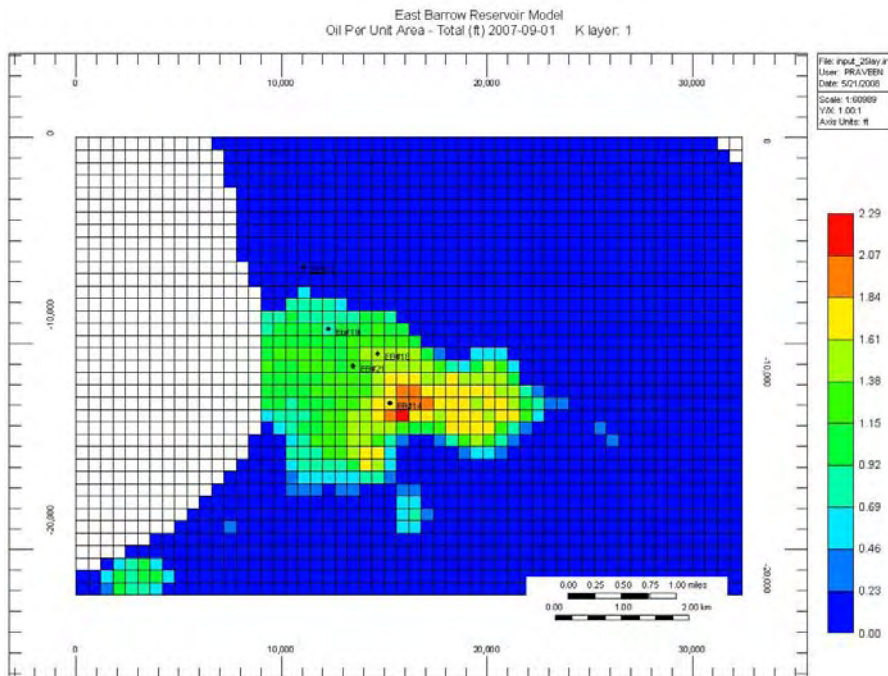


Figure 89: Hydrate per Unit Area-Total (Sep 2007) for East Barrow

E. Hydrate/Free Gas Contribution

To calculate the total gas production from in situ hydrates, reservoir simulation was carried out from the onset of production in 1981 to the present. The difference in hydrate reserve between the two periods provides an estimate of the amount of hydrate dissociated. CMG-STARs calculates hydrate per unit area for each IJ block (all k layer). This information can be used to obtain initial and final hydrate in place, and can be extended to calculate total amount of gas produced from hydrate dissociation, percent hydrate dissociation and contribution of hydrate as percent of gas produced. The area for each grid block is 600' x 600'. Figures 88 and 89 present hydrate per unit area for initial and final conditions, respectively. Total gas produced from hydrate dissociation and percent hydrate dissociation for the best case model is presented in Table E-13.

DESCRIPTION	RESULT
Initial Free Gas in Place	15.8 BSCF
Initial volume of hydrates	1.50 E+8 res ft ³
Initial Standard Condition volume of hydrates	26.1 BSCF
Volume of hydrate dissociated	4.04 E+7 res ft ³
Gas produced by hydrate dissociation	7.04 B SCF
% Hydrate Dissociation (To Sep 2007)	27.0%
Cumulative gas produced (To Sep 2007)	8.11 B SCF
Hydrate contribution as % of gas produced	86.8%

Table E-13: Hydrate Contribution in recharging gas reservoir for East Barrow

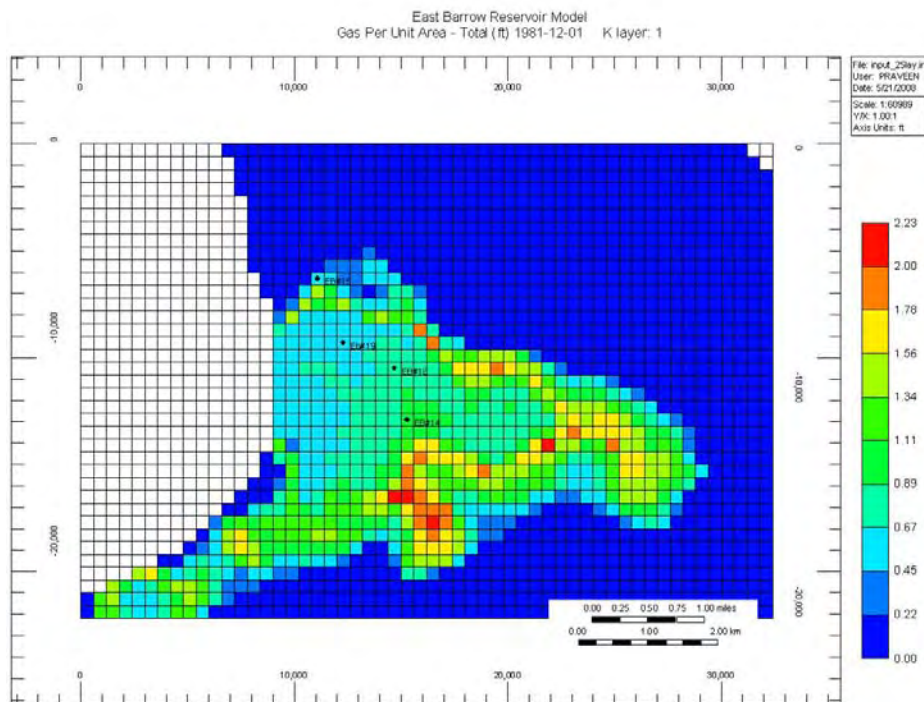


Figure 90: Free Gas per Unit Area-Total (Dec 1981) for East Barrow

Similarly, current free gas reserve is calculated by using “Total Free Gas per unit Area” data obtained using CMG-STARs results. Figures 90 and 91 show initial (Dec 1981) and current (Sep 2007) total-free gas per unit area, respectively, for the East Barrow reservoir model. The initial free gas in place calculated for the East Barrow reservoir model is 15.8 BCF, whereas the current free gas in place is approximately 15.4 BCF. A total of 8.11 BCF of gas has been produced to date; hence the additional free gas available currently has been supplied by dissociating hydrates, based on these model results.

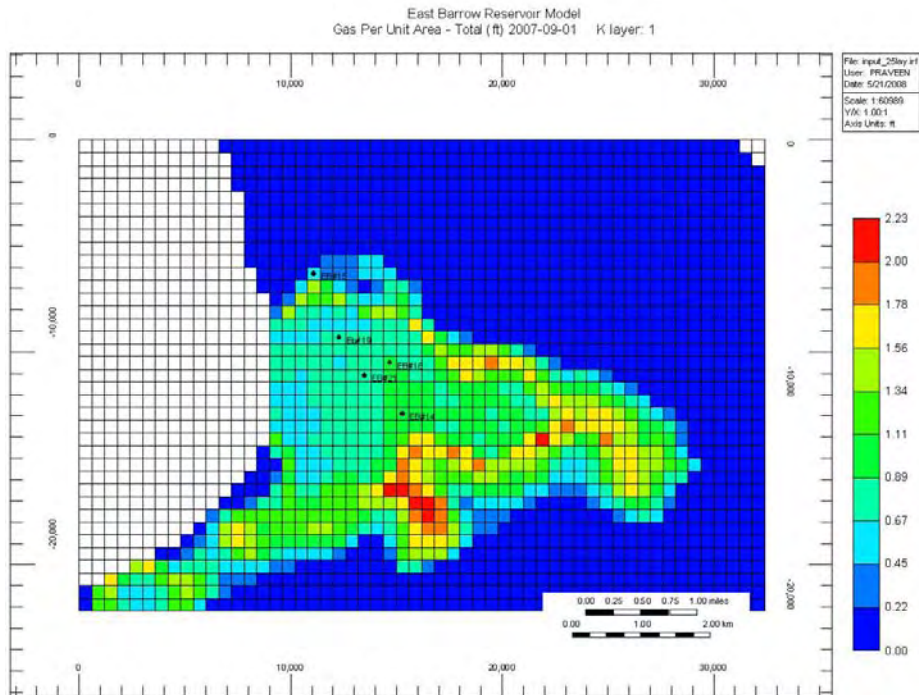


Figure 91: Free Gas per Unit Area-Total (Sep 2007) for East Barrow

III. SELECTING LOCATIONS FOR INFILL AND HYDRATE TEST WELLS FOR EAST BARROW

The methodology/approach for selecting optimum locations for future infill wells is to target grid blocks with high concentration of free gas in place. In order to do that a reservoir mapping exercise has been done to obtain current concentration of free gas throughout the reservoir. This is done very similar to previous exercise. Figure 92 is essentially a reproduction of Figure 91. The figure clearly shows 6 locations best suited for drilling infill wells. The co-ordinates of these locations are presented in Table E-14. Out of all the available options, the grid block which is at the highest location has been selected for forecasting purposes. The co-ordinate of selected grid block is 25, 10, (IJ Plane).

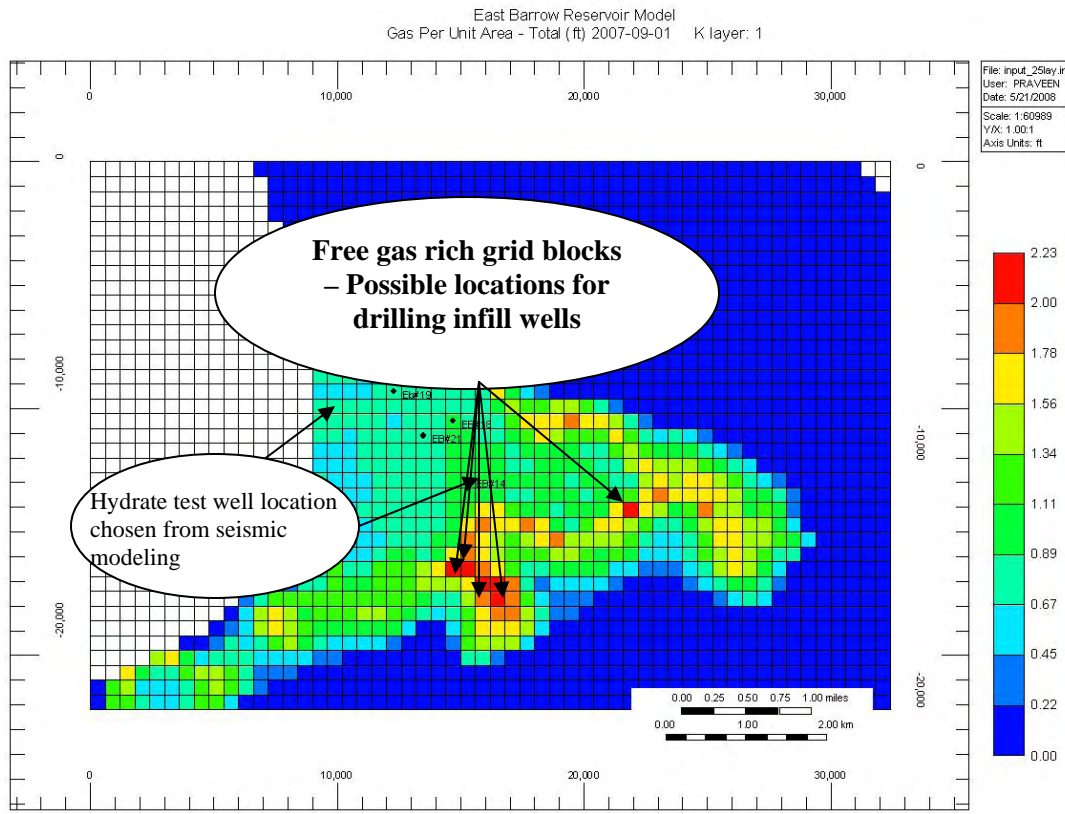


Figure 92: Selected location for infill wells (Free Gas per Unit Area-Total) for East Barrow

GRID BLOCK CO-ORDINATES (I J PLANE)	FREE GAS (res ft ³ /ft ²)
--	--

25, 10 (Selected for Drilling Infill Well)	2.1481
Refer – FORECASTING Section	
26, 10	2.1424
27, 9	2.0359
28, 9	2.0187
28, 8	2.2177
37, 14	2.0284

Table E-14: Optimum locations for drilling future infill wells for East Barrow

While these well locations are optimally suited for infill production wells, they are not necessarily the best locations for a hydrate test well. Our criteria for selection of a hydrate test well location include: very high chance of encountering and collecting a core of in situ hydrate from the reservoir; close to the free gas-hydrate interface; and dipping reservoir suitable for drilling high angle sidetrack downdip from

the hydrate zone into the free gas zone. The locations best matching these three criteria are also shown on Figure 92. One location happens to be a twin to the existing and still producing E.B. #14 well, which based on the hydrate per unit area map (Figure 89) is a location of high hydrate concentration. The other location to the northwest is slightly higher structurally, and is likely to be an area less affected by gas production. It is quite possible that the hydrate in the E.B.#14 area has been partially or completely depleted due to free gas offtake. Therefore, the location to the northwest at the crest of the reservoir is our favored location for a hydrate test well in the East Barrow Gas Field.

IV. EAST BARROW SENSITIVITY STUDY

As discussed previously, the sensitivity parameters have been categorized into five major groups. These categories have been identified based on their importance in quantifying methane hydrate resource potential of East Barrow gas field. These are:

1. Free Gas Zone Size
2. Hydrate Saturation
3. Hydrate Zone Size
4. Aquifer Strength and Size

1. Free Gas Zone Size

Five different free gas zone sizes have been studied. The reservoir response have been recorded and compared by plotting cumulative gas production, cumulative water production and average reservoir pressure for all the scenarios (including the history matched-best case scenario). The sensitivity runs performed were:

- a. Free Gas Water Contact – 2060'
- b. Free Gas Water Contact – 2070'
- c. Free Gas Water Contact – 2080' (best case model)
- d. Free Gas Water Contact – 2090'
- e. No Free Gas Water Contact (HYD + Free Gas model)

Figures 93, 94 and 95 show the reservoir sensitivity (gas production, water production and average reservoir pressure) to variation in free gas zone size. From Figure 93, we observed that for GWC of 2060', the cumulative gas production is slightly less than production history data indicates. For all other free gas zone sizes, the gas production data matches perfectly. In case of Figure 94, the free gas water contact at 2090' and 2080' (best case) closely matches the water production profile. The amount of water produced in the case of GWC-2090' is slightly less than base case (GWC at 2080'). This can be attributed to the fact that the deeper gas-water contact keeps the moving aquifer farther away from producing wells. Secondly, the thicker free gas zone size easily supplies free gas for production and hence, reduces hydrate dissociation rates. This in turn reduces mobile water build up in the hydrate zone. GWC-2060' and 2070' produce tremendous volumes of water, due to the fact that the gas-aquifer contact is closer to the well bore, leading to higher water production. The only mobile water available in the no aquifer scenario is the water produced during hydrate dissociation.

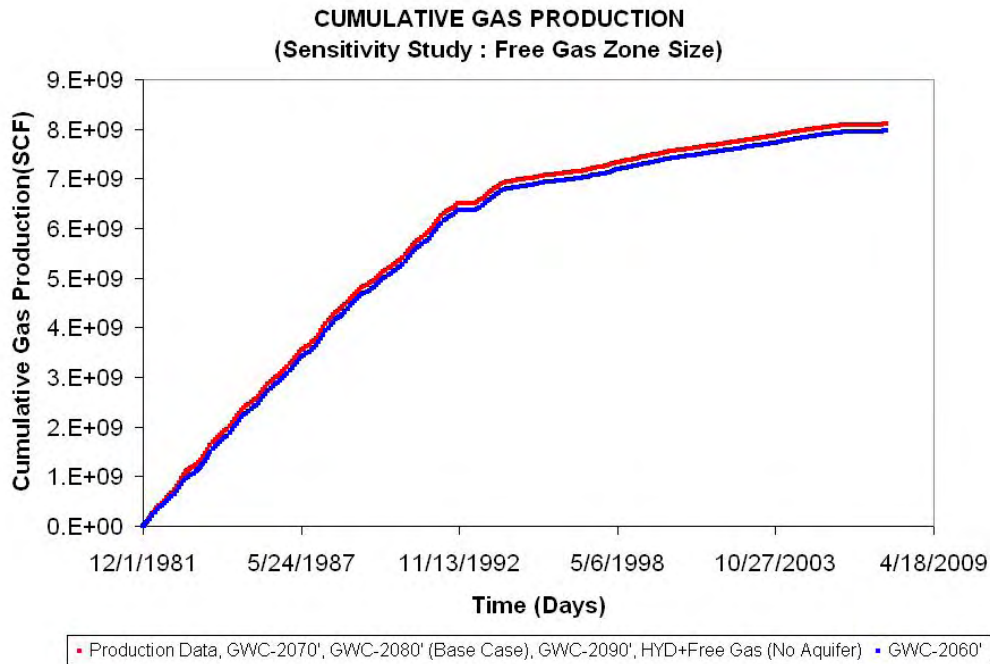


Figure 93: Cumulative Gas Production (Sensitivity - Free Gas Zone Size) for East Barrow

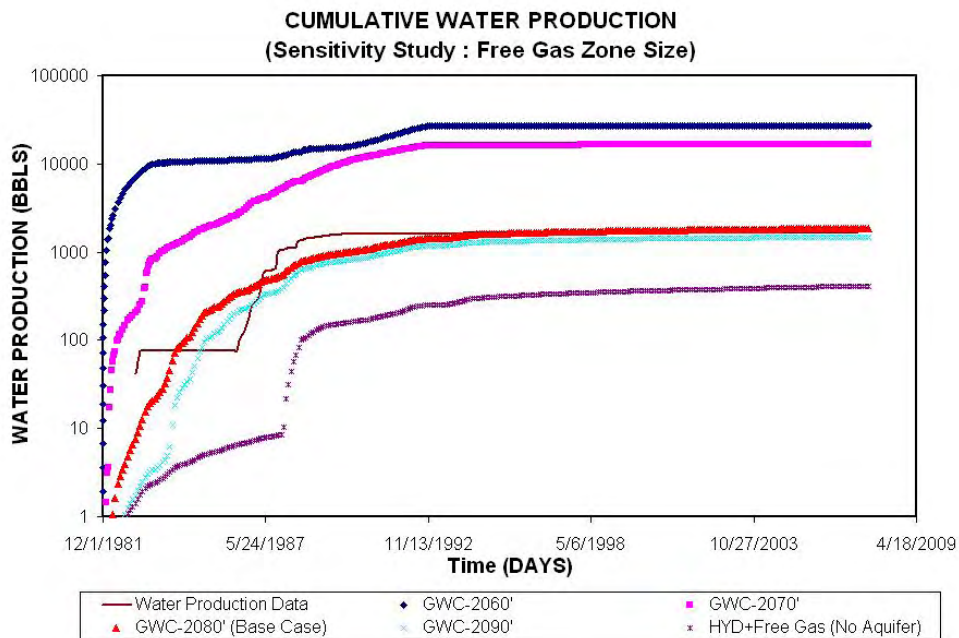


Figure 94: Cumulative Water Production (Sensitivity - Free Gas Zone Size) for East Barrow

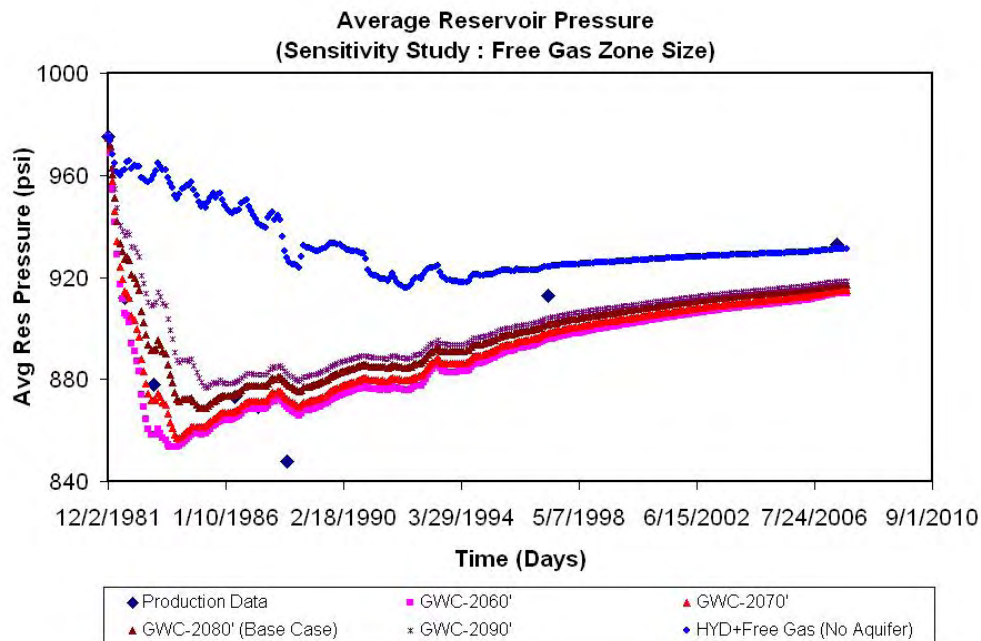


Figure 95: Average Reservoir Pressure (Sensitivity - Free Gas Zone Size) for East Barrow

The average reservoir pressure response has been recorded and compared in Figure 95. The scenario GWC-2090' closely follows the best case model. However, due to the large free gas volume, the scenario fails to match the production data during the initial gas production period. GWC-2060' and 2070' manage to achieve better match during initial production but fail to catch up during later stages of production. This is primarily due to the fact that the higher aquifer zone contact charges the reservoir with more water influx and hence, prevents hydrate dissociation. However, the moving water fails to match desired reservoir pressure.

2. Hydrate Saturation

Sensitivity of hydrate saturation on reservoir is a very crucial parameter that needs to be evaluated. A simulation run was performed with the hydrate zone completely saturated with hydrates (45%) and bounded water (55%). Numerical difficulties were observed while running the simulation and eventually the run could not be completed. The unavailability of free gas in the hydrate bearing zone was causing problems during gas production. Five hydrate saturations were studied to see the impact of hydrate saturation on reservoir response. These scenarios are:

- a. Hydrate Saturation = 0% (Gas +Aquifer Model)
- b. Hydrate Saturation = 5%
- c. Hydrate Saturaton = 15%
- d. Hydrate Saturation = 31% (Best case model)
- e. Hydrate Saturation = 40%

Figures 96, 97 and 98 show the comparative plots of all these scenarios. The cumulative gas production remains unchanged for all of the scenarios, except one, where hydrate saturation has been increased to 40%. Unavailability of free gas in the hydrate zone causes deficiency of mobile fluid in the hydrate zone and hence, reduces gas production.

The water production plot is an interesting comparison. Negligible water production has been observed with lower hydrate saturations of 0%, 5% and 15%, but as soon as hydrate saturation increases to 31%, a sudden jump in water production is observed. Again at 40% hydrate saturation, the water production comes down.

The possible explanation to this observation is that at lower hydrate saturation, more free gas is available for production. Free water generation due to hydrate dissociation is also low. 31% hydrate saturation provides optimum free gas for initial production followed by higher rates of hydrate dissociation. This eventually causes the immobile produced water to flow towards the wellbore, where it joins the production stream. But for hydrate saturation in the range of 40%, the free gas production is very low and hence the associated water is also low. With time, some hydrate dissociation is observed, and this causes a slight jump in the water production slope for this case.

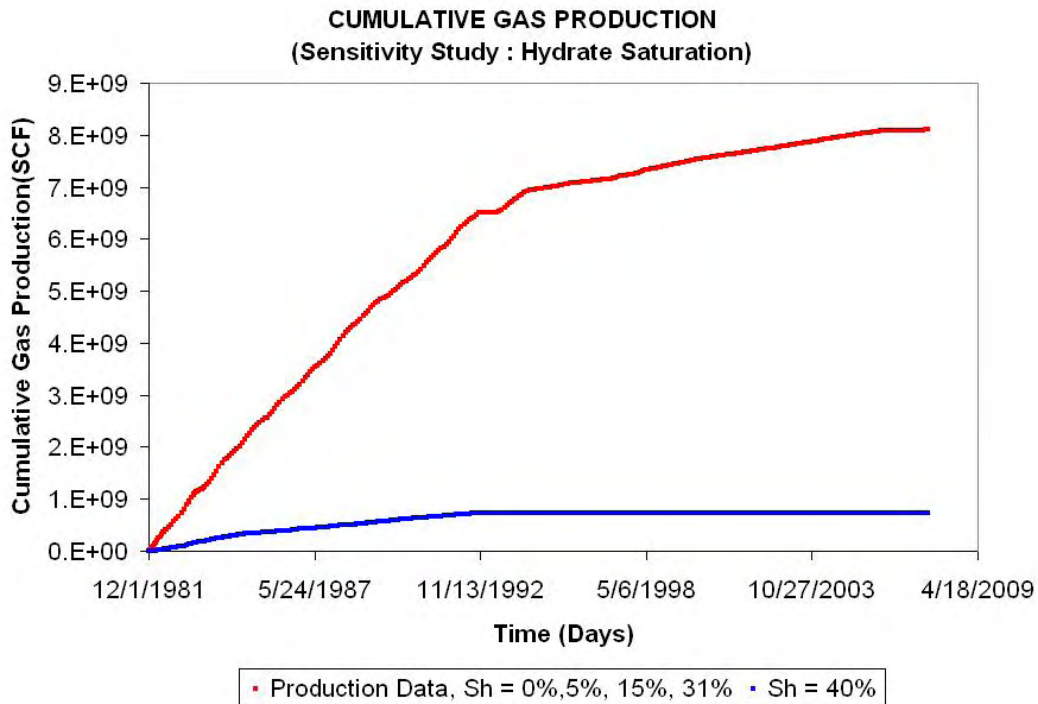


Figure 96: Cumulative Gas Production (Sensitivity – Hydrate Saturation) for East Barrow

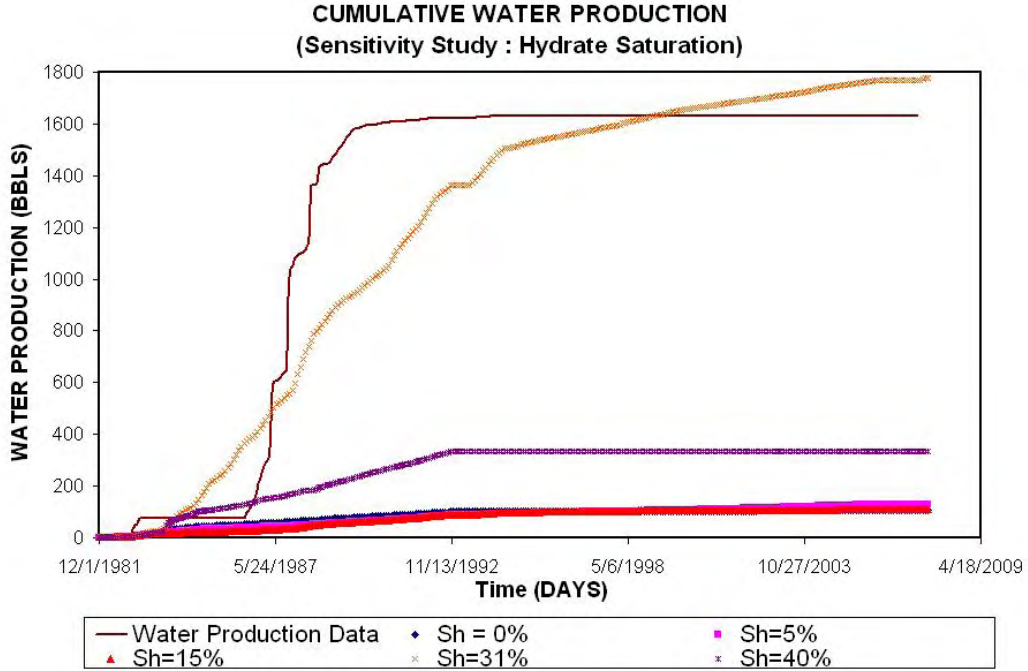


Figure 97: Cumulative Water Production (Sensitivity – Hydrate Saturation) for East Barrow

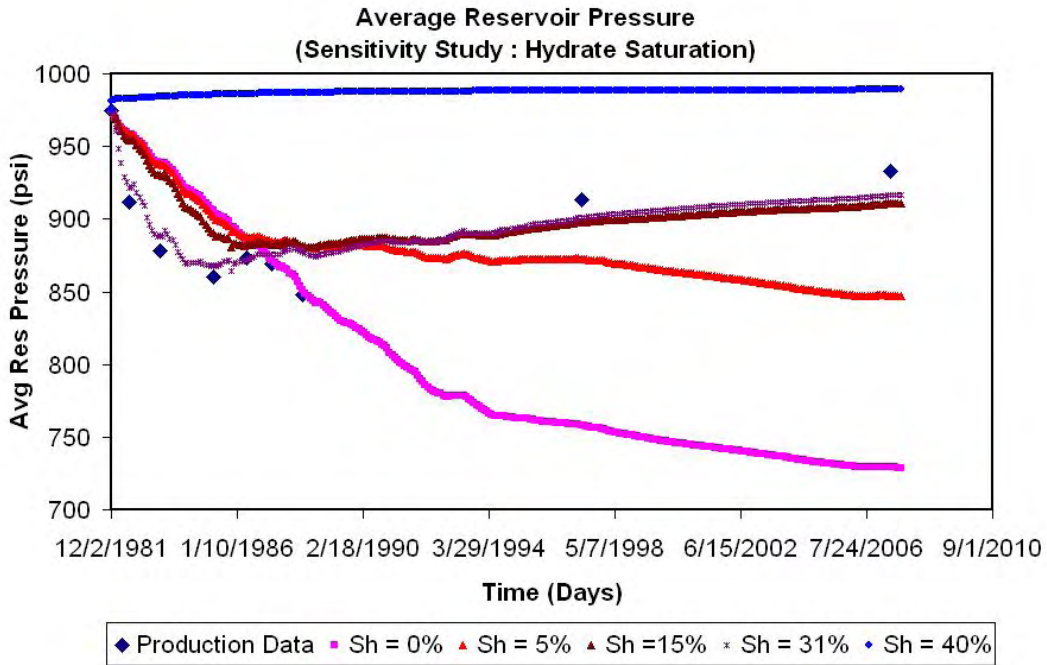


Figure 98: Average Reservoir Pressure (Sensitivity – Hydrate Saturation) for East Barrow

Figure 98 is the average reservoir pressure response for different hydrate saturations. Lower hydrate saturation is unable to maintain reservoir pressure for long periods of time. Dissociating hydrates maintain the reservoir pressure initially, and after complete dissociation of hydrates, the reservoir depletes by gas expansion. This is characterized by higher pressure decline observed in later times. Hydrate saturation of 15% matches the pressure history in later times, but due to higher hydrate dissociation rates, the scenario fails to match the response during initial production life of the reservoir. The base case model (hydrate saturation 31%) manages to support the reservoir pressure and match the production history. The scenario with hydrate saturation of 41% fails to produce gas from the reservoir and hence, there is not a drop in reservoir pressure. Slow hydrate dissociation actually accounts for an increases in the average reservoir pressure in this case.

3. Hydrate Zone Size

Hydrate zone size is changed by altering the hydrate-free gas contact. Changing the hydrate zone size changes the cumulative water production and average reservoir pressure. Six different cases have been studied by changing hydrate zone size. These are:

- a. No Hydrate Zone (Gas + Aquifer model)
- b. Hydrate – Free Gas Contact – 2030'
- a. Hydrate – Free Gas Contact – 2040'
- b. Hydrate – Free Gas Contact – 2050' (Best case model)
- c. Hydrate – Free Gas Contact – 2060'
- d. Hydrate – Water Contact – 2080' (HYD + Aquifer model)

Figures 99, 100 and 101 compare the reservoir performance due to changing hydrate zone thickness. The cumulative gas production profile observed in Figure 99 shows one scenario in which the modeled gas production fails to match the production history data. This scenario represents a hydrate-water contact at 2080', so there is no space for a free gas zone. The absence of a free gas zone, as one would expect, causes reduced gas production.

Figure 100 shows water production for all scenarios. Starting with a hydrate-aquifer system, i.e. thick hydrate zone overlying the aquifer zone produces tremendous volumes of water. This is attributed to unavailability of sufficient gas in the system. The gas production reduces reservoir pressure, and this reduction in reservoir pressure causes hydrate to dissociate slowly and the aquifer zone to migrate upward into the hydrate zone. The combined effect of the two scenarios results in high rates of water production. The cumulative water produced in this case has reached 9000 barrels. The impact of lower hydrate zone thickness in the cases of HGC-2030', 2040', 2050' and 2060' slightly changes the water production profile. The impact of encroaching aquifer in these cases is minimal (as the rate of encroachment is not very high). The water production depends mainly on the rate of hydrate dissociation. Thus, water production corresponds to the size of hydrate zone. With no hydrate zone (free gas-aquifer), the water production is negligible.

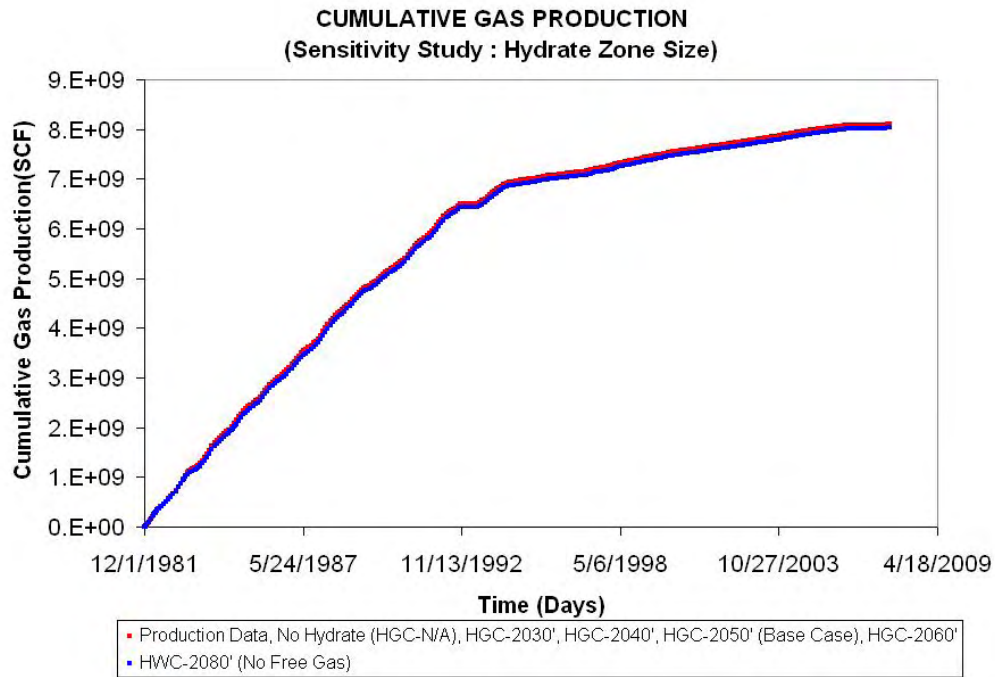


Figure 99: Cumulative Gas Production (Sensitivity – Hydrate Zone Size) for East Barrow

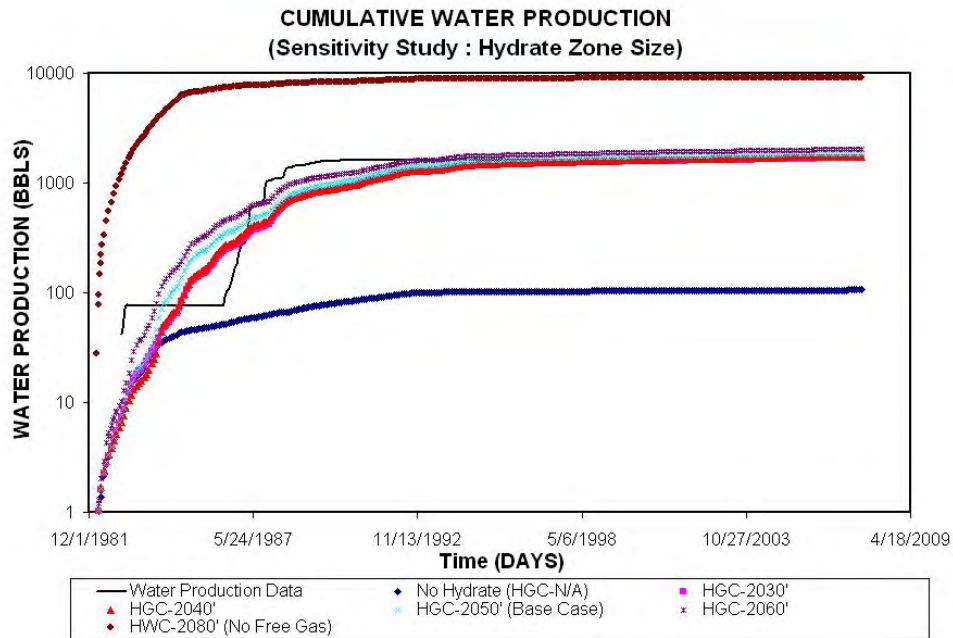


Figure 100: Cumulative Water Production (Sensitivity – Hydrate Zone Size) for East Barrow

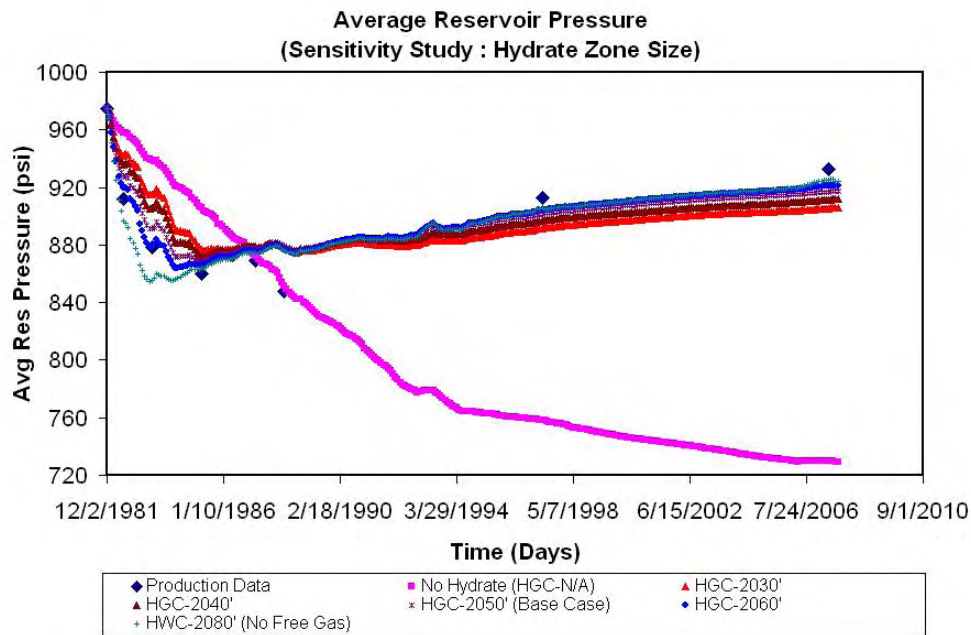


Figure 101: Average Reservoir Pressure (Sensitivity – Hydrate Zone Size) for East Barrow

Figure 101 shows the impact of hydrate zone size on average reservoir pressure. The plot clearly shows that the change in hydrate zone size has a small impact on reservoir pressure. The primary reason for such observation is that with reducing hydrate zone thickness, the gas zone thickness increases and it compensates for the loss of hydrates to a certain extent. However, when observed closely, the plot shows that for thinner hydrate zone, the initial reduction in reservoir pressure over predicts the reservoir response. Also, in later times, due to unavailability of sufficient hydrates, the model under predicts reservoir response. The no hydrate situation clearly shows a free gas type (volumetric) expansion pattern, with reservoir pressure reducing at a faster rate even in presence of aquifer support.

4. Aquifer Strength and Size

Following are the categories under which aquifer sensitivities have been studied. Figures 102-118 show the reservoir response for each sensitivity study.

- a. All Aquifer Sensitivity
- b. Bottom Aquifer Sensitivity
- c. Edge Aquifer Sensitivity
- d. Infinite Aquifer Sensitivity
- e. Finite Aquifer Sensitivity
- f. Aquifer Sensitivity at Gas-Water contact 2080'
- g. Aquifer Sensitivity at Gas-Water contact 2070'
- h. Aquifer Sensitivity at Gas-Watre contact 2045'

a. All Aquifer Sensitivity

The aquifer study was performed to understand the impact of aquifer strength and size on reservoir pressure response in absence of a hydrate cap. This exercise has been initiated to further evaluate the possibility of matching reservoir performance by changing aquifer strength. Figures 102, 103 and 104 presents a summary of all the scenarios studied as part of aquifer study. Figure 102 shows cumulative gas production with time. It has been observed that the effect of numerical aquifer strength has no major impact on gas production. However, increasing model aquifer size and /or decreasing gas saturation (i.e. by increasing bounded water saturation) substantially decreases the gas production. Figures 103 and 104 present summary of all the cases. Each will be discussed in detail under individual sensitivity study.

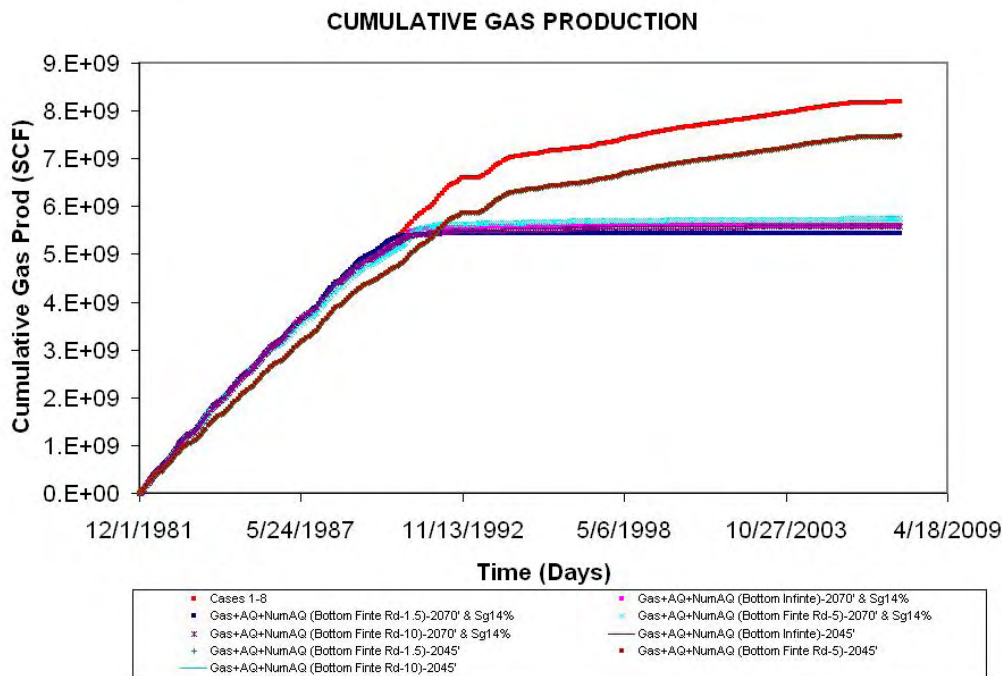


Figure 102: Cumulative Gas Production (Sensitivity – Aquifer Shape and Size, All) for East Barrow

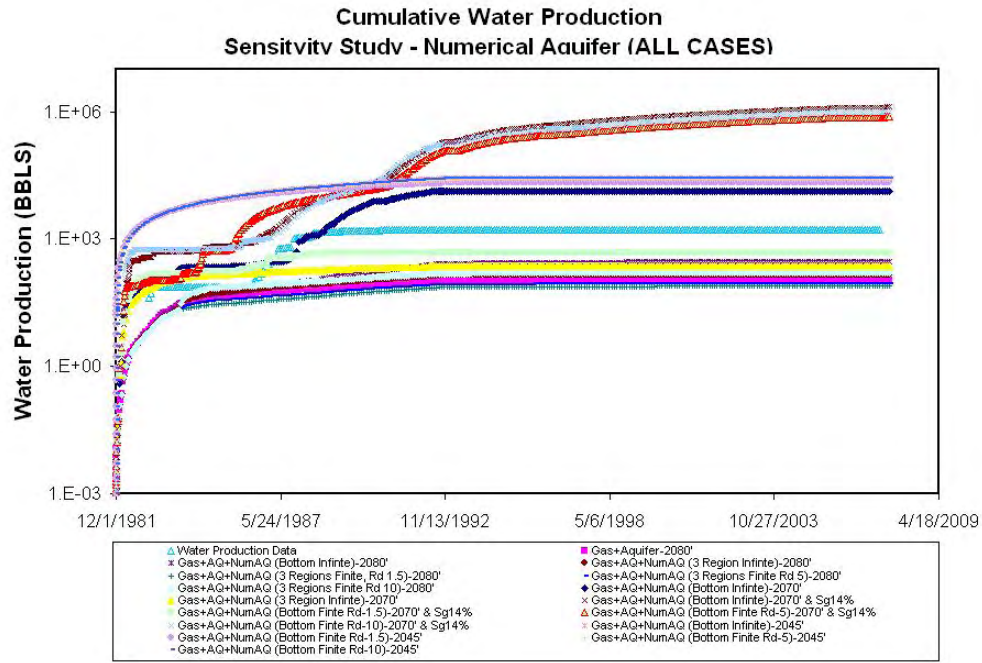


Figure 103: Cumulative Water Production (Sensitivity – Aquifer Shape and Size, All) for East Barrow

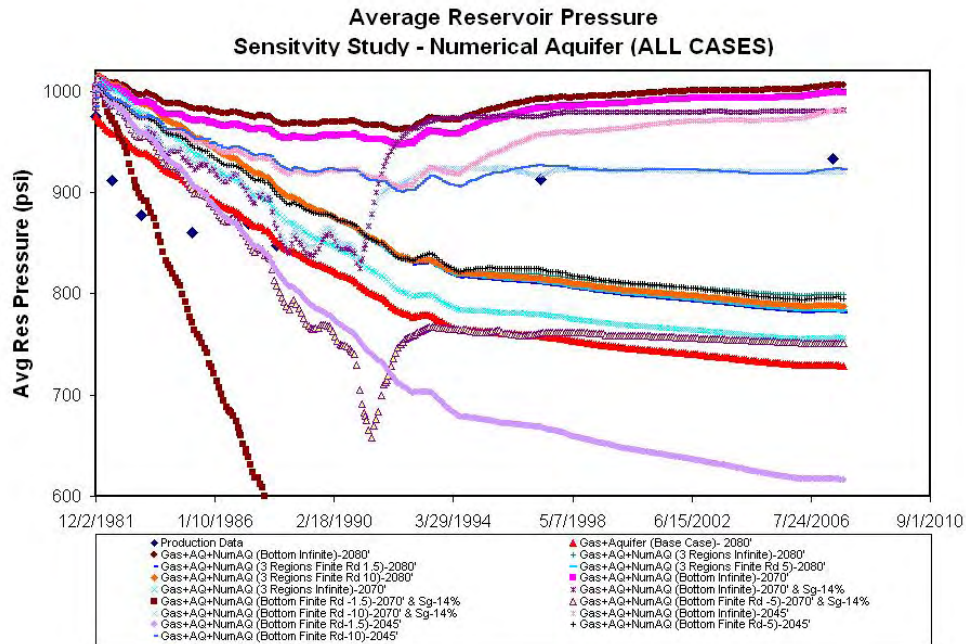


Figure 104: Average Reservoir Pressure (Sensitivity – Aquifer Shape and Size, All) for East Barrow

b. Bottom Aquifer Sensitivity

A bottom aquifer sensitivity study has been performed with finite and infinite aquifer strengths. All the scenarios studied in this case show (refer to Figure 105) higher water production with cases where gas-water contact has been shifted to a higher location eg. 2045' and 2070'. Scenarios studied in this study are:

1. Bottom Aquifer – Infinite Size (GWC-2080')
2. Bottom Aquifer – Infinite Size (GWC-2070')
3. Bottom Aquifer – Infinite Size (GWC-2070', $S_g=14\%$)
4. Bottom Aquifer – Finite Size- $R_d-1.5$ (GWC-2070', $S_g=14\%$)
5. Bottom Aquifer – Finite Size- R_d-5 (GWC-2070', $S_g=14\%$)
6. Bottom Aquifer – Finite Size- R_d-10 (GWC-2070', $S_g=14\%$)
7. Bottom Aquifer – Infinite Size (GWC-2045')
8. Bottom Aquifer – Finite Size, $R_d-1.5$ (GWC-2045')
9. Bottom Aquifer – Finite Size, R_d-5 (GWC-2045')
10. Bottom Aquifer – Finite Size, R_d-10 (GWC-2045')

Figure 105 shows the average reservoir pressure response in presence of a bottom aquifer. Aquifer supports like the infinite strength bottom aquifer and finite strength aquifer (where $R_d = 10$) present very strong support to the reservoir. The pressure of the reservoir is maintained much higher than the observed value. On the other hand cases with weak bottom aquifer strengths are unable to maintain constant pressure in the reservoir.

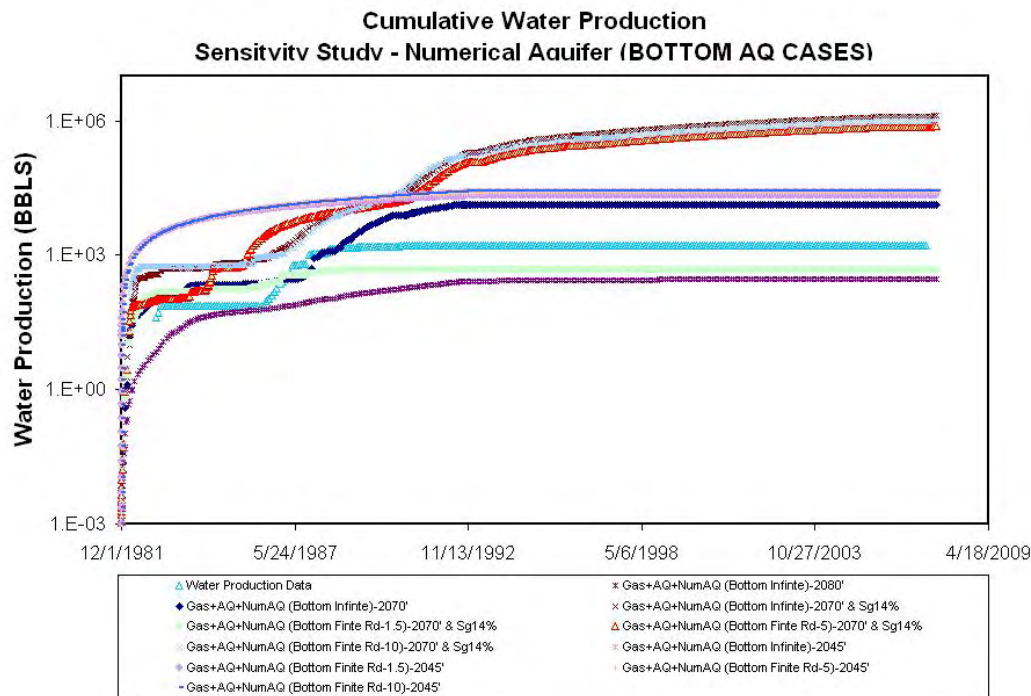


Figure 105: Cumulative Water Production (Sensitivity – Bottom Aquifer) for East Barrow

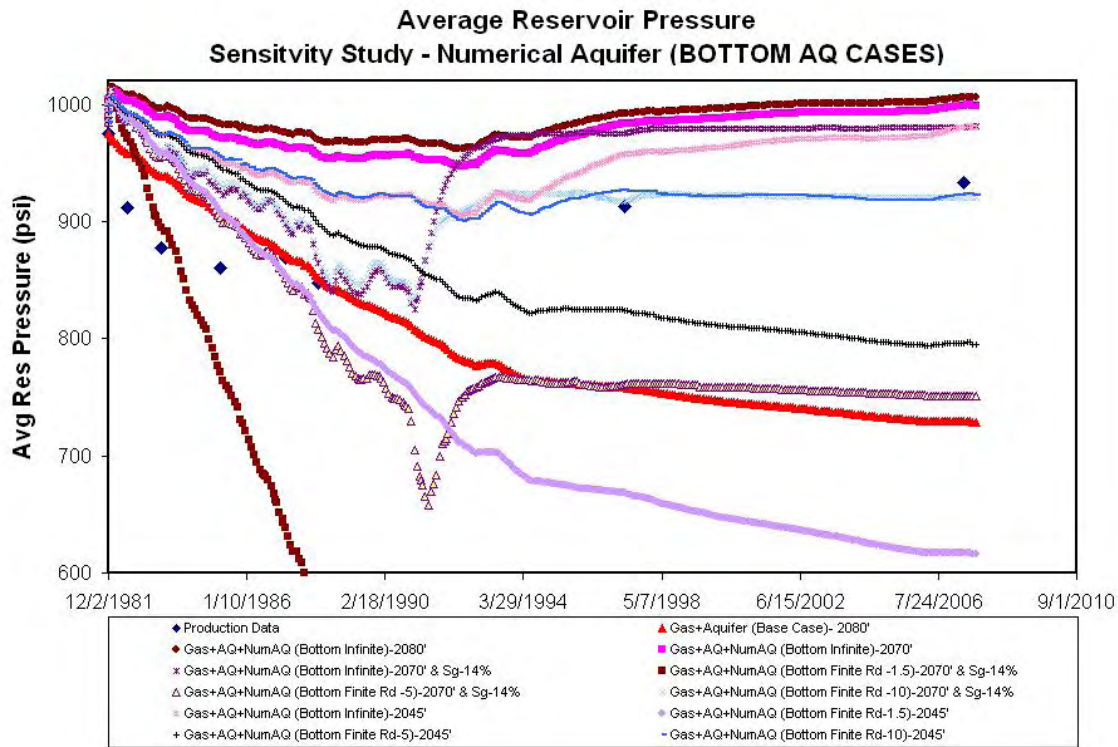


Figure 106: Average Reservoir Pressure (Sensitivity – Bottom Aquifer) for East Barrow

c. Edge Aquifer Sensitivity

Limited edge aquifer sensitivity studies were performed to see if they can explain the pressure support (along with model aquifer). Five scenarios were studied, these are:

1. Edge Aquifer Infinite (GWC-2080')
2. Edge Aquifer Finite, $R_d-1.5$ (GWC-2080')
3. Edge Aquifer Finite, R_d-5 (GWC-2080')
4. Edge Aquifer Finite, R_d-10 (GWC-2080')
5. Edge Aquifer Infinite (GWC-2070')

Figures 107 and 108 show the reservoir performance with edge aquifer sensitivity. It should be noted that the edge water strength and sizes were studied mostly at the gas-water contact of 2080'. The effect of edge water drive is negligible as far as water production is concerned. This shows that the edge water is unable to move higher and closer to the producing wells in the reservoir. Water production of all scenarios is lower than water production history.

Corresponding to this, the effect of edge aquifer on reservoir pressure maintenance is also minimal. Comparing the pressure profile with the free gas-aquifer model, the pressure response shows slight improvement due to the numerical edge water influx.

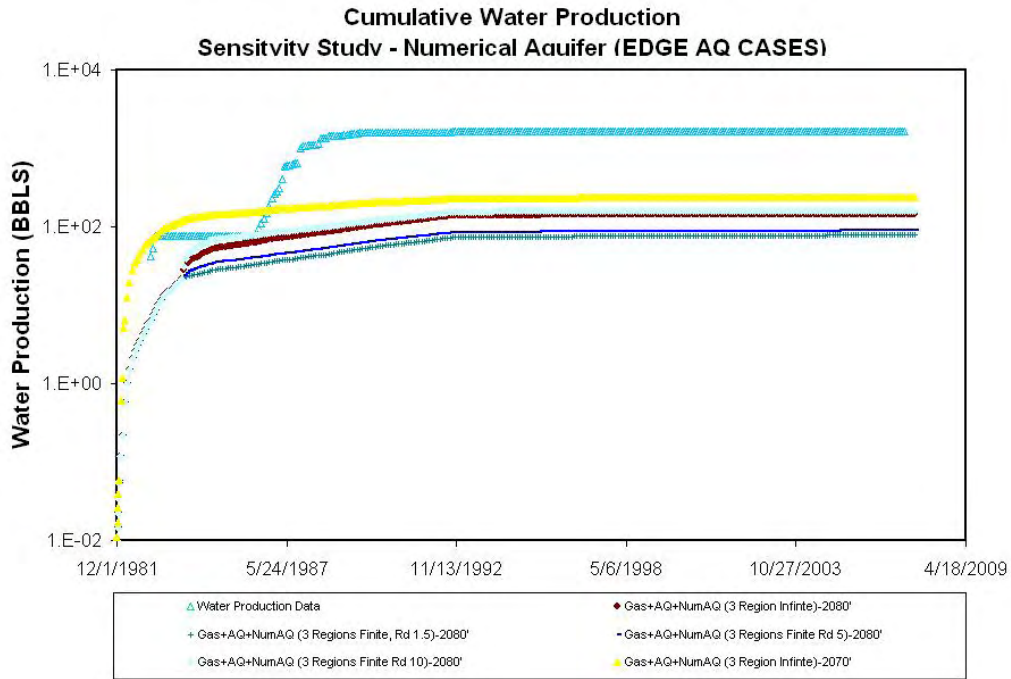


Figure 107: Cumulative Water Production (Sensitivity – Edge Aquifer) for East Barrow

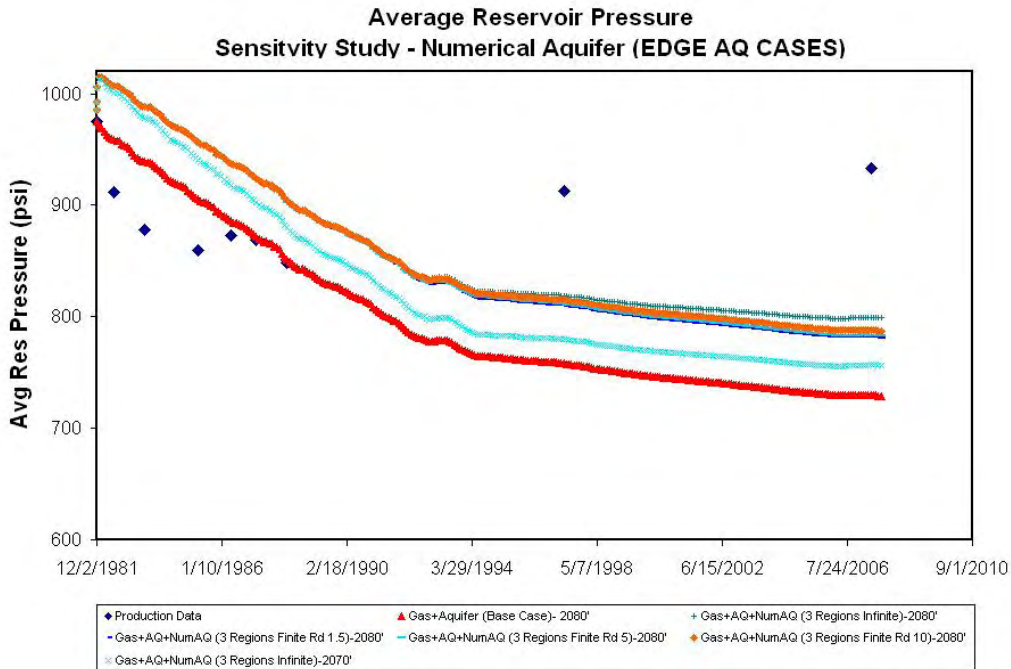


Figure 108: Average Reservoir Pressure (Sensitivity – Edge Aquifer) for East Barrow

d. Infinite Aquifer Sensitivity

The scenarios studied under this category are:

1. Bottom Aquifer Infinite (GWC-2080')
2. Edge Aquifer Infinite (GWC-2080')
3. Bottom Aquifer Infinite (GWC-2070')
4. Bottom Aquifer Infinite (GWC-2070', S_g -14%)
5. Edge Aquifer Infinite (GWC-2070')
6. Bottom Aquifer Infinite (GWC-2045')

Cumulative water production for several infinite sized aquifers were compared (refer to Figure 109). The plot clearly shows an increase in water production for bottom aquifer cases where the gas-water contact has been shifted to a location structurally higher in the reservoir (i.e. GWC 2070' and 2045') and for cases where free gas saturation has been decreased to 14%. Again, the effect of higher GWC on water production is negligible in the case of edge aquifer of infinite size.

The pressure response (refer to Figure 110) shows greater impact of bottom (infinite) aquifer on reservoir pressure. The bottom aquifer tends to stabilize at higher reservoir pressures; whereas the edge aquifer strength has no effect on reservoir pressure maintenance.

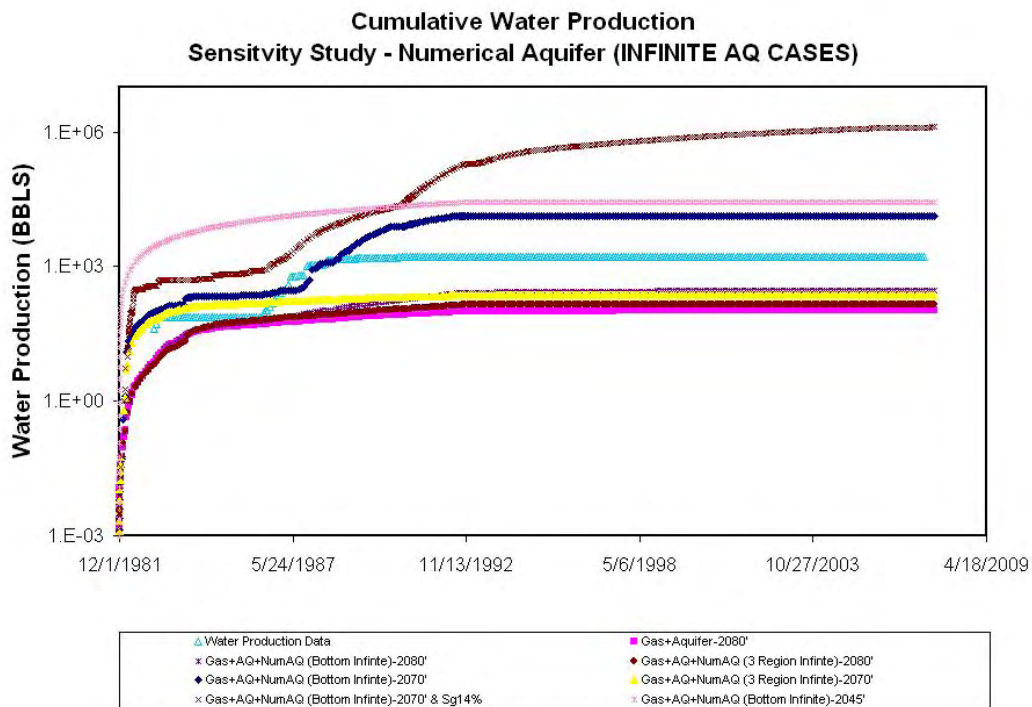


Figure 109: Cumulative Water Production (Sensitivity – Infinite Aquifer) for East Barrow

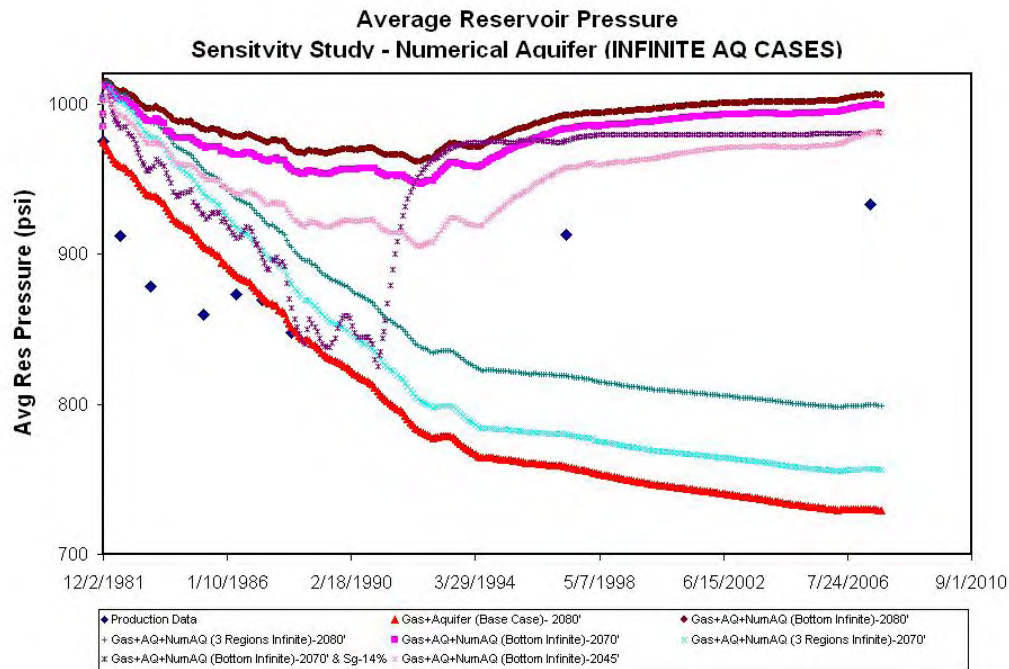


Figure 110: Average Reservoir Pressure (Sensitivity – Infinite Aquifer) for East Barrow

e. Finite Aquifer Sensitivity

The reservoir size is made finite by keeping the radius of aquifer close to the reservoir radius (approx). Three different finite aquifer sizes have been studied. These are R_d -1.5, 5 and 10, where R_d is the ratio of “effective aquifer radius to effective reservoir radius”. Following scenarios have been investigated under this category. Refer to Figure 111 and 112 for results of these scenarios.

The scenarios studied under this category are:

1. Edge Aquifer Finite, R_d -1.5 (GWC-2080')
2. Edge Aquifer Finite, R_d -5 (GWC-2080')
3. Edge Aquifer Finite, R_d -10 (GWC-2080')
4. Bottom Aquifer Finite, R_d -1.5 (GWC-2070', S_g -14%)
5. Bottom Aquifer Finite, R_d -5 (GWC-2070', S_g -14%)
6. Bottom Aquifer Finite, R_d -10 (GWC-2070', S_g -14%)
7. Bottom Aquifer Finite, R_d -1.5 (GWC-2045')
8. Bottom Aquifer Finite, R_d -5 (GWC-2045')
9. Bottom Aquifer Finite, R_d -10 (GWC-2045')

Figure 111 suggest that even with finite aquifer limits, the bottom aquifer manages to enter the reservoir in large volumes and hence, increases the water production substantially. However, the finite edge aquifer models are weak and are not capable of supplying comparable amounts of water to the reservoir.

The reservoir pressure response has been presented for finite aquifer models (Figure 112). The plot shows that for higher aquifer radius and bottom numerical aquifer, the reservoir pressure is maintained at a higher pressure than edge water driven models.

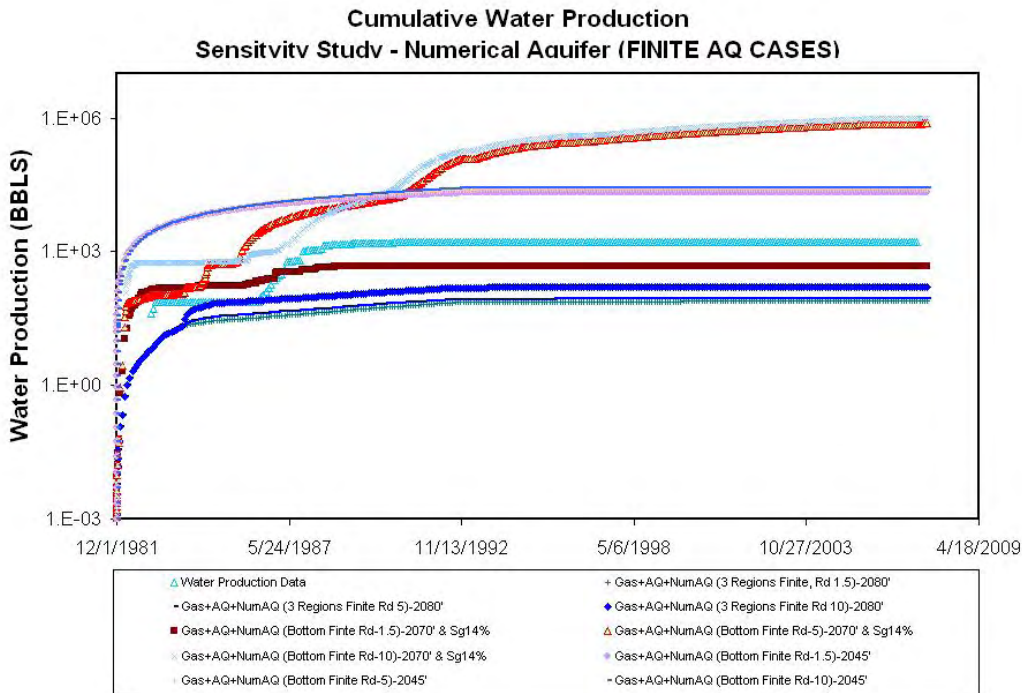


Figure 111: Cumulative Water Production (Sensitivity – Finite Aquifer) for East Barrow

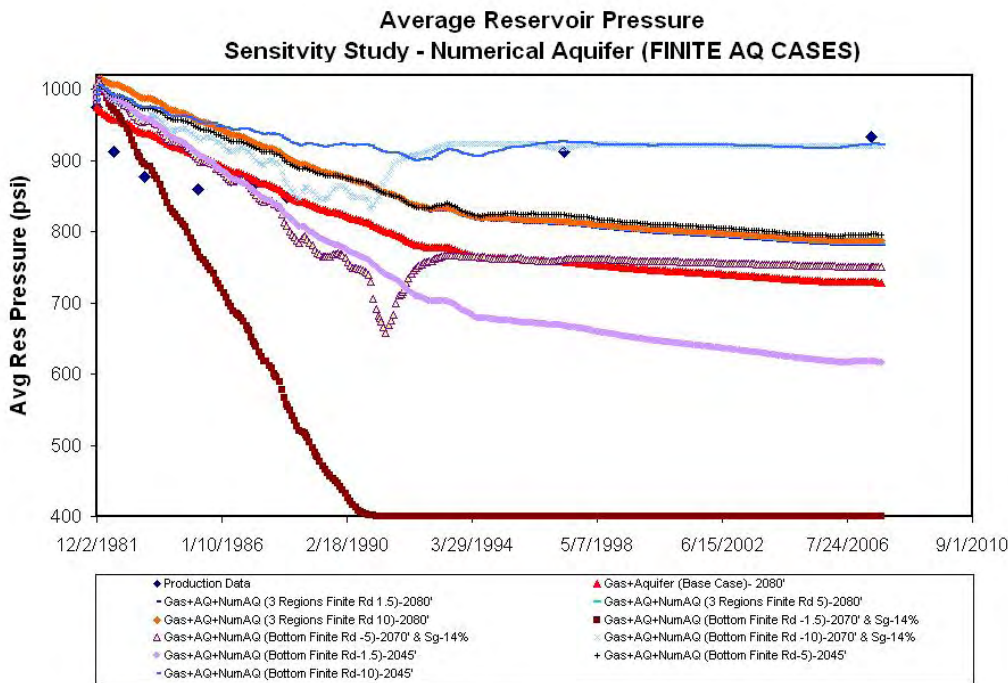


Figure 112: Average Reservoir Pressure (Sensitivity – Finite Aquifer) for East Barrow

f. Aquifer Sensitivity at Gas-Water contact 2080'

Scenarios compared are:

1. Bottom Aquifer Infinite (GWC-2080')
2. Edge Aquifer Infinite (GWC-2080')
3. Edge Aquifer Finite, R_d -1.5 (GWC-2080')
4. Edge Aquifer Finite, R_d -5 (GWC-2080')
5. Edge Aquifer Finite, R_d -10 (GWC-2080')

g. Aquifer Sensitivity at Gas-Water contact 2070'

Scenarios compared are:

1. Bottom Aquifer Infinite (GWC-2070')
2. Edge Aquifer Infinite (GWC-2070')
3. Bottom Aquifer Infinite (GWC-2070', S_g -14%)
4. Bottom Aquifer Finite, R_d -1.5 (GWC-2070', S_g -14%)
5. Bottom Aquifer Finite, R_d -5 (GWC-2070', S_g -14%)
6. Bottom Aquifer Finite, R_d -10 (GWC-2070', S_g -14%)

h. Aquifer Sensitivity at Gas-Water contact 2045'

Scenarios compared are:

1. Bottom Aquifer Infinite (GWC-2045')
6. Bottom Aquifer Finite, R_d -1.5 (GWC-2045')
7. Bottom Aquifer Finite, R_d -5 (GWC-2045')
8. Bottom Aquifer Finite, R_d -10 (GWC-2045')

These categories are derived from previous analysis and therefore have similar explanations. Figures 113 to 118 present these results for these comparisons.

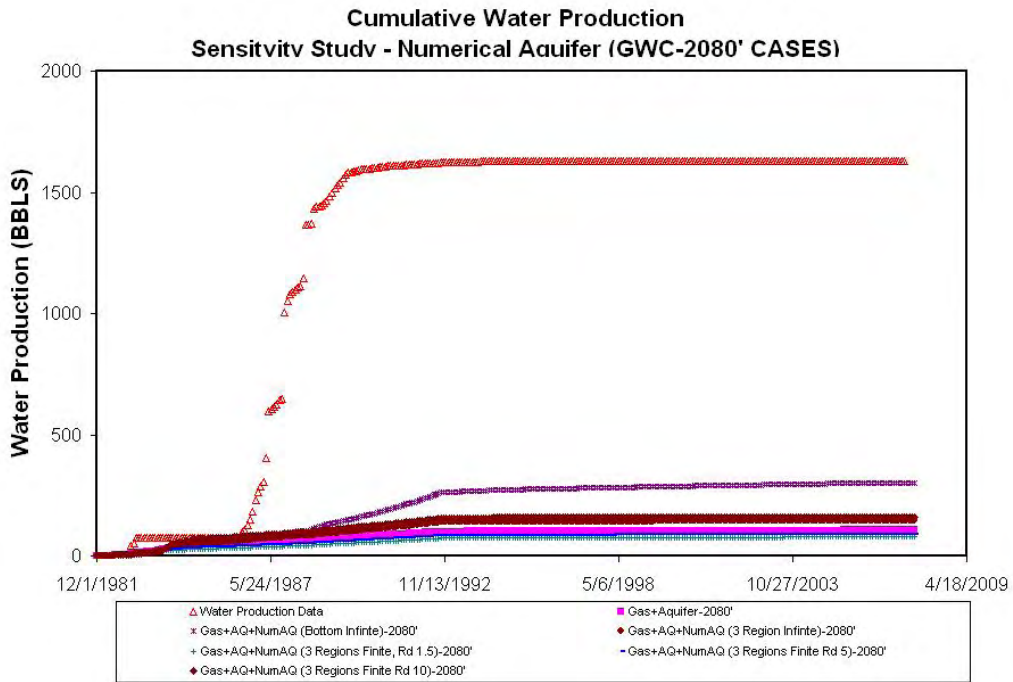


Figure 113: Cumulative Water Production (Sensitivity – GWC 2080') for East Barrow

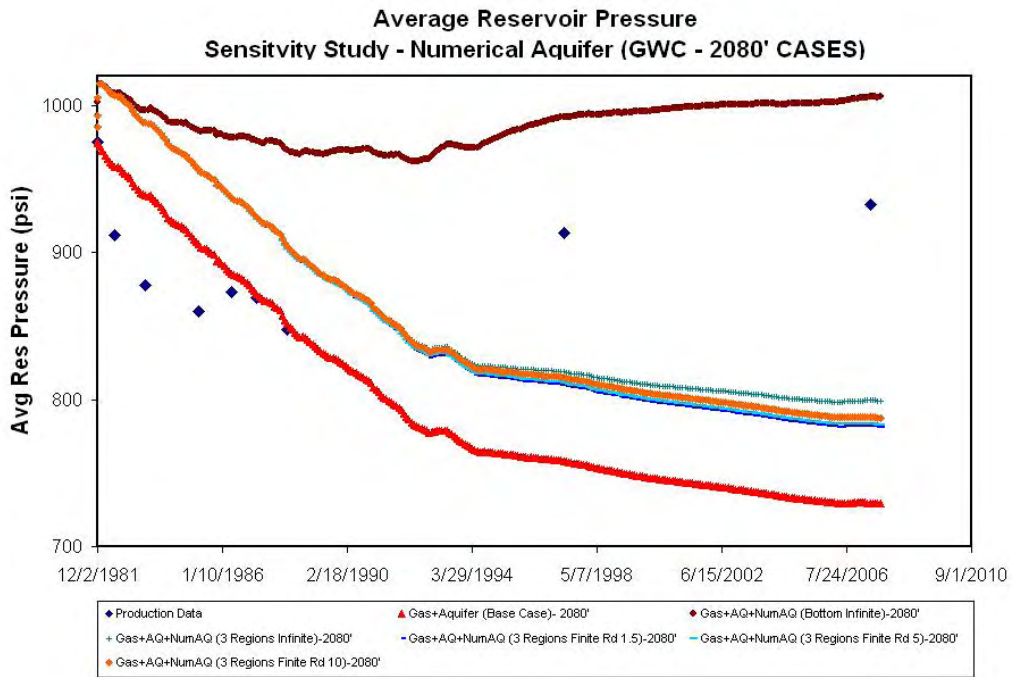


Figure 114: Average Reservoir Pressure (Sensitivity – GWC 2080') for East Barrow

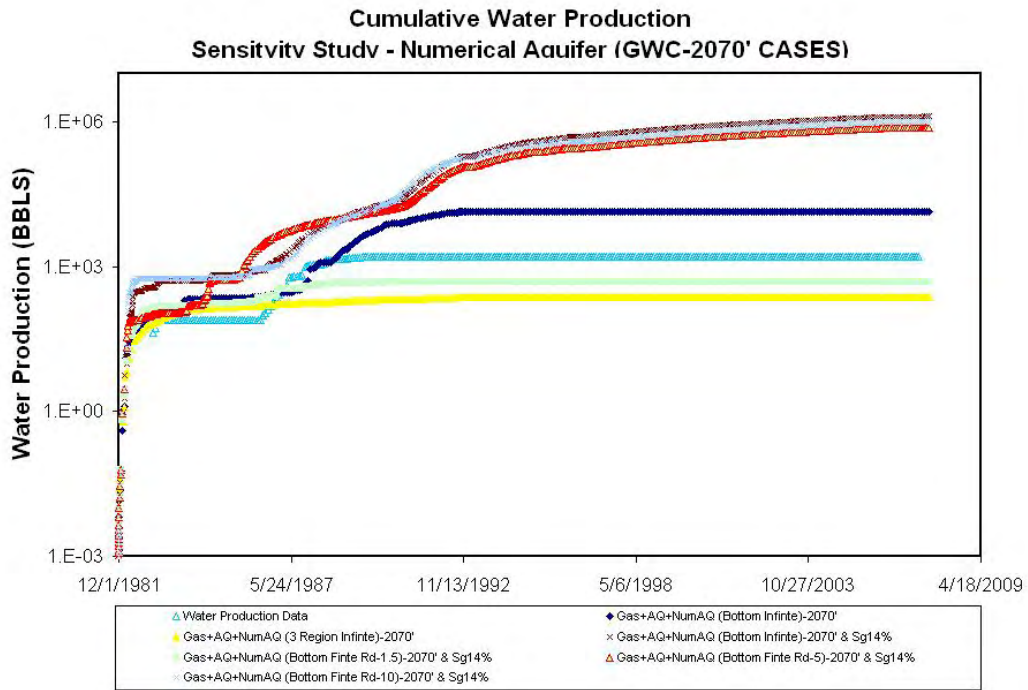


Figure 115: Cumulative Water Production (Sensitivity – GWC 2070') for East Barrow

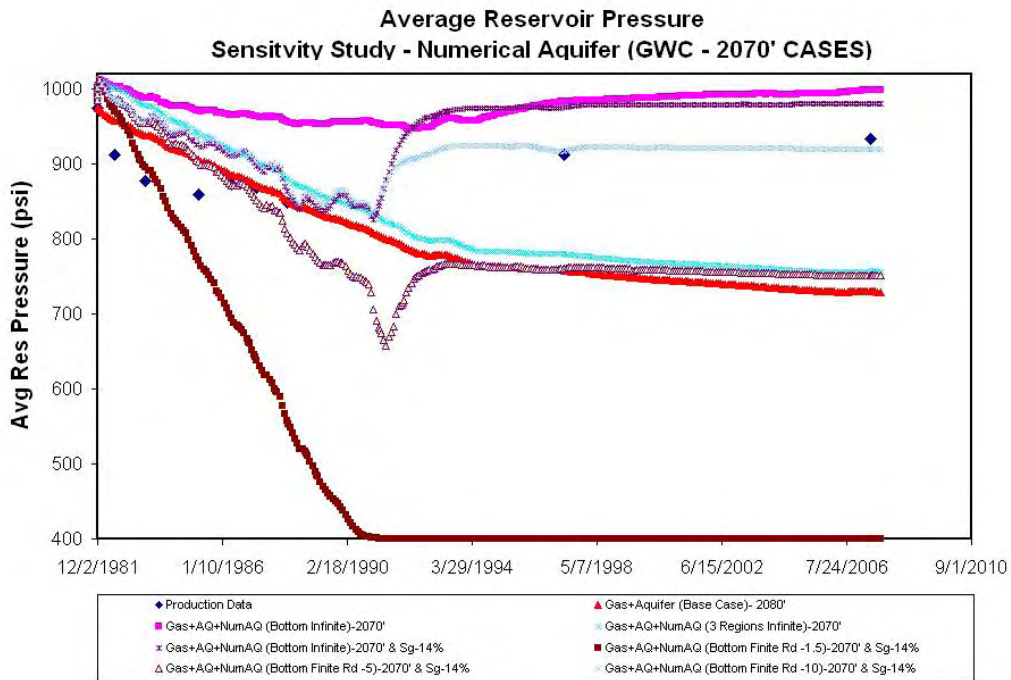


Figure 116: Average Reservoir Pressure (Sensitivity – GWC 2070') for East Barrow

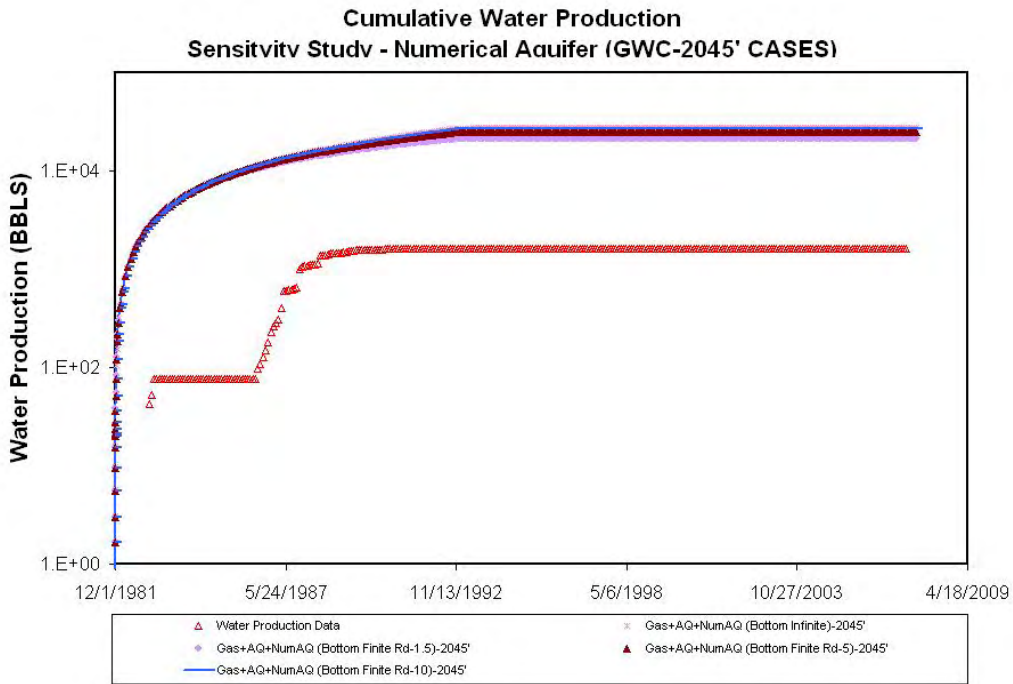


Figure 117: Cumulative Water Production (Sensitivity – GWC 2045') for East Barrow

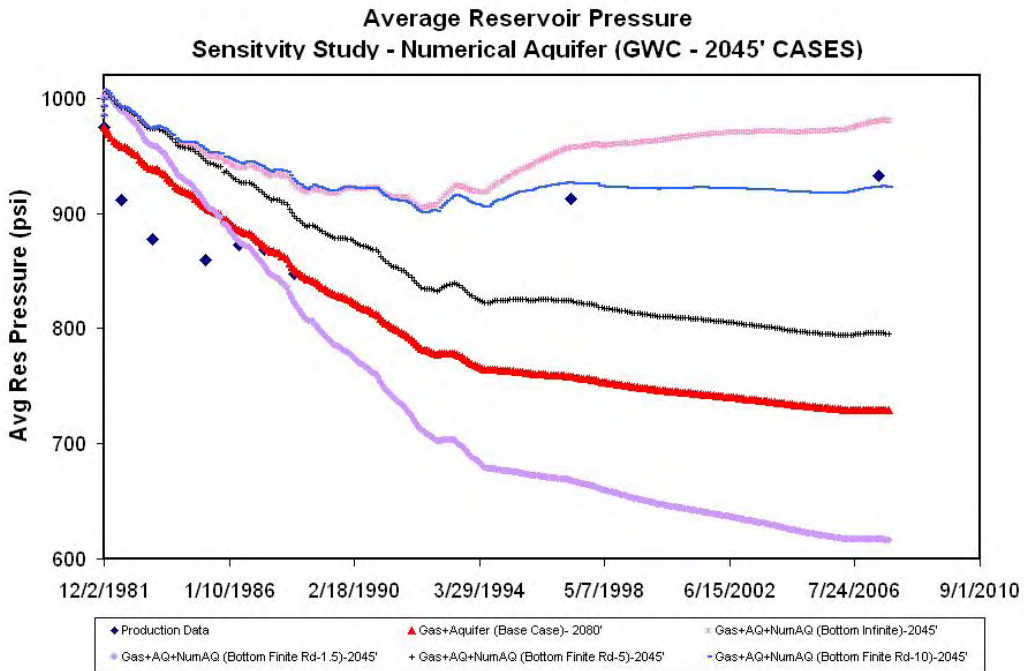


Figure 118: Average Reservoir Pressure (Sensitivity – GWC 2045') for East Barrow

V. EAST BARROW FORECASTING STUDY

The objectives and aim of performing forecasting studies have already been discussed in previous sections. This section compares the predicted responses of eight different scenarios.

1. Producing EB#14 (only)
2. Producing EB#19 (only)
3. Producing EB#14 and EB#19 together
4. Completing and producing EB#14 in horizontal plane (~1000' long)
5. Completing and producing EB#19 in horizontal plane (~1000' long)
6. Completing and producing EB#14 and EB#19 in horizontal plane (~1000' long)
7. Producing EB#14 and EB#19 with Vertical Infill Well (New Test Well)
8. Producing EB#14 and EB#19 with Horizontal Infill Well (New Test Well, ~1000')

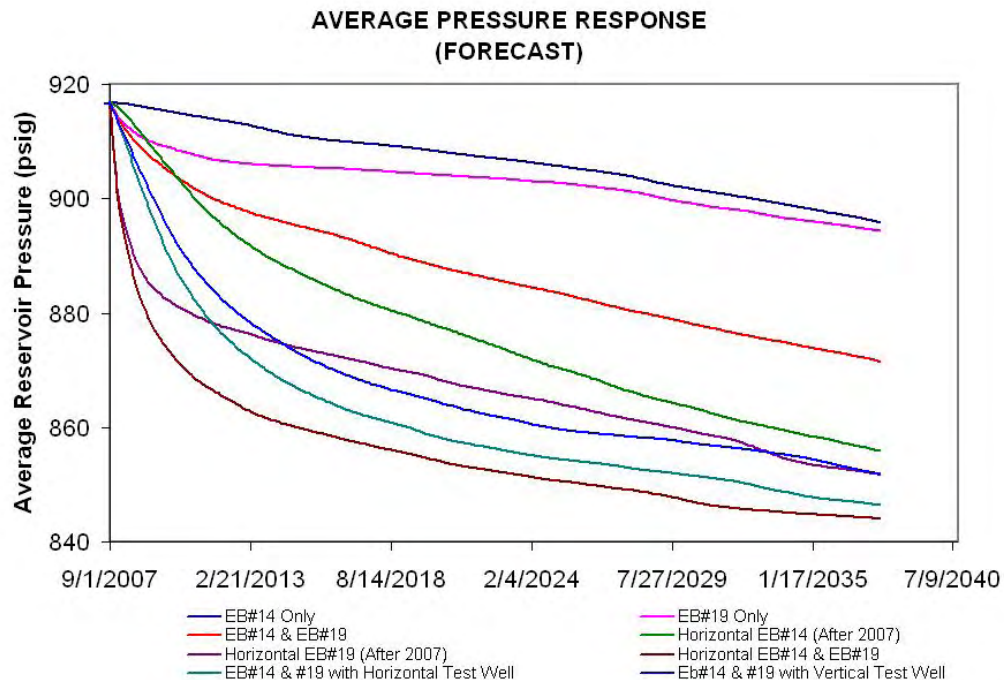


Figure 119: Average Reservoir Pressure (Forecasting Study) for East Barrow

Average reservoir pressure predicted for 30 years has been displayed in a common plot (Figure 119). The response clearly shows that when both EB#14 and EB#19 (completed horizontally) are producing, the reservoir pressure depletes at the maximum rate. This was not observed for cases where both existing vertical wells were either produced along with a new horizontal or vertical test well.

In all these cases, the average reservoir pressure indicates a change in pressure slope after 15-20 years of production. The dissociating hydrates within the reservoir were observed to be tapering off within 15-20 years. This causes pressure to deplete by gas expansion and hence, the reservoir average pressure depletes at a faster rate.

Figure 120 compares water production of all the scenarios. In the case in which both the wells (completed horizontally) are produced, the water production is observed to be extremely high. The wells have been completed as horizontal completions at the base of the existing vertical well. This has opened the entire surface area of the horizontal section to water flow. With higher gas flow rates, dissociating hydrates, and water influx from the aquifer, the water production from the horizontal section increases drastically. Contrary to this, the use of a new horizontal well, along with the two existing wells produces less water.

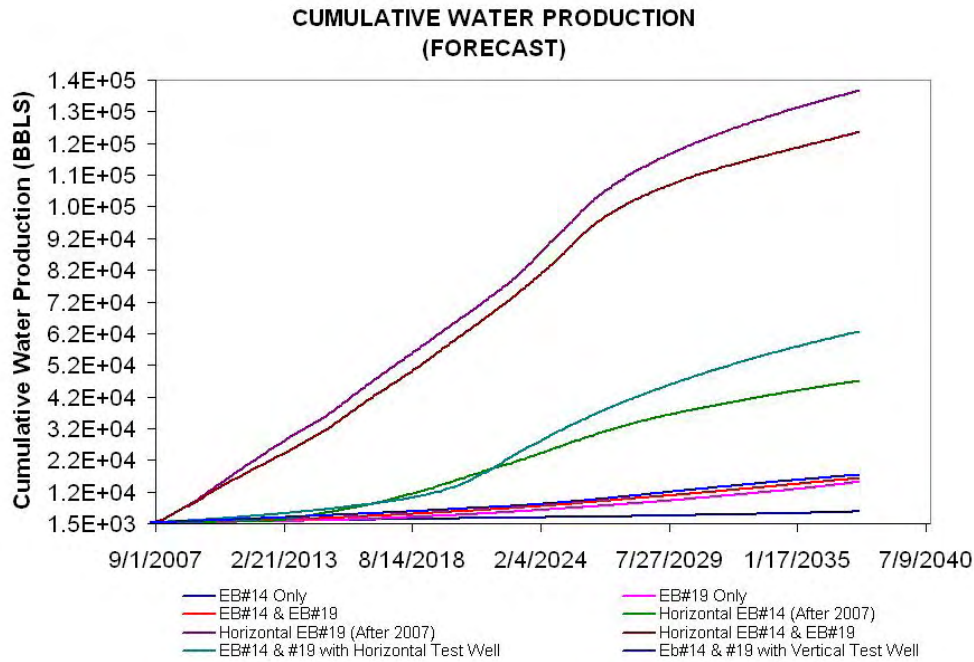


Figure 120: Cumulative Water Production (Forecasting Study) for East Barrow

The cumulative gas produced and gas recovered have been studied using Figures 121 and 122. The figures show that the cumulative gas produced in the case of completing two existing wells horizontally is equal to producing two existing wells with a new horizontal well. This is primarily due to the fact that the high water production observed in former case reduces the gas recovery. The gas production, recoveries and corresponding water production are listed in Table E-15 for all the scenarios. The last scenario offers the best combination of lower water production and higher recovery, and hence, this option can be chosen as the best option for future reservoir development.

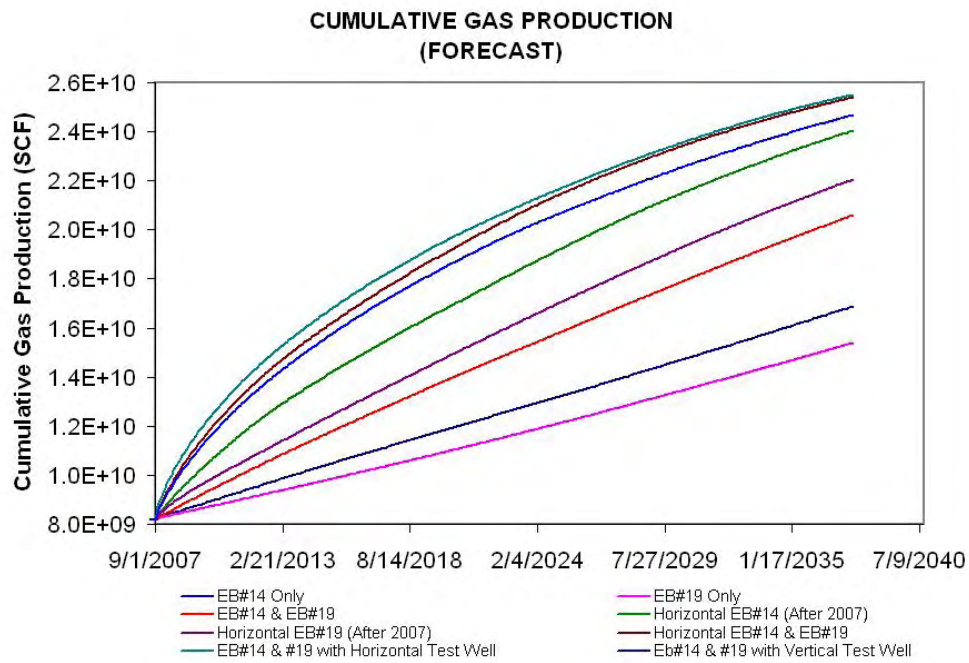


Figure 121: Cumulative gas production (Forecast Study) for East Barrow

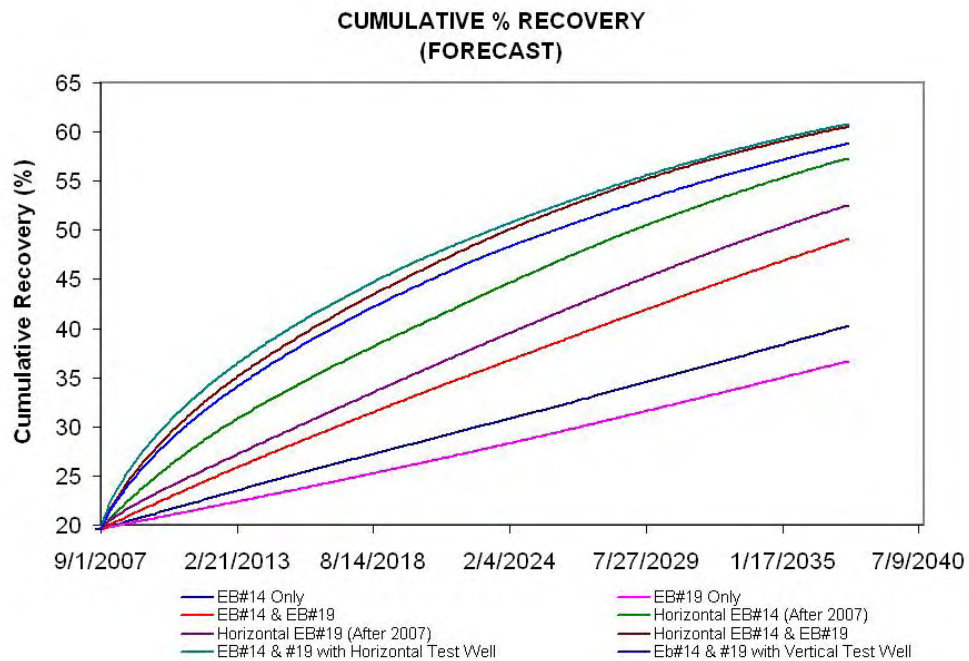


Figure 122: Recovery (Forecast Study) for East Barrow

SCENARIOS	CUMULATIVE GAS PRODUCTION (BSCF)	% RECOVERY	CUMULATIVE WATER PRODUCTION (BBLs)
Producing EB#14 (only)	16.9	40.20%	5,270
Producing EB#19 (only)	15.4	36.65%	14,610
Producing EB#14 and EB#19 together	20.6	49.10%	15,730
Completing and producing EB#14 in horizontal plane (~1000' long)	24.0	57.30%	46,450
Completing and producing EB#19 in horizontal plane (~1000' long)	22.0	52.50%	137,990
Completing and producing EB#14 and EB#19 in horizontal plane (~1000' long)	25.4	60.50%	125,060
Producing EB#14 and EB#19 with Vertical Infill Well (New Test Well)	25.5	60.75%	62,040
Producing EB#14 and EB#19 with Horizontal Infill Well (New Test Well, ~1000')	24.7	58.77%	16,825

Table E-15: Cumulative gas production and recovery on Sep 2037 (Forecast Study) for East Barrow

EAST BARROW CONCLUSIONS

A full-scale history matched reservoir simulation model has been performed on the East Barrow gas reservoir. The developed reservoir model is capable of evaluating and quantifying methane hydrate resource potential. A top-down approach has been employed to build the reservoir model and match the production history using an advanced reservoir simulator. This model is capable of evaluating and testing sensitivity to all reservoir parameters. The future reservoir performance has also been evaluated for different scenarios.

Following are the conclusions drawn from the reservoir simulation of the East Barrow reservoir:

- A. The East Barrow reservoir model, constructed and initialized in CMG-STAR3, successfully matched the reservoir production and pressure history data. The best match to production history is represented by a gas reservoir overlain by a thick layer of hydrate, and associated with aquifer support from the bottom.
 - a. The total initial gas (total = free + hydrate associated) in place is found to be 42 BCF.
 - b. The pressure-temperature condition of the hydrate zone is such that the three phases, water-gas-hydrate, exist in thermodynamic equilibrium.
 - c. The hydrate dissociation occurs due to depressurization and heat transfer from the surroundings.
 - d. As of 2007, 27% of initial hydrate in place has been dissociated (from 1981 to 2007).
 - e. Dissociating hydrates have charged the free gas reservoir by supplying more than 86% of total gas produced to date.
 - f. The hydrate-free gas contact has shifted upwards from an initial depth of 2050' to 2045' sub-sea.
 - g. The free gas-water contact has shifted from an initial depth of 2080' to a depth of 2070' sub-sea.
 - h. The possibility of having a strong aquifer support associated with free gas type reservoir has been evaluated; however, water influx alone failed to explain the production and pressure history of the reservoir.
- B. Sensitivity studies were performed to understand the impact of parameters on reservoir performance and also to investigate the possibility of explaining reservoir behavior with the help of free gas-aquifer system.
 - a. Hydrate saturations of 31% in the hydrate zone best matched the reservoir performance.
 - b. The simulator was unsuccessful in running the reservoir model with hydrate saturation of 45%, i.e. the reservoir saturated with hydrate and bounded water phases only. Free gas within the hydrate zone was required for the model to run.

- c. The free-gas aquifer sensitivity study failed to match the observed reservoir performance, thus confirming the previous history matching results that reservoir performance cannot be solely explained by a water aquifer.
- C. Forecasting studies were performed for next 30 years of production life of the reservoir. The conclusions drawn from this study are:
 - a. Complete hydrate dissociation (100% dissociation) was predicted within 15-20 years (between years 2022 and 2027) for all the forecasting scenarios.
 - b. The forecasting study showed that the best reservoir performance, of maximizing gas recovery while minimizing water production, was observed when the existing wells EB#14 and EB#19 were produced, along with a new horizontal infill well (~1000 ft long). The scenario produced a total of 25 BCF (from 1981-2037), which is equivalent to a recovery of 58.8% of total initial gas in place. The cumulative water production in this scenario was predicted to be lowest for equivalent gas recoveries, with a predicted cumulative water production of 16,825 BBLS.

WALAKPA METHODOLOGY

The CMG STARS simulator was used to build the top-down reservoir model for the Walakpa reservoir. The same methodology as described in the East Barrow study in this report was followed while constructing the Walakpa model and will not be repeated in this section of the report. Two Walakpa models were constructed:

- A SMALL MODEL included the mapped free gas interval, an aquifer and a 4000' length of hydrate updip of the hydrate/free gas interface. This model was history matched to confirm that the reservoir performance was not simply volumetric or a waterdrive reservoir mechanism, but required hydrate dissociation to make the best history match.
- A LARGE MODEL that included the free gas zone and aquifer and included the regionally extensive hydrate volume based on the geologic mapping of the Walakpa sand with well control to the north into the Barrow Gas Field wells. There was no attempt to history match this large model, due to the limited production data associated with such a large reservoir model. The purpose of the LARGE MODEL was to define in place hydrate resources and simulate the dissociation of the hydrate in the future, as the hydrate is dissociated and the hydrate/free gas interface migrates updip.

WALAKPA MODEL INTIALIZATION

Walakpa Reservoir Model - Base Case

The Walakpa model initialization, history matching and forecasting techniques are based on previous full scale field simulation studies performed on the East Barrow gas field, as previously described in this report. In this section, the model intialization (in CMG-STARS) for the best case is discussed.

The most likely scenario consists of a hydrate cap overlying a free gas field, and underlain with model aquifer. This scenario is confirmed by the aquifer observed to the south in the Brontosaurus #1 and a hydrate stability zone determined by the temperature/pressure regime. Additionally, hydrates appear to be observed in the Walakpa sandstone in Walakpa #1 and NSB #6 well logs, as well as others. This section will discuss the reservoir properties and wellbore model initialized for the base case. All parameters have been initialized in field units.

A. Reservoir Grid – SMALL MODEL

Based on reservoir geology and well log data, a detailed reservoir model, depicting the Walakpa gas reservoir was built using RMS¹⁹. The data file generated using RMS was directly imported into CMG-STARS by using *INCLUDE keyword. The geological description and geostatistical modeling procedures are described in Panda and Morahan, 2008¹⁹.

The model has been generated using a Cartesian co-ordinate system by choosing a grid having 100 blocks in the I direction, 63 blocks in J direction, and 10 blocks in K direction, making a total of 63,000 grid blocks. The dimension of each grid block is 500' by 500' (IJ plane). The grid block thickness in K direction is variable and ranges anywhere between 1.6 ft and 4.5 ft. The topmost section of the reservoir is at a depth of 1879 ft below sea level, whereas the deepest section is at a depth of 3111 ft below sea level. However, the pay zone depth ranges between 1879 ft to 3109 ft below sea level. The 3D reservoir grid is shown in Figure 123.

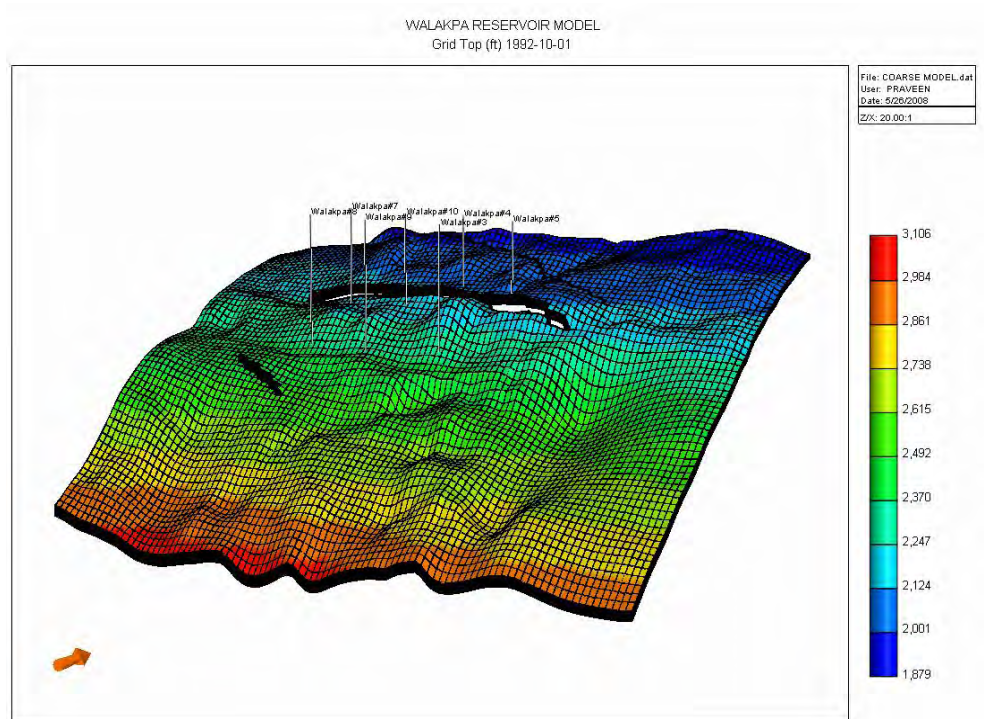


Figure 123: 3D reservoir grid (Grid Top) – Walakpa Reservoir Model

B. Reservoir Properties – SMALL MODEL

1. Porosity

For details regarding porosity distribution and estimation procedure, refer to the topical report by Panda and Morahan, 2008¹⁹. The porosity distribution data file is loaded into the CMG-STARs data file using *INCLUDE keyword. The porosity of the reservoir ranges from 8.5% (min) to 24.7% (max). Figure 124 shows a 3D view of porosity distribution within the reservoir.

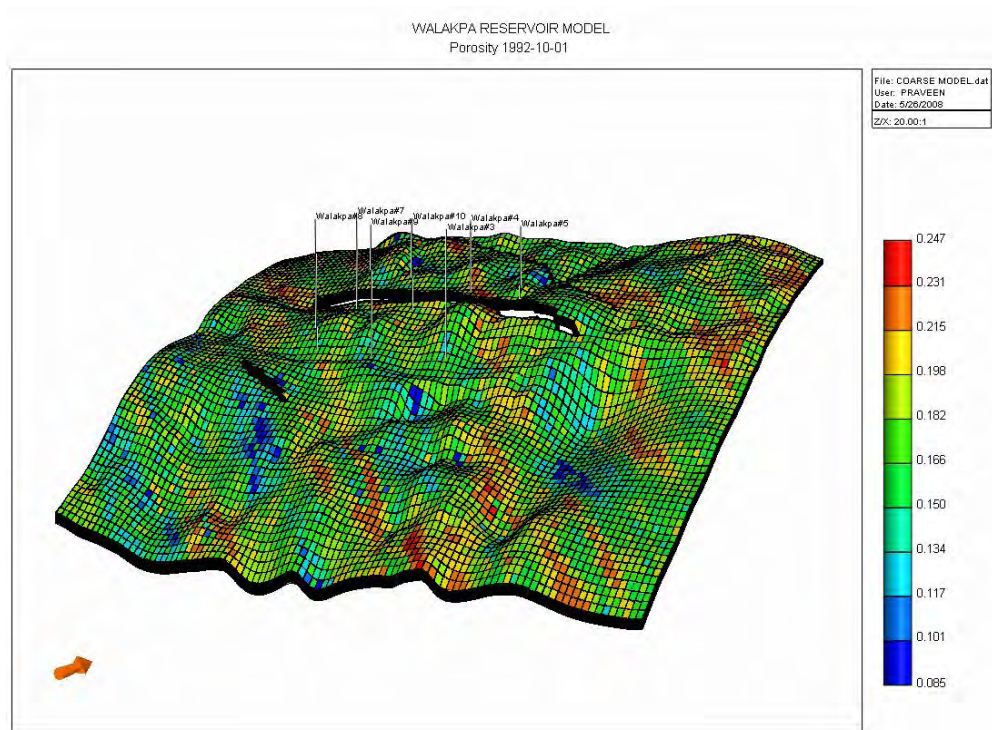


Figure 124: Porosity (3D view) – Walakpa Reservoir SMALL MODEL

2. Permeability

Reservoir permeability was calculated on the basis of well log data. Details about reservoir characterization and geostatistical modeling approach have already been discussed in “geology and characterization” report¹⁹. The *INCLUDE keyword is used to load these permeability data directly into the reservoir model. The reservoir permeability (I-J-K directions) is mostly in the range of 0.1-250 mD. Figure 125 shows a 3D view of permeability distribution within the reservoir in I direction. The permeability distribution in J and K direction is similar.

WALAKPA RESERVOIR MODEL
Permeability I (md) 1992-10-01

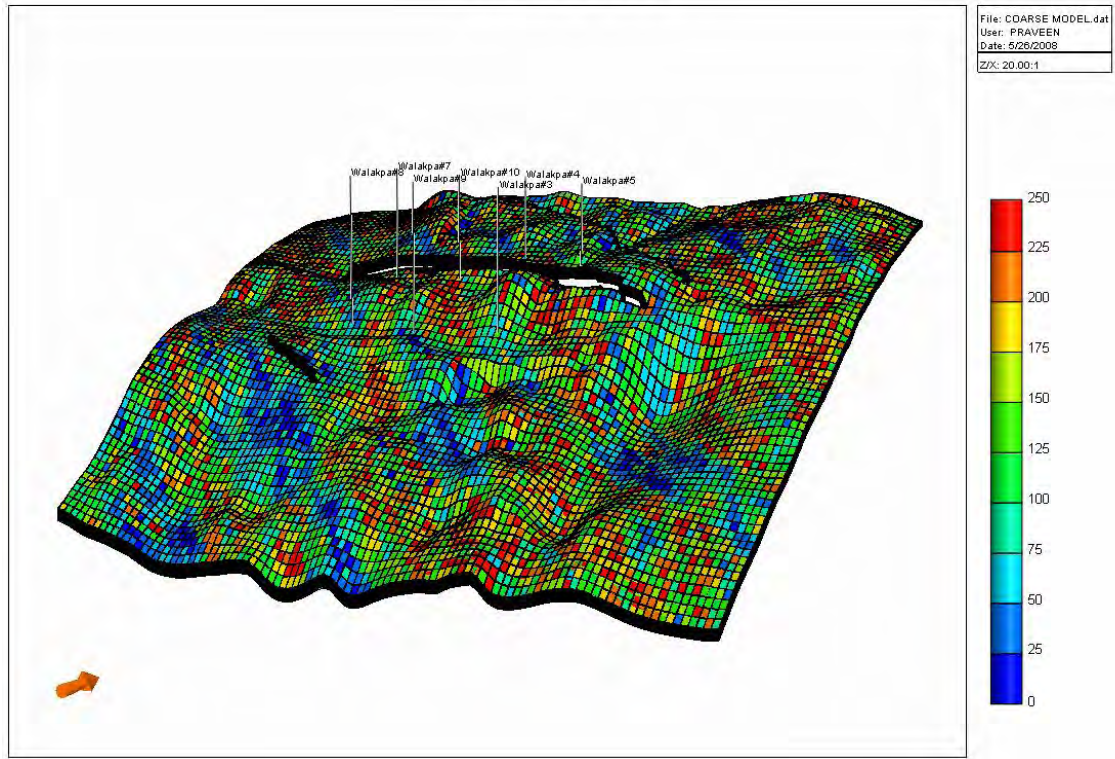


Figure 125: Walakpa Permeability-I (3D view) – SMALL MODEL

3. Initial Temperature

Geothermal gradient data obtained for Walakpa reservoir is 1.88⁰F/100ft. The reservoir top temperature is 49.6⁰F and bottommost region has a temperature of 72.4⁰F. The temperature distribution within the reservoir is initialized on the basis of reservoir depth. The temperature distribution is shown in Figure 126.

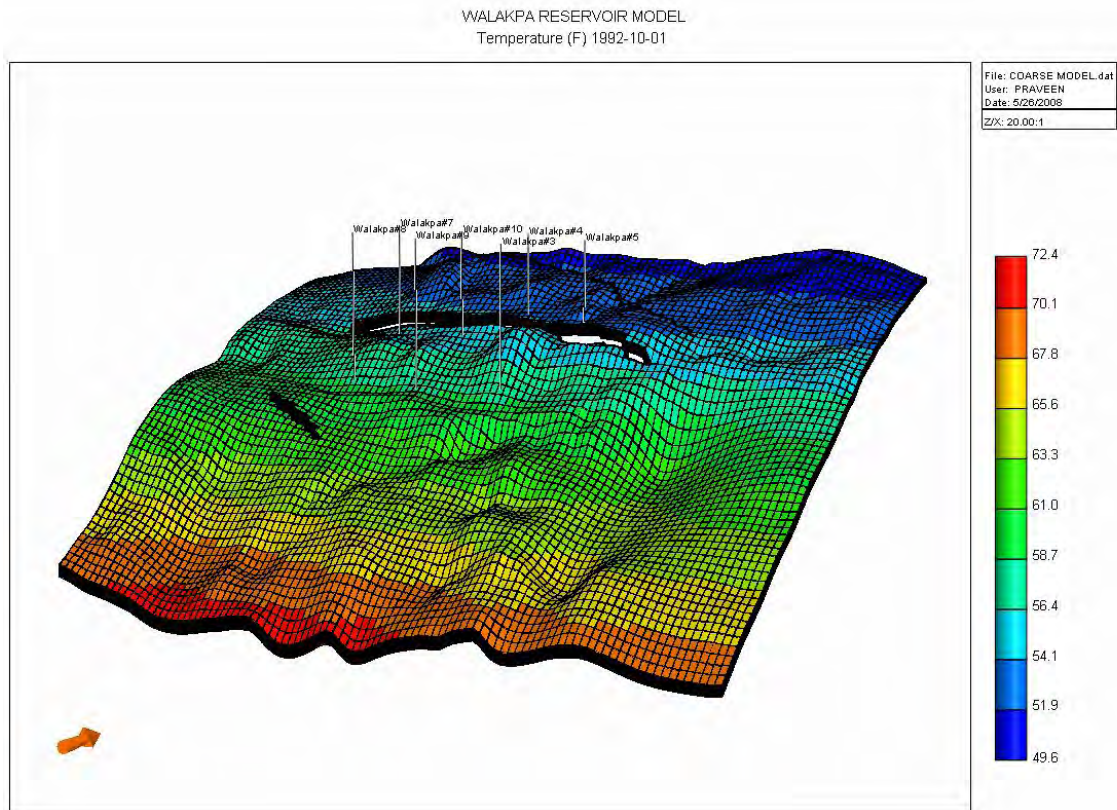


Figure 126: Walakpa Temperature, Deg F (3D view) – SMALL MODEL

4. Initial Reservoir Pressure

Well testing and pressure gradient data reported in previous studies conducted for Walakpa gas pool conclude that the initial reservoir pressure of the reservoir is 1037 psi²⁰. Since the model consists of hydrate cap and free gas zone underlain with model aquifer, the effect of gravity on reservoir pressure in the free gas zone has been neglected. The pressure gradient in the aquifer zone has been initialized based on a pressure gradient of 0.433 psi/ft. Figure 127 shows the initial condition as specified in CMG-STARS.

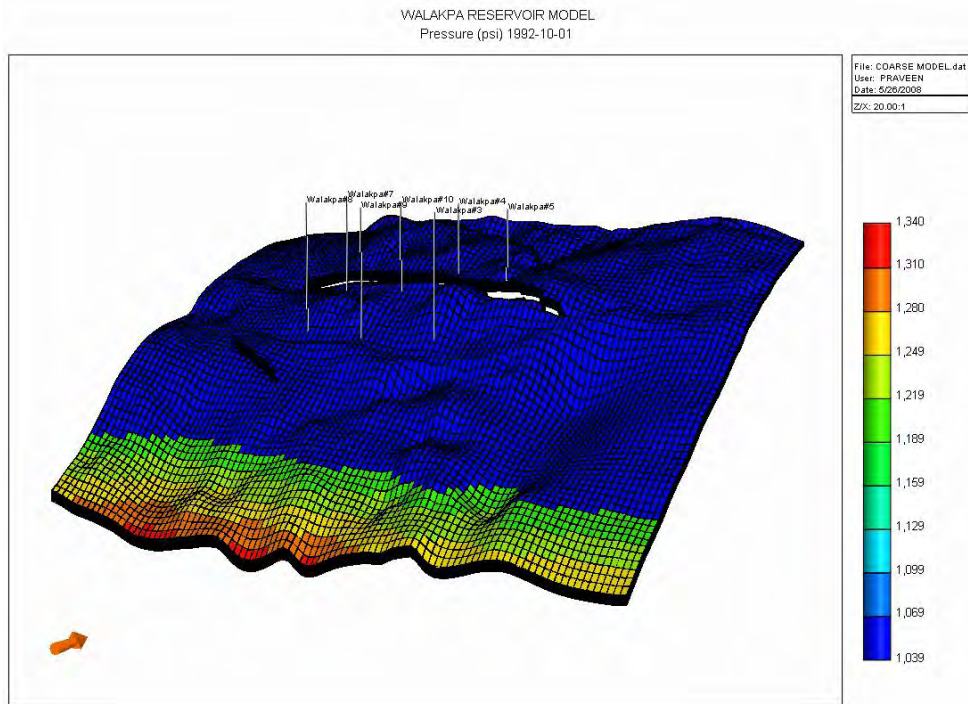


Figure 127: Walakpa Pressure, psi (3D view) – SMALL MODEL

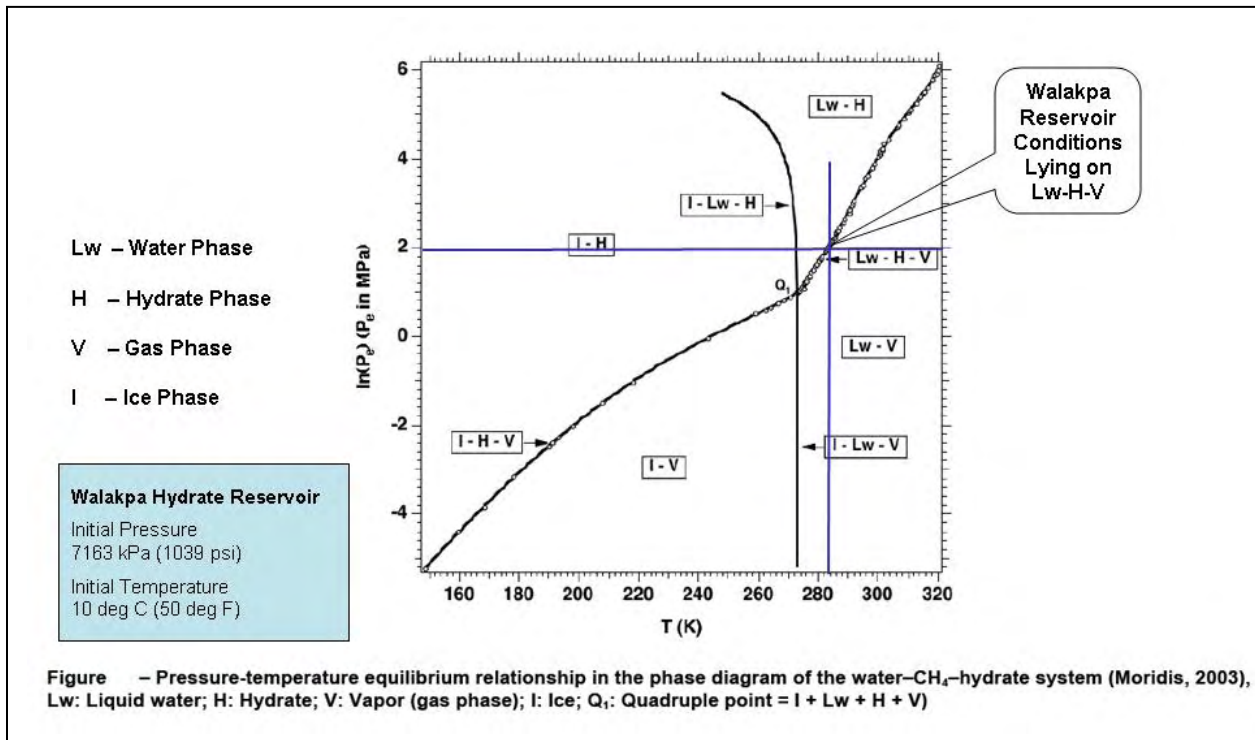


Figure 128: Pressure-temperature equilibrium relationship for water-hydrate-free gas system

5. Hydrate Saturation

The hydrate-free gas contact for Walakpa gas reservoir is estimated to be -2000'. The pressure-temperature condition (refer to Figure 128)¹⁸ for Walakpa gas field lies on the three phase pressure-temperature equilibrium curve (Lw-H-V, basis 100% methane). This clearly suggests that the hydrate zone is saturated with all the three phases i.e. hydrates, free gas and bounded water. The hydrate saturation in hydrate zone has been initialized as 30%. A hydrate zone of 0% is initialized in the free gas and aquifer zones.

Figure 129 shows a 3D view of hydrate distribution. Figure 130 is a magnified 2D (JK plane) image showing hydrate saturation in the hydrate zone down to the hydrate-free gas contact at -2000'.

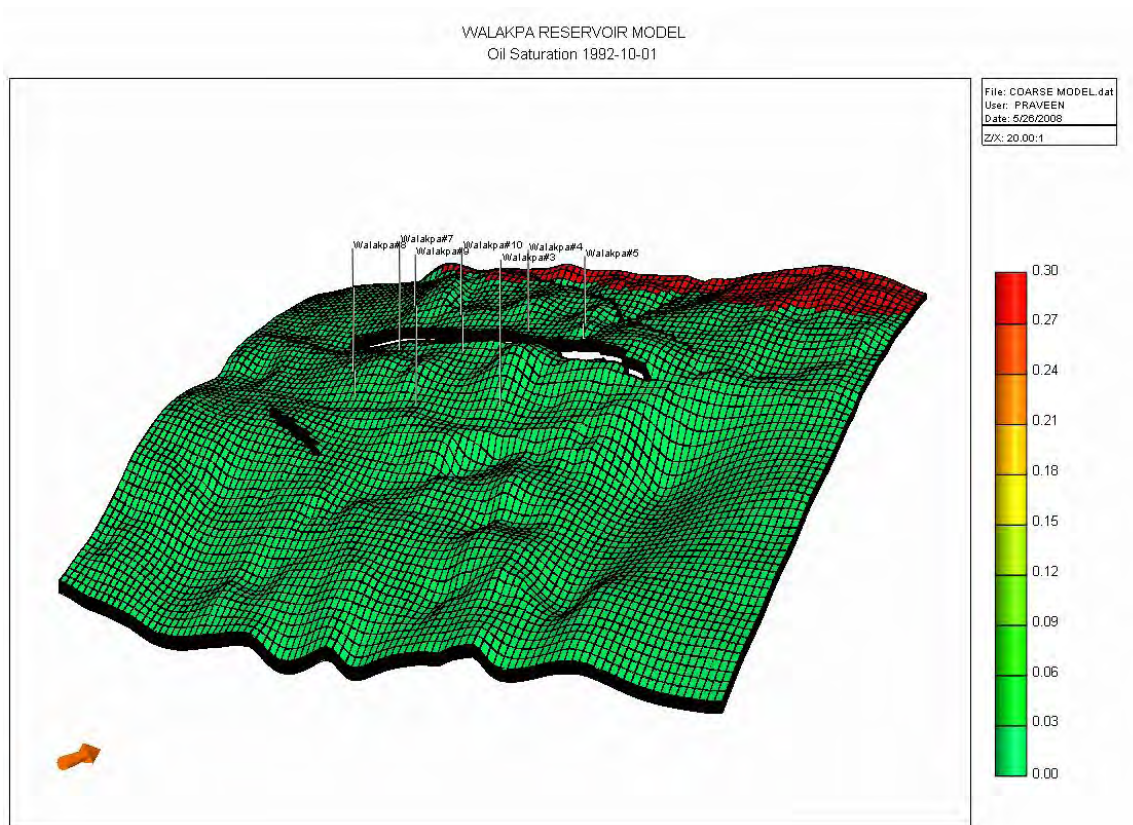


Figure 129: Walakpa Hydrate Saturation, S_h (3D view) – SMALL MODEL

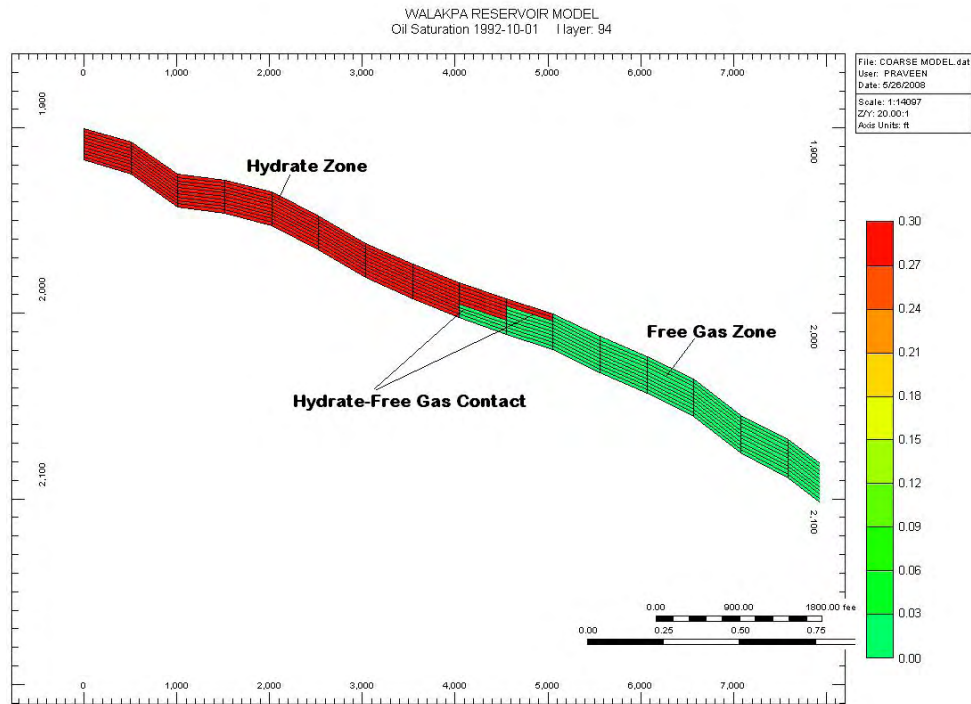


Figure 130: Walakpa Hydrate –Free Gas Zone Contact at 2000’ (JK Plane view) - SMALL MODEL

5. Gas Saturation

The thermodynamic condition of the hydrate zone is such that the hydrate phase exists in equilibrium with free gas phase and bounded water phase. Hence, the gas phase saturation is defined for both the hydrate and free gas zones. The well logs for East Barrow have shown that the irreducible (bounded) water saturation for both the hydrate and free gas zones is 55%, the same has been followed for Walakpa gas field and the estimated gas water contact is at 2750’. Hence, the free gas saturation initialized in the hydrate zone is 15% and for the free gas zone is 45%.

Figure 131 shows a 3D view of gas distribution. Figure 132 is a 2D (JK plane) image showing hydrate-free gas and free gas-water contacts at 2000’ and 2750’, respectively.

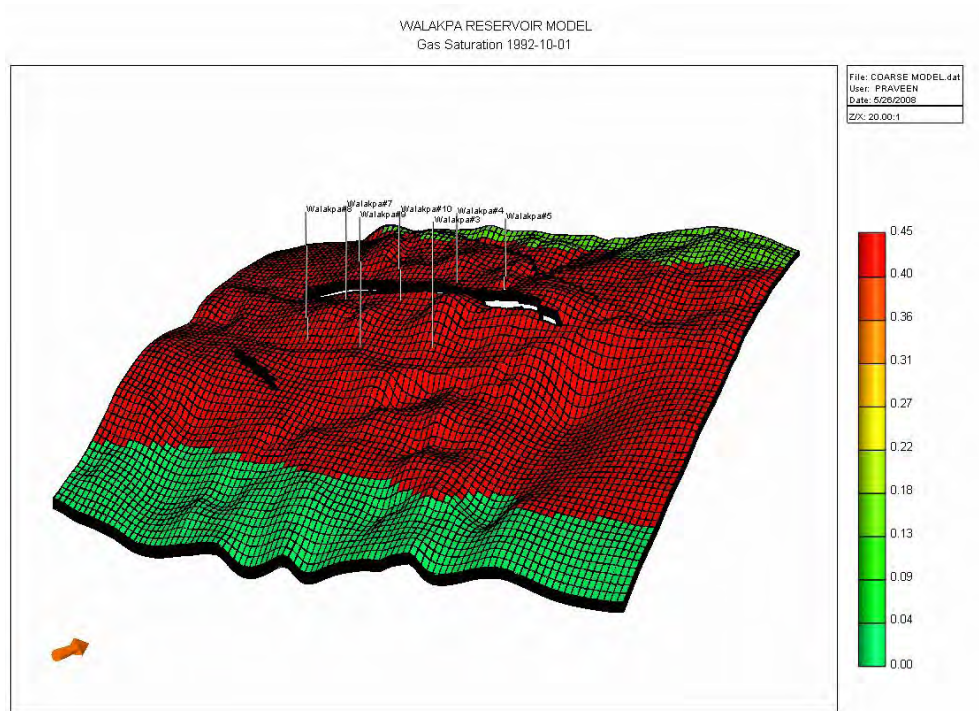


Figure 131: Gas Saturation, S_g (3D view) – SMALL MODEL

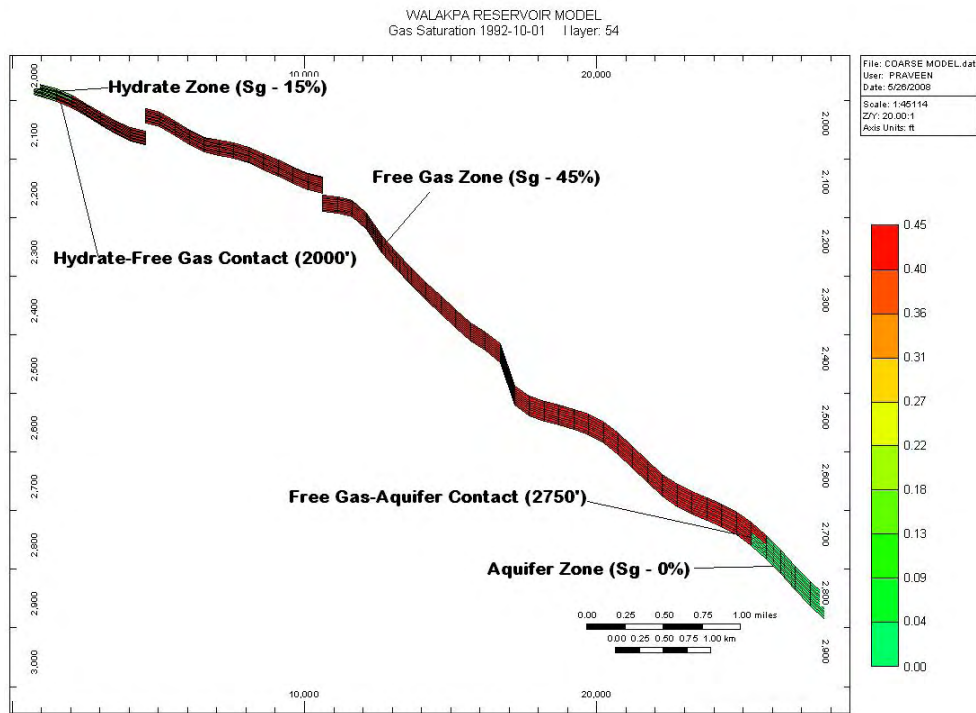


Figure 132: Walakpa Hydrate –Free Gas Zone Contact at 2000' and Gas-Water Contact at 2750' (JK Plane view) – SMALL MODEL

6. Water Saturation

As stated earlier, well log and core analysis data clearly suggest that the irreducible/connate water saturation in the hydrate and free gas zones is very high, i.e. S_w of 55%. To model the aquifer zone, water saturation of 100% has been initialized. Figure 133 shows a 3D view of water distribution. Figure 134 is a 2D (JK plane) image showing free gas-water contact 2750’.

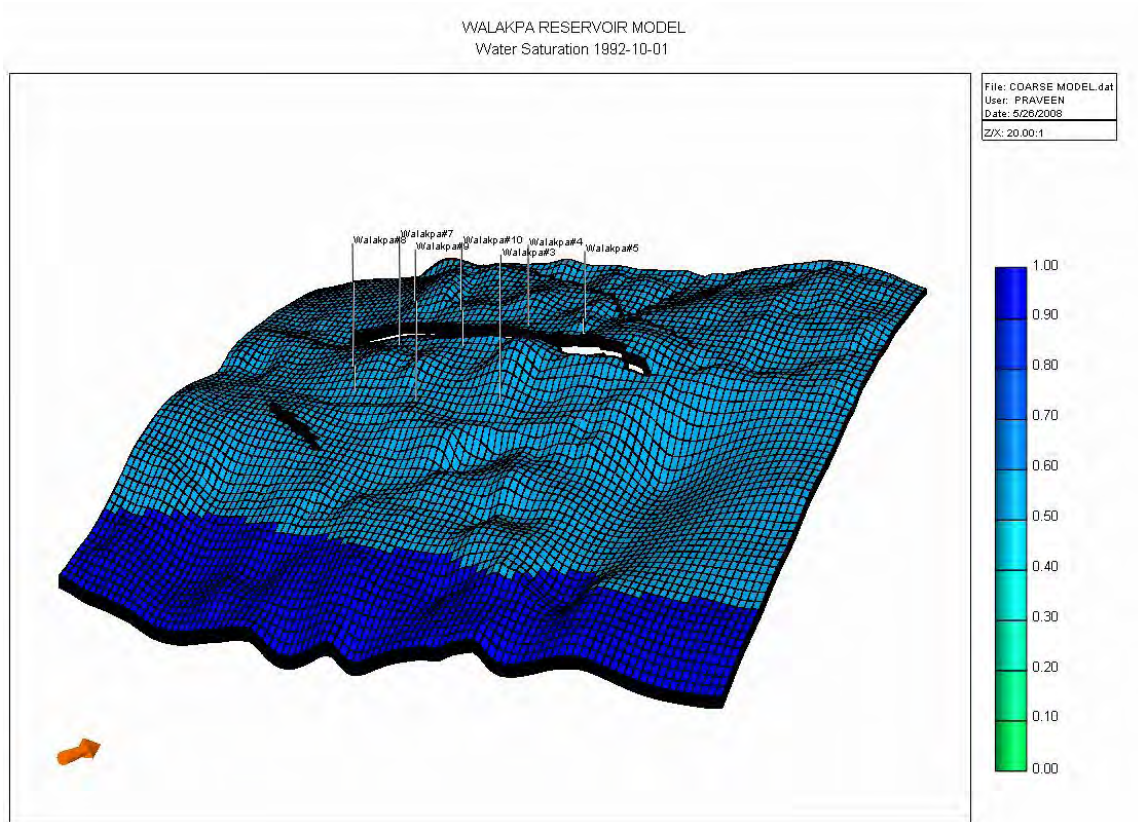


Figure 133: Walakpa Water Saturation, S_w (3D view) – SMALL MODEL

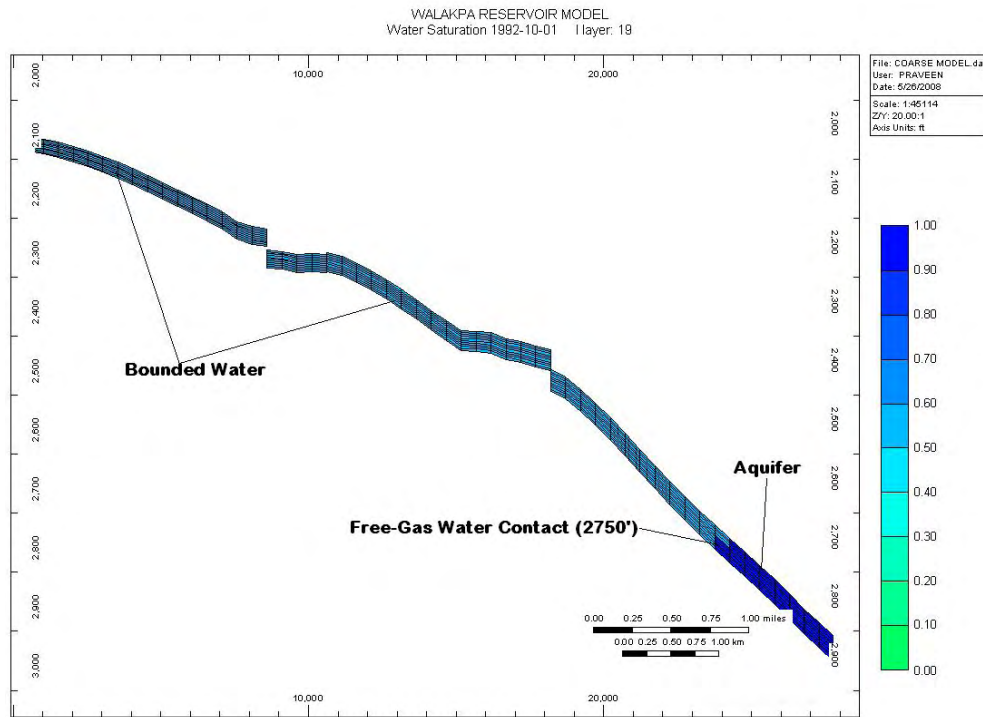


Figure 134: Walakpa Gas-Water Contact at 2750' (JK Plane view) – SMALL MODEL

Zone	Pressure	Temperature	Saturation	Remarks
Hydrate			$S_h = 30\%$ $S_g = 15\%$ $S_w = 55\%$	(Lw-H-V) close to Equilibrium
Free Gas*	1037 psi	Temperature Gradient $1.88^{\circ}\text{F}/100\text{ft}$	$S_g = 45\%$ $S_w = 55\%$	*Hydrate-Free Gas Contact- 2000'
Aquifer**		Top Temp 49.6°F	$S_w = 100\%$	**Free Gas-Water Contact-2750' **Press Grad 0.433 psi/ft

Table W-1: Walakpa reservoir model – Initial reservoir conditions

C. Thermal Properties

Thermal properties have been initialized similar to the East Barrow reservoir model described earlier in this report.

D. Fluid/Component Properties

Fluid and component properties have been initialized similar to East Barrow reservoir model described earlier in this report.

E. Relative Permeabilities and Capillary Pressure Functions

Relative permeabilities and capillary pressure functions have been initialized similar to East Barrow reservoir model described earlier in this report.

F. Production Well Modeling

The production history data and well details for the Walakpa gas field are presented in Table W-2. Table W-3 presents location and completion date of each well. Figure 135 shows a 2D image of wells in the Walakpa gas field.

PRODUCTION DATA WALAKPA GAS FIELD

Number of Wells	Walakpa #2, #3, #4, #5, #6, #7, #8, #9, #10 (Total 9 producing wells)
Completion	All in gas zone
Production Period	October, 1992 – September, 2007
Cumulative gas production	17.13 BCF (STD Condition)
Cumulative water production	None Reported

Table W-2: Production history data – Walakpa gas field

Well Name	Co-ordinate (Reservoir Top) I, J, K	Well Direction	Well Radius	Well Completion Date
WAL#2	54, 22, 1	K-Direction (Vertical Well)	0.4933 ft	Apr 01, 2000
WAL#3	51, 34, 1		0.5305 ft	Oct 01, 1992
WAL#4	49, 45, 1		0.5305 ft	Oct 01, 1992
WAL#5	59, 43, 1		0.5305 ft	Oct 01, 1992
WAL#6	66, 31, 1		0.5305 ft	Apr 01, 1997
WAL#7	29, 43, 1		0.5305 ft	Oct 01, 1992
WAL#8	27, 34, 1		0.5305 ft	Oct 01, 1992
WAL#9	38, 33, 1		0.5305 ft	Oct 01, 1992
WAL#10	40, 42, 1		0.5305 ft	Oct 01, 1992

Table W-3: Location (co-ordinates) and dimensions of Walkakpa Wells

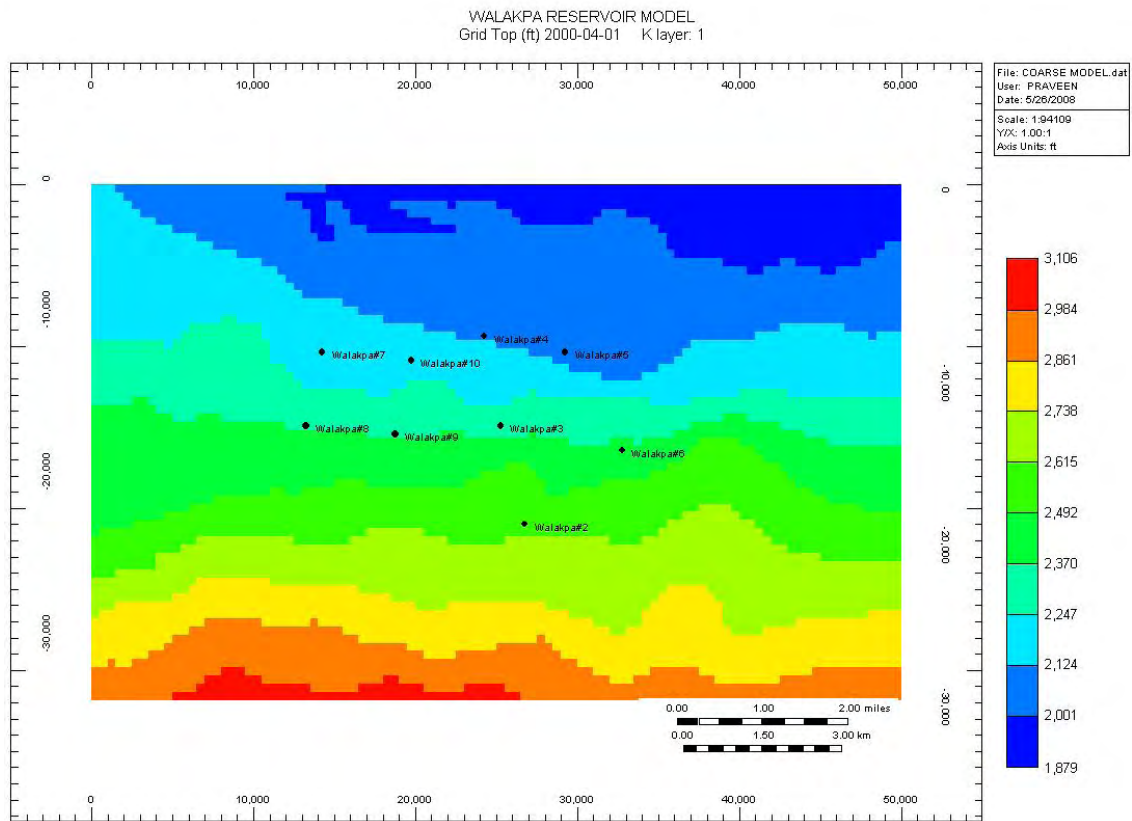


Figure 135: Walakpa Well locations (IJ Plane View)

WALAKPA RESULTS AND DISCUSSIONS

I. WALAKPA HISTORY MATCHING – SMALL MODEL

Two scenarios were developed and the performance was studied and matched with reservoir history data. The history matching was performed both at the reservoir level and well level. The reservoir level match has been initiated for both scenarios. Upon achieving a close match, individual well level match was performed for the best case scenario. The initial estimates of free gas, hydrates and associated (bounded) water have been estimated for each scenario. Table W-4 presents the estimates for each case.

SMALL MODEL Scenario	Reservoir Model	Hydrate	Free Gas		Water
		res ft ³	res ft ³	SCF	reservoir ft ³
A.	<i>Gas + Aquifer model</i>	0.00	3.05 E+9	245.3 E+9	6.03 E+9
B.	<i>HYD + Gas + Aquifer model (Best Case)</i>	8.88 E+7	2.96 E+9	237.9 E+9	6.03 E+9

Table W-4: Initial estimates of free gas, hydrate and water for Walakpa – SMALL MODEL

Table W-5 shows initial free gas estimates (at STD condition). These estimates include gas associated with hydrates. Conversion from in place hydrates to gas in standard conditions is one reservoir volume of hydrate (res ft³) is equal to 174 STD cubic ft of free gas.

SMALL MODEL Scenario	Reservoir Model	Hydrate Associated Free Gas	Free Gas	Total Initial Gas In Place (Free + Hydrate Associated)
		STD condition	STD cond ⁿ	STD condition
A.	<i>Gas + Aquifer model</i>	0.00	245.3 E+9	245.3 E+9
B.	<i>HYD + Gas + Aquifer model (Best Case)</i>	15.45 E+9	237.9 E+9	253.4 E+9

Table W-5: Walakpa Initial Gas In Place (Free Gas + Hydrate Associated Gas) – SMALL MODEL

Field Level Match

1. Cumulative gas production

Figure 136 is a plot showing cumulative gas production obtained for the two scenarios. The production history data has also been plotted on the same graph. The cumulative gas production profile for both the cases matches perfectly with the production data.

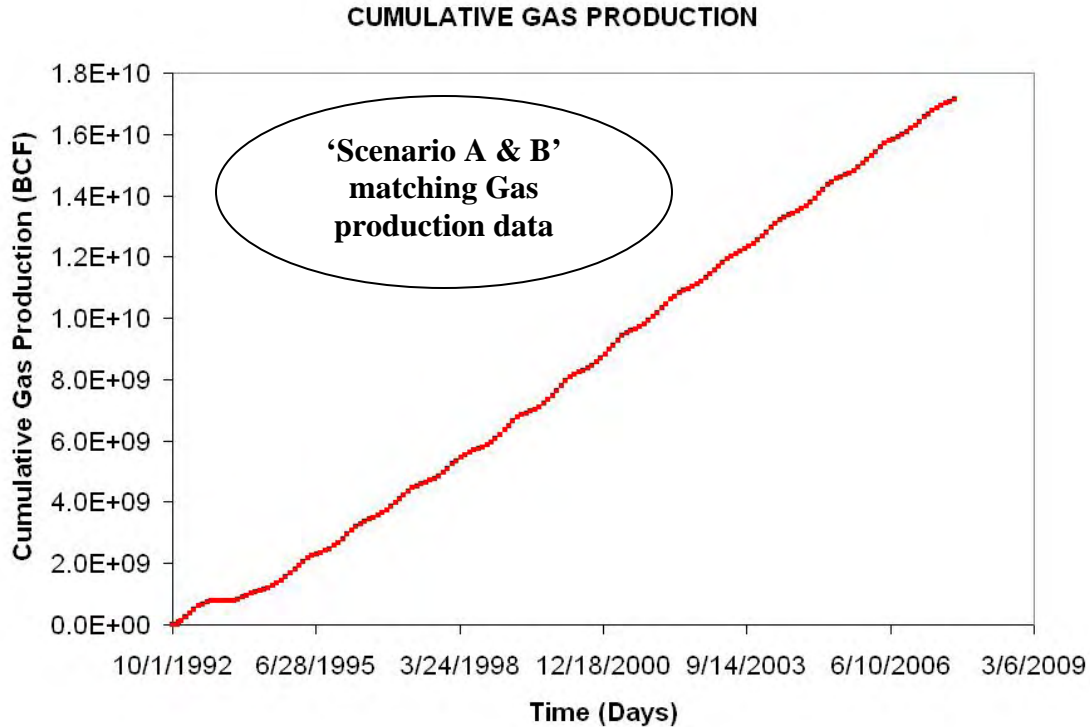


Figure 136: Walakpa Cumulative gas production profile (History Matching) – SMALL MODEL

SMALL MODEL SCENARIO	SIMULATION RESULT Cumulative Gas Production (Septemeber 2007)
Production History Data	17.10 E+9 SCF
Scenario A	17.10 E+9 SCF
Scenario B	17.10 E+9 SCF

Table W-6: Cumulative gas production (September 2007) for Walakpa

2. Reservoir pressure

Horner pressure and pressure history data has been matched for each scenario individually. Figures 137 and 138 present the pressure profile of Scenario A and B, respectively. The pressure co-ordinates, representing reservoir pressure distribution, have been compared with pressure history data (refer to Figure 139).

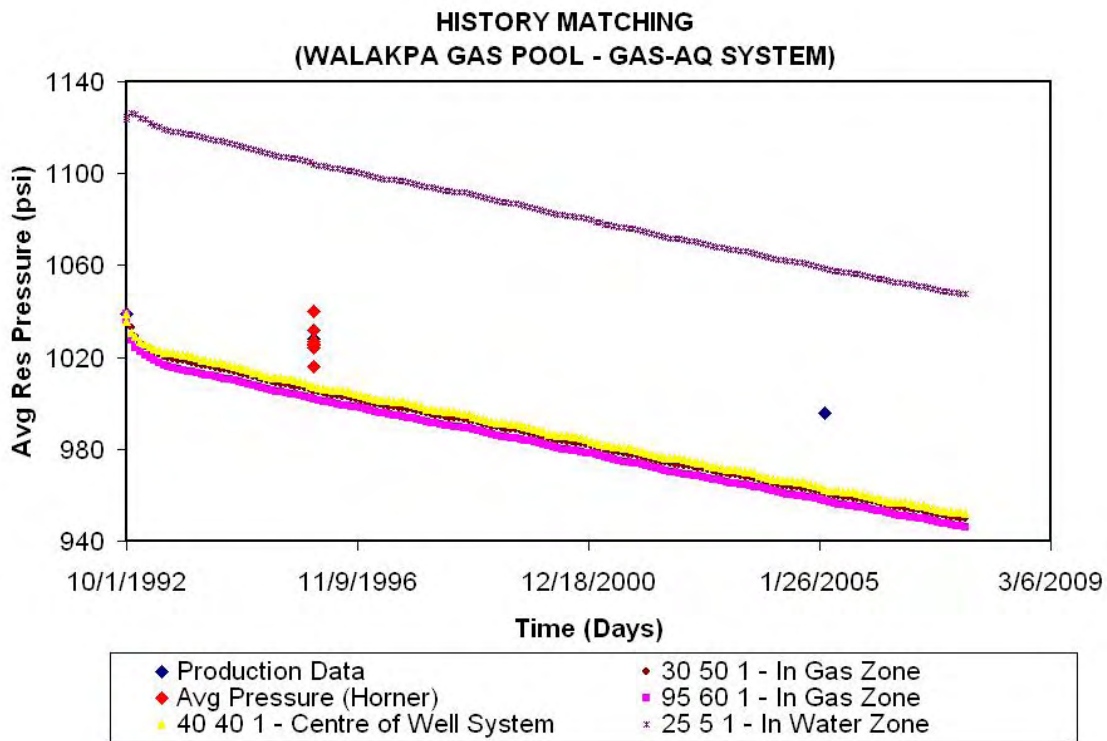


Figure 137: Reservoir Pressure Match (Scenario-A) – SMALL MODEL

Root mean square error for pressure co-ordinates in Scenario-A are given in Table W-7.

SMALL MODEL SCENARIO-A (Reservoir Pressure Co-ordinate)	SIMULATION RESULT Root Mean Square Error
Free Gas Zone (30, 50, 1)	2.40
Free Gas Zone (95, 60, 1)	2.67
Cente of Well System (40, 40, 1)	2.26
Aquifer Zone (25, 5, 1)	7.32

Table W-7: Root Mean Square Error-Scenario A (Res Press Data vs Model Output) for Walakpa – SMALL MODEL

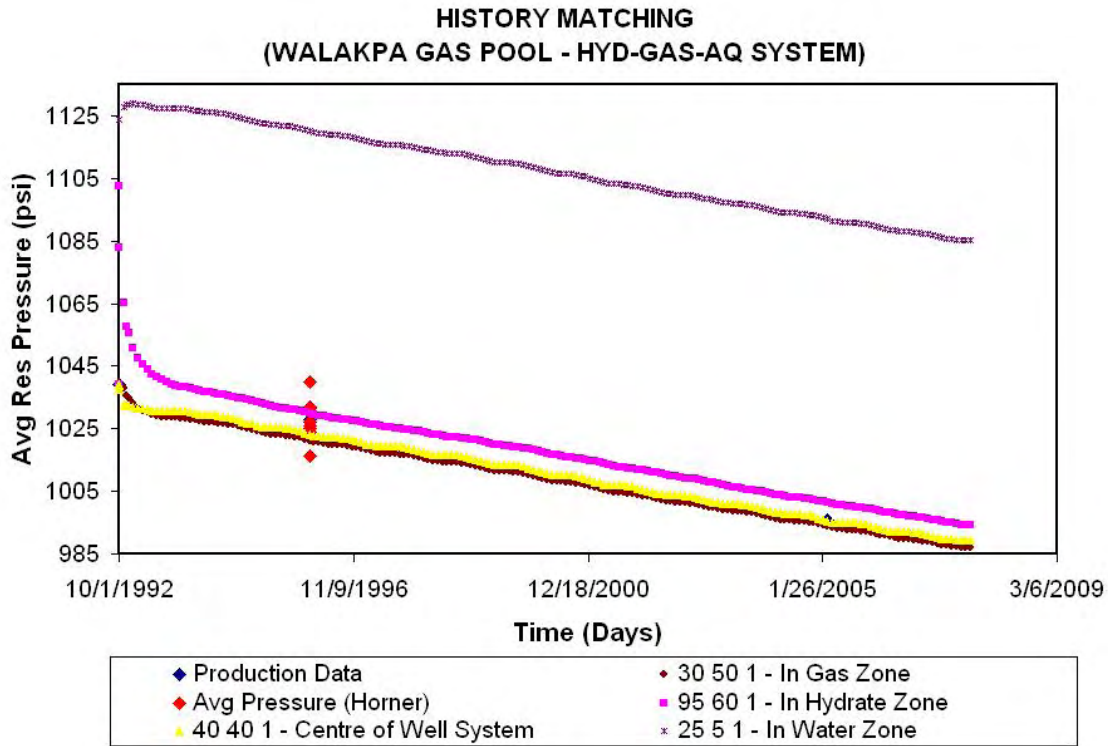


Figure 138: Reservoir Pressure Match (Scenario-B) for Walakpa – SMALL MODEL

Root mean square error for pressure co-ordinates in Scenario-B are given in Table W-8.

SMALL MODEL SCENARIO-B (Reservoir Pressure Co-ordinate)	SIMULATION RESULT Root Mean Square Error
Gas Zone (30, 50, 1)	0.40
Hydrate Zone (95, 60, 1)	2.45
Center of Well System (40, 40, 1)	0.27
Aquifer Zone (25, 5, 1)	8.94

Table W-8: Root Mean Square Error-Scenario B (Res Press Data vs Model Output) for Walakpa – SMALL MODEL

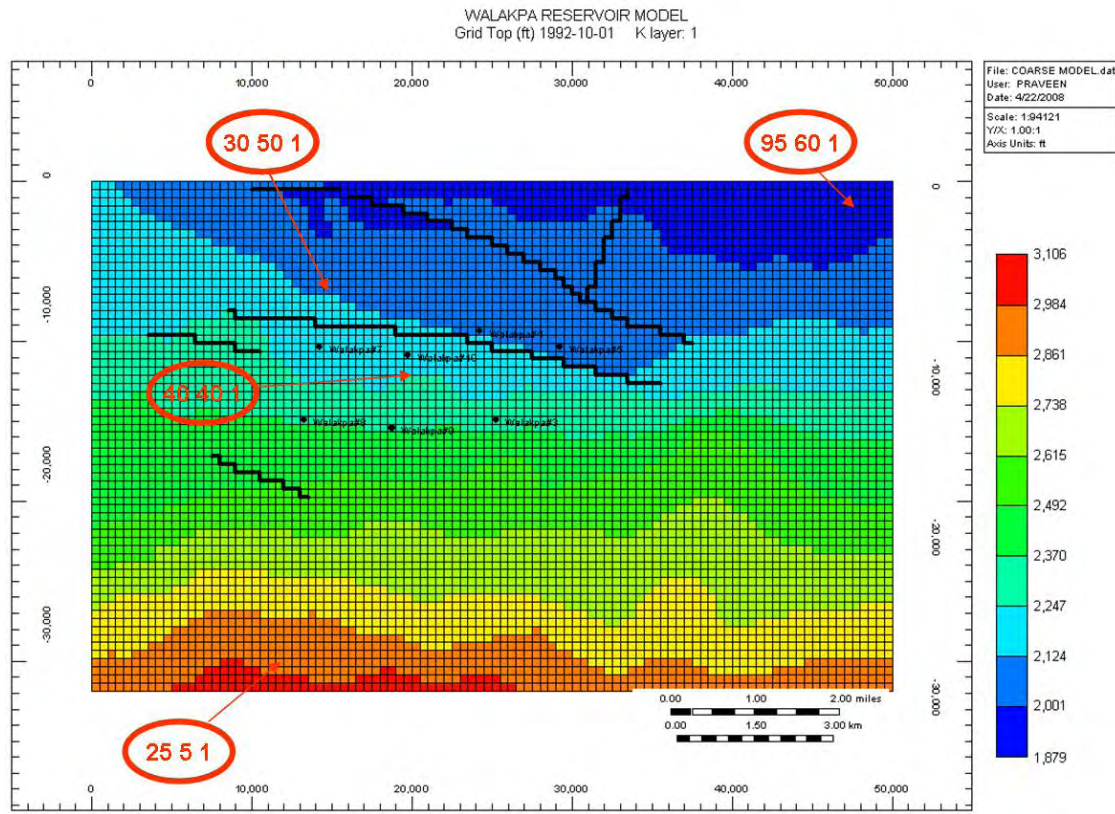


Figure 139: Pressure co-ordinates selected to represent reservoir pressure for Walakpa

The field level match shows that the ‘Scenario B’ matches the reservoir pressure much better than ‘Scenario A’. Therefore, the Walakpa gas reservoir is most likely associated with hydrates and aquifers with hydrate-gas contact at -2000’ and gas-water contact at -2750’.

II. WALAKPA DATA ANALYSIS

Hydrate/Free Gas Contribution

To calculate the total gas production from in situ hydrates, detailed reservoir mapping was performed. The difference in hydrate reserve between the two periods provides an estimate of the amount of hydrate dissociated. CMG-STARS calculates hydrate per unit area for each IJ block (all k layer). This information can be used to obtain initial and final hydrate in place, and can be extended to calculate total amount of gas produced from hydrate dissociation, percent hydrate dissociation and contribution of hydrate as a percent of gas produced. Total gas produced from hydrate dissociation and percent hydrate dissociation for the best case model has been presented in the Table W-9.

DESCRIPTION	RESULT
Initial volume of hydrates	8.88 E+7 res ft ³
Volume of hydrate dissociated	6.15 E+7 res ft ³
Gas produced by hydrate dissociation	10.7 BSCF
% Hydrate Dissociation (to Sep 2007)	69.25%
Cumulative gas produced (to Sep 2007)	17.1 BSCF
Hydrate contribution as % of gas produced	62.58%

Table W-9: Hydrate Contribution in recharging gas reservoir for Walakpa for SMALL MODEL

Similarly, current free gas reserve is calculated by using “Total Free Gas per unit Area” data obtained using CMG-STARS results. The initial free gas in place calculated for Walakpa reservoir model is 237.9 BCF, whereas the current free gas in place is approximately 219 BCF. A total of 17.11 BCF of gas has been produced to date, the volume of free gas supplied by hydrate is less than the free gas produced, and hence, the pressure depletion is faster.

III. WALAKPA FORECASTING STUDY

Initial conditions of the forecast run are shown in Table W-10.

SIMULATION PERIOD	30 Years (2007-2037)
WELL PRODUCED	ALL EXISTING WELLS
CONSTANT PRODUCTION RATE	500 MSCF/DAY/WELL (TOTAL 4.5 MMSCF/Day)

Table W-10: Initialization of Forecast Run for Walakpa

Forecasting runs were performed for both the SMALL MODEL and LARGE MODEL that was developed based on the geologic study performed by Panda & Morahan, 2008¹⁹. The larger model extended in up dip locations of the reservoir and was based on predictions of limited geologic and seismic data. This larger model was initialized similar to the previous model and forecast runs were studied.

Figures 140, 141 and 142 present the cumulative gas production, gas production rate and reservoir pressure, respectively, for the Walakpa reservoir from 1992 to 2037. Table W-11 quantifies the forecast results.

SCENARIO	CUMULATIVE GAS PRODUCTION (BSCF)	% RECOVERY	CUMULATIVE WATER PRODUCTION (BBLS)
SMALL MODEL			
All existing wells producing: 1992-2007	17.1 BSCF	6.75%	NIL
1992-2037 (FORECAST)	65.0 BSCF	25.65%	300 BBLS
LARGE MODEL			
All existing wells producing: 1992-2007	17.1 BSCF	3.23%	NIL
1992-2037 (FORECAST)	65.0 BSCF	11.10%	450 BBLS

Table W-11: Summary of forecast run from Forecasting Study for Walakpa

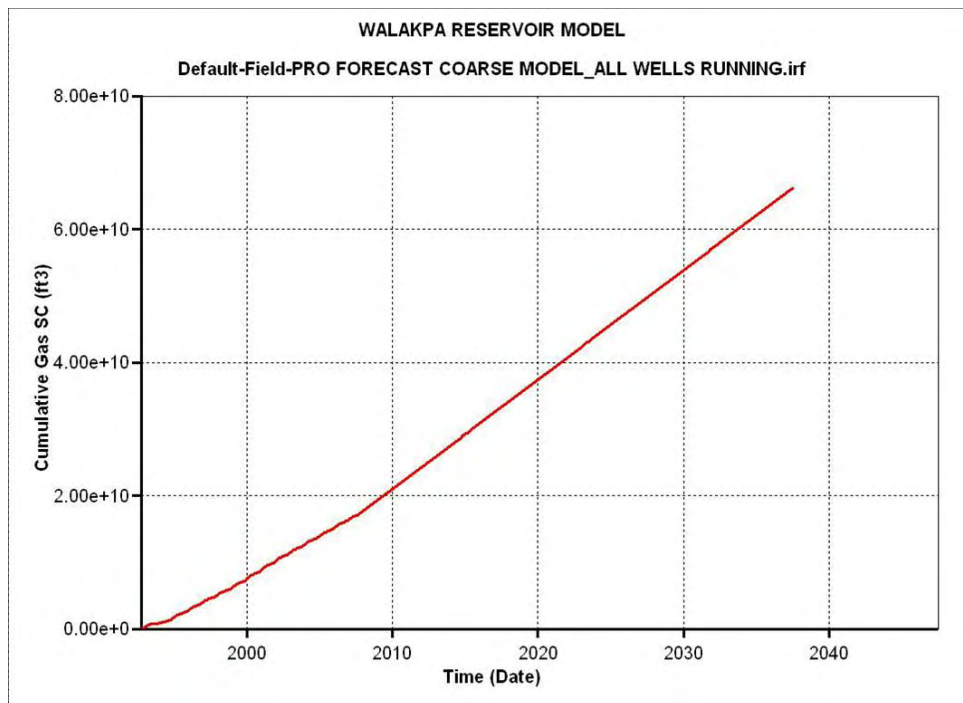


Figure 140: Cumulative gas production from Forecasting Study for Walakpa

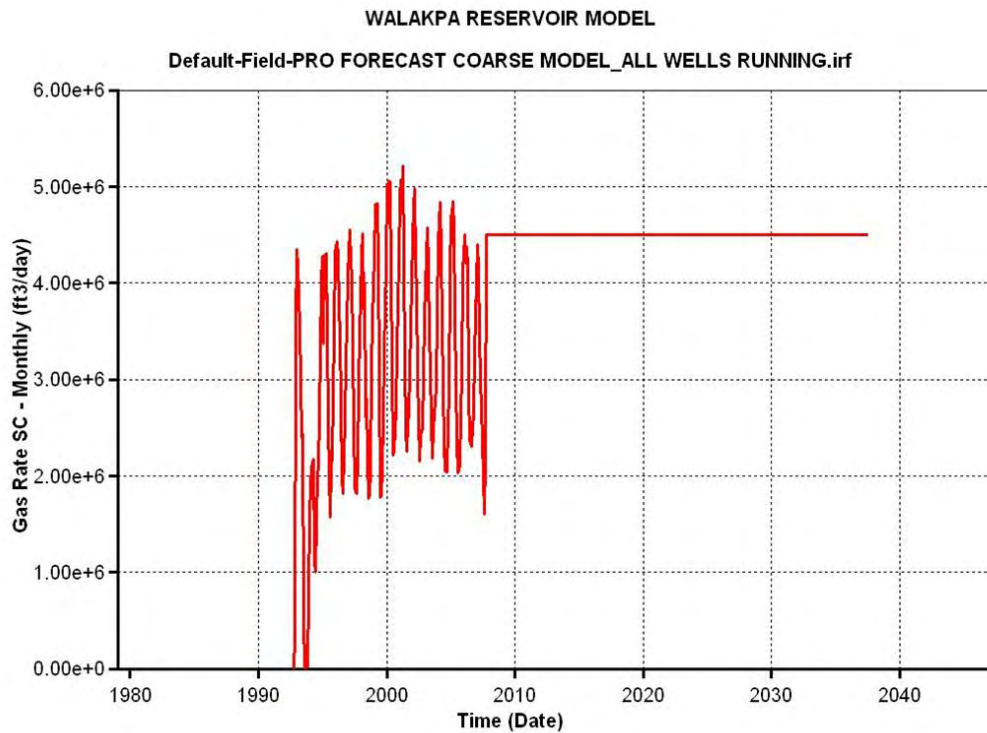


Figure 141: Cumulative gas production rate from Forecasting Study for Walakpa

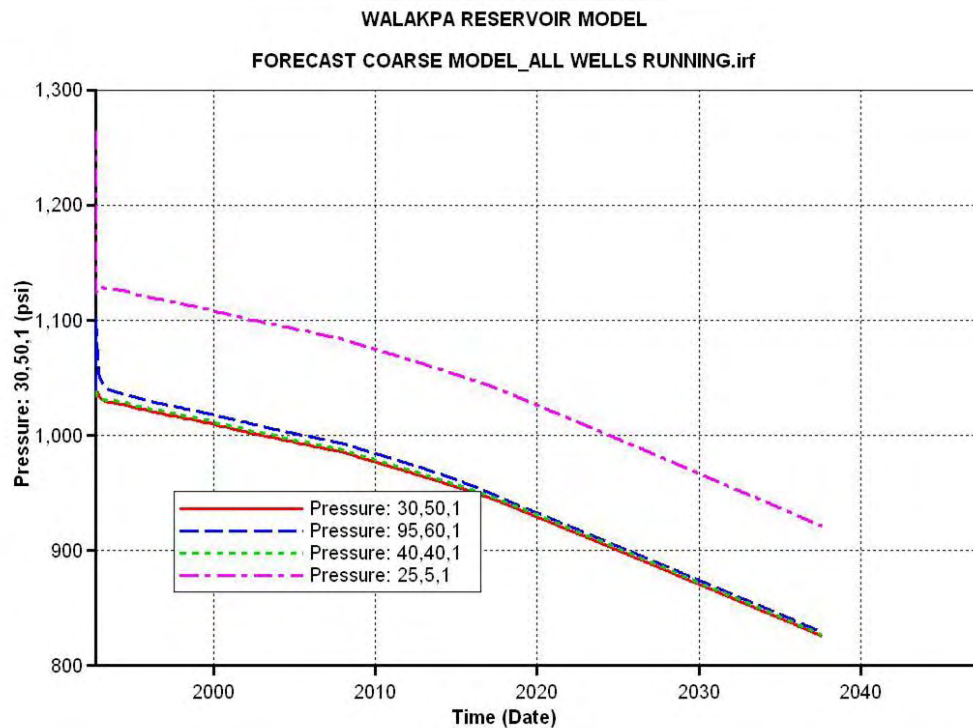


Figure 142: Reservoir Pressure Forecasting Study for Walakpa SMALL MODEL

Original in place volumes are shown for the SMALL MODEL and the LARGE MODEL in Table W-12

WALAKPA SIMULATION	SMALL MODEL	LARGE MODEL
Initial Free Gas in Place	235 BSCF	298 BSCF
Hydrate Gas in Place	15 BSCF	284 BSCF
Total Initial Gas in Place	250 BCF	582 BCF

Table W-12: Initial in-place gas and hydrate volumes Walakpa reservoir models

The forecasting results for the Walakpa reservoir simulation studies are summarized in Table W-13. Figure 143 shows the percent dissociation of the hydrates over time for the LARGE MODEL.

WALAKPA SIMULATION	SMALL MODEL	LARGE MODEL
Cumulative Gas Production (1992-2007)	17.1 BSCF	17.1 BSCF
Cumulative Gas Production (1992-2037)	65 BSCF	65 BSCF
Cumulative Water Production (1992-2037)	300 BBLS	450 BBLS
% Hydrate Dissociated (1992-2007) Production to Date	70% (of in place hydrates)	10.4% (of in place hydrates)
% Hydrate Dissociated (1992-2037) FORECASTING RUN	100% (of in place hydrates)	20.1% (of in place hydrates)

Table W-13: Comparison of simulation results between the Small and Large models for Walakpa

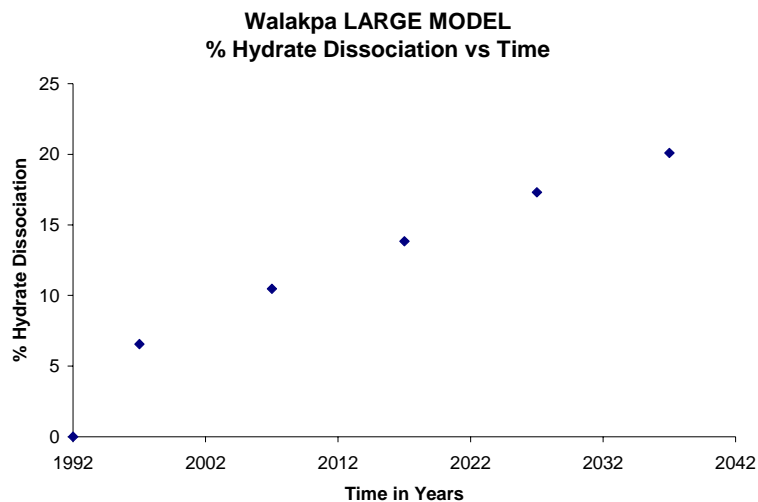


Figure 143: Walakpa LARGE MODEL Hydrate dissociation over forecast

WALAKPA CONCLUSIONS

A full scale reservoir simulation has been performed on the Walakpa gas reservoir model. The developed reservoir model is capable of evaluating and quantifying methane hydrate resource potential. A topdown approach has been employed to build the reservoir model and match the production history using advanced reservoir simulator. The SMALL MODEL was initially history matched to confirm that the reservoir pressure/production history was just due to volumetric or water-drive performance.

Following are the conclusions drawn from this study:

1. The Walakpa reservoir model, constructed and initialized in CMG-STAS, successfully matched the reservoir production and pressure history data in the SMALL MODEL, which only included an updip band of hydrates of 4000' in length, and associated with aquifer support from the bottom. A LARGE MODEL was also initialized that included hydrates updip to the extent mapped by the reservoir characterization study. Results of the history match are:
 - a. SMALL MODEL - The total initial gas (free gas + hydrate associated gas) in place is found to be 250 STD BCF (free gas = 235 BCF + hydrate associated gas = 15 BCF*).
 - b. LARGE MODEL - The total initial gas (free gas + hydrate associated gas) in place is found to be 582 STD BCF (free gas = 298 BCF + hydrate associated gas = 284 BCF*).
 - c. The pressure-temperature condition of the hydrate zone is such that the three phases, water-gas-hydrate, exist in thermodynamic equilibrium.
 - d. History matching studies were performed for the SMALL MODEL after including a large aquifer supporting the Walakpa gas reservoir. This was done by initializing a numerical aquifer of infinite strength (edge water system) along with pre-initialized model aquifer.
 - e. SMALL MODEL - 70% of initial hydrate in place was dissociated during the 15 year production life of the reservoir, from 1992 to 2007.
 - f. LARGE MODEL - 10.5% of initial hydrate in place was dissociated during the 15 year production life of the reservoir, from 1992 to 2007.
2. Forecasting studies were performed for the next 30 years of production life of the reservoir using both the SMALL MODEL and the LARGE MODEL, from 2007 through 2037. All existing wells were produced at a constant rate of 500 MSCF/Day. The conclusions drawn from these model predictions are:
 - a. SMALL MODEL - Total hydrate dissociation (100% dissociation) was observed during 30 years of future production, from years 2007 – 2037.
 - b. LARGE MODEL - 20.1% hydrate dissociation was observed at the end of 30 years of forecast run, from years 2007 – 2037.
 - c. SMALL MODEL - The forecasting resulted in total gas production of 65 BCF from 1992-2037, which is equivalent to a recovery of 26% of total initial gas in place. The

cumulative water production was predicted to be very low at 300 BBLs from years 1992-2037.

- d. LARGE MODEL - The forecasting resulted in total gas production of 65 BCF, from years 1992-2037, which is equivalent to a recovery of 11% of total initial gas in place. The cumulative water production was predicted to be 450 BBLs, from years 1992-2037.

REFERENCES

1. Walsh, T., “Characterization and Quantification of methane hydrate resource potential associated with Barrow gas fields, Alaska”, Sixth Quarterly Progress Report, May 2008, NETL website, www.netl.doe.gov.
2. Darvish, M., “Gas production from hydrate reservoir and its modeling”, June 2004, SPE-86827, www.spe.org.
3. Moridis, G., Kowalsky and Pruess, K “Depressurization induced gas production from Class-1 hydrate deposits”, October 2005, SPE-97266, www.spe.org
4. Moridis, G. and Reagan, M., “Gas production from Class-2 hydrate accumulations in the permafrost”, November 2007, SPE-110858, www.spe.org
5. Moridis, G, Collett, T. S., Boswell R., Kurihara, M., Reagan, M. T., Koh, C. and Sloan, E. D., “Toward Production From Gas Hydrates: Current Status, Assessment of Resources, and Simulation-Based Evaluation of Technology and Potential”, February 2008, SPE-114163, www.spe.org
6. Walsh, T., Singh, P., “Characterization and quantification of methane hydrate resource potential associated with Barrow Gas Fields”, May 2007, Phase 1 A, Final Technical Report, NETL website, www.netl.doe.gov.
7. Kim, H. C. et. al., “Kinetics of methane hydrate decomposition”, 1987, Chemical Engineering Science, vol 42, pp 1645-1653.
8. Uddin, M., Coombe, D. A., Law, D. A. and Gunter, D. W., “Numerical Studies of Gas-Hydrates Formation and Decomposition in a geologic reservoir”, May 2006, SPE-100460, www.spe.org.
9. Kamath, V. A. and Holder, G. D., “Dissociation heat transfer characteristics of methane hydrates”, 1987, AIChE J, 33, pp, 347-350.
10. Hong, M. and Pooladi-Darvish, M.: “A Numerical Study on Gas Production from Formations Containing Gas Hydrates”. *June 10 – 12, 2003, Paper CIMMP 2003-060, presented at the Canadian International Petroleum Conference 2003, Calgary, Alberta, Canada.*
11. Van Genuchten, M. T.: “A closed-form equation for predicting the hydraulic conductivity of unsaturated soils”, 1980, *Soil Science Society of America Journal*, vol. 44, pp. 892-898.
12. Parker, J.J., Lenhard, R.J., and Koppusamy, T.: “A Parametric Model for Constitutive Properties Governing Multiphase Flow in Porous Media”. 1987, *Water Resources Research*, Vol. 23, No. 4, pp. 618-624.
13. Gruy, H. J., “*Reservoir Engineering and Geologic Study of the East Barrow Field, National Petroleum Reserves in Alaska*”, 1978, under USGS Contract
14. Howe, S., “Production modeling and economic evaluation of a potential gas hydrate pilot production program on the north slope of Alaska”, 2004, MS Thesis, University of Alaska, Fairbanks.

15. PRA, Stokes, P., and Walsh, T., “*South and East Barrow Reserves Study*”, July 2007, report submitted to North Slope Borough.
16. Allen, W. W. and Crouch, W. J., “*Engineering Study South and East Barrow Fields, North Slope Alaska, Alaska*”, 1988, technical report prepared for North Slope Borough Gas Development Project, Alaska.
17. Singh, P., Panda, M. and Stokes, P., “Material Balance Study to Investigate Methane Hydrate Resource Potential in the East Pool of the Barrow Gas Field”, March 2008, a Topical Report for DOE Project Number DE-FC26-06NT42962, NETL website, www.netl.doe.gov.
18. Moridis, G. J., “ Numerical Studies of Gas Production from Methane Hydrates:”, pp 359-70, SPE Journal, December 2003.
19. Panda, M. and Morahan, G. T., “An Integrated Reservoir Model Description for East Barrow and Walakpa Gas Fields, Alaska”, June 2008, a Topical Report for DOE Project Number DE-FC26-06NT42962, NETL website, www.netl.doe.gov.
20. PRA, Stokes P., Walsh T. and Walsh, C., “*Walakpa Field Reserves Study*”, June 2005, report submitted to North Slope Borough.

National Energy Technology Laboratory

626 Cochrans Mill Road
P.O. Box 10940
Pittsburgh, PA 15236-0940

3610 Collins Ferry Road
P.O. Box 880
Morgantown, WV 26507-0880

One West Third Street, Suite 1400
Tulsa, OK 74103-3519

1450 Queen Avenue SW
Albany, OR 97321-2198

2175 University Ave. South
Suite 201
Fairbanks, AK 99709

Visit the NETL website at:
www.netl.doe.gov

Customer Service:
1-800-553-7681

